

UC Santa Barbara

UC Santa Barbara Electronic Theses and Dissertations

Title

Tandem chemo- and bio-catalysis enabled by micellar technology

Permalink

<https://escholarship.org/uc/item/0vp1b0zz>

Author

Singhania, Vani

Publication Date

2023

Peer reviewed|Thesis/dissertation

UNIVERSITY OF CALIFORNIA

Santa Barbara

Tandem chemo- and bio-catalysis enabled by micellar technology

A dissertation submitted in partial satisfaction of the
requirements for the degree Doctor of Philosophy
in Chemistry

by

Vani Singhania

Committee in charge:

Professor Bruce H. Lipshutz, Chair

Professor Craig Hawker

Professor Liming Zhang

Professor Song-I Han

June 2023

The dissertation of Vani Singhanian is approved.

Craig Hawker

Liming Zhang

Song-I Han

Bruce H. Lipshutz, Committee Chair

May 2023

Tandem chemo- and bio-catalysis enabled by micellar technology

Copyright © 2023

by

Vani Singhania

ACKNOWLEDGEMENTS

My graduate school journey would have been incomplete without the constant support from my friends and family. A special shout out to my parents and my sister for being there with me through thick and thin.

I feel grateful to have been advised by an extremely dedicated mentor, Prof. Bruce H. Lipshutz. A special thank you to all my lab mates, co-workers, mentors and mentees who not only helped me progress in the field of chemistry but also assisted in my personal growth.

Finally, to each and every individual who has played a part in helping me reach where I am in life, today. Nothing but immense amount of gratitude.

VANI SINGHANIA

Curriculum Vitae May 2023

PROFILE

- PhD Candidate in Organic Chemistry with 7+ years of experience in a research laboratory and 2 industry experiences as a research and development chemist
- Passionate about green chemistry while focused on sustainable syntheses of pharmaceuticals through creative application of techniques to effectively meet project goals
- Motivated and organized leader with strong interpersonal skills gained from leading research teams, training junior researchers, managing lab safety, and heading the professional development team
- Excellent written and oral (3 languages) scientific communication skills gained through 5 publications, 2 oral, and 5 poster presentations (2 received outstanding poster awards)

EDUCATION

Ph.D. Organic Chemistry, University of California, Santa Barbara June 2023
B.Sc. Chemistry and Applied Mathematics, Purdue University June 2018

INTERNSHIP EXPERIENCE

Process Research and Development Intern, Merck - NJ June 2021 - Sep 2021

- Scientific problem solving of Sulfur-35 isotope exchange in pharmaceuticals containing sulfones and sulfonamides
- Conducted High Throughput Experiments to test for transition metal catalysts and ligands
- Developed LCMS and UPLC-MS methods to identify and analyze complex samples

Process Technology and Development Chemist, BASF – MO May 2017 - Dec 2017

- Designed and delivered time sensitive analytical tests to facilitate launch of a new target compound

- Managed purity analysis of intermediates and products from production test batches
- Synthesized complex organic compounds to assay for impurities in agricultural products

RESEARCH EXPERIENCE

Graduate Student Researcher, Lipshutz Group, UCSB Aug 2018 - Current

- Conducted research and development of environmentally friendly and sustainable technologies to perform organic synthesis under aqueous micellar conditions
- Amalgamated biocatalysis and chemocatalysis to develop tandem 1-pot methodologies
- Experienced in palladium-catalyzed cross-couplings, reduction reactions using catalytic nickel, and enzyme enabled organic transformations
- Conducted mechanistic and kinetic studies including deuterium incorporation using designer surfactants
- Incorporated the 12 Principles of Green Chemistry and integrated them into industrial product designs including pharmaceuticals, cosmetics, and paints
- 6+ years of teaching and mentoring to develop leadership and scientific-communication skills

Undergraduate Research Assistant, Mei Lab, Purdue University Jan 2015 - May 2018

- Synthesized, characterized and studied the physical and electronic properties of semiconducting, donor-acceptor type pure polymers and polymer blends
- 3 poster presentations on influence of molecular weight on charge transport properties in blends

LEADERSHIP

Co-President, Chemistry Professional Development team, UCSB Aug 2019 – Aug 2022

- Organized three Chemistry Career Fests and hosted over 20 companies virtually and in-person
- Coordinated and collaborated with industry and faculty to promote careers beyond academia

- Managed over 150 participating graduate students

Primary Safety Officer and Instrument Manager, UCSB Aug 2018 – Dec 2022

- Maintained and repaired lab instruments while training new users on operation and analysis
- Implemented safe and clean laboratory practices and organized chemical inventory
- Trained new graduate and undergraduate students and encouraged a collaborative environment

Graduate Student Mentor, Women in Science, UCSB May 2019 - Current

- Mentored undergraduate students looking to pursue careers in STEM

TEACHING EXPERIENCE

Teaching Assistant, Chemistry, UCSB Aug 2018 - Current

- Managed over 35 senior undergraduate students in organic chemistry lab
- Trained students on safe laboratory techniques
- Responsible for lectures and discussion of coursework which resulted in a UCSB teaching award

Head Teaching Assistant, Mathematics, Purdue University Aug 2016 - May 2018

- Designed new teaching techniques and trained fellow teaching assistants
- Taught differential equations and calculus to a class of 40 students using MATLAB

TECHNICAL SKILLS

- **Spectroscopy:** FTIR, NMR, GCMS, LCMS, UPLC-MS, HPLC, DLS, GPC
- **Drug Discovery and Synthesis**
- **Organic, Medicinal and Process Chemistry**
- **High Throughput Experimentation**
- **Purification Techniques:** Chromatography, Crystallization
- **Qualitative and Quantitative Analysis**

AWARDS

- **Mananya Tantiwivat Fellowship Award**, UCSB 2022
- **Exceptional Leadership and Outstanding Service**, UCSB 2022
- **Distinguished Teaching Fellow Award**, UCSB 2022
- **Chair's Fellowship**, UCSB 2022
- **Outstanding Poster**, U. C. Chemical Symposium 2021
- **Outstanding Academic and Research Record**, Fellowship, UCSB 2018
- **Outstanding Student of Mathematics**, Purdue University 2017
- **Outstanding Poster**, Symposium on Soft Matter and Polymers, Notre Dame 2016

POSTER AND PRESENTATIONS

Singhania, V., Cortes-Clerget, M., Dussart-Gautheret, J., Akkachairin, B., Yu, J., Akproji, N., Lipshutz, B. H. Tandem, 1-Pot Chemo and Biocatalysis...*in Water*. **Poster** presented at: National Organic Chemistry Symposium; **2022** June; San Diego, CA

Singhania, V., Lipshutz, B. H. Tandem, 1-Pot Chemo and Biocatalysis in Water. **Oral presentation** at: 2021 International Chemical Congress of Pacific Basin Societies; **2021** December; Virtual

Singhania, V., Lipshutz, B. H. Tandem, 1-Pot Chemo and Biocatalysis in Water. **Oral presentation** at: 25th Annual Green Chemistry and Engineering Conference; **2021** June; Virtual

Singhania, V., Akkachairin, B., Cortes-Clerget, M., Lipshutz, B. H. Tandem, 1-Pot Chemo and Biocatalysis in Water. **Poster** presented at: University of California Chemical Symposium; **2021** March; Virtual

Singhania, V., Akkachairin, B., Cortes-Clerget, M., Lipshutz, B. H. Lipase catalyzed esterification...in water. **Poster** presented at: Bristol Myers Squibb Women in Chemistry Outreach Event; **2020** November; Virtual

Singhania, V., Zhao, X., Zhao, Y., Mei, J. Influence of Molecular Weight on Charge Transport Properties in Complementary Semiconducting Polymer Blends. **Poster** presented at: 19th Annual Undergraduate Research Symposium; **2016** October; University of Maryland Baltimore County, MD

Singhania, V., Zhao, X., Zhao, Y., Mei, J. Influence of Molecular Weight on Charge Transport Properties in Complementary Semiconducting Polymer Blends. **Poster** presented at: Notre Dame-Purdue Symposium on Soft Matter and Polymers; **2016** October; University of Notre Dame, IN

PUBLICATIONS

Singhania, V., Nelson, C., Reamey, M., Morin, E., Kavthe, R., "A streamlined, green, and sustainable synthesis of the anticancer agent erdafitinib", *Submitted*

Singhania, V., Cortes-Clerget, M., Dussart-Gautheret, J., Akkachairin, B., Yu, J., Akporji, N., Gallou, F., Lipshutz, B. H., "Lipase-catalyzed esterification in water enabled by nanomicelles. Applications to 1-pot multi-step sequences", *Chem. Sci.* **2022**, *1*, 1440-1445

Akporji, N., **Singhania, V.**, Dussart-Gautheret, J., Gallou, F., Lipshutz, B. H., "Nanomicelle-enhanced, asymmetric ERED-catalyzed reductions of activated olefins. Applications to 1-pot chemo- and bio-catalysis sequences in water", *Chem. Comm.* **2021**, *57*, 11847-11850

Thakore, R. R., Takale, B. S., **Singhania, V.**, Gallou, F., Lipshutz, B. H., "Late stage Pd-catalyzed cyanations of aryl/heteroaryl halides in aqueous micellar media", *ChemCatChem*, **2021**, *13*, 212-216

Wood, A. B., Cortes-Clerget, M., Kincaid, J. R. A., Akkachairin, B., **Singhania, V.**, Gallou, F., Lipshutz, B. H., "Nickel Nanoparticle-Catalyzed Mono- and Di-Reductions of gem-Dibromocyclopropanes Under Mild, Aqueous Micellar Conditions", *Angew. Chem. Int. Ed.*, **2020**, *59*, 17587-17593

Zhao, X., Xue, G., Qu, G., **Singhania, V.**, Zhao, Y., Butrouna, K., Gumyusenge, A., Diao, Y., Graham, K. R., Li, H., Mei, J., "Complementary Semiconducting Polymer Blends: Influence of Side Chains of Matrix Polymers', *Macro molecules*, **2017**, *50*, 6202-6209

ABSTRACT

Tandem chemo- and bio-catalysis enabled by micellar technology

by

Vani Singhanian

The world of modern organic chemistry, a very traditional but unsustainable 200-year-old discipline, relies heavily on the use of environmentally harmful chemicals. From the 12 Principles of Green Chemistry it is evident that waste-generating and toxic organic solvents must be eliminated and replaced by the greenest solvent, recyclable water. New surfactants were developed by the Lipshutz lab which forms nano-micelles in water to serve as organic reaction vessels. Micellar catalysis has been advantageous by enabling a myriad of synthetic organic reactions.

Recent advancements utilize enzymes such as lipases for bio-catalytic processes that benefit significantly when run in the presence of these nanomicelles, offering an advantageous and unprecedented “reservoir effect” that minimizes textbook enzymatic inhibition. In addition, the study of substrate promiscuity for lipases that catalyze esterification reactions, focuses on the use of a simple, economical and commercially available additive. The common aqueous micellar reaction medium provides the synergy between chemo- and bio-catalytic processes giving rise to the blossoming field of “chemoenzymatic catalysis” that can now occur sequentially in 1-pot in various permutations and combinations.

These cascade reactions abide by many principles of green chemistry such as time- and pot-economy and illustrate the potential of conducting sequential organic transformations including industrial drug development, under ambient condition with low levels of precious metal catalyst loadings. One such example is the synthesis of an anticancer drug, erdafitinib which is achieved in a 3-step, 2-pot sequence under aqueous micellar conditions enabled by a biodegradable surfactant, Savie.

TABLE OF CONTENTS

1. LIPASE-CATALYZED ESTERIFICATION IN WATER ENABLED BY NANOMICELLES. APPLICATION TO 1-POT MULTI-STEP SEQUENCES.	1
1.1. INTRODUCTION AND BACKGROUND	2
1.2. RESULTS AND DISCUSSION	8
1.2.1. Optimization of lipase-catalyzed esterification reaction.....	8
1.2.2. Substrate scope of esterification reaction in water	13
1.2.3. Influence of additive on reactivity of challenging substrates.....	15
1.2.4. “Reservoir effect” caused by aqueous micellar system	20
1.2.5. Chemoselectivity of these bio-catalytic reactions	22
1.2.6. Tandem, 1-pot, chemo- and bio-catalysis	25
1.3. CONCLUSION	29
1.4. REFERENCES.....	30
1.5. EXPERIMENTAL INFORMATION	33
1.5.1. General Information.....	33
1.5.2. Preparation of the buffer solution	34
1.5.3. Conversion measurement	35
1.6. EXPERIMENTAL PROCEDURE	35
1.6.1. General approach to optimization of esterification reactions	35
1.6.2. Optimized procedure for esterification reactions	36
1.6.3. General procedure for esterification using the additive PhCF ₃	36
1.6.4. Buffer concentration study	37
1.6.5. Surfactant concentration study.....	37
1.6.6. 2-step, 1-pot: esterification, Suzuki-Miyaura cross-coupling.....	38
1.6.7. 3-step, 1-pot sequence: Pd/C reduction, esterification, gem-dibromocyclopropane reduction	39
1.6.8. 3-step, 1-pot sequence: Sonogashira cross-coupling reaction, esterification, ADH reduction	41
1.6.9. 3-step, 1-pot sequence: esterification, Suzuki cross-coupling reaction, Pd/C reduction	42
1.7. CHARACTERIZATION (NMR AND HRMS)	44

1.8.	NMR SPECTRA	59
2.	A STREAMLINED, SUSTAINABLE SYNTHESIS OF THE ANTICANCER DRUG ERDAFITINIB.....	91
2.1.	INTRODUCTION AND BACKGROUND	92
2.2.	RESULTS AND DISCUSSION.....	97
2.2.1.	<i>Optimization of Step 1: Suzuki-Miyaura reaction.....</i>	<i>98</i>
2.2.2.	<i>Optimization of Step 2: amination reaction</i>	<i>103</i>
2.2.3.	<i>Optimization of the final step to erdafitinib</i>	<i>106</i>
2.2.4.	<i>Greener route to erdafitinib</i>	<i>110</i>
2.3.	CONCLUSION	112
2.4.	REFERENCES.....	113
2.5.	GENERAL INFORMATION	116
2.6.	EXPERIMENTAL PROCEDURES	117
2.6.1.	<i>Suzuki-Miyaura cross coupling reaction.....</i>	<i>117</i>
2.6.2.	<i>Amination reaction.....</i>	<i>118</i>
2.6.3.	<i>S_N2 reaction.....</i>	<i>118</i>
2.6.4.	<i>Procedure for synthesis of step 1 and step 2 in 1-pot</i>	<i>119</i>
2.7.	E FACTOR CALCULATION FOR ERDAFITINIB.....	120
2.8.	PRODUCT CHARACTERIZATION (NMR AND HRMS)	123
2.9.	NMR SPECTRA	125
3.	NICKEL NANOPARTICLE CATALYZED MONO- AND DI-REDUCTIONS OF GEM-DIBROMOCYCLOPROPANES UNDER MILD, AQUEOUS MICELLAR CONDITIONS.....	131
3.1.	INTRODUCTION AND BACKGROUND	132
3.2.	RESULTS AND DISCUSSION.....	135
3.2.1.	<i>Mechanistic studies of mono-reduction of gem-dibromocyclopropane</i>	<i>136</i>
3.2.2.	<i>Reduction of mono-bromocyclopropane</i>	<i>139</i>
3.2.3.	<i>Mechanistic studies of di-reduction of gem-dibromocyclopropanes</i>	<i>140</i>
3.2.4.	<i>Access to a variety of isotopic analogs of reduced products of gem-dibromocyclopropanes.....</i>	<i>141</i>
3.3.	CONCLUSION	143
3.4.	REFERENCES.....	144
3.5.	GENERAL EXPERIMENTAL INFORMATION	145

3.6.	GENERAL PROCEDURE.....	146
3.6.1.	<i>General procedure for the di-reduction of gem-dibromocyclopropanes</i>	146
3.6.2.	<i>General procedure for the mono-reduction of gem-dibromocyclopropanes</i>	146
3.6.3.	<i>General procedure for deuteration studies</i>	147
3.7.	PRODUCT CHARACTERIZATION (NMR AND HRMS)	148
3.8.	NMR SPECTRA	153
4.	SYNTHESIS OF SULFAMATE ESTERS.....	165
4.1.	INTRODUCTION AND BACKGROUND	165
4.2.	RESULTS AND DISCUSSION.....	171
4.3.	CONCLUSION	177
4.4.	REFERENCES.....	179
5.	HYDROSILYLATION OF CARBOXYLIC ACID TO PRIMARY ALCOHOL ...	181
5.1.	INTRODUCTION AND BACKGROUND	181
5.2.	RESULTS AND DISCUSSION.....	189
5.3.	CONCLUSION	199
5.4.	REFERENCES.....	199

1. Lipase-catalyzed esterification in water enabled by nanomicelles.

Application to 1-pot multi-step sequences.

Singhania, V.; Cortes-Clerget, M.; Dussart-Gautheret, J.; Akkachairin, B.; Yu, J.; Akporji, N.; Gallou, F.; Lipshutz, B. H. Lipase-catalyzed esterification in water enabled by nanomicelles. Applications to 1-pot multi-step sequences *Chem. Sci.* **2022**, *13*, 1440-1445.

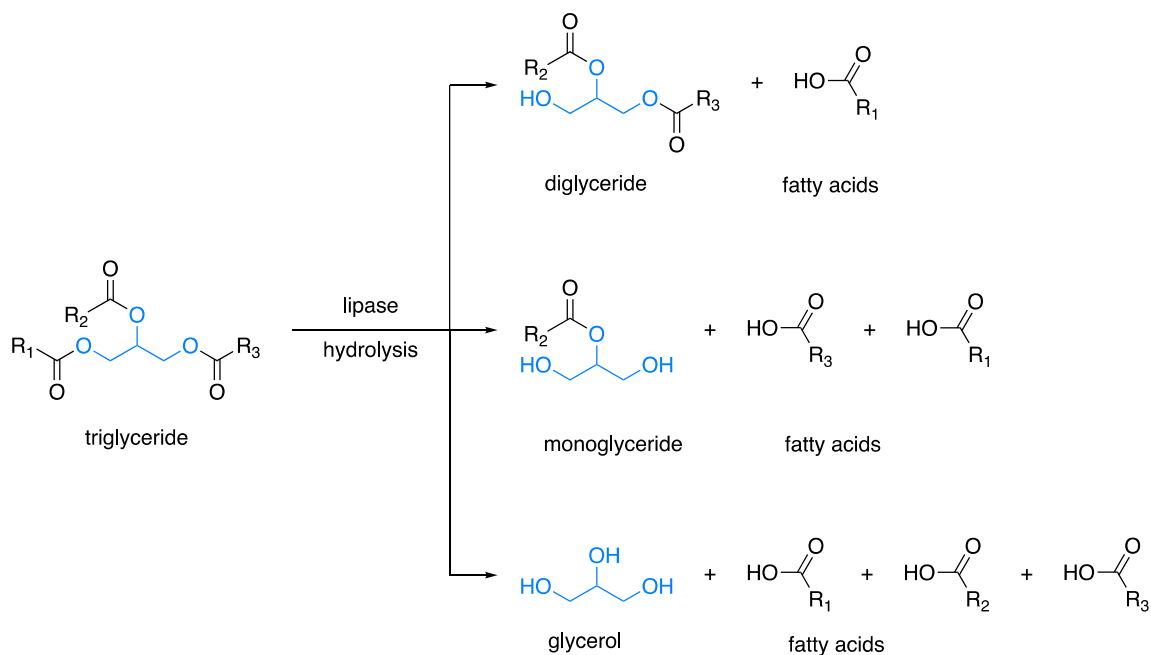
Copyright 2022 Royal Society of Chemistry.

Reproduced with permission.

1.1. Introduction and background

Lipases are water-soluble enzymes that catalyze hydrolysis of fats and oils (triacylglycerides) to release free fatty acids, diglycerides, monoglycerides and glycerol (Figure 1).¹ They are naturally found in plants, animals and microbes, where their function is to metabolize lipids. Lipases are either extracted from animal or plant tissue or cultivated from microorganisms. These enzymes are very popular in organic synthesis due to their commercial availability and broad specificity. They are very important industrial enzymes that are generally used in different chemical sectors such as detergents, food, bioenergy, flavors, pharmaceuticals, fine chemicals and agrochemicals.¹

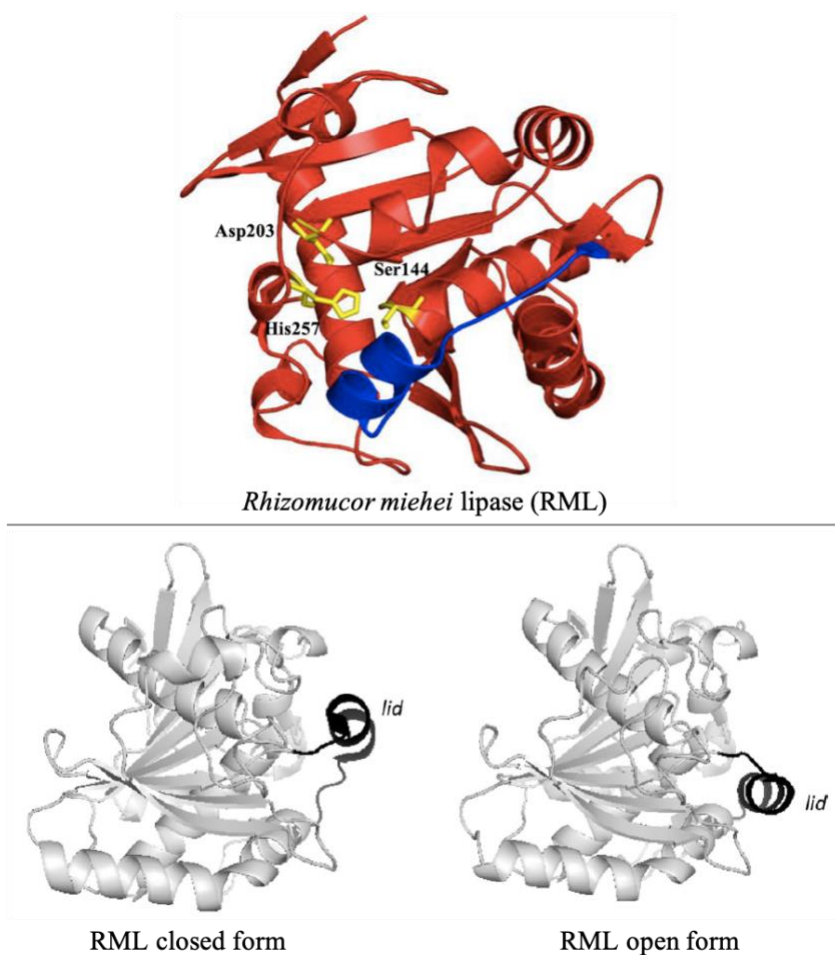
Figure 1. Hydrolysis of triglycerides catalyzed by lipase



Lipases show varied stability toward the presence of organic solvents, extreme pH conditions and ionic liquids. Esterification, transesterification and interesterification catalyzed by lipases have also been investigated however, at very low levels or absence of water.

The structures of lipases are composed of a core of mainly parallel β strands surrounded by α helices. The active site of lipases is made of a catalytic triad consisting of amino acids serine, histidine and aspartic acid/glutamic acid. This active site is covered by a lid or flap formed by an amphiphilic α helix peptide sequence (Figure 2).²

Figure 2. Structure of lipase, *Rhizomucor miehei*



Most lipases in pure aqueous media are in their inactive state, since the amphiphilic lid is predominantly in the closed formation protecting the active site from the environment with their hydrophilic side facing the solvent and the hydrophobic side directed towards the catalytic pocket.²

The enzyme gains catalytic activity on adsorption onto a hydrophobic interface, a phenomenon as known as “interfacial activation.” The lid undergoes displacement (opening) or rotation around two hinge regions at the lipid–water interface. This exposes the catalytic triad and creates a large hydrophobic patch around it resulting in activation of the lipase, thus allowing substrates access to the otherwise inaccessible active site.³

The mechanism of lipase-catalyzed esterification involves formation of two tetrahedral intermediates (Figure 3). The first step is a nucleophilic attack by a hydroxyl group of a serine residue (present in the active site) on the carboxylic acid substrate. This forms the tetrahedral intermediate which then loses a water molecule to give an acyl-enzyme complex. Then there is a nucleophilic attack on the complex by the alcohol to give the tetrahedral intermediate, which finally releases the ester product to regenerate the enzyme in its native form. Both tetrahedral intermediates are stabilized by the hydrogen bonding interactions between the oxyanion and the oxyanion hole, bringing down the activation energy. The oxyanion hole is formed by two backbone amides of a residue in the *N*-terminal region of the lipase and the *C*-terminal neighbor of the catalytic serine.³

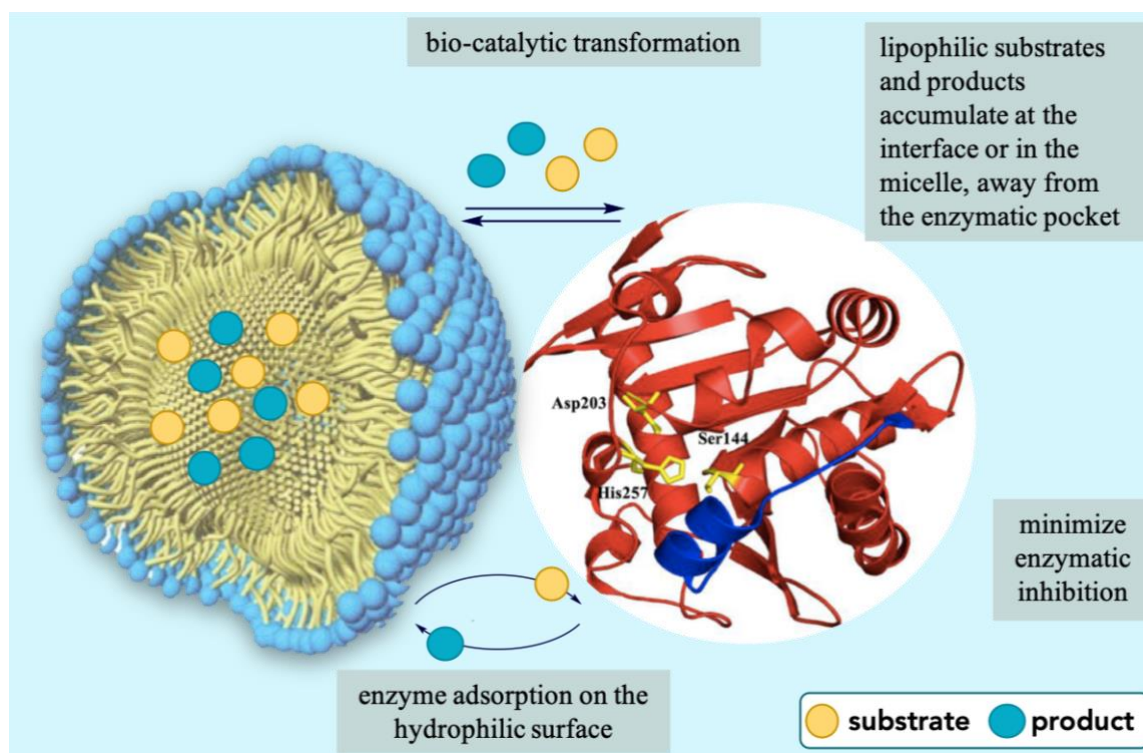
Esterification is a popular transformation using acids and alcohols, commonly performed in organic solvents under anhydrous conditions to drive the equilibrium to favor ester synthesis. Esters are applicable in various industries including food, beverage, cosmetic, personal care products, and pharmaceuticals. Esters are also used as antioxidants and surfactants.⁵ Bio-catalytic processes often offer mild conditions, high selectivity, and, in general, environmental friendliness. They are typically used in aqueous buffered media due to enzyme solubility and stability.⁶⁻¹⁰

Lipases have been studied for use in the synthesis of esters but they typically require dry conditions to avoid the reversible reaction, i.e., hydrolysis. Many chemical methods to remove water involve using sacrificial substrates and esters making it difficult to scale up for industrial applications. Lipases are often immobilized; non-covalently or covalently modified by attaching to surfactants, matrices, porous inorganic carriers or polymers. The enzymes are then lyophilized or precipitated out to suspend in organic solvent. Other special conditions (*e.g.*, prior acid activation, membrane-bound, solid supports or reverse micellar technology, etc.) have also been employed to address enzyme-solvent incompatibility issues.¹¹⁻¹² These methods are tedious, expensive and toxic and certainly do not follow the *12 Principles of Green Chemistry*.¹³⁻¹⁴

Even though esterification *in water*, where water is the by-product, seems counterintuitive,¹⁵⁻¹⁸ we developed use of an economical, commercially available lipase to catalyze esterification in water as the reaction medium. An important contributor to the reaction is the designer surfactant TPGS-750-M that forms micelles that enhance the solubility of organic molecules in water.¹⁹ The reservoir effect, first discovered in 2019,²⁰ explains the dynamic exchange of hydrophobic substrates and products between the micelle and the

enzyme, adsorbed to its surface (Figure 4). This phenomenon thus reduces crowding around the lipase and reduces enzymatic inhibition. This newly developed method for esterification uses only a 1:1 stoichiometric ratio of acid and alcohol and is performed in the complete absence of any co-factor. Enhanced reactivity was found in the presence of a simple additive (1 equiv). Moreover, this esterification process could be further applied to chemoenzymatic tandem sequences, all in 1-pot, all done in water.

Figure 4. Illustration of the “reservoir effect”

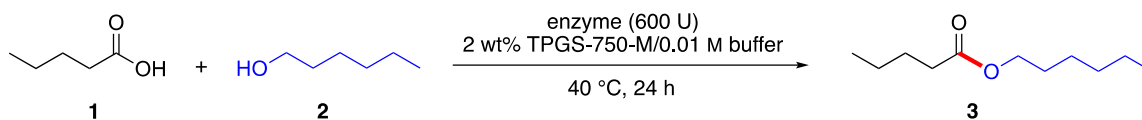


1.2. Results and discussion

1.2.1. Optimization of lipase-catalyzed esterification reaction

To optimize the reaction parameters, a lipase-catalyzed esterification reaction between valeric acid (1) and hexanol (2) was used as a model (Table 1). Esterification was tested using four commercially available lipases: *candida rugosa*, *rhizopus niveus*, *rhizomucor miehei* and *burkholderia cepacian*. Among these, *rhizomucor miehei* and *burkholderia cepacian* initially provided the most satisfactory results.

While keeping the concentration of valeric acid constant at either 0.25 M or 0.5 M, varied equivalences of hexanol were examined at varied concentrations and temperatures. At 0.25 M global concentration and fixed temperature of 40°C (entry 1-3), for reactions catalyzed by *rhizomucor miehei*, increasing the quantity of hexanol improved levels of conversion to the corresponding ester. No significant effect was seen at 0.5 M global concentration (entry 4-8). Entry 5 emphasizes the importance of surfactant being present in the reaction mixture as the conversion to product dramatically decreases from 83% to 47% in the absence of TPGS-750-M. The acidic pH of the reaction is also deemed important since the reaction is completely shut down at a neutral pH of 7 (entry 7).

Table 1. Optimization of reaction conditions using commercially available lipases

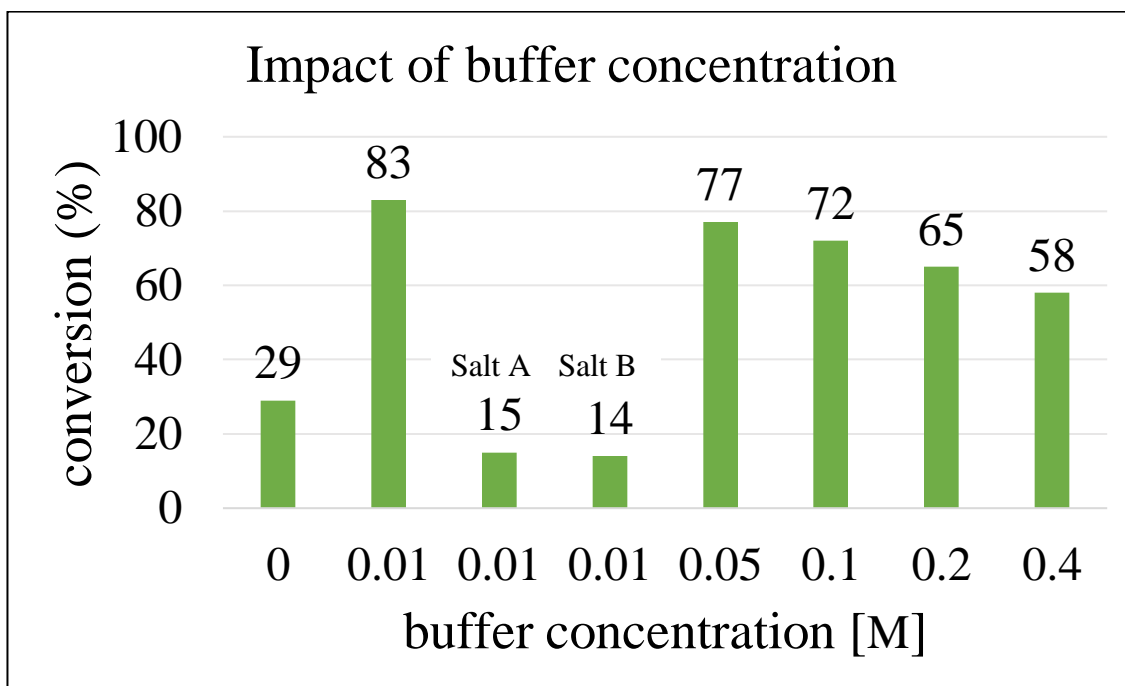
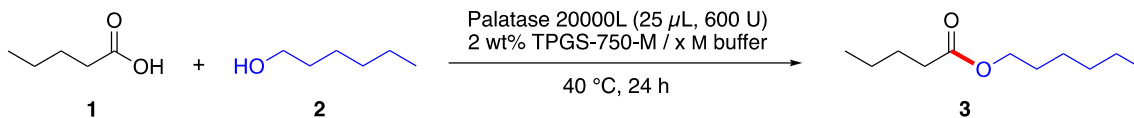
entry	conc. [M] ^[a]	ratio acid/alcohol	lipase (conversion)			
			<i>candida</i>	<i>rhizopus</i>	<i>rhizomucor</i>	<i>burkholderia</i>
			<i>rugosa</i>	<i>niveus</i>	<i>miehei</i>	<i>cepacia</i>
1		1:1	32	52	66	-
2	0.25	1:3	22	60	78	54
3		1:5	21	33	91	80
4		1:1	17	-	83	58
5		1:1	-	-	47 ^[b]	-
6	0.5	1:3	16	33	79	85
7		1:3	-	-	0 ^[c]	-
8		1:5	22	41	79	74

Conversion determined by crude ¹H NMR. ^[a] concentration, ^[b] performed in the absence of surfactant, ^[c] pH adjusted to 7 at t = 0.

Based on the best results in terms of reaction conditions outlined in Table 1, entry 4, further optimizations were carried out to better understand the need for a buffer, in hopes of driving the reaction to full conversion. Figure 5 indicates that in the absence of the buffer in aqueous solution, the conversion to the product plummets to 29%. A concentration as low as 0.01 M is deemed sufficient, since increasing the concentration only reduces the formation of

ester **3**. It was also observed that the neither the presence of kosmotropic anion, SO_4^{2-} nor that of chaotropic anion, SCN^- , was beneficial for the reaction.

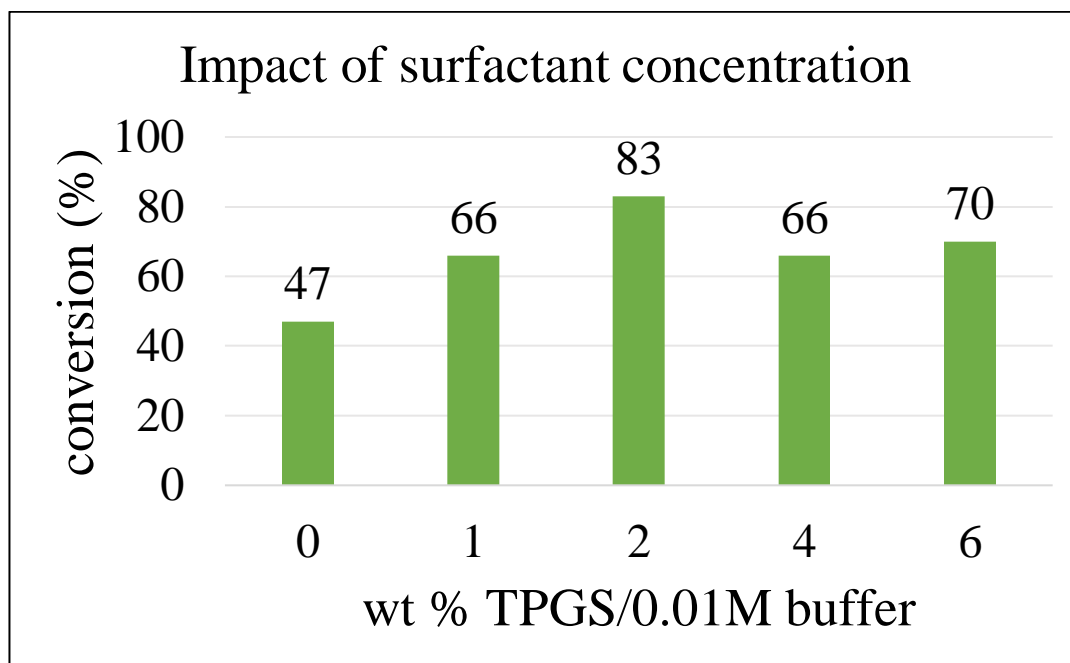
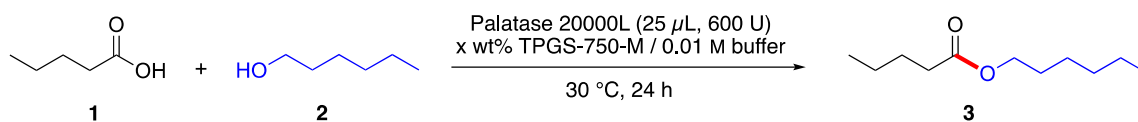
Figure 5. Impact of buffer concentration on lipase-catalyzed esterification reaction



Salt A: Na_2SO_4 ; Salt B: NaSCN

Since the presence of surfactant in the reaction pot was essential (Table 1, entry 5), along with the ideal buffer concentration of 0.01 M, the concentration of the surfactant, TPGS-750-M was altered. It was surprising to observe that increasing the amount of surfactant to either 4% or 6%, unlike that observed in KRED, did not lead to further increase in conversion (Figure 6).

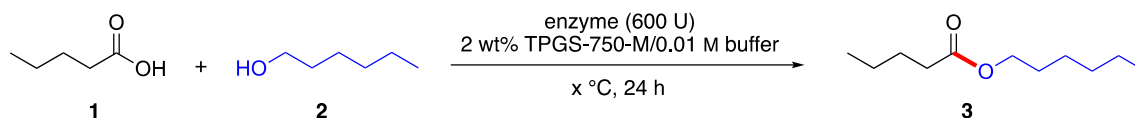
Figure 6. Impact of surfactant concentration on lipase-catalyzed esterification reaction



After understanding the impact of 2 wt % TPGS-750-M in 0.01 M buffer solution, three optimal parameters (marked in green in Table 1) were further investigated to find the ideal reaction conditions. High conversions (> 90%) were witnessed at 30 $^{\circ}$ C and 40 $^{\circ}$ C (entries 2, 5 and 9; Table 2). With respect to the above data (Table 1), decreasing the temperature to room temperature (entry 4) or increasing it to 50 $^{\circ}$ C (entry 3, 7 and 10) was detrimental for the reaction. At a low temperature of 30 $^{\circ}$ C, with no excess alcohol and high global concentration of 0.5 M, full conversion was observed, thus defining our ideal reaction conditions (entry 5). The 1:1 ratio of acid to alcohol helped maintain the goals of green chemistry, especially from the atom economy and prevention of waste perspective. It was also

beneficial during the process of purification, as well as when performing high concentration tandem processes.

Table 2. Optimization of esterification in aqueous buffer + surfactant



entry	temp (° C) ^[a]	enzyme	ratio acid/alcohol	conc [M] ^[b]	conv (%) ^[c]
1	30	<i>Rhizomucor miehei</i>	1:5	0.25	83
2	40	<i>Rhizomucor miehei</i>	1:5	0.25	91
3	50	<i>Rhizomucor miehei</i>	1:5	0.25	21
4	rt (22)	<i>Rhizomucor miehei</i>	1:1	0.5	74
5	30	<i>Rhizomucor miehei</i>	1:1	0.5	99
6	40	<i>Rhizomucor miehei</i>	1:1	0.5	83
7	50	<i>Rhizomucor miehei</i>	1:1	0.5	9
8	30	<i>burkholderia cepacia</i>	1:3	0.5	72
9	40	<i>burkholderia cepacia</i>	1:3	0.5	91
10	50	<i>burkholderia cepacia</i>	1:3	0.5	81

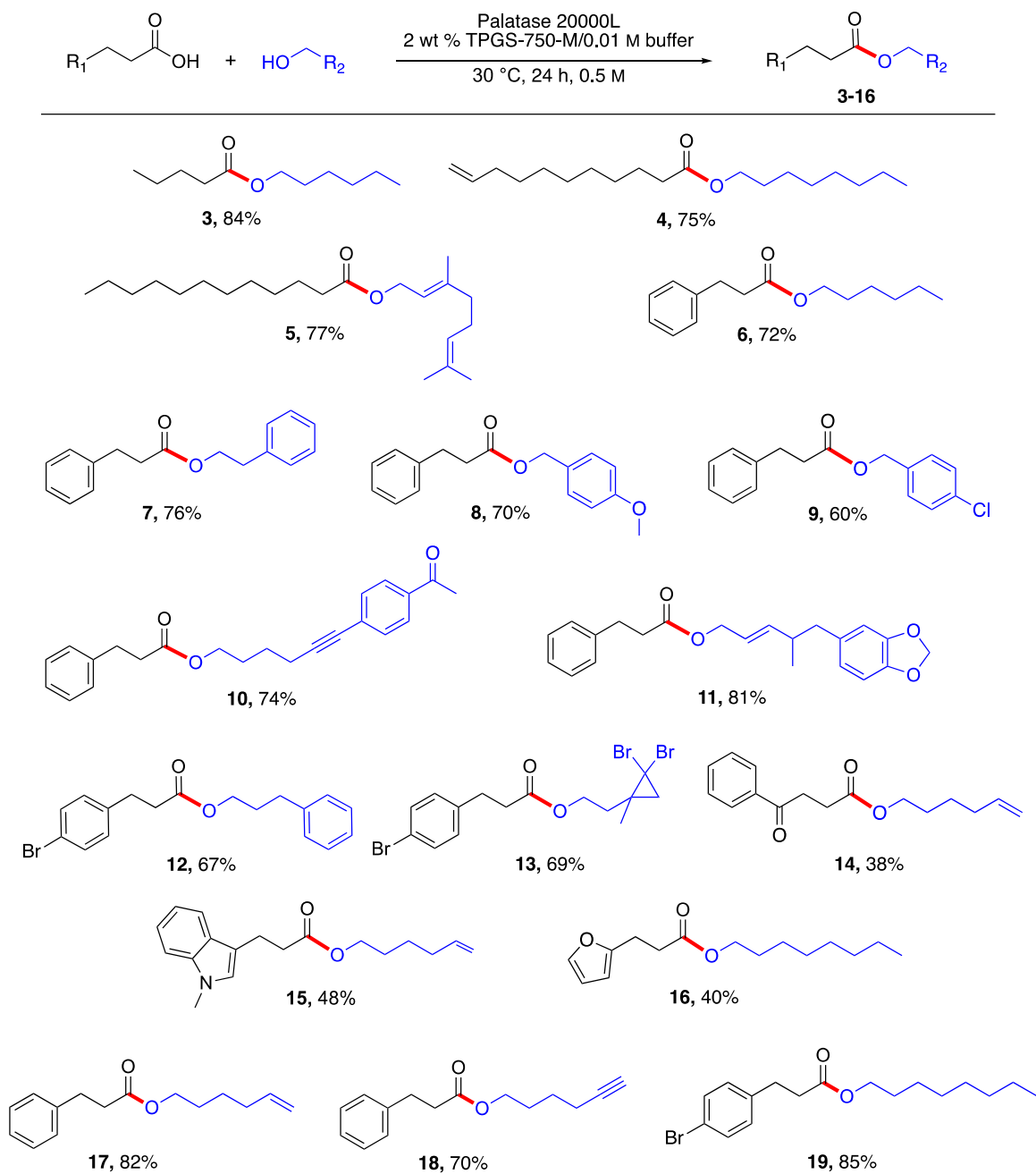
Conversion determined by crude ¹H NMR. ^[a] temperature, ^[b] concentration, ^[c] conversion.

1.2.2. Substrate scope of esterification reaction in water

To determine the generality of the optimized reaction conditions (i.e., 1:1 acid : alcohol, 30 °C), various esterification reactions were investigated, catalyzed by a commercially available lipase derived from *Rhizomucor miehei* (Scheme 1). Although, given an enzyme's typical preference for certain structural features associated with reaction partners, as witnessed with carboxylic acids, somewhat greater flexibility was observed in terms of the alcohol that participated in the esterification process. While these esterifications in water seem unexpected, the key to success may be the presence of the micelles. The presence of 2 wt % TPGS-750-M (i.e., 20 mg/mL of water) in the buffered aqueous medium proved beneficial for most lipophilic substrates. Hence, the water-insoluble product esters are likely located within the hydrophobic pocket or the inner cores of the micelles. Thus, opportunities for competitive hydrolysis by water are absent due to this “reservoir” effect.²⁰

Both saturated and unsaturated aliphatic and aromatic alcohols and carboxylic acids **3-19** were well tolerated. The methodology was tolerant towards various functional groups on both the alcohol and the carboxylic acid. Halogen (Cl and Br) containing compounds **9**, **12** and **13**, did not inhibit the enzymatic process. A strained cyclopropane ring containing alcohol also afforded product **13** in moderate yield. Even though the aromatic ketone **14** and heteroaromatic compounds **15-16** were challenging cases due to partial solubilities, modest yields of the derived esters were obtained for these reaction partners. Although the isolated yields differed for each substrate pair, the reactions were clean as no side products were observed.

Scheme 1. Substrate scope: lipase-catalyzed esterification

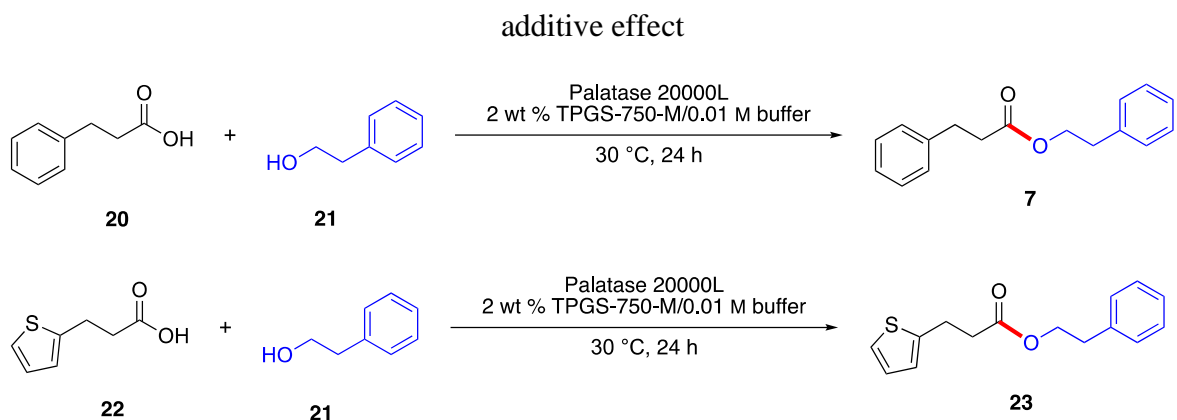


Conditions: carboxylic acid (0.5 mmol; 1 equiv), alcohol (0.5 mmol; 1 equiv), *Rhizomucor miehei* enzyme (25 μ L), 2 wt % TPGS-750-M in 0.01 M phosphate buffer solution (1 mL) at 30 $^\circ$ C for 24 h. Isolated yields reported.

1.2.3. Influence of additive on reactivity of challenging substrates

To enhance the reactivity of challenging heteroaromatic substrates, (i.e., beyond those leading to products **15** and **16**; Scheme 1), the influence of small amounts (1 equiv) of organic additives was investigated. This concept emerged when 3-(thiophen-2-yl)propanoic acid (**22**), the analog of reactive 3-phenylpropionic acid (**20**) (which had successfully led to product **7**, Table 3, entry 1) was examined with 2-phenylethan-1-ol (**21**) leading to complete shutdown (entry 2) under otherwise optimized reaction conditions. Even though both the thiophene and the phenyl analogs have identical distance from the reactive carboxyl site, their contrasting reactivities were surprising. Unexpectedly, when the thiophene acid (**22**) was admixed with either the 3-phenylpropionic acid (**20**) and the same alcohol (**21**), the major ester formed *contained the thiophene subunit*, product **23** (entry 4)!

It is important to note that this phenomenon appears to be unique, since the presence of additive does not inhibit enzymatic activity.^{4, 21} This occurrence is unlikely to be a simple solvent effect seen in previous work where the presence of a co-solvent positively impacted aqueous micellar catalysis, since common solvents like dichloromethane (0% yield), hexanes (25% yield), cyclohexane (29% yield) and toluene (50% yield) were comparatively less effective.²²

Table 3. Enhancement of reactivity in the presence of two substrates: emergence of the

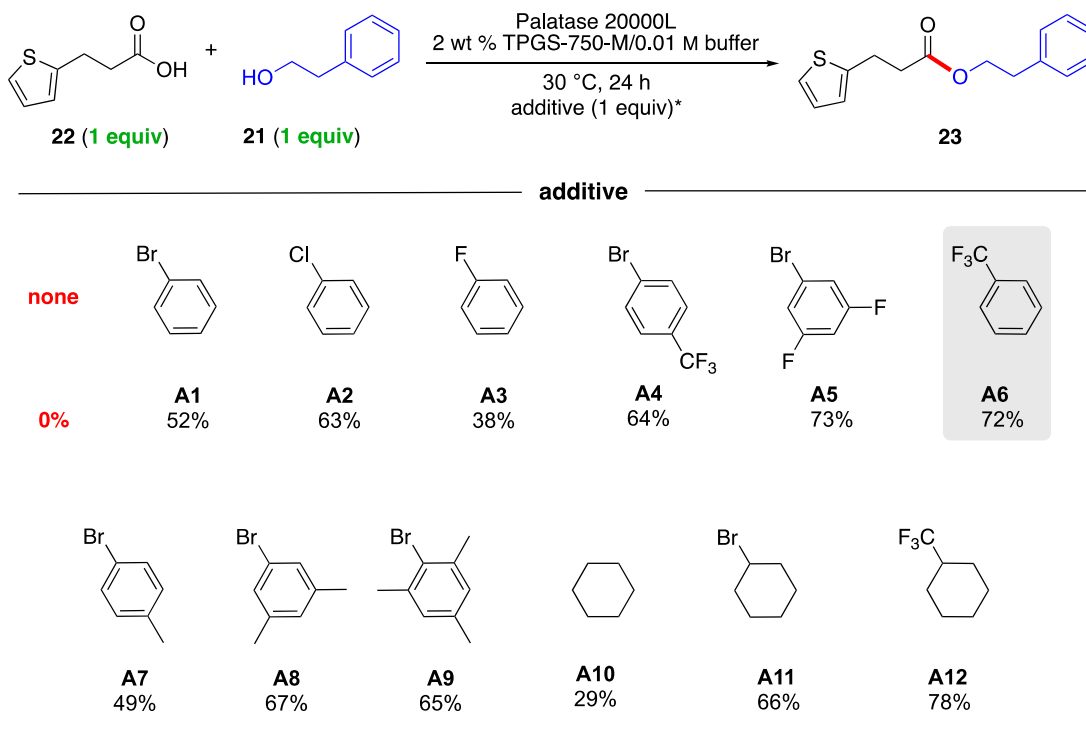
entry	equiv of 20	equiv of 22	conv of 7 (%)	conv of 23 (%)
1	1	-	76	-
2	-	1	-	0
3	1	1	0	trace
4	0.5	0.5	30	30

Conversion determined by crude ^1H NMR.

As seen in Figure 7, amongst monosubstituted aryl halides, chlorobenzene **A2** provided the highest yield. However, it was not pursued further to abide by the principles of green chemistry and eliminate the use of toxic chlorinated reagents. The reaction yield was further improved in the presence of electron-deficient aromatic rings **A5** and **A6**, affording ester **23** in 73% and 72% yields, respectively. More lipophilic aryl halide additives, **A7** - **A9** were not as effective. Use of compounds **A10** - **A12** proved that the π -conjugation is not contributing to the additive effect found in this enzymatic reaction. Among the additives

investigated, trifluoromethylbenzene (**A6**) was selected given its effectiveness, commercial availability, non-chlorinated status, and attractive economics.

Figure 7: Screening the effect of additives on an esterification reaction



*1 equiv relative to acid/alcohol

To optimize the effect on this esterification process catalyzed by the lipase derived from *Rhizomucor miehei*,²³ various equivalents of the additive were tested. The highest yield was observed with one equivalent of additive with respect to the acid and alcohol (Table 4, entry 3). Half the quantity (entry 2) or double the quantity (entry 4) of PhCF₃ led to decreases in yield. In the absence of the additive (entry 1) or in the absence of the surfactant (entry 5), no ester product formation was observed. Upon inverting the combination of acid and alcohol

partners to yield ester **24** (Figure 8), a similar additive effect was observed wherein there was no conversion in the absence of an additive but 50% isolated yield of the product was obtained in the presence of one equivalent of PhCF₃.

Table 4. Impact of reaction variables by the additive

entry	solvent ^[a]	additive (equiv.)	yield of 23 (%) ^[b]
1	2 wt % TPGS-750-M/0.01 M buffer	-	0
2	2 wt % TPGS-750-M/0.01 M buffer	PhCF ₃ (0.5)	14
3	2 wt % TPGS-750-M/0.01 M buffer	PhCF₃ (1)	72
4	2 wt % TPGS-750-M/0.01 M buffer	PhCF ₃ (2)	57
5	0.01 M buffer (no surfactant)	PhCF ₃ (1)	0

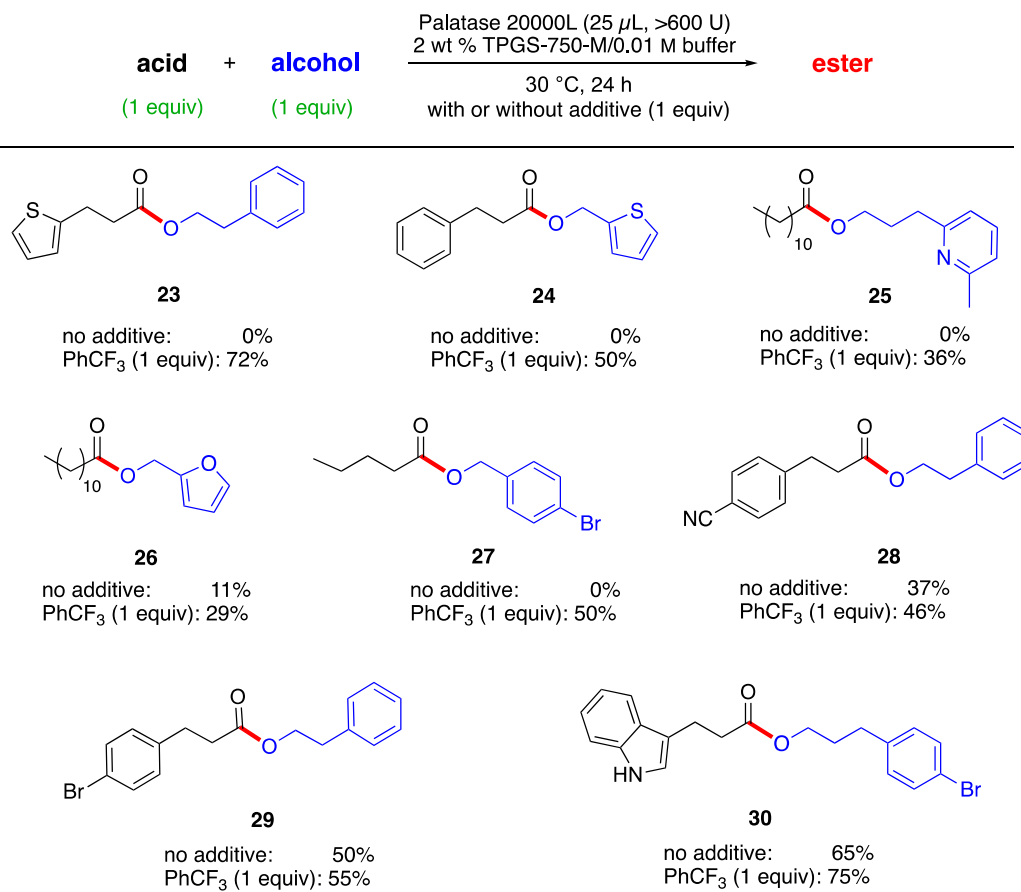
^[a] 1 mL of solvent used for 0.5 M global concentration; ^[b] Isolated.

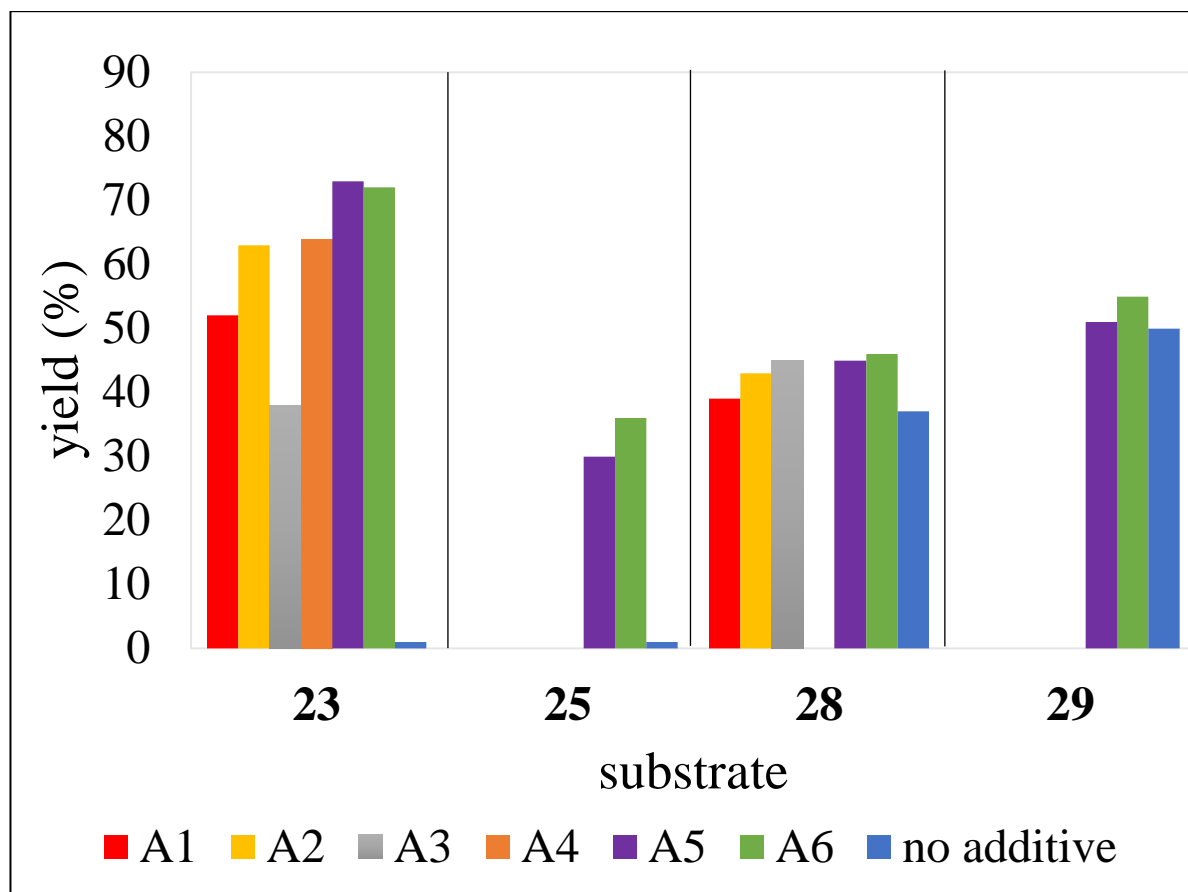
The effect of various additives **A1-A6**, was further investigated on other substrates **23**, **25**, **28**, and **29** (Figure 8). In addition to the initial discovery involving esterification to product **23**, the isolated yield using the additive, PhCF₃, of esters **25** and **27** increased from 0 to 36% and from 0 to 50%, respectively. Even though modest enhancements in yields were observed for some esters, the overall positive trend using this additive is clear.

The influence by PhCF₃ may be due to an allosteric effect that alters the enzymatic cavity.²⁴ Another explanation for this phenomenon could be adaptation of the entrance to the enzymatic pocket, adding a variable element of “promiscuity”, thus permitting functionality that was formerly forbidden to gain entry to the enzymatic cavity. Alternatively, this additive

may be providing a hydrophobic layer that enhances lid opening to the enzymatic pocket. A more definitive analysis as to which role is operative awaits further scrutiny.

Figure 8: Impact of various additives on lipase-catalyzed esterification reactions



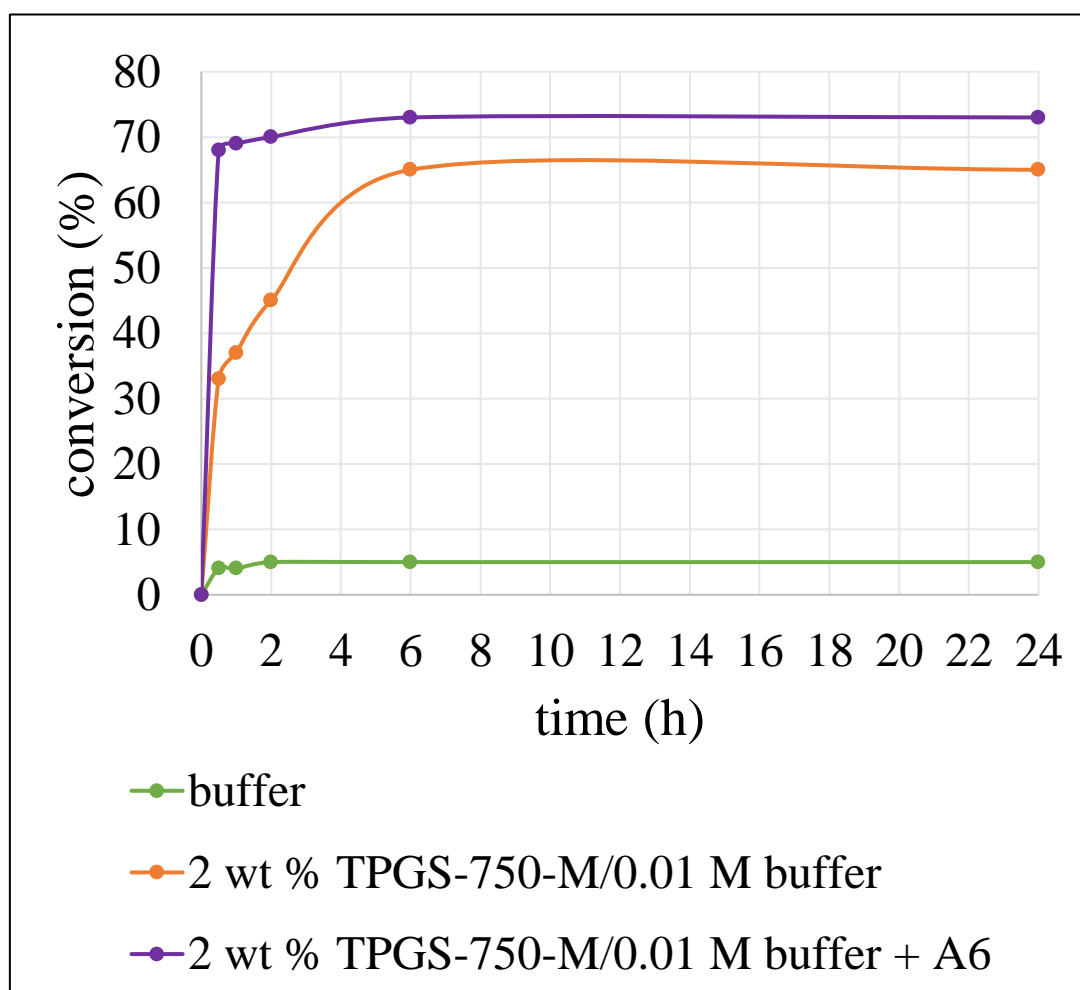
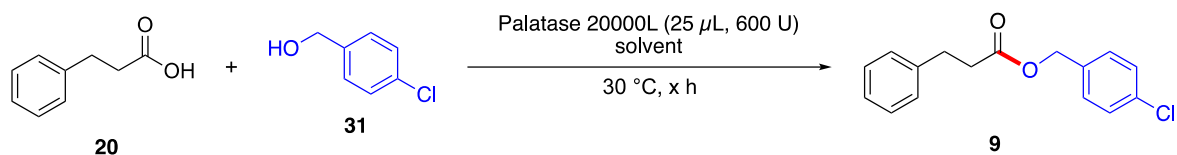


1.2.4. “Reservoir effect” caused by aqueous micellar system

The individual contributions of the surfactant and additive were evaluated based on the “reservoir effect” first detected in alcohol dehydrogenase.²⁰ For lipase-catalyzed esterifications, this phenomenon was observed in the reaction between 3-phenylpropanoic acid (**20**) and (4-chlorophenyl)methanol (**31**) to obtain product **9** (Figure 9). While the esterification in aqueous buffer only did not exceed 5% after a 24-hour period, the designer surfactant TPGS-750-M increased the level of conversion to 65%. The same reaction was

enhanced in the presence of additive PhCF₃ (**A6**) raising the conversion level to 73%, although the rate of increase was dramatic, reaching 70% after only two hours.

Figure 9: Impact of surfactant and additive on reaction between acid, **20** and alcohol, **31**

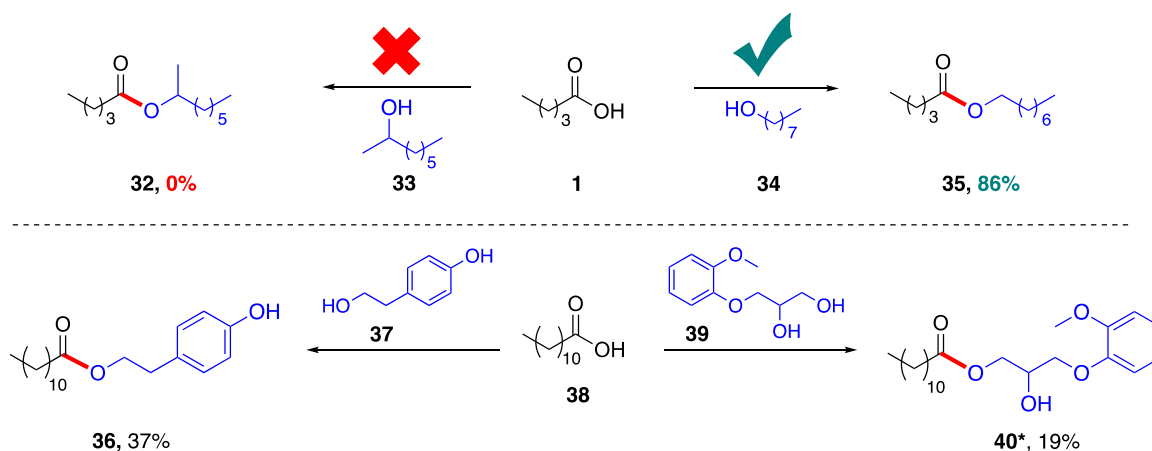


1.2.5. Chemoselectivity of these bio-catalytic reactions

The same lipase (*Rhizomucor miehei*) was also found to exclusively react with primary alcohols while secondary alcohols remained unperturbed. The selective catalysis to esters was tested with the primary alcohol, 1-octanol (**34**) and secondary alcohol, 2-octanol (**33**); valeric acid (**1**) only reacted with the former (Scheme 2) yielding ester **35** (86% yield), while no ester (**32**) formation was observed with the latter.

This exclusive reactivity also prevails when the alcohol functional groups are present within the same molecule. Irrespective of the alcohol's position on a sp^2 carbon (phenol, **37**) or a sp^3 carbon (secondary alcohol, **39**), the primary alcohol is esterified selectively. The same results favoring esterification of a primary alcohol is observed in the presence of the additive, $PhCF_3$.

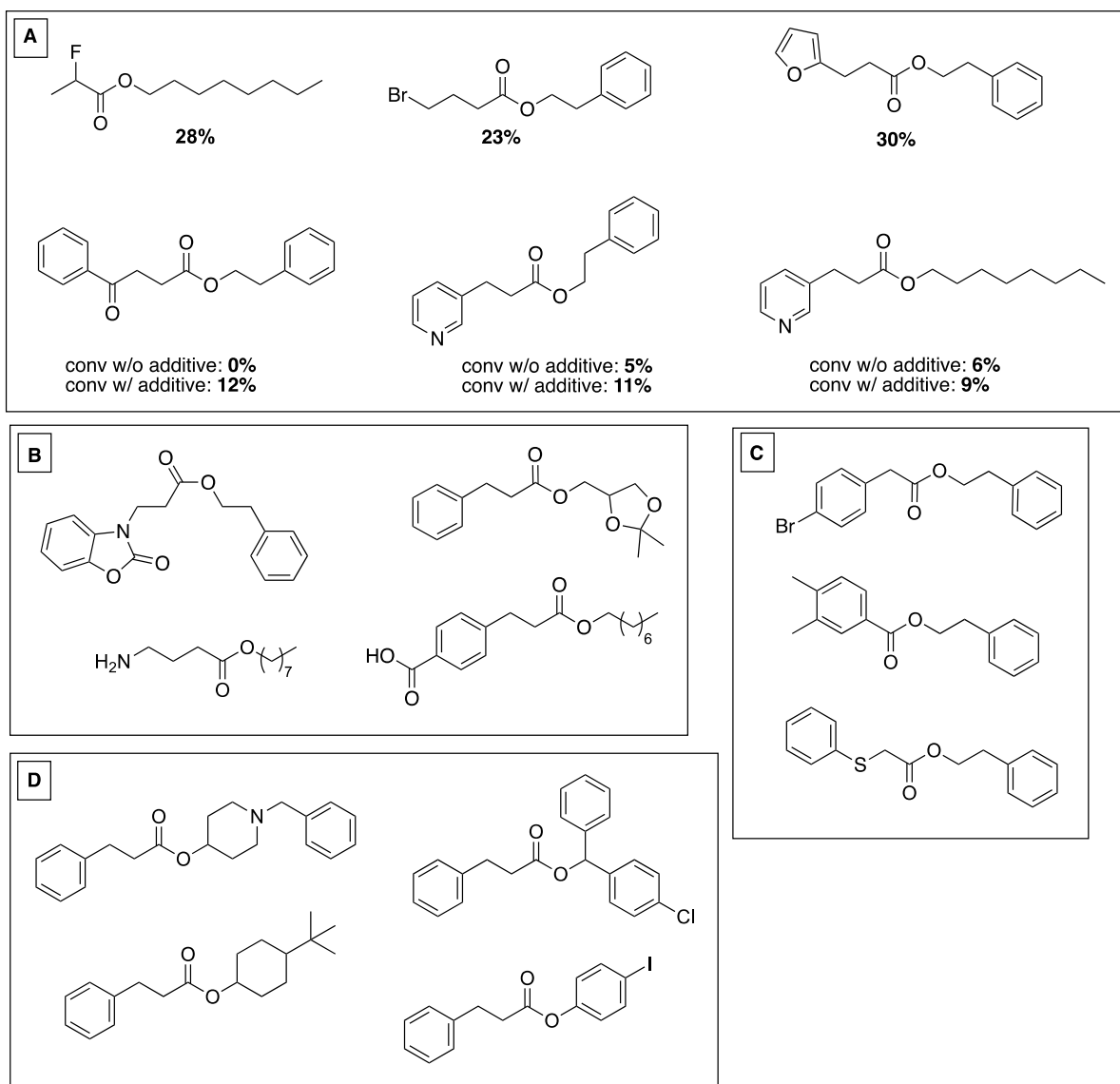
Scheme 2. Selective esterification of a primary alcohols catalyzed by lipase



Conditions: *Rhizomucor miehei* enzyme (25 μ L), 2 wt % TPGS-750-M/0.01 M buffer solution (1 mL) at 30 $^{\circ}$ C for 24 h. Only one product observed. Isolated yields reported. *Trace conversion in the absence of $PhCF_3$.

Even though the bio-catalytic process has a multitude of benefits, the process has a few shortcomings. Figure 10 represents some of the limitations of the lipase-catalyzed esterification process, providing a list of failed substrates. Figure 10A, demonstrates potential esters with challenging carboxylic acid partners that undergo low to no conversion. Heteroaromatics such as pyridine and furan rings are not very well tolerated. The use of additive was not beneficial as its presence did not enhance reaction conversions. Figure 10B illustrates examples of incompatible functional groups on both the alcohol and carboxylic acid components. Figure 10C indicates that the acid component requires two methylene residues between the carboxylic acid functionality and the rest of the molecules. Benzoic acids or phenylacetic acid analogs were not suitable for the reaction. Figure 10D confirms that a secondary alcohol functionality on a sp^2 carbon or a sp^3 carbon remains unreactive to the esterification process.

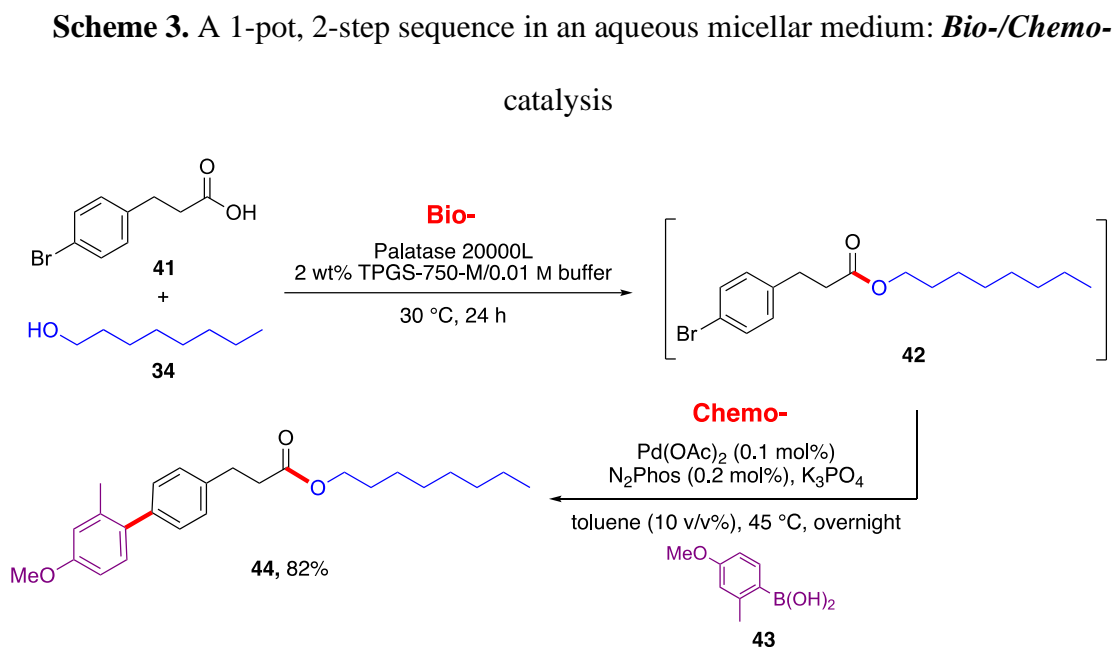
Figure 10: Esters that failed to form in the presence of lipase



1.2.6. Tandem, 1-pot, chemo- and bio-catalysis

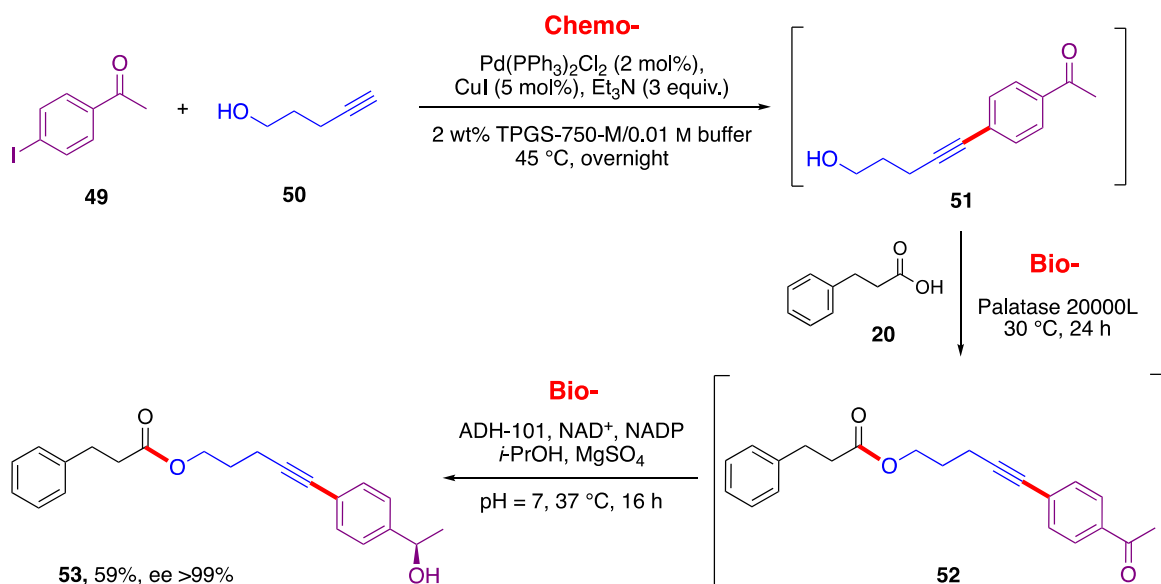
With water being the common denominator for chemo- and bio-catalysis, essentially unlimited opportunities arise to combine both in tandem 1-pot sequences, thereby not only minimizing workups, waste creation, and time invested (“time economy”),²⁵ but also handling (“pot economy”).²⁶ While maintaining the global concentration, the sequence of reactions is not affected by the order in which chemo- or bio-catalysis is performed.

An example of bio- followed by chemo-catalysis is shown in Scheme 3. Lipase-catalyzed esterification led to product **42** which was not isolated and was subsequently used as a precursor to a ppm Pd-catalyzed Suzuki-Miyaura coupling to afford final product **44** in 82% overall yield.²⁷ It is important to note the lack of hydrolysis of the intermediate ester after the increase of pH with addition of base.



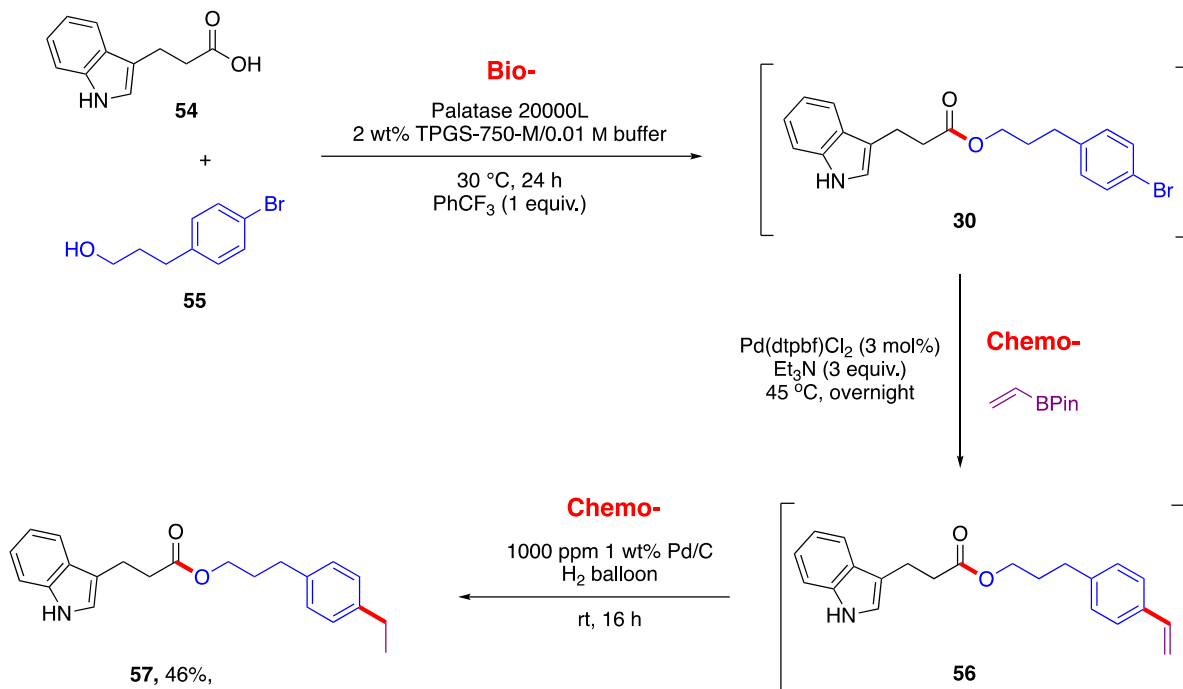
within this intermediate was reduced with KRED (ADH-101)²⁰ to provide secondary alcohol **53** in 59% overall yield, with high enantiomeric excess (ee >99%).

Scheme 5. A 1-pot, 3-step sequence in an aqueous micellar medium: *Chemo-/Bio-/Bio-* catalysis



To expand the tandem 1-pot process to more complex molecules, carboxylic acid containing indole (**54**) was studied without its N-H protection (Scheme 6). An initial lipase-catalyzed esterification, which benefited from the presence of the additive, PhCF₃, preceded two consecutive chemocatalytic steps: a Pd-catalyzed Suzuki-Miyaura vinylation²⁸ to **56** followed by olefin reduction to arrive at **57** in 46% overall yield.

Scheme 6. A 1-pot, 3-step sequence in an aqueous micellar medium: *Bio-/Chemo-
/Chemo-catalysis*



1.3. Conclusion

A methodology for esterification reaction catalyzed by a commercially available and economically attractive lipase, all performed “in water” has been developed, requiring no extra starting materials in an ideal 1 : 1 ratio of acid and alcohol. The lipase also showcases chemo-selective esterification of primary alcohols. The presence of the nanomicelles derived from TPGS-750-M, in the aqueous medium is not only tolerated by the enzymatic process but also enhances the reaction conversion and discourages the competitive reversible hydrolysis. An unusual and unexpected additive, PhCF₃, has been found to broaden the substrate scope and further advances the reaction conversion with only one equivalent relative to substrate. Unprecedented 1-pot sequences have been described that demonstrate that chemo- and bio-catalysis can be performed in various combinations in the same reaction medium (2 wt % TPGS-750-M / H₂O), making this approach environmentally friendly, as well as synthetically attractive in terms of time and pot economy.

1.4. References

- 1) Kapoor, M.; Gupta, M. N. Lipase Promiscuity and its Biochemical Applications. *Process Biochem.* **2012**, *47*, 555-569.
- 2) Pleiss, J.; Fischer, M. Schmid R. D. Anatomy of Lipase Binding Sites: the Scissile Fatty Acid Binding Site. *Chem. Phys. Lipids* **1998**, *93*, 67-80.
- 3) a) Rodrigues, R. C.; Fernandez-Lafuente, R. Lipase from *Rhizomucor miehei* as an industrial biocatalyst in chemical process. *J. Mol. Catal. B Enzym.* **2010**, *64*, 1-22. b) Khan, F. I.; Lan, D.; Durrani, R.; Huan, W.; Zhao, Z.; Wang, Y. The Lid Domain in Lipases: Structural and Functional Determinant of Enzymatic Properties. *Front. Bioeng. Biotechnol.* **2017**, *5*. c) Brzozowski, A. M.; Derewendat, U.; Derewendat, Z. S.; Lawson, D. M. Turkenburg, J. P.; Bjorkling, F.; Hüge-Jensen, B.; Patkar, S. A.; Thim, L. A Model for Interfacial Activation in Lipases from the Structure of a Fungal Lipase-Inhibitor Complex. *Nature.* **1991**, *351*, 491-494. d) Roussel, A.; Amara, S.; Nyssölä, A.; Mateos-Diaz, E.; Blangy, S.; Kontkanen, H.; Westerholm-Parvinen, A.; Carrière, F.; Cambillau, C. A Cutinase from *Trichoderma Reesei* with a Lid-Covered Active Site and Kinetic Properties of True Lipases. *J. Mol. Biol.* **2014**, *426*, 3757-3772.
- 4) Tweddell, R. J.; Kermasha, S.; Combes, D.; Marty, A. Esterification and Interesterification Activities of Lipases from *Rhizopus niveus* and *Mucor miehei* in Three Different Types of Organic Media: A Comparative Study. *Enzyme Microb. Technol.* **1998**, *22*, 439-445.
- 5) Otera, J.; Nishikido, J. Esterification: Methods, Reactions, and Applications. Wiley-VCH, New York, **2009**. DOI: [10.1002/9783527627622](https://doi.org/10.1002/9783527627622).
- 6) de Souza, R. O. M. A.; Miranda, L. S. M.; Bornscheuer, U. T. A Retrosynthesis Approach for Biocatalysis in Organic Synthesis. *Chem. Eur. J.* **2017**, *23*, 12040-12063.
- 7) Wu, S.; Snajdrova, R.; Moore, J. C.; Baldenius, K.; Bornscheuer, U. T. Biocatalysis: Enzymatic Synthesis for Industrial Applications. *Angew. Chem., Int. Ed.* **2021**, *60*, 88-119.
- 8) Hammer, S. C.; Knight, A. M.; Arnold, F. H. Design and Evolution of Enzymes for Non-Natural Chemistry. *Curr. Opin. Green Sustain. Chem.* **2017**, *7*, 23-30.
- 9) Arnold, F. H. Directed Evolution: Bringing New Chemistry to Life. *Angew. Chem., Int. Ed.* **2018**, *57*, 4143-4148.
- 10) Sheldon, R. A.; Woodley, J. M. Role of Biocatalysis in Sustainable Chemistry. *Chem. Rev.* **2018**, *118*, 801-838.
- 11) Larsen, M. W.; Zielinska, D. F.; Martinelle, M.; Hidalgo, A.; Jensen, L. J.; Bornscheuer, U. T.; Hult, K. Suppression of Water as a Nucleophile in *Candida Antarctica* Lipase B Catalysis. *Chem. Bio. Chem.* **2010**, *11*, 796-801.
- 12) Gandhi, N. N.; Patil, N. S.; Sawant, S. B.; Joshi, J. B.; Wangikar, P. P.; Mukesh, D. Lipase-Catalyzed Esterification. *Catal. Rev.* **2000**, *42*, 439-480.

- 13) Anastas, P. T.; Warner, J. C. Green Chemistry: Theory and Practice. *Oxford University Press*. **1998**.
- 14) R. A. Sheldon, D. Brady and M. L. Bode, *Chem. Sci.*, **2020**, *11*, 2587–2605.
- 15) Sá, A. G. A.; de Meneses, A. C.; de Araújo, P. H. H. de Oliveira, D. A Review on Enzymatic Synthesis of Aromatic Esters Used as Flavor Ingredients for Food, Cosmetics and Pharmaceuticals Industries. *Trends Food Sci. Technol.* **2017**, *69*, 95–105.
- 16) Karmee, S. K. Biocatalytic Synthesis of Ascorbyl Esters and Their Biotechnological Applications. *Appl. Microbiol. Biotechnol.* **2009**, *81*, 1013–1022.
- 17) a) Müller, J.; Sowa, M. A.; Fredrich, B.; Brundiek, H.; Bornscheuer, U. T. Enhancing the Acyltransferase Activity of *Candida Antarctica* Lipase A by Rational Design. *Chem. Bio. Chem.* **2015**, *16*, 1791–1796. b) Sandstrom, A. G.; Wikmark, Y.; Engstrom, K.; Nyhlen, J.; Backvall, J. E. Combinatorial Reshaping of the *Candida Antarctica* Lipase A Substrate Pocket for Enantioselectivity Using an Extremely Condensed Library. *Proc. Natl. Acad. Sci.* **2012**, *109*, 78–83.
- 18) Mestrom, L.; Claessen, J. G. R.; Hanefeld, U. Enzyme-Catalyzed Synthesis of Esters in Water. *ChemCatChem*, **2019**, *11*, 2004–2010.
- 19) Lipshutz, B. H.; Ghorai, S.; Abela, A. R.; Moser, R.; Nishikata, T.; Duplais, C.; Krasovskiy, A.; Gaston, R. D.; Gadwood, R. C. TPGS-750-M: A Second-Generation Amphiphile for Metal-Catalyzed Cross-Couplings in Water at Room Temperature. *J. Org. Chem.* **2011**, *76*, 4379–4391.
- 20) Cortes-Clerget, M.; Akporji, N.; Zhou, J.; Gao, F.; Guo, P.; Parmentier, M.; Gallou, F.; Berthon, J.-Y.; Lipshutz, B. H. Bridging the Gap between Transition Metal- and Bio-Catalysis via Aqueous Micellar Catalysis. *Nat. Commun.* **2019**, *10*, 2169.
- 21) Fevrier, P.; Guégan, P.; Yvergnaux, F.; Callegari, J. P.; Dufossé, L.; Binet, A. Evaluation of Regioselectivity of Lipases Based on Synthesis Reaction Conducted with Propyl Alcohol, Isopropyl Alcohol and Propylene Glycol. *J. Mol. Catal. B Enzym.* **2001**, *11*, 445–453.
- 22) Villo, P.; Dalla-Santa, O.; Szabó, Z.; Lundberg, H. Kinetic Analysis as an Optimization Tool for Catalytic Esterification with a Moisture-Tolerant Zirconium Complex. *J. Org. Chem.* **2020**, *85*, 6959–6969.
- 23) (a) Cuendet, M. A., Weinstein, H.; LeVine, M. V. The Allosteric Landscape: Quantifying Thermodynamic Couplings in Biomolecular Systems. *J. Chem. Theory Comp.* **2016**, *12*, 5758–5767. (b) Koshland, D. E.; Némethy, G.; Filmer, D. Comparison of Experimental Binding Data and Theoretical Models in Proteins Containing Subunits. *Biochem.* **1966**, *5*, 365–385. (c) Jacque, M.; Wyman, J.; Changeux, J. On the Nature of Allosteric Transitions: A Plausible Model. *J. Mol. Biol.* **1965**, *12*, 88–118.
- 24) The additive, PhCF₃, was not nearly as effective upon evaluation in the presence of other lipases used in this study (*Candida rugosa*, *Rhizopus niveus*, and *Burkholderia cepacian*).
- 25) Hayashi, Y. Time economy in Total Synthesis. *J. Org. Chem.* **2021**, *86*, 1–23.

- 26) Hayashi, Y. Pot Economy and one-pot synthesis. *Chem. Sci.* **2016**, *7*, 866.
- 27) Akporji, N.; Thakore, R. R.; Cortes-Clerget, M.; Andersen, J.; Landstrom, E.; Aue, D. H.; Gallou, F.; Lipshutz, B. H. N₂Phos – an Easily Made, Highly Effective Ligand Designed for Ppm Level Pd-Catalyzed Suzuki–Miyaura Cross Couplings in Water. *Chem. Sci.* **2020**, *11*, 5205–5212.
- 28) Takale, B. S.; Thakore, R. R.; Gao, E. S.; Gallou, F.; Lipshutz, B. H. Environmentally responsible, safe, and chemoselective catalytic hydrogenation of olefins: ppm level Pd catalysis in recyclable water at room temperature. *Green Chem.* **2020**, *22*, 6055-6061.
- 29) Wood, A. B.; Cortes-Clerget, M.; Kincaid, J. R. A.; Akkachairin, B.; Singhanian, V.; Gallou, F.; and Lipshutz, B.H. Nickel Nanoparticle Catalyzed Mono- and Di-Reductions of Gem-Dibromocyclopropanes Under Mild, Aqueous Micellar Conditions. *Angew. Chem., Int. Ed.* **2020**, *7*.
- 30) Chinchilla, R.; Najera, C. Recent Advances in Sonogashira Reactions. *Chem. Soc. Rev.* **2011**, *40*, 5084-5121.
- 31) National Research Council (US) Chemical Sciences Roundtable. The Role of the Chemical Sciences in Finding Alternatives to Critical Resources: A Workshop Summary. Washington (DC): National Academies Press (US); 2012. *4*, Replacing Critical Materials with Abundant Materials.
- 32) We have no experimental proof at this time as to why enzymatic denaturation has yet to be seen independent of the amounts and nature of the metals present in the medium. Nonetheless, we suggest that the explanation may be attributed to the likelihood that the catalysts are predominantly localized in and around the micellar array; hence, as far as the enzyme is concerned, it may not be exposed to the high levels of potentially denaturing metals present, which is a textbook phenomenon.

1.5. Experimental information

1.5.1. General Information

Palatase 20000L (originating from *Rhizomucor miehei*) was purchased from Strem Chemicals Inc. (cat. no. 06-3118).

https://www.strem.com/catalog/v/06-3118/101/biocatalysts_9001-62-1

Lipozyme ® RM was purchased from Strem Chemicals Inc. (cat. no. 06-3120).

https://www.strem.com/catalog/v3/06-3120/101/biocatalysts_9001-62-1

Amano Lipase PS was purchased from Aldrich (cat. no. 534641).

<https://www.sigmaaldrich.com/US/en/product/aldrich/534641>

Lipase from *Candida rugosa* was purchased from Sigma (cat. no. L1754).

<https://www.sigmaaldrich.com/US/en/product/sigma/l1754>

Lipase from *Rhizopus niveus* was purchased from Sigma (cat. no. 62310).

<https://www.sigmaaldrich.com/US/en/product/sigma/62310>

ADH101, 1, 2, 3, ADH1054 ADH1105 and ADH1126, 7 are commercially available from the enzyme kit EZK-001 from Johnson Matthey. TPGS-750-M is available from Sigma-Aldrich (catalog #733857 (solution) or #763896 (wax)) or can be prepared following the reported procedure.¹ Potassium phosphate monobasic and dibasic were purchased from Sigma

¹ Lipshutz, B. H.; Ghorai, S.; Abela, A. R.; Moser, R.; Nishikata, T.; Duplais, C.; Krasovskiy, A.; Gaston, R. D.; Gadwood, R. C. TPGS-750-M: A Second-Generation Amphiphile for Metal-Catalyzed Cross-Couplings in Water at Room Temperature. *J. Org. Chem.* **2011**, 76, 4379–4391.

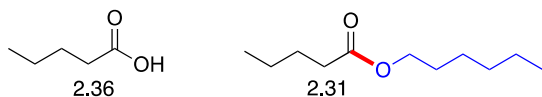
Aldrich. All commercially available reagents were used without further purification. Thin layer chromatography (TLC) was done using Silica Gel 60 F254 plates (Merck, 0.25 mm thick). Flash chromatography was done in glass columns using Silica Gel 60 (EMD, 40-63 μm). ^1H and ^{13}C NMR were recorded at 25 $^\circ\text{C}$ either on a Varian Unity Inova 400 MHz, a Varian Unity Inova 500 MHz or on a Varian Unity Inova 600 MHz spectrometers in CDCl_3 with residual CHCl_3 ($^1\text{H} = 7.27$ ppm, $^{13}\text{C} = 77.16$ ppm) as internal standard. Chemical shifts are reported in parts per million (ppm). Data are reported as follows: chemical shift, multiplicity (s = singlet, d = doublet, t = triplet, q = quartet, quin = quintet, m = multiplet), coupling constant (if applicable) and integration. Chiral HPLC data was collected using an Agilent 1220 HPLC. HRMS data were recorded on a Waters Micromass LCT TOF ES+ Premier mass spectrometer using ESI ionization.

1.5.2. Preparation of the buffer solution

Aqueous 1 M stock solutions of potassium phosphate monobasic (A) and potassium phosphate dibasic (B) were prepared. A pH=7 phosphate buffer solution was then prepared by mixing 38.5 mL of solution A with 61.5 mL of solution B. The pH was controlled and adjusted, if needed, with a 1 M solution of NaOH or HCl. The buffer solution was diluted with HPLC grade water (to 0.01 M, 0.05 M, 0.2 M or 0.4 M). 2 wt % of TPGS-750-M, as a wax, was dissolved and used as media of the reaction. 1, 4 and 6 wt % of TPGS-750-M in the buffer solution have also been prepared.

1.5.3. Conversion measurement

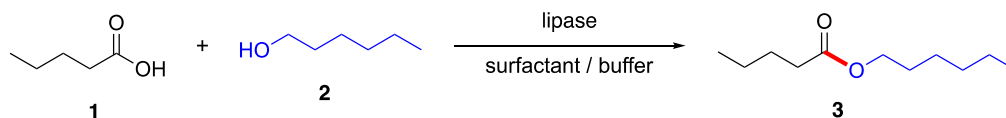
From the general procedure, the crude material was analyzed by ^1H NMR. The ratio between the triplet at 2.36 ppm (acid) and the triplet at 2.31 ppm (ester) was calculated to determine the conversion of the reaction.



1.6. Experimental procedure

1.6.1. General approach to optimization of esterification reactions

The evaluation of the impact of various parameters has been set up on the esterification between valeric acid and hexanol.



All the reactions have been set up on a 0.5 mmol scale. The source of the enzyme, acid/alcohol ratio, the concentration regarding the limiting starting material, the buffer concentration, the temperature and the TPGS-750-M amount have been evaluated.²

To a 1 dr vial was added, in succession valeric acid (54 μL , 0.5 mmol, 1 equiv.), *n*-hexanol (63-314 μL 0.5-2.5 mmol, 1-5 equiv) and 1 mL of 1-6 wt % TPGS-750-M/buffer [0.01-0.4

² Cortes-Clerget, M.; Akporji, N.; Zhou, J.; Gao, F.; Guo, P.; Parmentier, M.; Gallou, F.; Berthon, J.-Y.; Lipshutz, B. H. Bridging the Gap between Transition Metal- and Bio-Catalysis via Aqueous Micellar Catalysis. *Nat. Comm.* **2019**, *10*, 2169.

M]. The lipase (25 μ L; 600 U – enzyme activity is 20000 lipase units per gram) was added and the reaction was stirred at the defined temperature (22-50 ° C) for 24 h. After completion, the pH of the reaction was lowered to 1-2 with a 1 M HCl solution. The product and remaining starting materials were extracted with 2 x 1 mL of EtOAc. The organic layer was dried with anhydrous MgSO₄ and concentrated *in vacuo*.

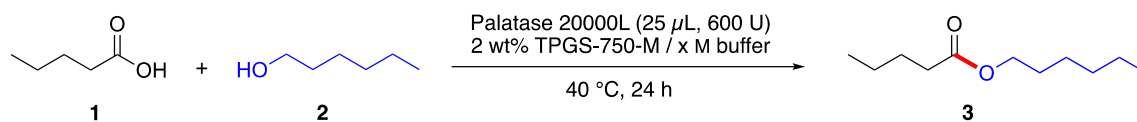
1.6.2. Optimized procedure for esterification reactions

To a 1 dr vial was added, in succession the carboxylic acid (0.5 mmol, 1 equiv.), the alcohol (0.5 mmol, 1 equiv.) and 1 mL of 2 wt % TPGS-750-M/buffer [0.01 M]. The lipase (600 U) was added and the reaction was stirred at the defined temperature (30 ° C) for 24 h. After completion, the reaction was extracted with 2 x 1 mL of EtOAc. The organic layer was dried with anhydrous MgSO₄, filtered through a pad of silica to remove residual surfactant and concentrated *in vacuo*.

1.6.3. General procedure for esterification using the additive PhCF₃

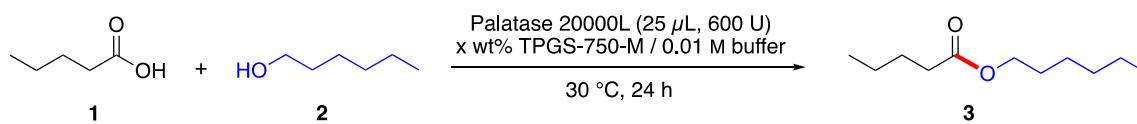
To a 1 dr vial containing a stir bar the carboxylic acid (0.5 mmol, 1 equiv.), the alcohol (0.5 mmol, 1 equiv.) and 1 mL of 2 wt % TPGS-750-M/buffer [0.01 M] was added in that order. The additive was added (0.5 mmol, 1 equiv) followed by the lipase (600 U) and the reaction was stirred at the defined temperature (30 ° C). After 24 h, the reaction was extracted with 2 x 1 mL of EtOAc. The organic layer was dried with anhydrous MgSO₄, filtered through a pad of silica to remove residual surfactant and concentrated *in vacuo*.

1.6.4. Buffer concentration study



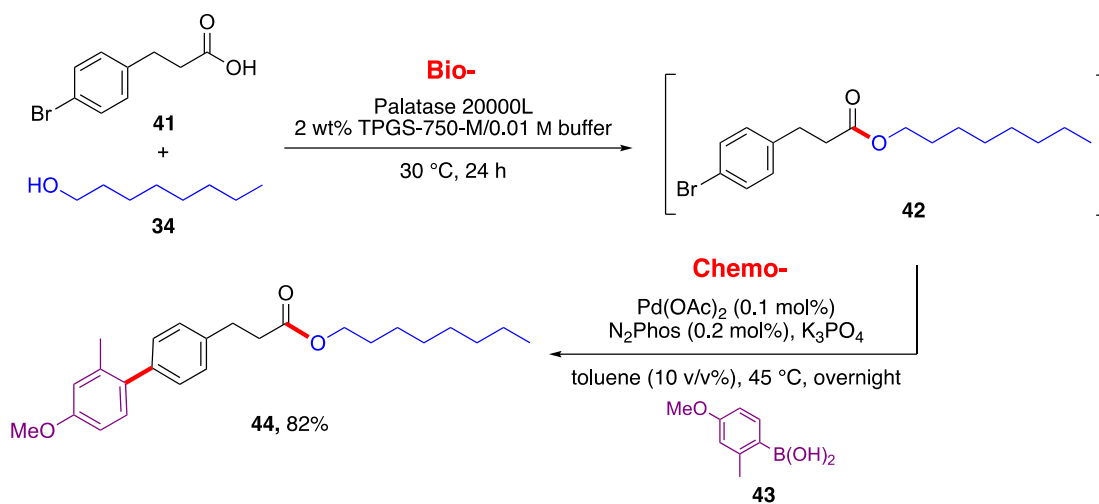
To evaluate the impact of the buffer concentration on the conversion of the ester, **3**, various concentrations of buffer were studied. To a 1 dr vial was added, in succession the carboxylic acid (0.5 mmol, 1 equiv), the alcohol (0.5 mmol, 1 equiv) and 1 mL of 2 wt % TPGS-750-M/buffer [0-0.4 M]. The lipase (600 U) was added and the reaction was stirred at the defined temperature (30 °C) for 24 h. After completion, the reaction was extracted with 2 x 1 mL of EtOAc. The organic layer was dried with anhydrous MgSO₄, filtered through a pad of silica to remove residual surfactant and concentrated *in vacuo*. The samples were analyzed by ¹H NMR to determine the conversion.

1.6.5. Surfactant concentration study



To evaluate the impact of the surfactant concentration on the conversion of reaction between **1** and **2**, various concentrations were studied. To a 1 dr vial was added, in succession the carboxylic acid (0.5 mmol, 1 equiv), the alcohol (0.5 mmol, 1 equiv.) and 1 mL of 0-6 wt % TPGS-750-M/buffer [0.01 M]. The lipase (600 U) was added and the reaction was stirred at the defined temperature (30 °C) for 24 h. After completion, the reaction was extracted with 2 x 1 mL of EtOAc. The organic layer was dried with anhydrous MgSO₄, filtered through a pad of silica to remove residual surfactant and concentrated *in vacuo*. The samples were analyzed by ¹H NMR to determine the conversion.

1.6.6. 2-step, 1-pot: esterification, Suzuki-Miyaura cross-coupling

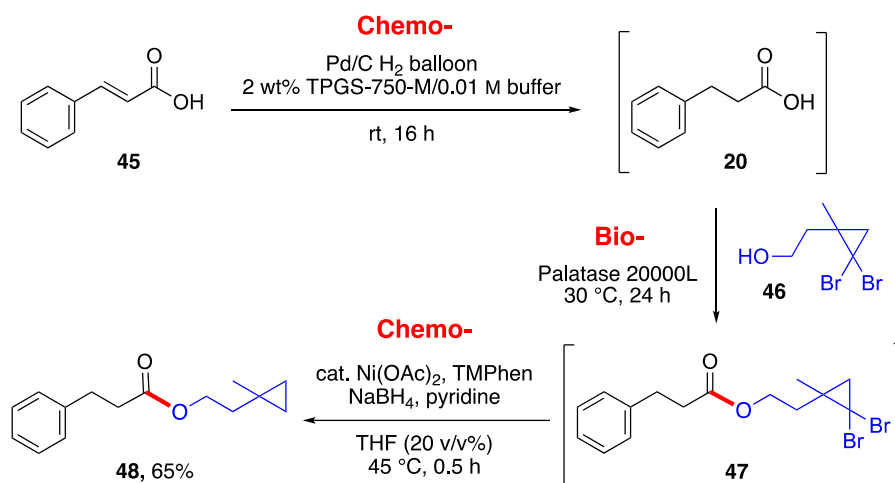


To a 1 dr vial was added 3-(4-bromophenyl)propionic acid (116.9 mg, 0.5 mmol, 1 equiv), octanol (78 μ L, 0.5 mmol, 1 equiv.) and 2 wt % TPGS-750-M/buffer (1 mL [0.5 M]/0.01 M phosphate buffer at pH = 7). Palatase 20000L (25 μ L) was added and the reaction was stirred at 30 °C for 24 h. After completion, 2-methyl-4-methoxyphenyl boronic acid (124.5 mg, 0.75 mmol, 1.5 equiv) was added, followed by K₃PO₄ (159.2 mg, 0.75 mmol, 1.5 equiv). Finally, the catalyst solution* (0.1 mL, 1000 ppm) was added and the reaction was stirred at 45 °C overnight. Upon completion of the reaction, the vial was cooled to rt. The mixture was extracted with ethyl acetate (3 x 3 mL), and the organic layer was washed with brine three times. The layers were then separated and the organic layer was dried over anhydrous MgSO₄. The mixture was concentrated *in vacuo*.

* Catalyst stock solution contains Pd(OAc)₂ (1.1 mg) and N₂Phos (7.6 mg) in toluene (1 mL).³

³ Akporji, N.; Thakore, R. R.; Cortes-Clerget, M.; Andersen, J.; Landstrom, E.; Aue, D. H.; Gallou, F.; Lipshutz, B. H. N₂Phos – an Easily Made, Highly Effective Ligand Designed for Ppm Level Pd-Catalyzed Suzuki–Miyaura Cross Couplings in Water. *Chem. Sci.* **2020**, *11*, 5205–5212.

1.6.7. 3-step, 1-pot sequence: Pd/C reduction, esterification, gem-dibromocyclopropane reduction



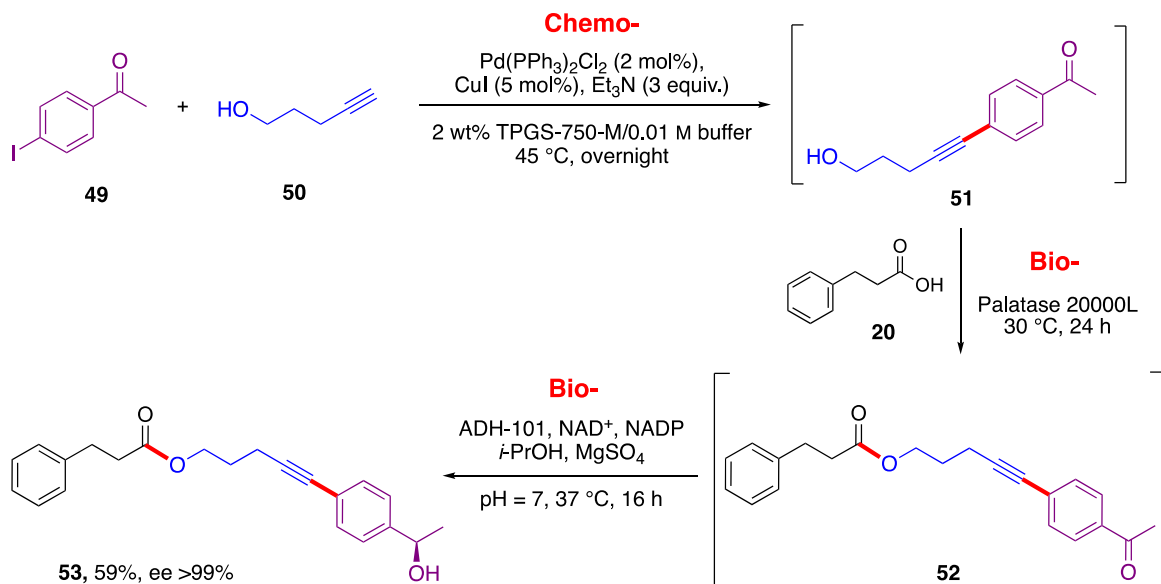
In a 1-dram vial containing equipped with a stir bar, 1 wt % Pd/C (2.6 mg), alkene (74.1 mg, 0.5 mmol, 1 equiv) and 2 wt % TPGS-750-M/buffer (1 mL [0.5 M]/0.01 M phosphate buffer at pH = 7) were added.⁴ The reaction vial was sealed with a septum which was punctured with a needle (18 G) attached with pre-filled balloon of hydrogen gas. The vial was purged with the H₂ and a vent needle for ca. 2 min. The vent needle was removed and another H₂ filled balloon was then attached to the reaction vial. The reaction mixture was stirred at rt or 45 °C. Upon completion, Palatase 20000L (25 μL) was added and the reaction was set to stir for 24 h. Upon completion the intermediate was extracted with MTBE and concentrated *in vacuo*. In a 25 mL round-bottom flask equipped with a stir bar was added

⁴ Takale, B. S.; Thakore, R. R.; Gao, E. S.; Gallou, F.; Lipshutz, B. H. Environmentally responsible, safe, and chemoselective catalytic hydrogenation of olefins: ppm level Pd catalysis in recyclable water at room temperature. *Green Chem.* **2020**, *22*, 6055-6061.

Ni(OAc)₂ (9 mg) under argon. The reaction vial was cooled to 0 °C and 2 wt % TPGS-750-M/H₂O (1.5 mL) was added to the reaction vial and the mixture was set to stir for 10 min. Pyridine (0.1 mL) was added to the reaction vial and the mixture was set to stir for an additional 5 min. NaBH₄ (189.15 mg, 2.5 mmol, 5 equiv) was then added in one portion. The crude reaction material from the previous step was dissolved in THF (300 μL) and added as a solution to the flask through the septum. The vial containing the crude mixture was rinsed with another portion of THF (300 μL, 20 v/v % total). A 12 mL syringe (containing 0.1 mL of THF) was added through the top of the septum to accept evolving hydrogen gas. The reaction was stirred for 30 min at 45 °C. If the volume of gas generated exceeds the volume of the syringe, the syringe must be emptied outside of the flask and adapted again.⁵ After completion, the reaction was dissolved in EtOAc (10 mL) and filtered through a pad of silica. The pad was rinsed with EtOAc (3 x 10 mL). The organic layer was dried over anhydrous MgSO₄, filtered, and concentrated under vacuum. Purification by flash chromatography using hexanes and EtOAc (85:15) was performed to afford the product.

⁵ Wood, A. B.; Cortes-Clerget, M.; Kincaid, J. R. A.; Akkachairin, B.; Singhania, V.; Gallou, F.; and Lipshutz, B.H. Nickel Nanoparticle Catalyzed Mono- and Di-Reductions of Gem-Dibromocyclopropanes Under Mild, Aqueous Micellar Conditions. *Angew. Chem., Int. Ed.* **2020**, *59*, 17587-17593.

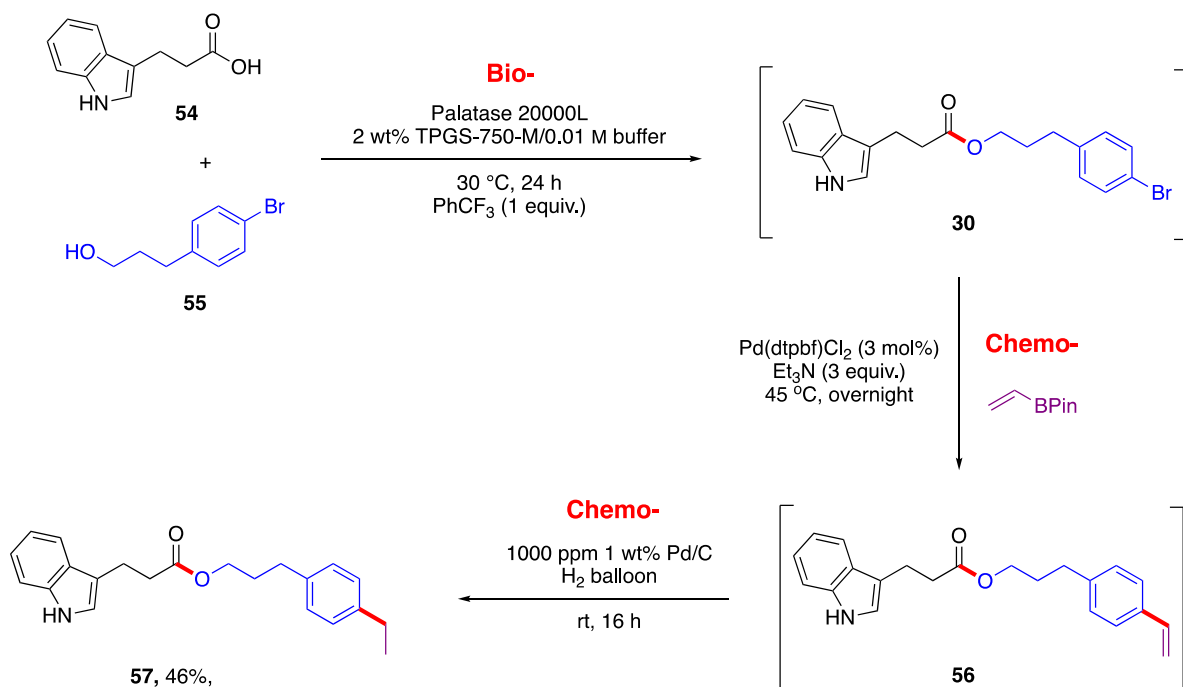
1.6.8. 3-step, 1-pot sequence: Sonogashira cross-coupling reaction, esterification, ADH reduction



To a dried 1-dram vial were added, under an argon atmosphere, $\text{Pd(PPh}_3)_3\text{Cl}_2$ (2.8 mg, 2 mol %), CuI (1.9 mg, 5 mol %), aryl iodide (49.2 mg, 1 equiv, 0.2 mmol), alkyne (27.9 μL , 1 equiv., 0.2 mmol) and Et_3N (84.0 μL , 3 equiv). The vial was capped with a rubber septum. A 2 wt % TPGS-750-M/buffer (0.4 mL [0.5 M]/0.01 M phosphate buffer at pH = 7) was added. The reaction was stirred at 45 °C under argon until completion. The pH was adjusted to 3 with a solution of HCl (1 M) and the mixture became opaque white. Then, 3-phenylpropionic acid (30.0 mg, 1 equiv, 0.2 mmol) and Palatase 20000L (10 μL) were added and the reaction was set to stir at 30 °C for 24 h. The concentration was adjusted to [0.056 M] by adding 2.6 mL of a 2 wt % TPGS-750-M/buffer solution (phosphate, [0.23 M], pH = 7). MgSO_4 (0.8 mg), NAD^+ (2.6 mg), NADP^+ (2.4 mg), $i\text{-PrOH}$ (0.6 mL) and ADH101 (20.0 mg) was added in succession. The reaction was stirred at 37 °C until completion. The reaction was extracted in EtOAc . The organic layer was washed with H_2O , dried over anhydrous MgSO_4 , filtered and

concentrated under vacuum. Purification by flash chromatography using hexanes and EtOAc (85:15) was performed to afford (59%, 40 mg) of the product.

1.6.9. 3-step, 1-pot sequence: esterification, Suzuki cross-coupling reaction, Pd/C reduction

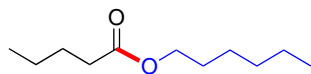


To a 1-dram vial equipped with a stirrer, 3-(4-bromophenyl)propan-1-ol (0.25 mmol, 53.8 mg, 1 equiv), 3-(1H-indol-3-yl), propanoic acid (0.25 mmol, 47.3 mg, 1 equiv) and trifluoromethyl-benzene (0.25 mmol, 36.5 mg, 1 equiv) were added. Followed by 2 wt % TPGS-750-M/buffer (0.5 mL [0.5 M]/0.01 M phosphate buffer at pH = 7). The resulting mixture was allowed to stir to emulsify. Finally, the enzyme was added. The reaction mixture was stirred vigorously at 30 °C for 24 h. To the reaction vial are then added Pd(dtpbf)Cl₂ (0.06 mmol, 4.9 mg, 3 mol %), triethylamine (0.75 mmol, 75.9 mg, 3 equiv) and vinylboronic acid pinacol ester (0.26 mmol, 40.4 mg, 1.05 equiv). The reaction was stirred at 45 °C. Upon

completion (monitored by TLC), the reaction was charged with Pd/C (1 wt % Pd loading; 2.6 mg). The reaction was stirred at rt under a balloon of hydrogen. After the reaction completed (monitored by proton NMR), the reaction was subjected to flash column chromatography to obtain purified product.

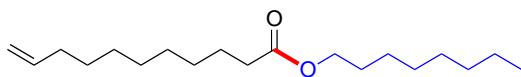
1.7. Characterization (NMR and HRMS)

n-Hexyl pentanoate (**3**)



¹H NMR (500 MHz, CDCl₃) δ 4.06 (t, J = 6.7 Hz, 2H), 2.30 (t, J = 7.6 Hz, 2H), 1.62 (dtt, J = 11.5, 7.7, 3.6 Hz, 4H), 1.41 – 1.23 (m, 8H), 0.98 – 0.85 (m, 6H); **¹³C NMR (126 MHz, CDCl₃)** δ 174.1, 64.5, 34.3, 31.6, 28.8, 27.2, 25.7, 22.7, 22.4, 14.1, 13.8. **Yield:** 84%, 78.2 mg; pale yellow oil. **R_f** = 0.73 (95:5 hexanes/EtOAc). Spectral data matched those previously reported.⁶

n-Octyl undec-10-enoate (**4**)

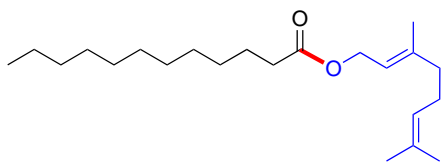


¹H NMR (600 MHz, CDCl₃) δ 5.82 (ddt, J = 16.9, 10.2, 6.7 Hz, 1H), 5.00 (dq, J = 17.1, 1.7 Hz, 1H), 4.94 (ddt, J = 10.2, 2.3, 1.2 Hz, 1H), 4.06 (t, J = 6.7 Hz, 2H), 2.30 (t, J = 7.5 Hz, 2H), 2.08 – 2.01 (m, 2H), 1.67 – 1.59 (m, 4H), 1.43 – 1.22 (m, 20H), 0.89 (t, J = 7.0 Hz, 3H); **¹³C NMR (151 MHz, CDCl₃)** δ 174.2, 139.3, 114.3, 64.6, 34.6, 33.9, 31.9, 29.4, 29.4, 29.3, 29.3, 29.2, 29.0, 28.8, 26.1, 25.2, 22.8, 14.2. **Yield:** 75%, 111.0 mg; colorless oil. **R_f** = 0.53 (90:10 hexanes/EtOAc). Spectral data matched those previously reported.⁷

⁶ Seitz, L. M.; Ram, M. S. Metabolites of Lesser Grain Borer in Grains. *J. Agric. Food Chem.* **2004**, *52*, 898–908.

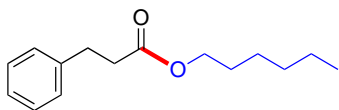
⁷ Stenhagen, E.; Abrahamsson, S.; McLafferty, F. W. (eds.) *Archives of Mass Spectral Data*. Interscience Publishers, New York 1970.

(*E*)-3,7-Dimethylocta-2,6-dien-1-yl dodecanoate (**5**)



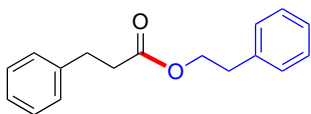
¹H NMR (500 MHz, CDCl₃) δ 5.34 (tt, $J = 7.0, 1.4$ Hz, 1H), 5.09 (tt, $J = 6.9, 1.5$ Hz, 1H), 4.60 (d, $J = 7.1$ Hz, 2H), 2.30 (t, $J = 7.6$ Hz, 2H), 2.15 – 2.08 (m, 2H), 2.05 (dd, $J = 8.7, 6.5$ Hz, 2H), 1.70 (dd, $J = 9.6, 1.4$ Hz, 6H), 1.67 – 1.56 (m, 5H), 1.28 (d, $J = 15.3$ Hz, 17H), 0.89 (t, $J = 6.9$ Hz, 3H); **¹³C NMR (126 MHz, CDCl₃)** δ 174.076, 142.237, 131.951, 123.912, 118.582, 61.313, 39.680, 34.553, 32.057, 29.750, 29.614, 29.480, 29.420, 29.305, 26.454, 25.817, 25.171, 22.830, 17.824, 16.606, 14.253. **Yield:** 77%, 133.1 mg; colorless oil. **R_f** = 0.61 (95:5 hexanes/EtOAc). **Chemical Formula:** HRMS (ESI) m/z : [M+Na]⁺ calcd. for C₂₂H₄₀O₂Na 359.2926; found 359.2928.

n-Hexyl 3-phenylpropanoate (**6**)



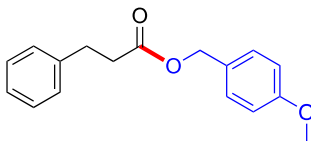
¹H NMR (600 MHz, CDCl₃) δ 7.31 – 7.26 (m, 2H), 7.23 – 7.18 (m, 3H), 4.06 (t, $J = 6.7$ Hz, 2H), 2.95 (t, $J = 7.8$ Hz, 2H), 2.65 – 2.61 (m, 2H), 1.62 – 1.56 (m, 2H), 1.35 – 1.22 (m, 6H), 0.89 (t, $J = 6.9$ Hz, 3H); **¹³C NMR (126 MHz, CDCl₃)** δ 173.0, 140.6, 128.5, 128.3, 126.2, 64.6, 35.9, 31.4, 31.0, 28.6, 25.5, 22.5, 14.0. **Yield:** 72%, 84.2 mg; colorless oil. **R_f** = 0.46 (90:10 hexanes/EtOAc). **Chemical Formula:** HRMS (CI) m/z : [M+H]⁺ calcd. for C₁₅H₂₃O₂ 235.1698; found 235.1694.

Phenethyl 3-phenylpropanoate (**7**)



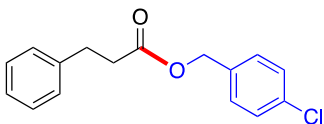
¹H NMR (600 MHz, CDCl₃) δ 7.31 – 7.25 (m, 4H), 7.25 – 7.15 (m, 6H), 4.29 (t, *J* = 7.1 Hz, 2H), 2.94 – 2.88 (m, 4H), 2.61 (t, *J* = 7.8 Hz, 2H); **¹³C NMR (126 MHz, CDCl₃)** δ 172.7, 140.4, 137.7, 128.8, 128.4, 128.2, 126.5, 126.2, 64.9, 35.8, 35.0, 30.8. **Yield:** 76%, 95.0 mg; colorless oil. **R_f** = 0.50 (90:10 hexanes/EtOAc). **Chemical Formula:** HRMS (ESI) *m/z*: [M+Na]⁺ calcd. for C₁₇H₁₈O₂Na 277.1205; found 277.1204.

4-Methoxybenzyl 3-phenylpropanoate (**8**)



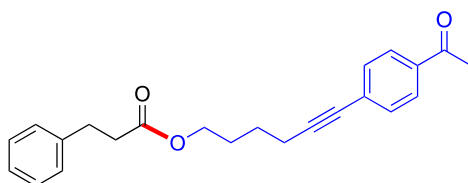
¹H NMR (500 MHz, CDCl₃) δ 7.31 – 7.25 (m, 4H), 7.24 – 7.17 (m, 3H), 6.92 – 6.87 (m, 2H), 5.06 (s, 2H), 3.83 (s, 3H), 2.97 (t, *J* = 7.8 Hz, 2H), 2.67 (dd, *J* = 8.4, 7.2 Hz, 2H); **¹³C NMR (126 MHz, CDCl₃)** δ 172.7, 159.6, 140.4, 130.0, 128.4, 128.3, 128.0, 126.2, 113.9, 66.1, 55.2, 35.9, 30.9. **Yield:** 70%, 95.2 mg; pale yellow oil. **R_f** = 0.49 (80:20 hexanes/EtOAc). **Chemical Formula:** HRMS (CI) *m/z*: [M]⁺ calcd. for C₁₇H₁₈O₃ 270.1256; found 270.1246.

4-Chlorobenzyl 3-phenylpropanoate (**9**)



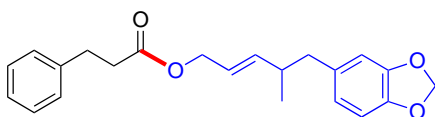
¹H NMR (500 MHz, CDCl₃) δ 7.33 – 7.25 (m, 4H), 7.24 – 7.16 (m, 5H), 5.07 (s, 2H), 2.97 (t, *J* = 7.8 Hz, 2H), 2.69 (dd, *J* = 8.2, 7.2 Hz, 2H); **¹³C NMR (126 MHz, CDCl₃)** δ 172.5, 140.2, 134.4, 134.0, 129.5, 128.7, 128.5, 128.2, 126.3, 65.4, 35.8, 30.9. **Yield:** 60%, 82.9 mg; pale yellow oil. **R_f** = 0.53 (80:20 hexanes/EtOAc). **Chemical Formula:** HRMS (ESI) *m/z*: [M+Na]⁺ calcd. for C₁₆H₁₅ClO₂Na 297.0658; found 297.0663.

6-(4-Acetylphenyl)hex-5-yn-1-yl 3-phenylpropanoate (**10**)



¹H NMR (600 MHz, CDCl₃) δ 7.90 – 7.86 (m, 2H), 7.48 – 7.44 (m, 2H), 7.31 – 7.27 (m, 2H), 7.22 – 7.18 (m, 3H), 4.13 (t, *J* = 6.5 Hz, 2H), 2.96 (t, *J* = 7.8 Hz, 2H), 2.64 (dd, *J* = 8.3, 7.3 Hz, 2H), 2.59 (s, 3H), 2.45 (t, *J* = 7.0 Hz, 2H), 1.82 – 1.75 (m, 2H), 1.67 – 1.61 (m, 2H); **¹³C NMR (126 MHz, CDCl₃)** δ 197.3, 172.9, 140.4, 135.7, 131.6, 128.8, 128.4, 128.2, 128.1, 126.2, 93.3, 80.5, 63.9, 35.8, 30.9, 27.8, 26.5, 24.9, 19.1. **Yield:** 74%, 129.3 mg; colorless oil. **R_f** = 0.50 (70:30 hexanes/EtOAc). **Chemical Formula:** HRMS (CI) *m/z*: [M+C₂H₅]⁺ calcd. for C₂₅H₂₉O₃ 377.2117; found 377.2112.

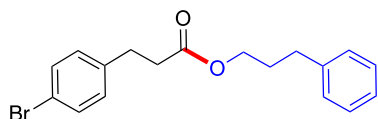
(*E*)-5-(Benzo[d][1,3]dioxol-5-yl)-4-methylpent-2-en-1-yl 3-phenylpropanoate (**11**)



¹H NMR (500 MHz, CDCl₃) δ 7.31 – 7.27 (m, 2H), 7.23 – 7.18 (m, 3H), 6.71 (d, *J* = 7.9 Hz, 1H), 6.62 (d, *J* = 1.7 Hz, 1H), 6.57 (dd, *J* = 7.9, 1.7 Hz, 1H), 5.90 (s, 2H), 5.69 (ddt, *J* = 15.4,

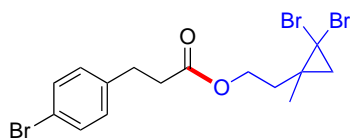
6.8, 1.2 Hz, 1H), 5.46 (dtd, $J = 15.5, 6.5, 1.2$ Hz, 1H), 4.50 (d, $J = 6.4$ Hz, 2H), 2.95 (t, $J = 7.8$ Hz, 2H), 2.64 (dd, $J = 8.5, 7.2$ Hz, 2H), 2.58 (dd, $J = 13.0, 6.4$ Hz, 1H), 2.47 – 2.35 (m, 2H), 0.98 (d, $J = 6.5$ Hz, 3H); ^{13}C NMR (126 MHz, CDCl_3) δ 172.6, 147.3, 145.6, 140.9, 140.5, 134.1, 128.4, 128.3, 126.2, 122.4, 122.0, 109.5, 107.9, 100.7, 65.1, 42.8, 38.2, 35.9, 30.9, 19.2. **Yield:** 81%, 142.1 mg; colorless oil. **R_f** = 0.54 (70:30 hexanes/EtOAc). **Chemical Formula:** HRMS (ESI) m/z : $[\text{M}+\text{Na}]^+$ calcd. for $\text{C}_{22}\text{H}_{24}\text{O}_4\text{Na}$ 375.1572; found 375.1576.

3-Phenylpropyl 3-(4-bromophenyl)propanoate (**12**)



^1H NMR (400 MHz, CDCl_3) δ 7.46 – 7.40 (m, 2H), 7.34 – 7.28 (m, 2H), 7.25 – 7.15 (m, 3H), 7.15 – 7.07 (m, 2H), 4.11 (t, $J = 6.5$ Hz, 2H), 2.93 (t, $J = 7.6$ Hz, 2H), 2.65 (dt, $J = 15.0, 7.5$ Hz, 4H), 2.00 – 1.90 (m, 2H); ^{13}C NMR (101 MHz, CDCl_3) δ 172.63, 141.16, 139.54, 131.61, 130.17, 128.51, 128.44, 126.09, 120.14, 77.48, 77.16, 76.84, 63.97, 35.62, 32.20, 30.39, 30.20. **Yield:** 67%, 116.6 mg; colorless oil. **R_f** = 0.45 (90:10 hexanes/EtOAc). **Chemical Formula:** HRMS (ESI) m/z : $[\text{M}+\text{Na}]^+$ calcd. for $\text{C}_{18}\text{H}_{19}\text{BrO}_2\text{Na}$ 369.0466; found 369.0465.

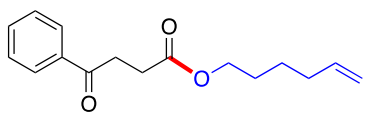
2-(2,2-Dibromo-1-methylcyclopropyl)ethyl 3-(4-bromophenyl)propanoate (**13**)



^1H NMR (500 MHz, CDCl_3) δ 7.44 – 7.38 (m, 2H), 7.12 – 7.06 (m, 2H), 4.28 (td, $J = 7.0, 1.7$ Hz, 2H), 2.93 (t, $J = 7.7$ Hz, 2H), 2.64 (t, $J = 7.7$ Hz, 2H), 1.99 (dp, $J = 14.3, 7.1$ Hz, 2H),

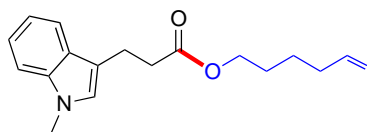
1.48 (d, $J = 7.5$ Hz, 1H), 1.42 (d, $J = 7.5$ Hz, 1H), 1.38 (s, 3H); ^{13}C NMR (151 MHz, CDCl_3) δ 172.6, 139.5, 131.7, 130.2, 120.3, 62.0, 38.2, 37.0, 35.8, 34.5, 30.4, 27.6, 22.7. **Yield:** 69%, 161.7 mg; pale yellow oil. $R_f = 0.33$ (95:5 hexanes/EtOAc). **Chemical Formula:** HRMS (ESI) m/z : $[\text{M}+\text{Na}]^+$ calcd. for $\text{C}_{15}\text{H}_{17}\text{Br}_3\text{O}_2\text{Na}$ 490.8656; found 490.8651.

Hex-5-en-1-yl 4-oxo-4-phenylbutanoate (**14**)



^1H NMR (400 MHz, CDCl_3) δ 7.98 (d, $J = 7.0$ Hz, 2H), 7.57 (t, $J = 7.4$ Hz, 1H), 7.46 (t, $J = 7.6$ Hz, 2H), 5.78 (ddt, $J = 17.0, 10.3, 6.7$ Hz, 1H), 5.04 – 4.92 (m, 2H), 4.10 (t, $J = 6.6$ Hz, 2H), 3.31 (t, $J = 6.6$ Hz, 2H), 2.76 (t, $J = 6.6$ Hz, 2H), 2.07 (q, $J = 7.0$ Hz, 2H), 1.70 – 1.60 (m, 2H), 1.45 (q, $J = 7.7$ Hz, 2H); ^{13}C NMR (101 MHz, CDCl_3) δ 198.23, 173.08, 138.48, 136.69, 133.33, 128.73, 128.15, 114.92, 77.48, 77.16, 76.84, 64.75, 33.50, 33.39, 28.39, 28.14, 25.28. **Yield:** 38%, 48.9 mg; white solid. $R_f = 0.45$ (80:20 hexanes/EtOAc). **Chemical Formula:** HRMS (ESI) m/z : $[\text{M}+\text{Na}]^+$ calcd. for $\text{C}_{15}\text{H}_{24}\text{O}_3\text{Na}$ 283.1310; found 283.1311.

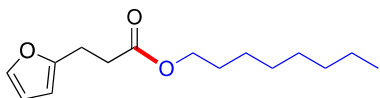
Hex-5-en-1-yl 3-(1-methyl-1H-indol-3-yl)propanoate (**15**)



^1H NMR (500 MHz, CDCl_3) δ 7.60 (dt, $J = 8.0, 1.0$ Hz, 1H), 7.29 (dt, $J = 8.3, 0.9$ Hz, 1H), 7.23 (ddd, $J = 8.2, 6.9, 1.2$ Hz, 1H), 7.11 (ddd, $J = 8.0, 6.9, 1.1$ Hz, 1H), 6.87 (s, 1H), 5.78 (ddt, $J = 16.9, 10.2, 6.6$ Hz, 1H), 5.01 (dq, $J = 17.1, 1.7$ Hz, 1H), 4.96 (ddt, $J = 10.2, 2.2, 1.2$

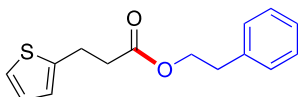
Hz, 1H), 4.08 (t, $J = 6.7$ Hz, 2H), 3.74 (s, 3H), 3.10 (t, $J = 7.5$ Hz, 2H), 2.71 (dd, $J = 8.2, 7.1$ Hz, 2H), 2.10 – 2.03 (m, 2H), 1.67 – 1.58 (m, 2H), 1.45 – 1.37 (m, 2H); ^{13}C NMR (126 MHz, CDCl_3) δ 173.4, 138.3, 136.9, 127.5, 126.2, 121.5, 118.7, 118.8, 114.7, 113.4, 109.1, 64.2, 35.1, 33.2, 32.5, 28.0, 25.1, 20.5. **Yield:** 48%, 68.6 mg; pale colorless oil. **R_f** = 0.45 (80:20 hexanes/EtOAc). **Chemical Formula:** HRMS (CI) m/z : $[\text{M}+\text{H}]^+$ calcd. for $\text{C}_{18}\text{H}_{25}\text{NO}_2$ 286.1807; found 286.1815.

n-Octyl 3-(furan-2-yl)propanoate (**16**)



^1H NMR (400 MHz, CDCl_3) δ 7.30 (d, $J = 1.8$ Hz, 1H), 6.30 – 6.25 (m, 1H), 6.01 (d, $J = 3.2$ Hz, 1H), 4.08 (t, $J = 6.7$ Hz, 2H), 2.96 (t, $J = 7.6$ Hz, 2H), 2.65 (t, $J = 7.6$ Hz, 2H), 1.61 (t, $J = 7.0$ Hz, 2H), 1.28 (dq, $J = 11.7, 4.6, 3.8$ Hz, 10H), 0.90 – 0.86 (m, 3H); ^{13}C NMR (101 MHz, CDCl_3) δ 172.75, 154.35, 141.31, 110.30, 105.36, 88.05, 77.48, 77.16, 76.84, 64.90, 32.87, 31.91, 29.33, 29.31, 28.73, 26.02, 23.63, 22.78, 14.22. **Yield:** 40%, 50.4 mg; yellowish oil. **R_f** = 0.64 (90:10 hexanes/EtOAc). **Chemical Formula:** HRMS (ESI) m/z : $[\text{M}+\text{Na}]^+$ calcd. for $\text{C}_{15}\text{H}_{24}\text{O}_3\text{Na}$ 275.1623; found 275.1625.

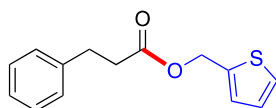
Phenethyl 3-(thiophen-2-yl)propanoate (**23**)



^1H NMR (600 MHz, CDCl_3) δ 7.34 (t, $J = 7.5$ Hz, 2H), 7.30 – 7.22 (m, 3H), 7.15 (dd, $J = 5.2, 1.2$ Hz, 1H), 6.94 (dd, $J = 5.1, 3.4$ Hz, 1H), 6.82 (dd, $J = 3.5, 1.3$ Hz, 1H), 4.35 (t, $J = 7.1$

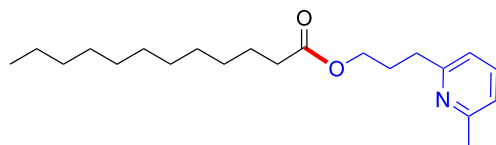
Hz, 2H), 3.20 – 3.14 (m, 2H), 2.96 (t, $J = 7.1$ Hz, 2H), 2.70 (t, $J = 7.6$ Hz, 2H); ^{13}C NMR (101 MHz, CDCl_3) δ 172.35, 143.10, 137.83, 128.97, 128.58, 126.91, 126.65, 124.72, 123.59, 65.13, 36.21, 35.15, 25.19. **Yield:** 72%, 93.9 mg; yellow-brown liquid. **R_f** = 0.3 (95:5 hexanes/EtOAc). **Chemical Formula:** HRMS (ESI) m/z : $[\text{M}+\text{Na}]^+$ calcd. for $\text{C}_{15}\text{H}_{16}\text{O}_2\text{SNa}$ 283.0769; found 283.0774.

Thiophen-2-ylmethyl 3-phenylpropanoate (**24**)



^1H NMR (400 MHz, CDCl_3) δ 7.36 – 7.17 (m, 6H), 7.09 (d, $J = 3.6$ Hz, 1H), 7.00 (dd, $J = 5.1, 3.5$ Hz, 1H), 5.29 (s, 2H), 2.98 (t, $J = 7.8$ Hz, 2H), 2.68 (t, $J = 7.8$ Hz, 2H); ^{13}C NMR (101 MHz, CDCl_3) δ 172.64, 140.43, 137.98, 128.60, 128.39, 128.32, 126.95, 126.91, 126.37, 60.58, 35.91, 30.94. **Yield:** 50%, 60.8 mg; yellowish oil. **R_f** = 0.33 (80:20 hexanes/EtOAc). **Chemical Formula:** HRMS (ESI) m/z : $[\text{M}+\text{Na}]^+$ calcd. for $\text{C}_{14}\text{H}_{14}\text{SO}_2$ 269.0700; found 269.0392.

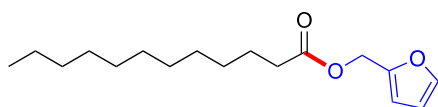
3-(6-Methylpyridin-2-yl)propyl dodecanoate (**25**)



^1H NMR (400 MHz, CDCl_3) δ 7.46 (t, $J = 7.7$ Hz, 1H), 6.94 (dd, $J = 9.9, 7.7$ Hz, 2H), 4.10 (t, $J = 6.5$ Hz, 2H), 2.80 (dd, $J = 8.8, 6.7$ Hz, 2H), 2.50 (s, 3H), 2.27 (t, $J = 7.5$ Hz, 2H), 2.10 – 1.99 (m, 2H), 1.65 – 1.54 (m, 2H), 1.25 (d, $J = 10.2$ Hz, 16H), 0.86 (t, $J = 6.6$ Hz, 3H); ^{13}C

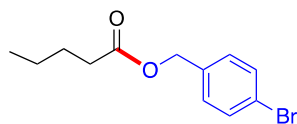
NMR (101 MHz, CDCl₃) δ 174.04, 160.43, 158.03, 136.69, 120.79, 119.69, 63.84, 34.86, 34.45, 32.01, 29.71, 29.57, 29.44, 29.38, 29.28, 28.91, 25.10, 24.62, 22.78, 14.22. **Yield:** 36%, 60.3 mg; colorless solid. **R_f** = 0.32 (80:20 hexanes/EtOAc). **Chemical Formula:** HRMS (ESI) *m/z*: [M+H]⁺ calcd. for C₂₁H₃₆NO₂ 334.2746; found 334.2748.

Furan-2-ylmethyl dodecanoate (**26**)



¹H NMR (400 MHz, CDCl₃) δ 7.42 (dd, *J* = 1.9, 0.9 Hz, 1H), 6.40 (d, *J* = 3.2 Hz, 1H), 6.36 (dd, *J* = 3.3, 1.8 Hz, 1H), 5.06 (s, 2H), 2.32 (t, *J* = 7.6 Hz, 2H), 1.68 – 1.56 (m, 2H), 1.34 – 1.22 (m, 16H), 0.88 (t, *J* = 6.8 Hz, 3H); **¹³C NMR (101 MHz, CDCl₃)** δ 173.63, 149.79, 143.32, 110.66, 110.61, 57.99, 34.29, 32.04, 30.09, 29.74, 29.72, 29.58, 29.47, 29.37, 29.21, 25.01, 22.83, 14.26. **Yield:** 29%, 40.3 mg; yellow oil. **R_f** = 0.73 (90:10 hexanes/EtOAc). **Chemical Formula:** HRMS (ESI) *m/z*: [M+Na]⁺ calcd. for C₁₇H₂₈O₃Na 303.1936; found 303.1938.

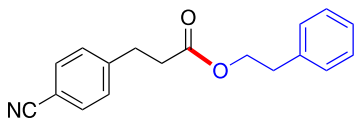
4-Bromobenzyl pentanoate (**27**)



¹H NMR (600 MHz, CDCl₃) δ 7.51 – 7.46 (m, 2H), 7.25 – 7.20 (m, 2H), 5.05 (s, 2H), 2.35 (t, *J* = 7.6 Hz, 2H), 1.66 – 1.58 (m, 2H), 1.38 – 1.31 (m, 2H), 0.91 (t, *J* = 7.4 Hz, 3H); **¹³C NMR (101 MHz, CDCl₃)** δ 173.68, 135.31, 131.82, 129.97, 122.32, 65.37, 34.12, 27.11,

22.38, 13.82. **Yield:** 50%, 27 mg; colorless oil. **R_f** = 0.30 (98:2 hexanes/EtOAc). Spectral data matched those previously reported.⁸

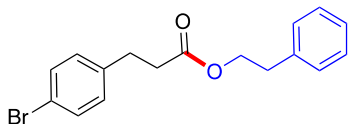
Phenethyl 3-(4-cyanophenyl)propanoate (**28**)



¹H NMR (600 MHz, CDCl₃) δ 7.60 – 7.56 (m, 2H), 7.33 (dd, J = 8.3, 6.8 Hz, 2H), 7.31 – 7.24 (m, 3H), 7.24 – 7.20 (m, 2H), 4.33 (t, J = 7.0 Hz, 2H), 3.00 (t, J = 7.5 Hz, 2H), 2.95 (t, J = 7.0 Hz, 2H), 2.66 (t, J = 7.6 Hz, 2H); **¹³C NMR (101 MHz, CDCl₃)** δ 172.16, 146.10, 137.71, 132.35, 129.21, 128.91, 128.58, 126.69, 118.99, 110.26, 77.47, 65.18, 35.06, 30.89.

Yield: 46%, 64.6 mg; white solid. **R_f** = 0.26 (85:15 hexanes/EtOAc). **Chemical Formula:** HRMS (ESI) m/z : [M+Na]⁺ calcd. for C₁₈H₁₇NO₂Na 302.1157; found 302.1161.

Phenethyl 3-(4-bromophenyl)propanoate (**29**)



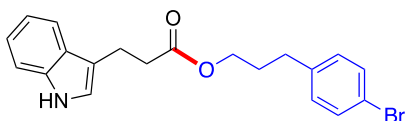
¹H NMR (600 MHz, CDCl₃) δ 7.43 – 7.38 (m, 2H), 7.35 – 7.29 (m, 2H), 7.28 – 7.23 (m, 1H), 7.23 – 7.18 (m, 2H), 7.07 – 7.02 (m, 2H), 4.31 (t, J = 7.0 Hz, 2H), 2.93 (t, J = 7.0 Hz, 2H),

⁸ Janssen, P. G. A.; Pouderoijen, M.; van Breemen, A. J. J. M.; Herwig, P. T.; Koeckelberghs, G.; Popa-Merticaru, A. R.; Meskers, S. C. J.; Valetton, J. J. P.; Meijer, E. W.; Schenning, A. H. J. Synthesis and Properties of α,ω -Phenyl-Capped Bithiophene Derivatives. *J. Mater. Chem.* **2006**, *16*, 4335–4342.

2.89 (t, $J = 7.7$ Hz, 2H), 2.61 (t, $J = 7.7$ Hz, 2H); ^{13}C NMR (101 MHz, CDCl_3) δ 172.57, 139.52, 137.83, 131.62, 130.18, 128.97, 128.60, 126.69, 120.15, 65.10, 35.69, 35.14, 30.35.

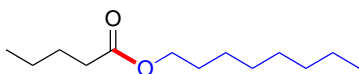
Yield: 55%, 91.3 mg; white solid. $R_f = 0.33$ (90:10 hexanes/EtOAc). **Chemical Formula:** HRMS (ESI) m/z : $[\text{M}+\text{Na}]^+$ calcd. for $\text{C}_{17}\text{H}_{17}\text{BrO}_2\text{Na}$ 355.0310; found 355.0310.

3-(4-Bromophenyl)propyl 3-(1H-indol-3-yl)propanoate (**30**)



^1H NMR (600 MHz, CDCl_3) 7.87 (s, 1H), 7.54 (dd, $J = 7.9, 1.2$ Hz, 1H), 7.32 – 7.16 (m, 3H), 7.12 (ddd, $J = 8.2, 7.0, 1.2$ Hz, 1H), 7.05 (ddd, $J = 8.0, 7.0, 1.0$ Hz, 1H), 6.93 (d, $J = 2.3$ Hz, 1H), 6.92 – 6.87 (m, 2H), 3.99 (t, $J = 6.4$ Hz, 2H), 3.06 – 3.01 (m, 2H), 2.65 (t, $J = 7.6$ Hz, 2H), 2.47 (dd, $J = 8.6, 6.8$ Hz, 2H), 1.83 – 1.76 (m, 2H); ^{13}C NMR (101 MHz, CDCl_3) δ 173.53, 140.28, 136.40, 131.57, 130.28, 127.30, 122.23, 121.54, 119.84, 119.50, 118.85, 115.08, 111.27, 63.59, 35.04, 31.65, 30.14, 20.83. **Yield:** 75%, 77 mg; white solid. $R_f = 0.34$ (85:15 hexanes/EtOAc). **Chemical Formula:** HRMS (ESI) m/z : $[\text{M}+\text{Na}]^+$ calcd. for $\text{C}_{20}\text{H}_{20}\text{BrNO}_2\text{Na}$ 408.0571; found 408.0575.

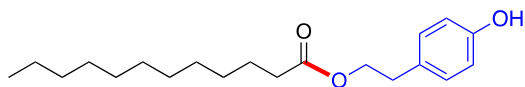
n-Octyl pentanoate (**35**)



^1H NMR (500 MHz, CDCl_3) δ 4.06 (t, $J = 6.7$ Hz, 2H), 2.30 (t, $J = 7.5$ Hz, 2H), 1.66 – 1.56 (m, 4H), 1.39 – 1.21 (m, 12H), 0.90 (dt, $J = 16.6, 7.2$ Hz, 6H); ^{13}C NMR (126 MHz, CDCl_3) δ 173.97, 64.38, 34.11, 31.77, 29.20, 29.18, 28.65, 27.10, 25.92, 22.63, 22.27, 14.06, 13.70.

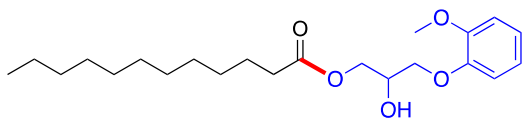
Yield: 86%, 43 mg; colorless liquid. **R_f** = 0.65 (95:5 hexanes/EtOAc). Spectral data matched those previously reported.⁹

4-Hydroxyphenethyl dodecanoate (**36**)



¹H NMR (400 MHz, CDCl₃) δ 7.10 – 7.03 (m, 2H), 6.80 – 6.74 (m, 2H), 4.25 (t, J = 7.1 Hz, 2H), 2.86 (t, J = 7.1 Hz, 2H), 2.35 (t, J = 7.5 Hz, 1H), 2.29 (t, J = 7.5 Hz, 2H), 1.70 – 1.53 (m, 3H), 1.26 (d, J = 3.9 Hz, 22H), 0.88 (t, J = 6.8 Hz, 4H). **¹³C NMR (126 MHz, CDCl₃)** δ 180.20, 174.24, 154.44, 130.17, 115.48, 65.17, 34.52, 34.41, 34.19, 32.05, 29.76, 29.74, 29.60, 29.57, 29.49, 29.47, 29.41, 29.38, 29.27, 29.20, 25.09, 24.83, 22.83, 14.25. **Yield:** 37%, 36.5 mg; white solid. **R_f** = 0.73 (80:20 hexanes/EtOAc). **Chemical Formula:** HRMS (ESI) m/z : [M+Na]⁺ calcd. for C₂₀H₃₂O₃Na 343.2249; found 343.2253. Sample contains some hexanes.

2-Hydroxy-3-(2-methoxyphenoxy)propyl dodecanoate (**40**)

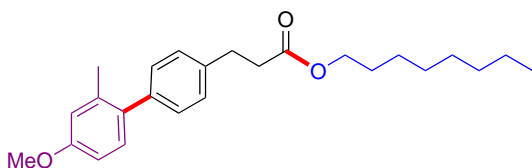


¹H NMR (400 MHz, CDCl₃) δ 7.03 – 6.87 (m, 4H), 4.33 – 4.17 (m, 3H), 4.12 – 3.93 (m, 2H), 3.86 (s, 3H), 2.34 (t, J = 7.6 Hz, 2H), 1.67 – 1.57 (m, 2H), 1.30 – 1.21 (m, 16H), 0.88 (t, J = 6.8 Hz, 3H). **¹³C NMR (126 MHz, CDCl₃)** δ 173.96, 150.03, 147.96, 122.56, 121.05, 115.73,

⁹ Cahiez, G.; Chaboche, C.; JeÂzeÂquel, M. Cu-Catalyzed Alkylation of Grignard Reagents: A New Efficient Procedure. *Tetrahedron* **2000**, *56*, 2733-2737.

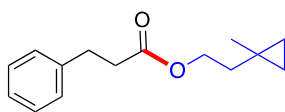
112.04, 71.50, 68.49, 64.95, 55.82, 34.15, 31.90, 29.59, 29.44, 29.32, 29.25, 29.13, 24.91, 22.67, 14.11. **Yield:** 19%, 35.2 mg; white solid. **R_f** = 0.35 (70:30 hexanes/EtOAc). **Chemical Formula:** HRMS (ESI) *m/z*: [M+Na]⁺ calcd. for C₂₂H₃₆O₅Na 403.2460; found 403.2447.

Octyl 3-(4'-methoxy-2'-methyl-[1,1'-biphenyl]-4-yl)propanoate (**44**)



¹H NMR (500 MHz, CDCl₃) δ 7.24 (s, 4H), 7.15 (d, *J* = 8.3 Hz, 1H), 6.83 (d, *J* = 2.7 Hz, 1H), 6.80 (dd, *J* = 8.3, 2.7 Hz, 1H), 4.10 (t, *J* = 6.8 Hz, 2H), 3.84 (s, 3H), 3.01 (dd, *J* = 8.5, 7.3 Hz, 2H), 2.69 (dd, *J* = 8.5, 7.2 Hz, 2H), 2.27 (s, 3H), 1.68 – 1.57 (m, 2H), 1.40 – 1.23 (m, 10H), 0.93 – 0.87 (m, 3H); **¹³C NMR (126 MHz, CDCl₃)** δ 173.2, 158.8, 139.7, 138.9, 136.9, 134.5, 131.0, 129.6, 128.1, 115.8, 111.2, 64.8, 55.4, 36.0, 31.9, 30.8, 29.3, 29.3, 28.8, 26.0, 22.8, 20.9, 14.2. **Yield:** 82%, 157.2mg, colorless oil. **R_f** = 0.50 (95:5 hexanes/EtOAc). **Chemical Formula:** HRMS (ESI) *m/z*: [M+Na]⁺ calcd. for C₂₅H₃₄O₃Na 405.2406; found 405.2404.

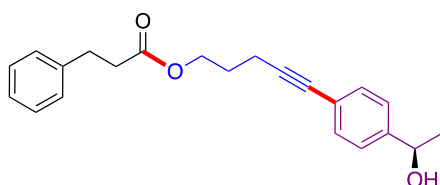
2-(1-Methylcyclopropyl)ethyl 3-phenylpropanoate (**48**)



¹H NMR (500 MHz, CDCl₃) δ 7.31 – 7.27 (m, 2H), 7.22 – 7.18 (m, 3H), 4.18 (t, *J* = 7.1 Hz, 2H), 2.95 (t, *J* = 7.9 Hz, 2H), 2.64 – 2.60 (m, 2H), 1.54 (t, *J* = 7.1 Hz, 2H), 1.04 (s, 3H), 0.31

– 0.23 (m, 4H); ^{13}C NMR (126 MHz, CDCl_3) δ 173.09, 140.73, 128.62, 128.43, 126.37, 63.35, 38.00, 36.14, 31.11, 22.90, 13.09, 12.84. **Yield:** 65%, 75.4 mg, colorless oil. **R_f** = 0.60 (85:15 hexanes/EtOAc). Spectral data matched those previously reported.¹⁰

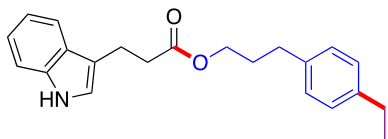
(*R*)-5-(4-(1-Hydroxyethyl)phenyl)pent-4-yn-1-yl 3-phenylpropanoate (**53**)



^1H NMR (500 MHz, CDCl_3) δ 7.37 (d, J = 8.1 Hz, 2H), 7.29 (d, 4H), 7.23-7.16 (m, 3H), 4.37 (q, J = 6.4 Hz, 1H), 4.22 (t, J = 6.3 Hz, 2H), 2.96 (t, J = 7.8 Hz, 2H), 2.65 (t, J = 7.8 Hz, 2H), 2.45 (t, J = 7.0 Hz, 2H), 1.90 (p, J = 6.7 Hz, 2H), 1.47 (d, J = 6.5 Hz, 3H), 1.27 (s, 1H); ^{13}C NMR (126 MHz, CDCl_3) δ 172.9, 145.4, 140.5, 131.7, 128.5, 128.3, 126.3, 125.3, 122.8, 88.5, 81.1, 70.1, 63.2, 35.9, 40.0, 27.8, 25.1, 16.2. **Yield:** 59%, 40 mg, colorless oil. **R_f** = 0.3 (85:15 hexanes/EtOAc). **Chemical Formula:** HRMS (ESI) m/z : $[\text{M}+\text{Na}]^+$ calcd. for $\text{C}_{22}\text{H}_{24}\text{O}_3\text{Na}$ 318.1620; found 318.1627.

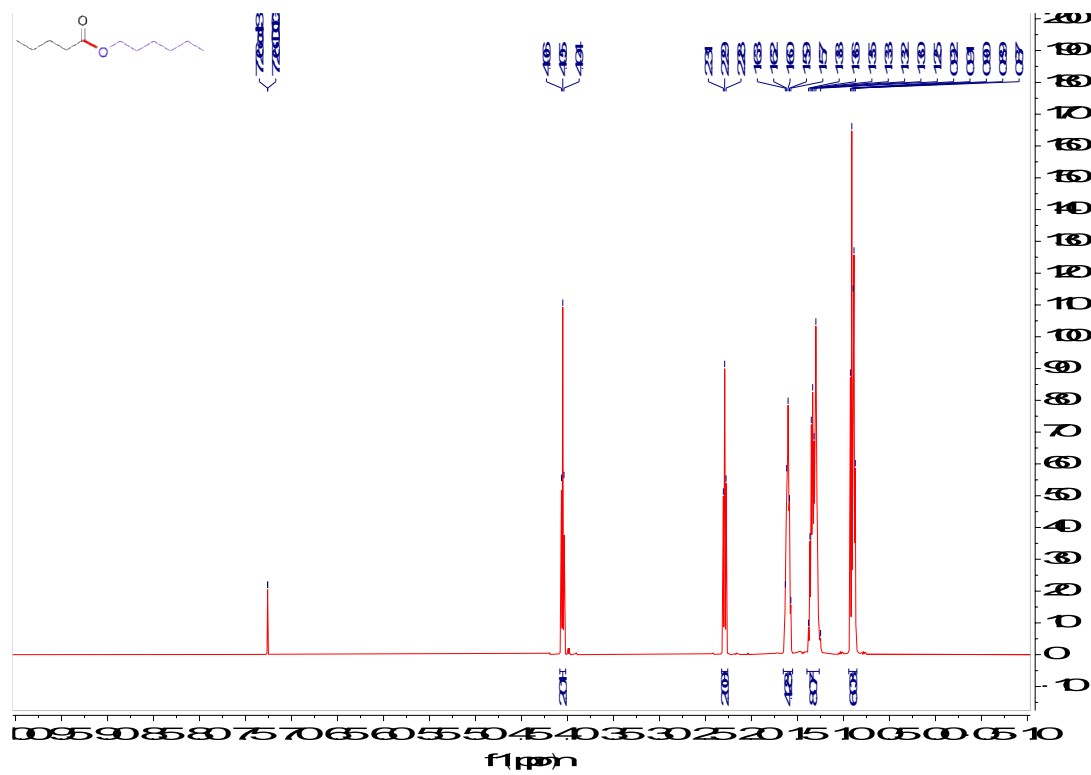
¹⁰ Wood, A. B.; Cortes-Clerget, M.; Kincaid, J. R. A.; Akkachairin, B.; Singhanian, V.; Gallou, F.; and Lipshutz, B.H. Nickel Nanoparticle Catalyzed Mono- and Di-Reductions of Gem-Dibromocyclopropanes Under Mild, Aqueous Micellar Conditions. *Angew. Chem., Int. Ed.* **2020**, *59*, 17587-17593.

3-(4-Ethylphenyl)propyl 3-(1H-indol-3-yl)propanoate (**57**)

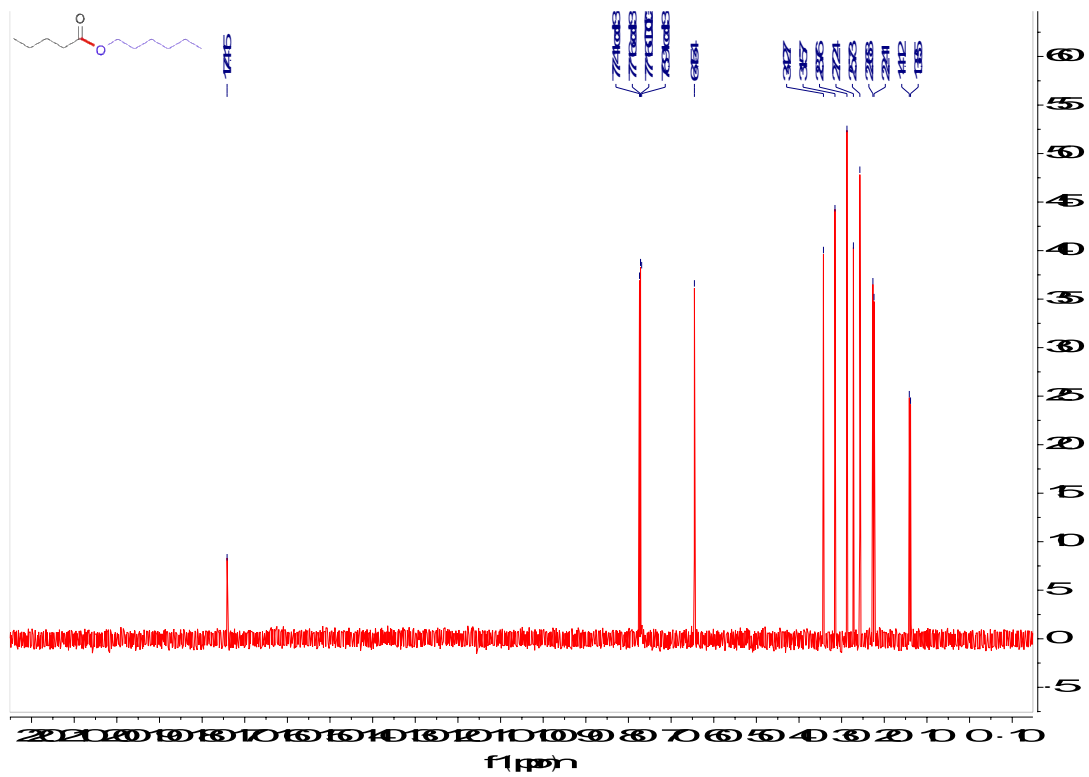


¹H NMR (400 MHz, CDCl₃) δ 7.93 (s, 1H), 7.61 (d, $J = 7.8$ Hz, 1H), 7.34 (d, $J = 8.1$ Hz, 1H), 7.22 – 7.07 (m, 4H), 7.04 (d, $J = 7.8$ Hz, 2H), 7.00 (s, 1H), 4.09 (t, $J = 6.5$ Hz, 2H), 3.11 (t, $J = 7.7$ Hz, 2H), 2.72 (t, $J = 7.6$ Hz, 2H), 2.60 (dt, $J = 12.2, 7.5$ Hz, 4H), 1.90 (p, $J = 6.9$ Hz, 2H), 1.21 (t, $J = 7.6$ Hz, 3H). **¹³C NMR (101 MHz, CDCl₃)** δ 173.42, 141.85, 138.36, 136.27, 128.30, 127.87, 127.19, 122.07, 121.35, 119.34, 118.72, 115.06, 111.10, 77.20, 63.79, 34.93, 31.66, 30.24, 28.41, 20.68, 15.62. **Yield:** 46%, 39 mg, yellow oil. **R_f** = 0.21 (90:10 hexanes/EtOAc). **Chemical Formula:** HRMS (ESI) m/z : [M+Na]⁺ calcd. for C₂₂H₂₅NO₂Na 358.1783; found 358.1789.

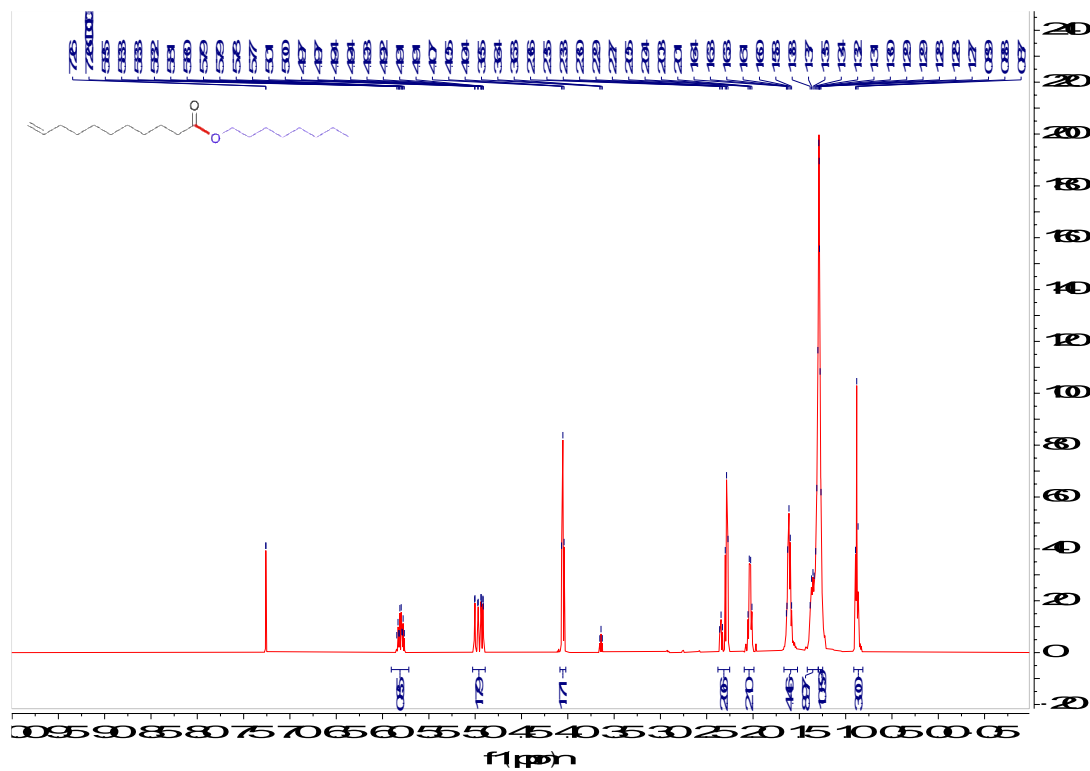
1.8. NMR spectra



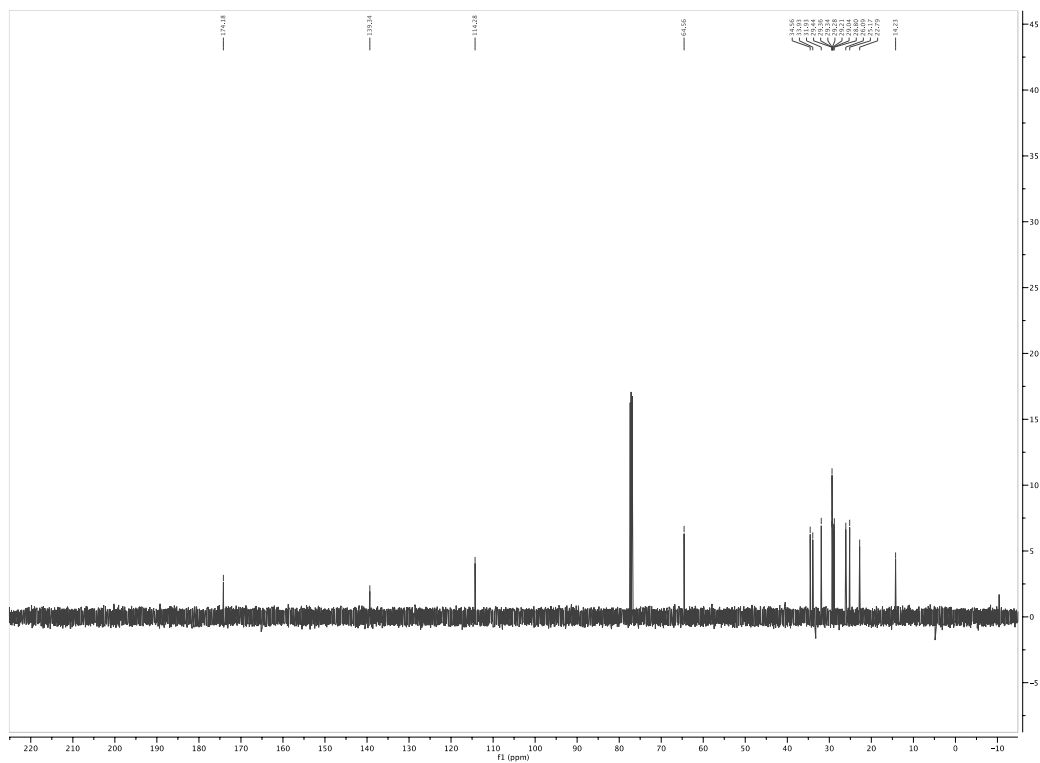
^1H NMR spectrum of *n*-Hexyl pentanoate (3)



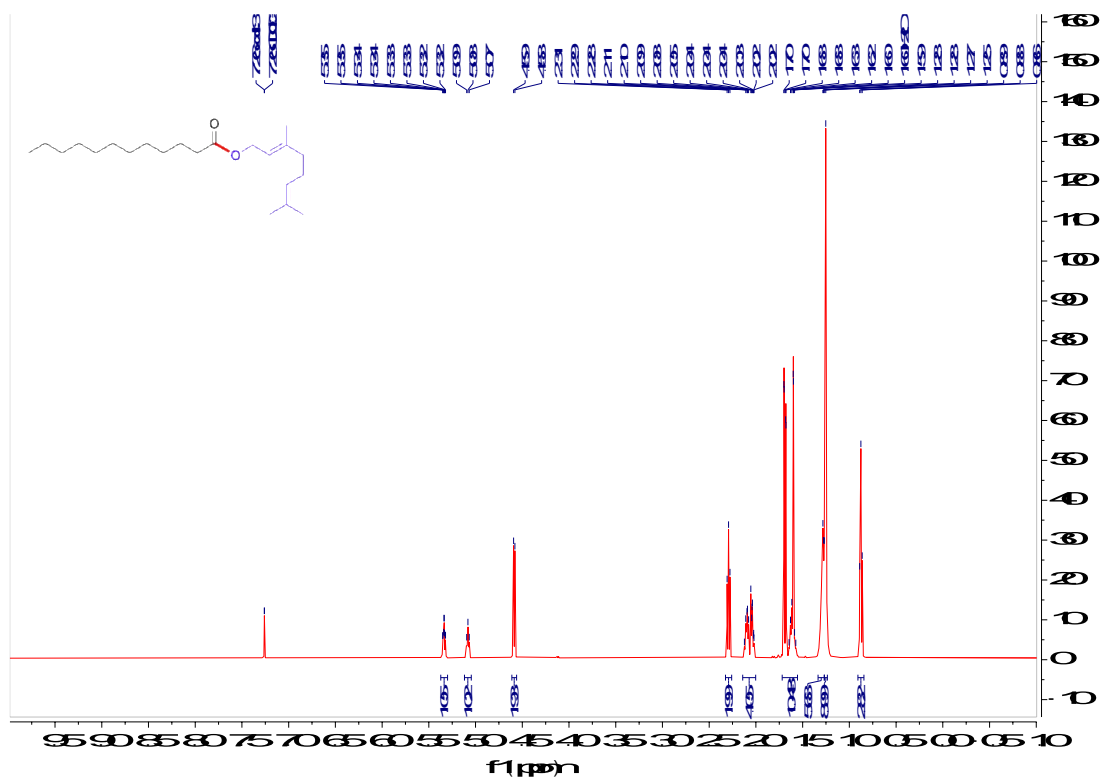
^{13}C NMR spectrum of *n*-Hexyl pentanoate (3)



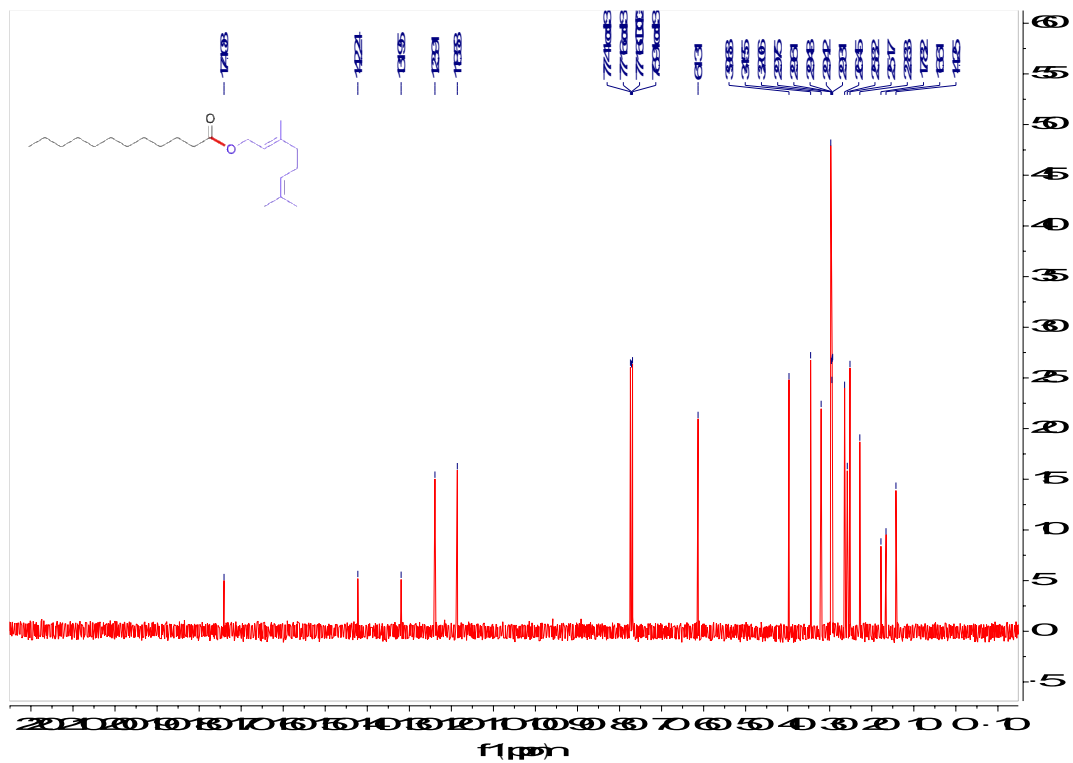
^1H NMR spectrum of *n*-Octyl undec-10-enoate (4)



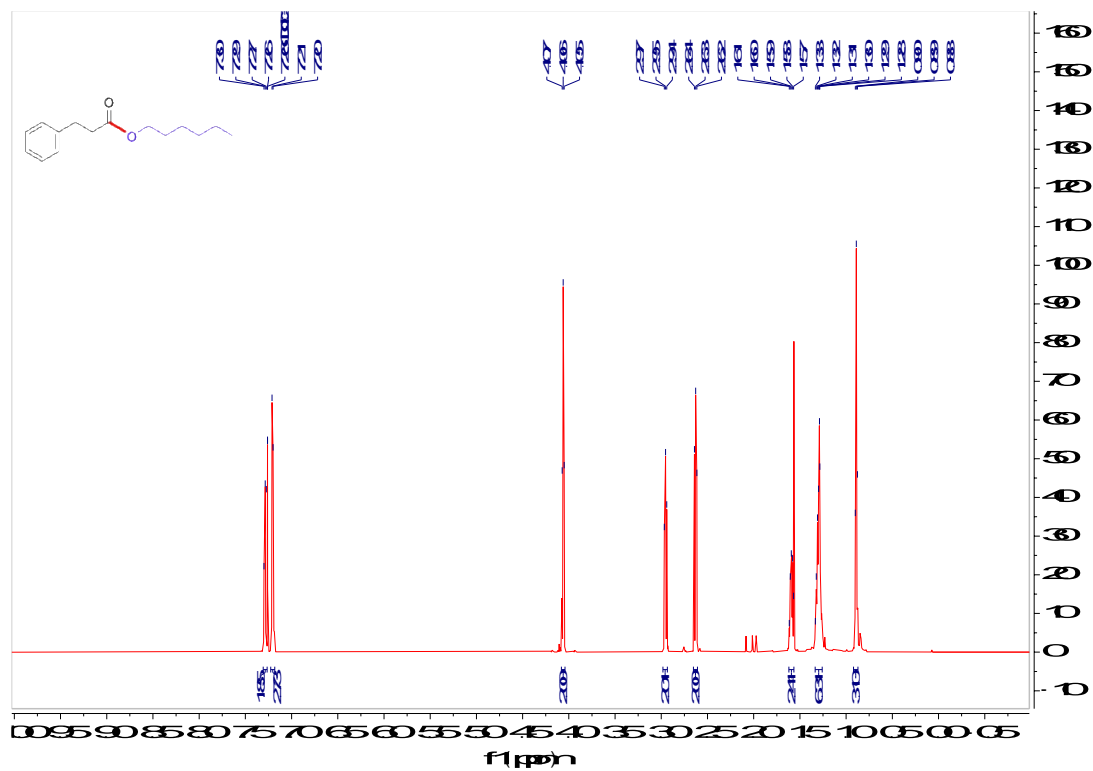
^{13}C NMR spectrum of *n*-Octyl undec-10-enoate (4)



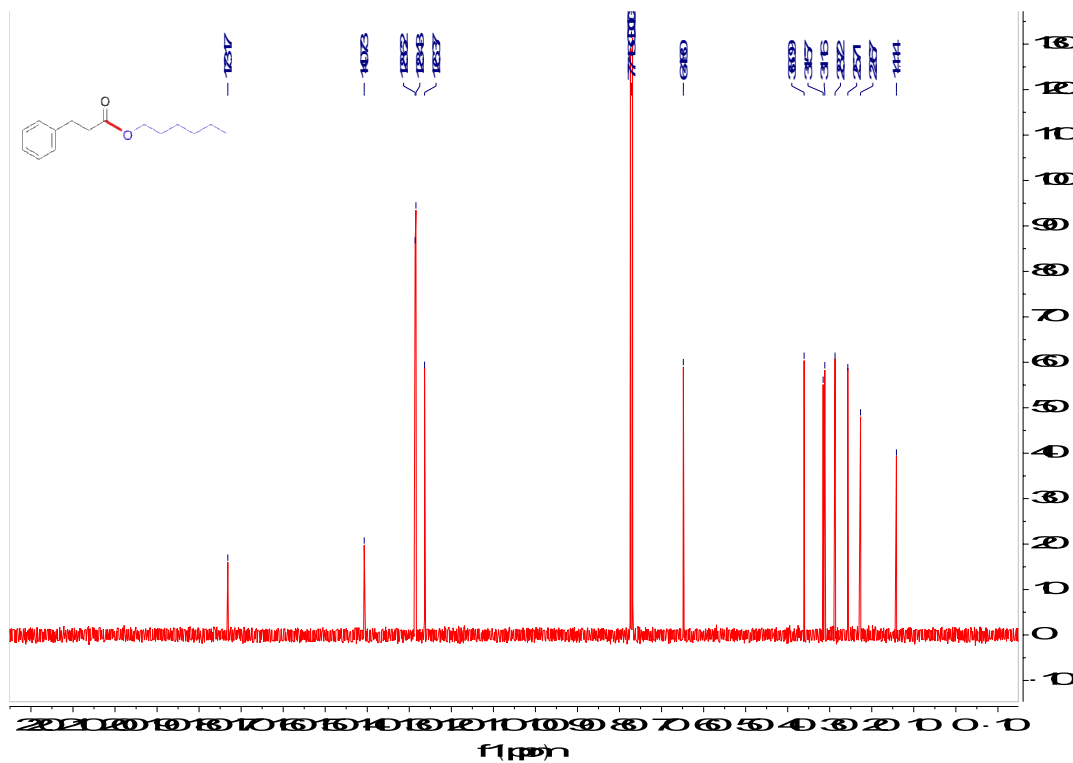
¹H NMR spectrum of (E)-3,7-Dimethylocta-2,6-dien-1-yl dodecanoate (5)



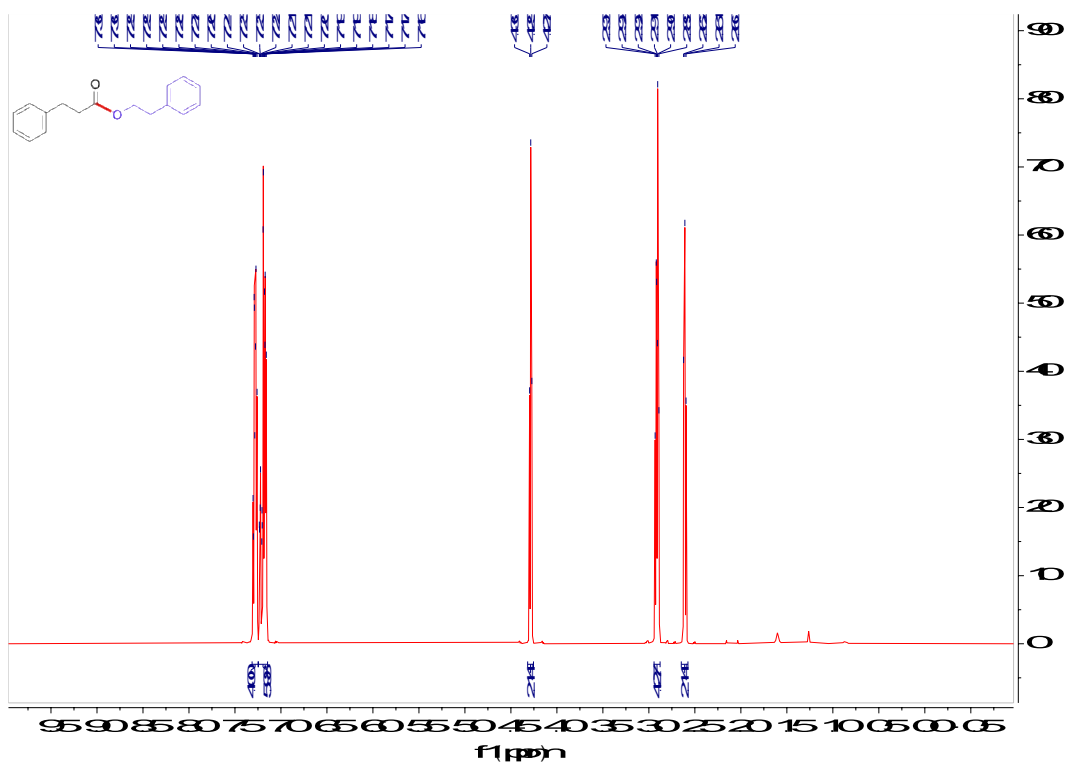
¹³C NMR spectrum of (E)-3,7-Dimethylocta-2,6-dien-1-yl dodecanoate (5)



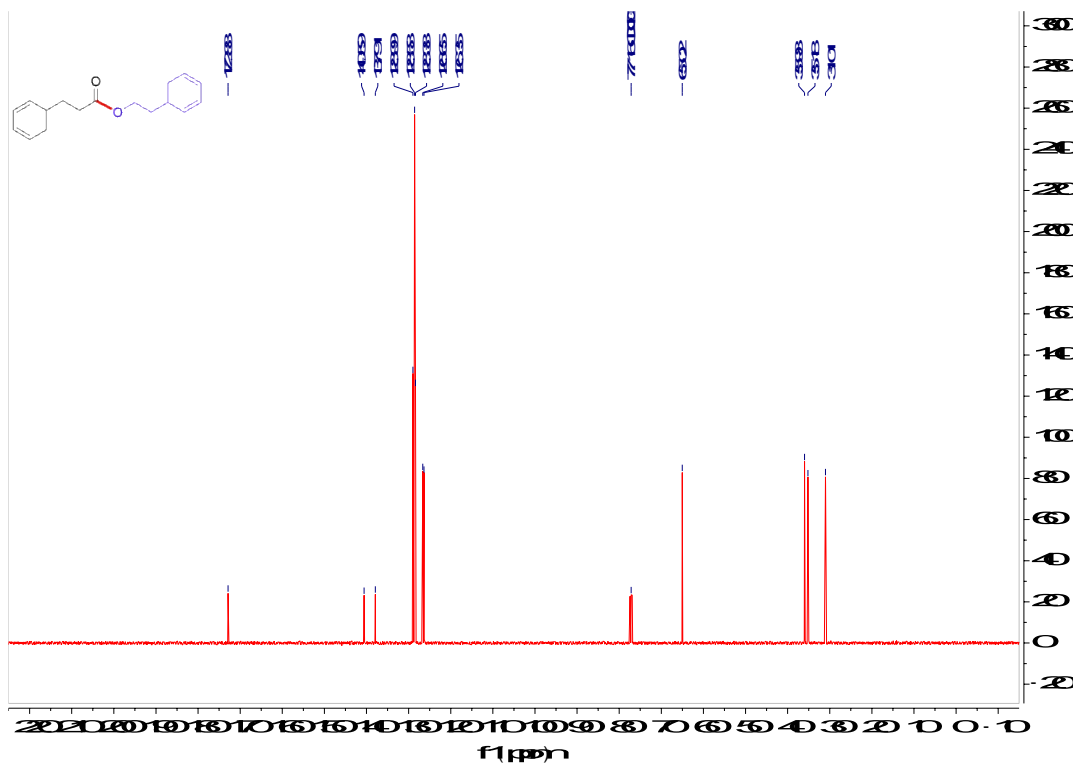
^1H NMR spectrum of *n*-Hexyl 3-phenylpropanoate (6)



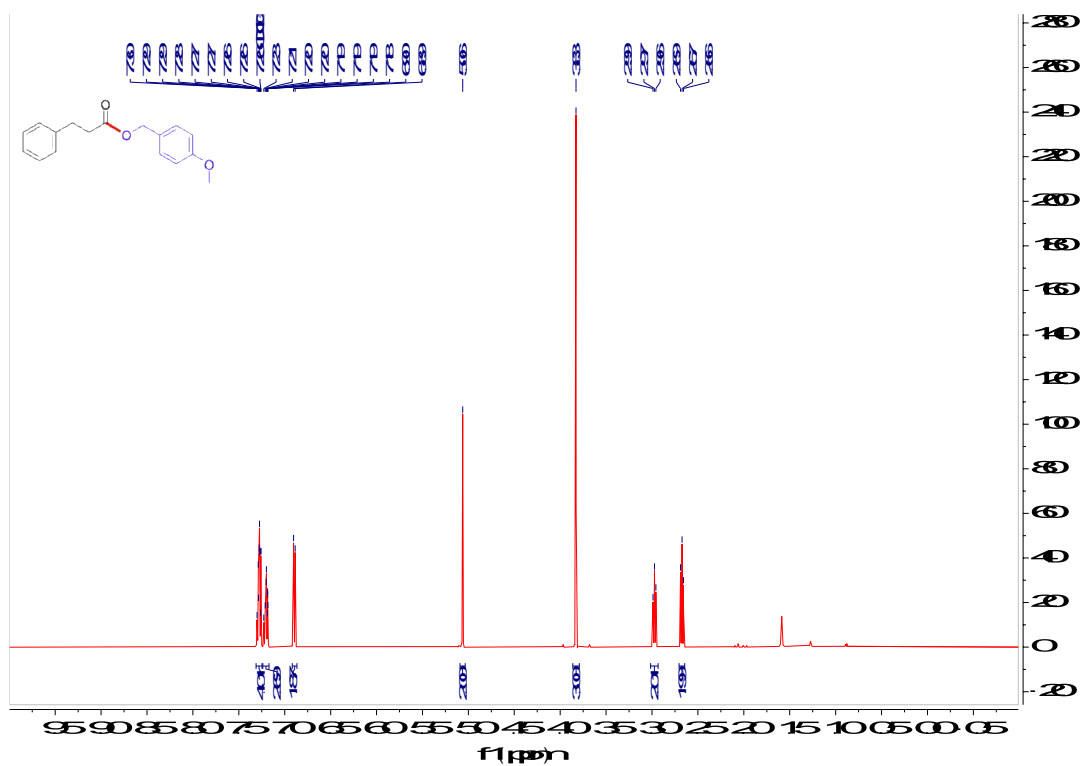
^{13}C NMR spectrum of *n*-Hexyl 3-phenylpropanoate (6)



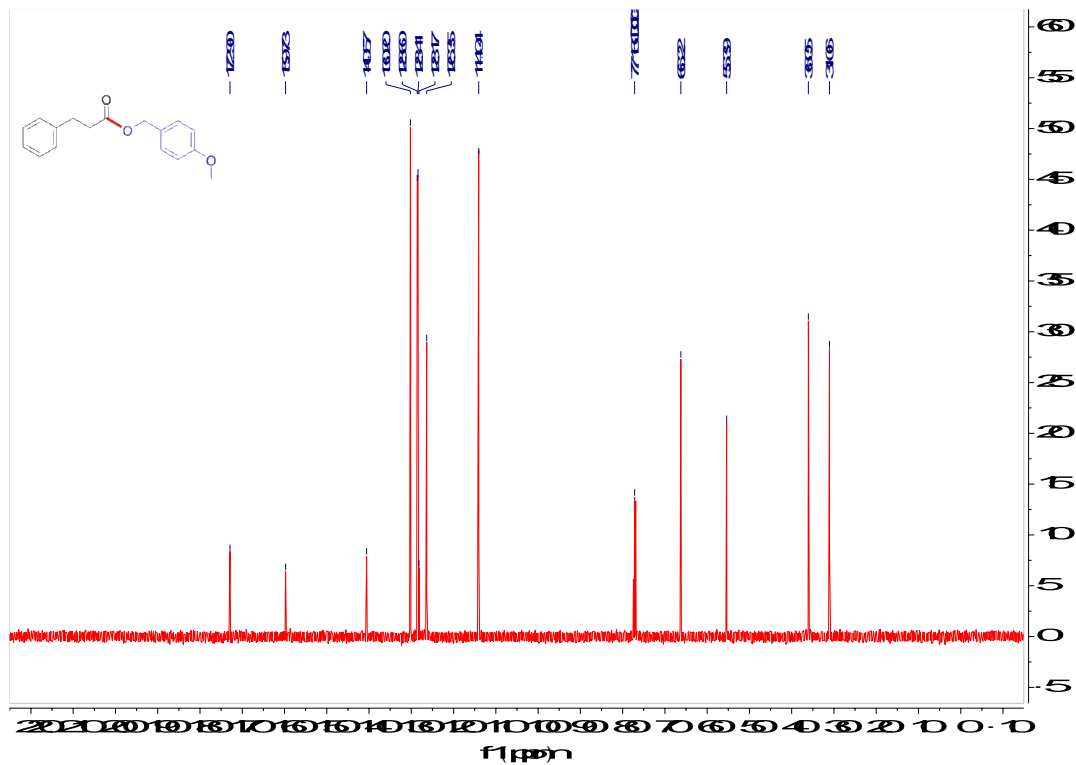
¹H NMR spectrum of Phenethyl 3-phenylpropanoate (7)



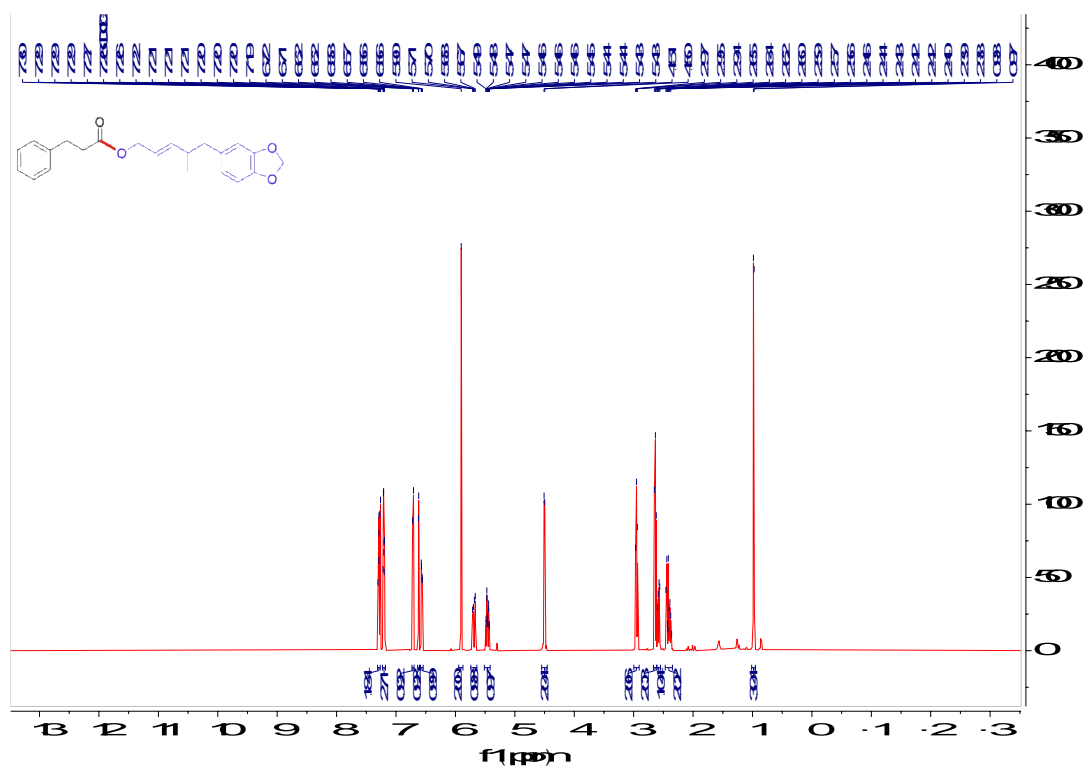
¹³C NMR spectrum of Phenethyl 3-phenylpropanoate (7)



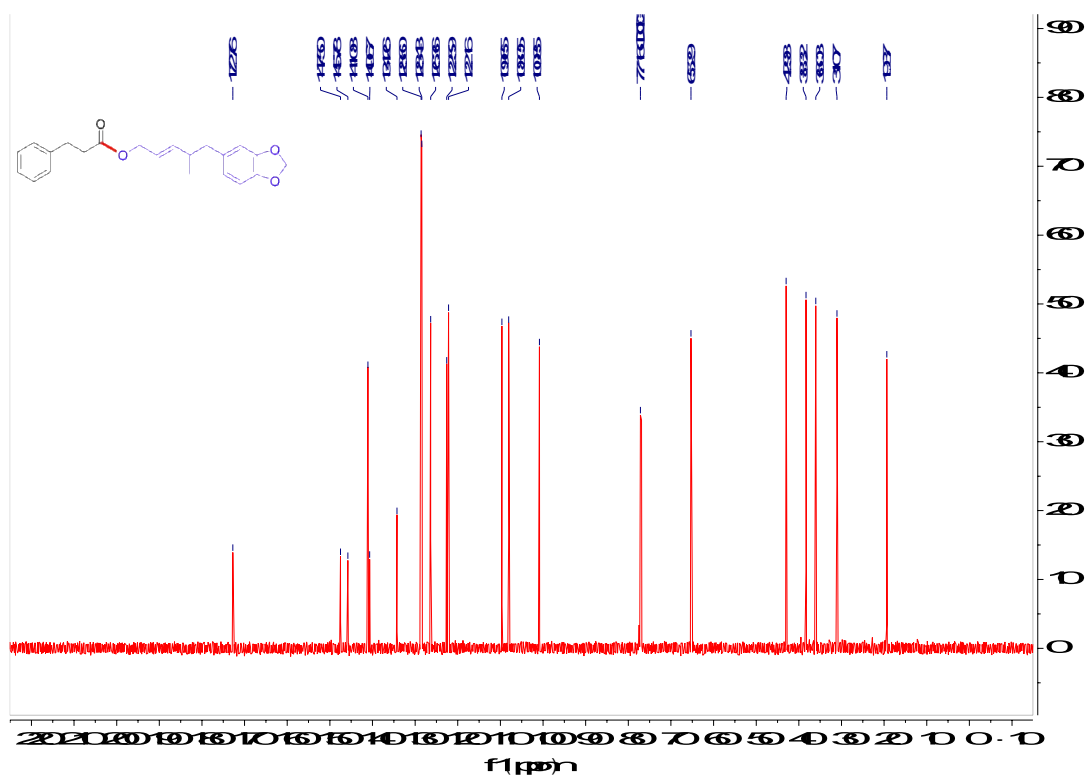
¹H NMR spectrum of 4-Methoxybenzyl 3-phenylpropanoate (8)



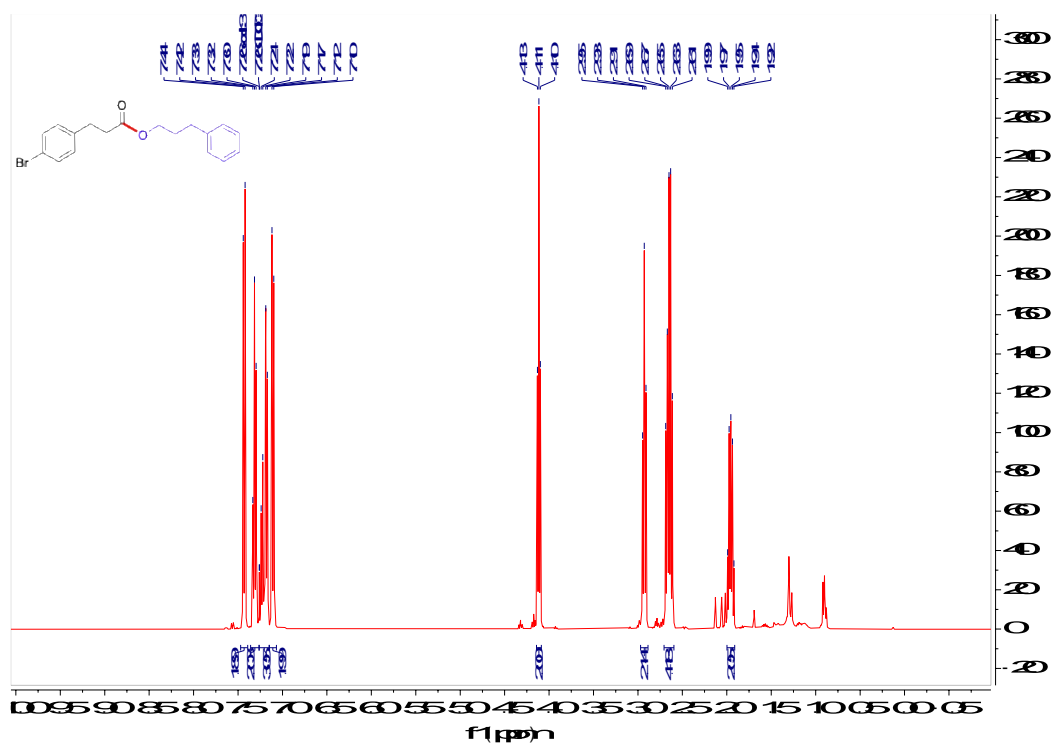
¹³C NMR spectrum of 4-Methoxybenzyl 3-phenylpropanoate (8)



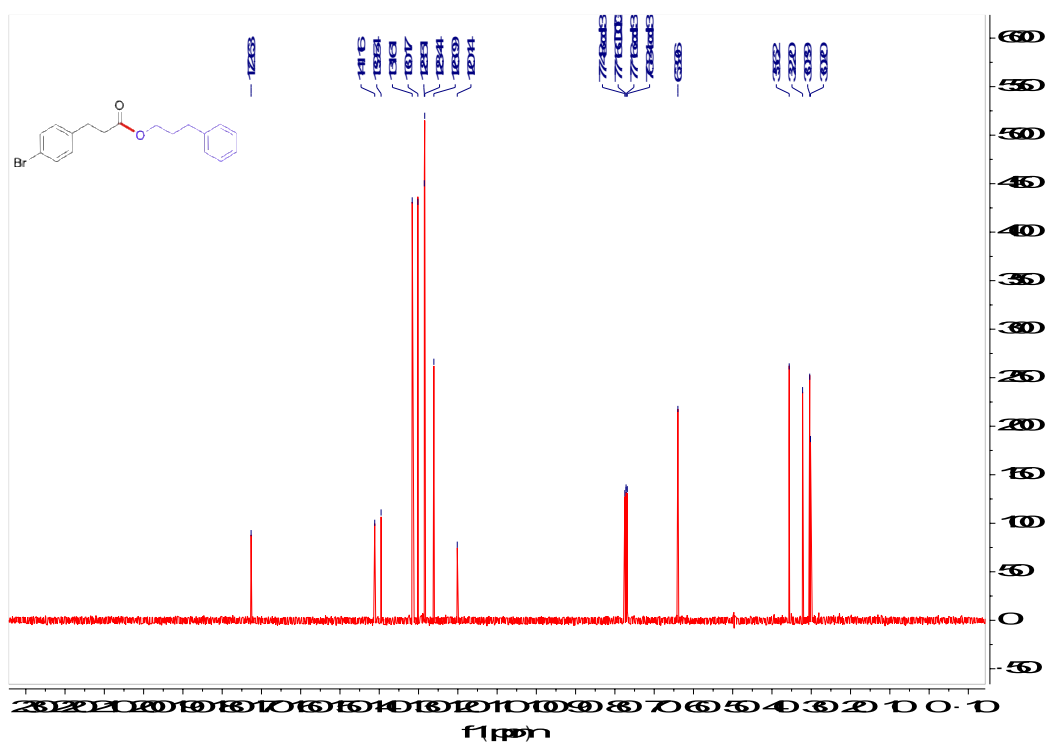
¹H NMR spectrum of (*E*)-5-(Benzo[d][1,3]dioxol-5-yl)-4-methylpent-2-en-1-yl 3-phenylpropanoate (**11**)



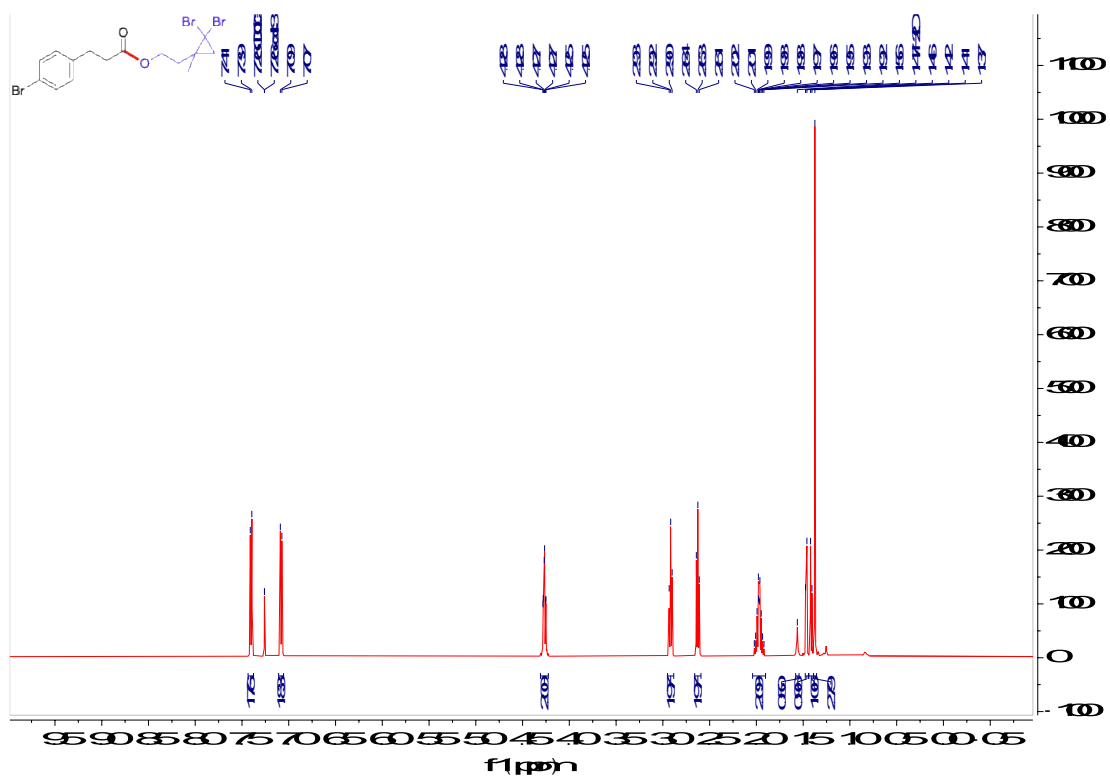
^{13}C NMR spectrum of (*E*)-5-(Benzo[d][1,3]dioxol-5-yl)-4-methylpent-2-en-1-yl 3-phenylpropanoate (**11**)



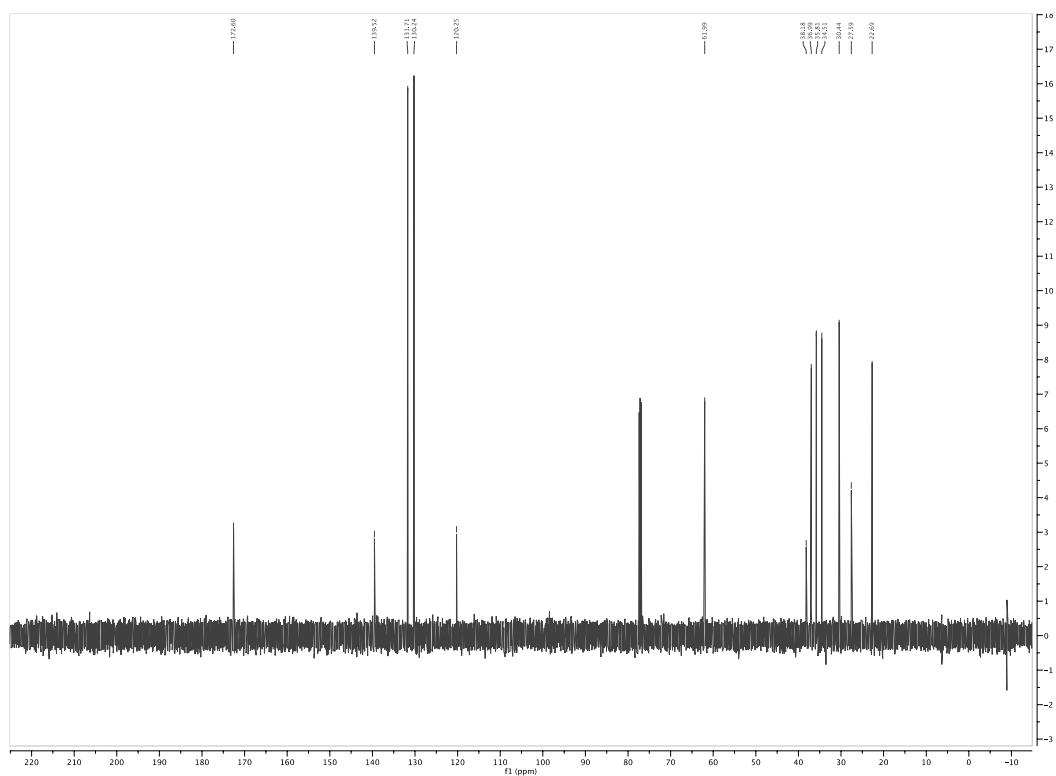
¹H NMR spectrum of 3-Phenylpropyl 3-(4-bromophenyl)propanoate (**12**)



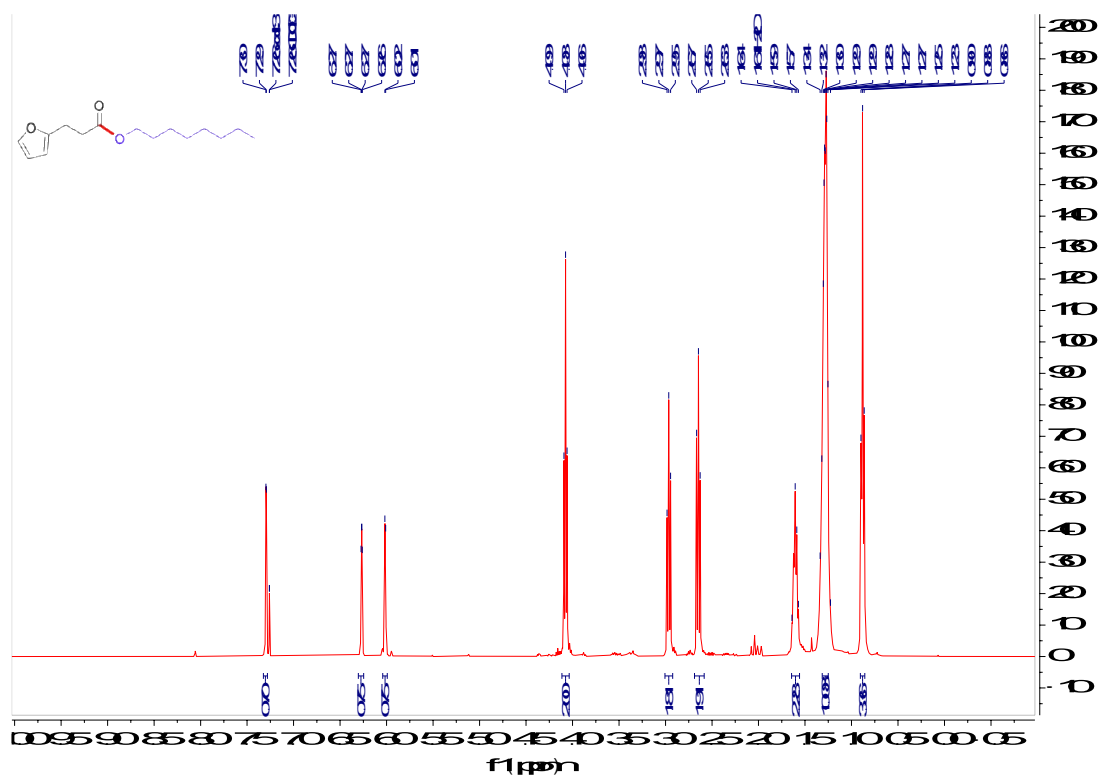
¹³C NMR spectrum of 3-Phenylpropyl 3-(4-bromophenyl)propanoate (**12**)



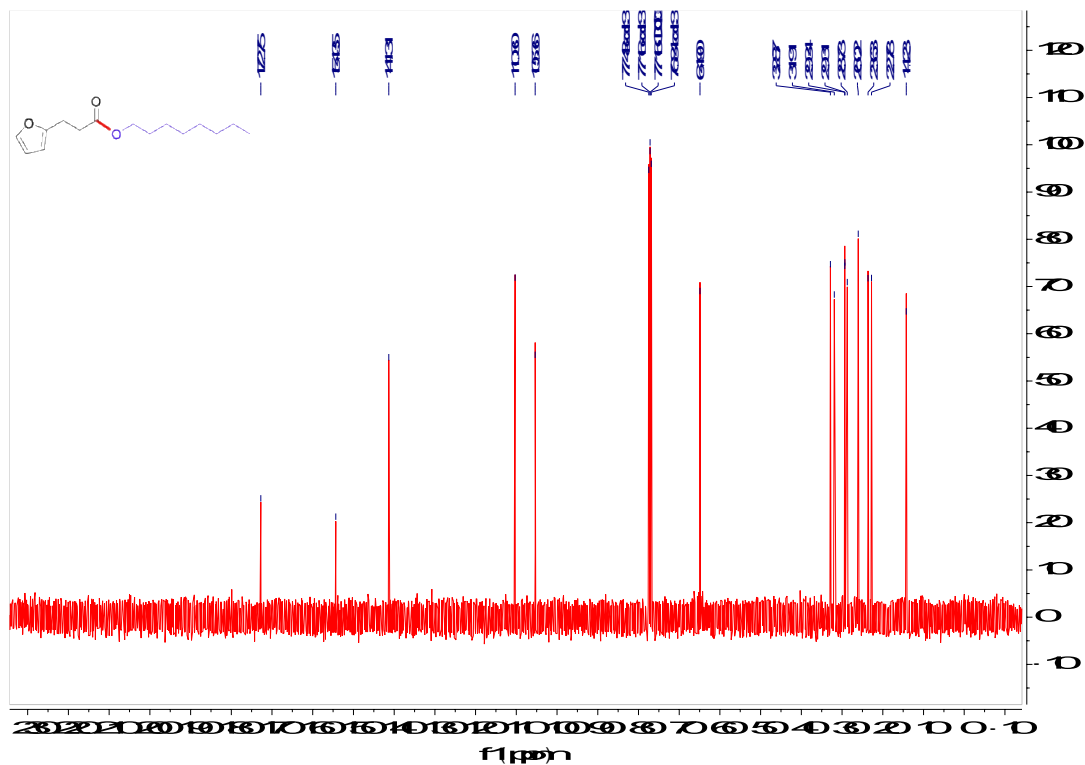
¹H NMR spectrum of 2-(2,2-Dibromo-1-methylcyclopropyl)ethyl 3-(4-bromophenyl)propanoate
(13)



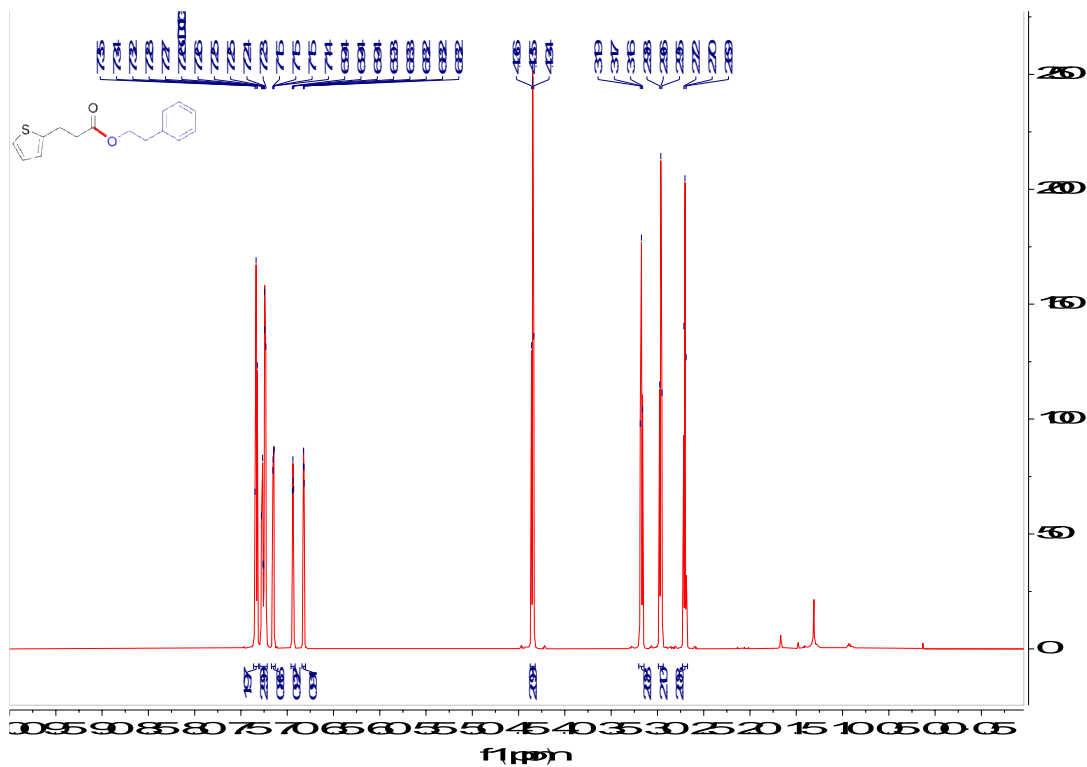
^{13}C NMR spectrum of 2-(2,2-Dibromo-1-methylcyclopropyl)ethyl 3-(4-bromophenyl)propanoate
(13)



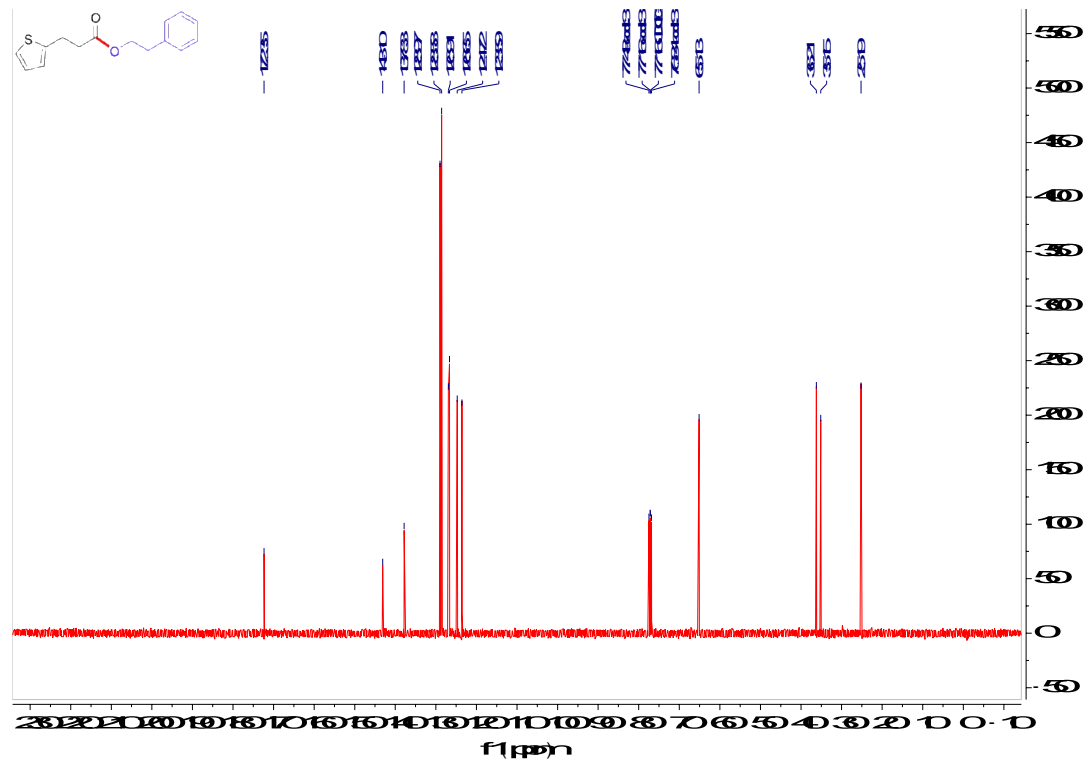
¹H NMR spectrum of *n*-Octyl 3-(furan-2-yl)propanoate (16)



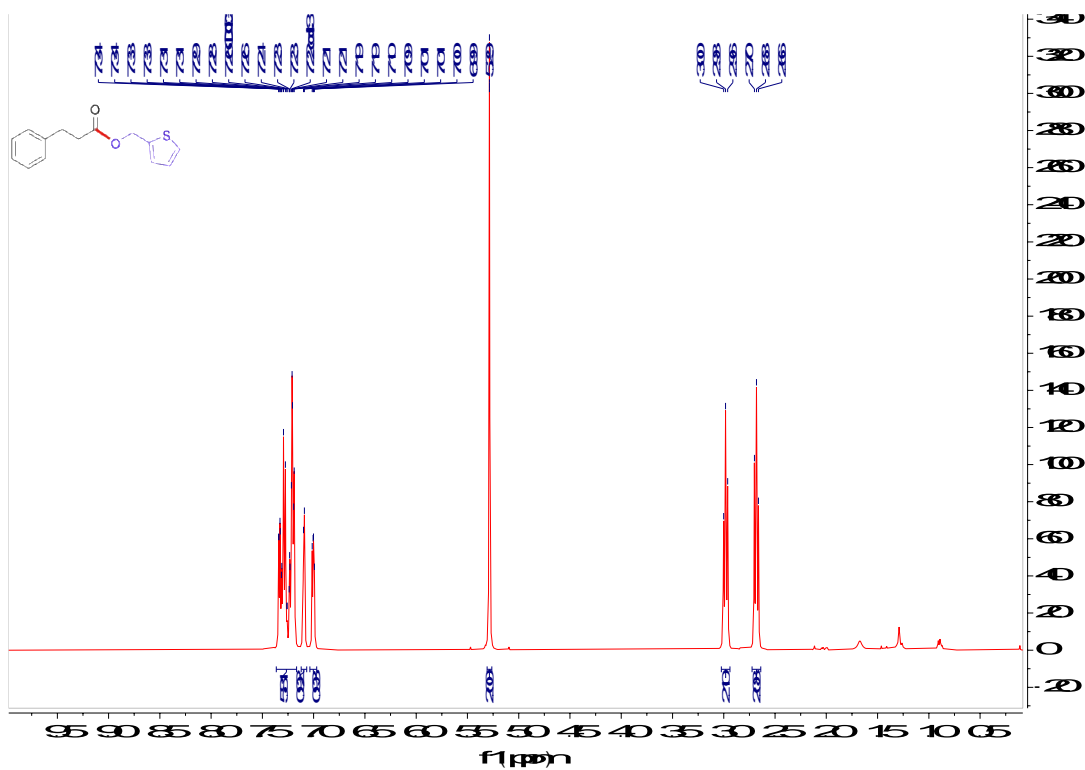
¹³C NMR spectrum of *n*-Octyl 3-(furan-2-yl)propanoate (16)



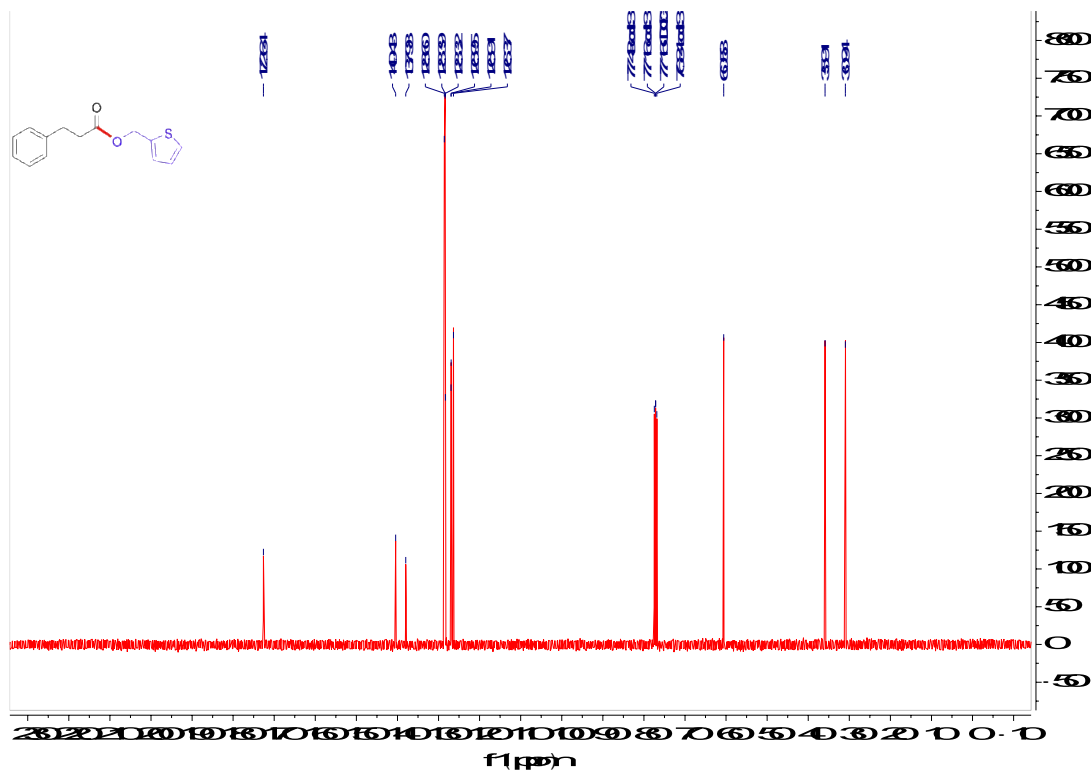
¹H NMR spectrum of Phenethyl 3-(thiophen-2-yl)propanoate (23)



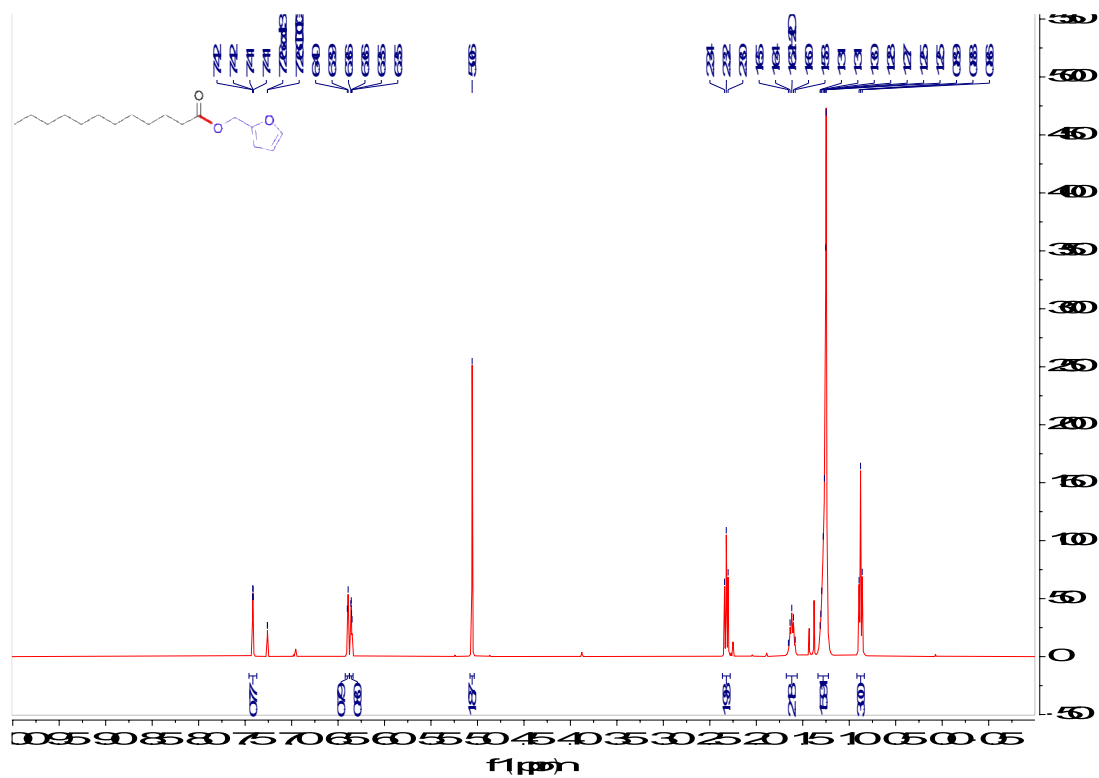
¹³C NMR spectrum of Phenethyl 3-(thiophen-2-yl)propanoate (23)



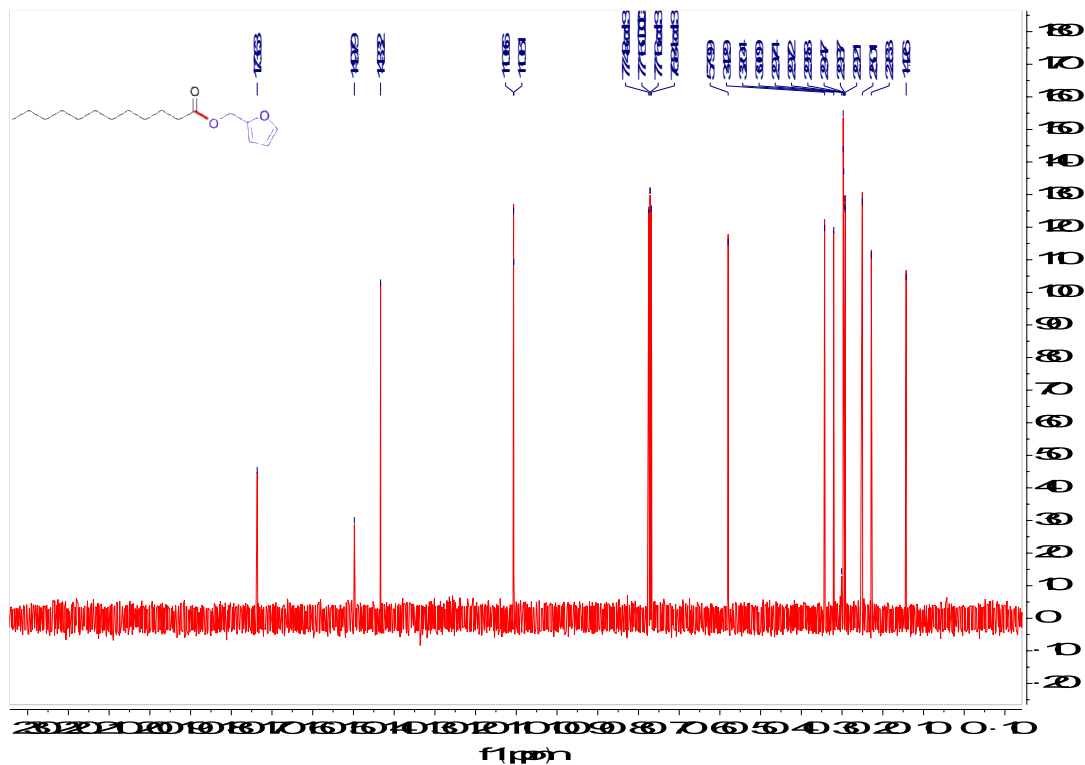
¹H NMR spectrum of Thiophen-2-ylmethyl 3-phenylpropanoate (24)



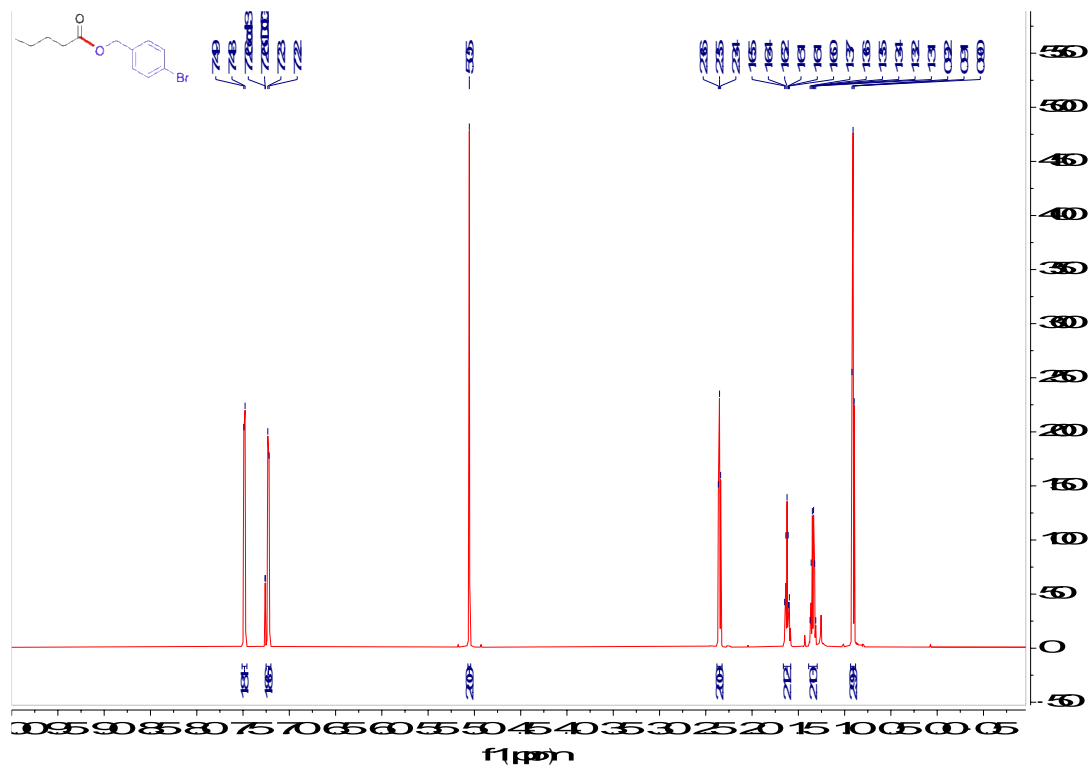
¹³C NMR spectrum of Thiophen-2-ylmethyl 3-phenylpropanoate (24)



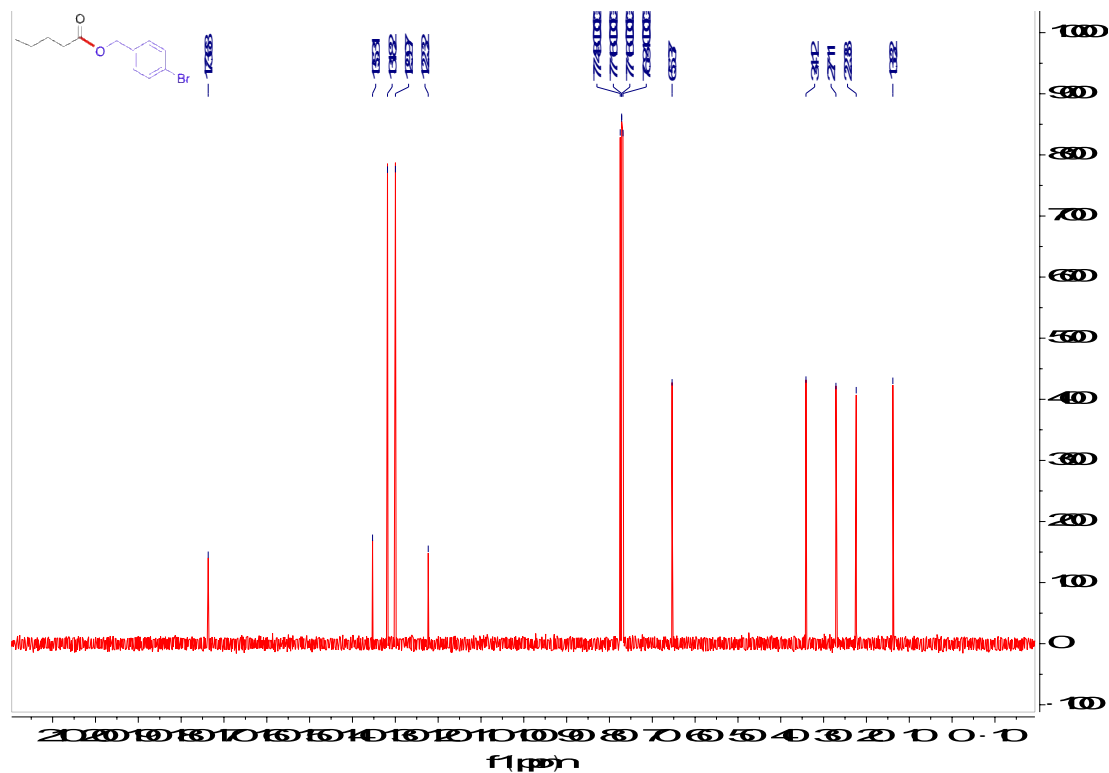
¹H NMR spectrum of Furan-2-ylmethyl dodecanoate (**26**)



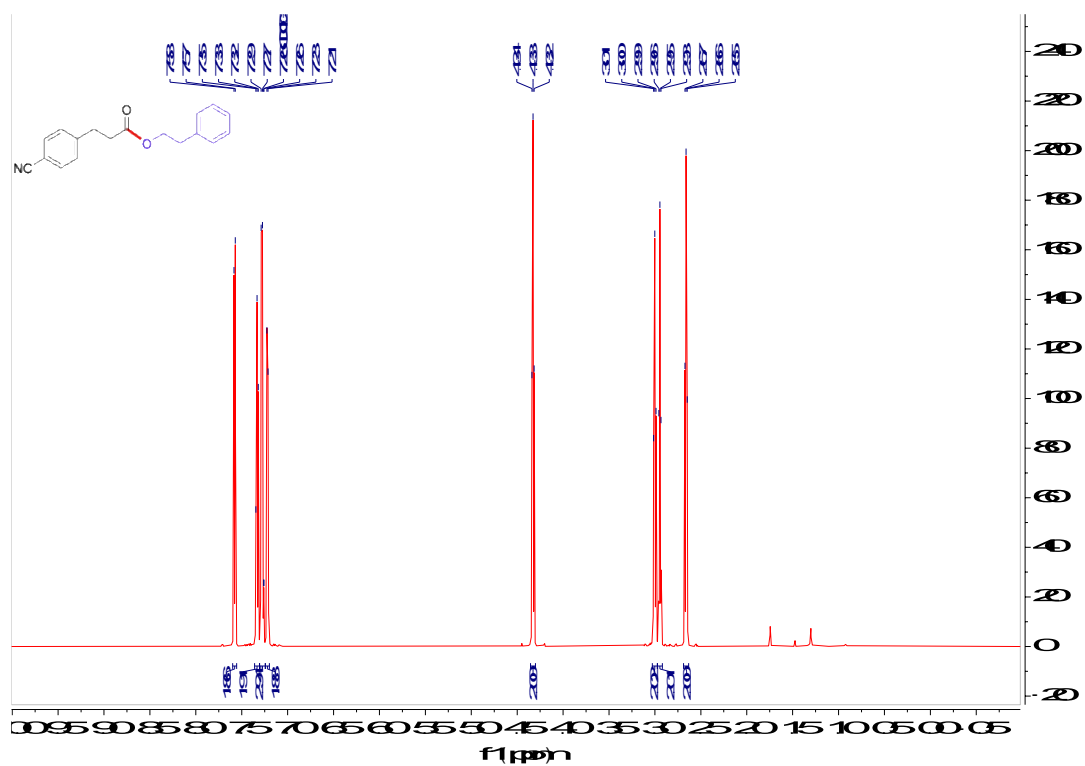
¹³C NMR spectrum of Furan-2-ylmethyl dodecanoate (**26**)



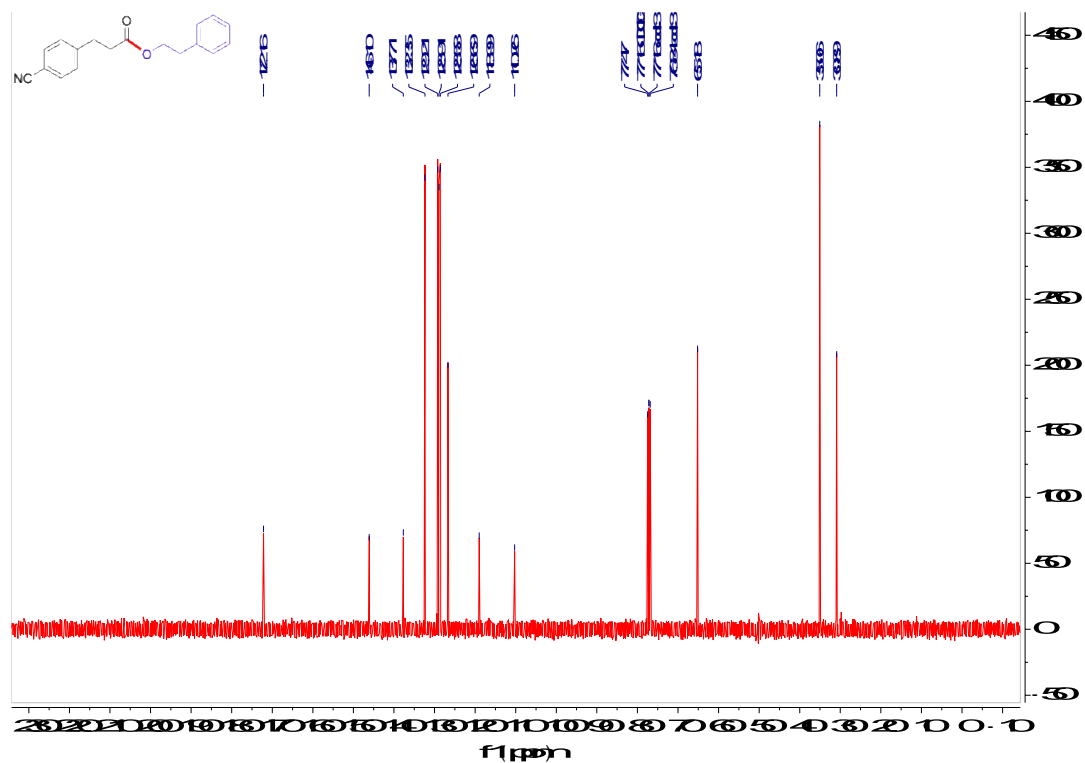
¹H NMR spectrum of 4-Bromobenzyl pentanoate (27)



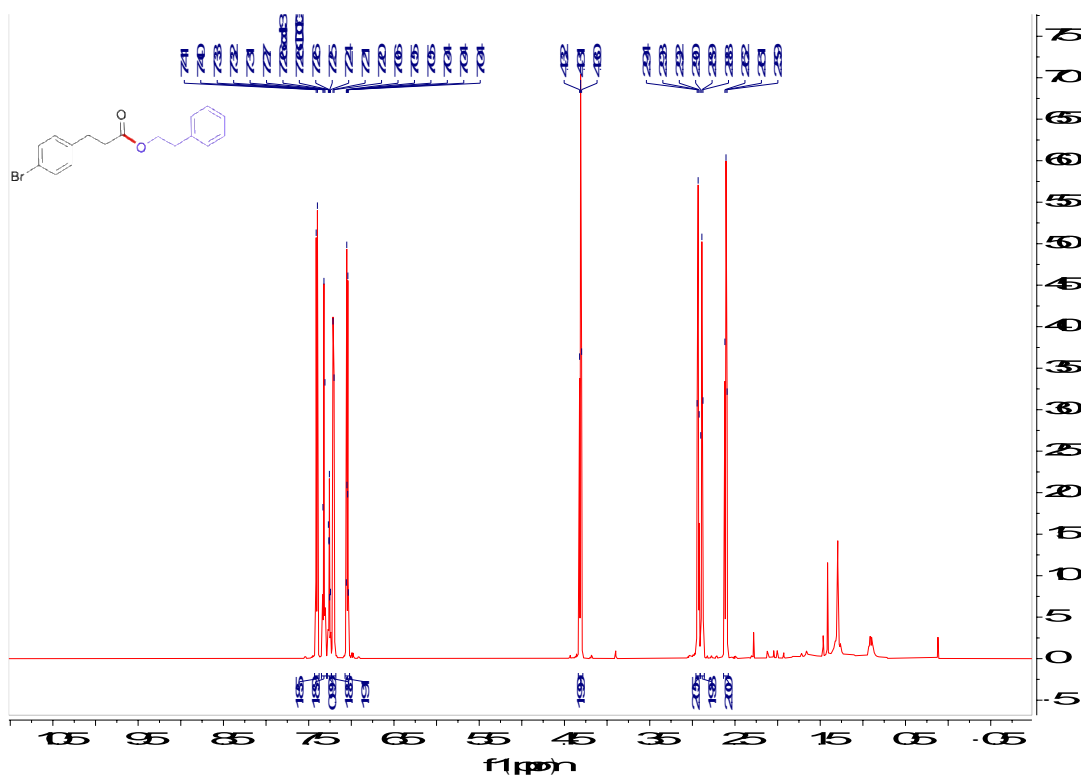
¹³C NMR spectrum of 4-Bromobenzyl pentanoate (27)



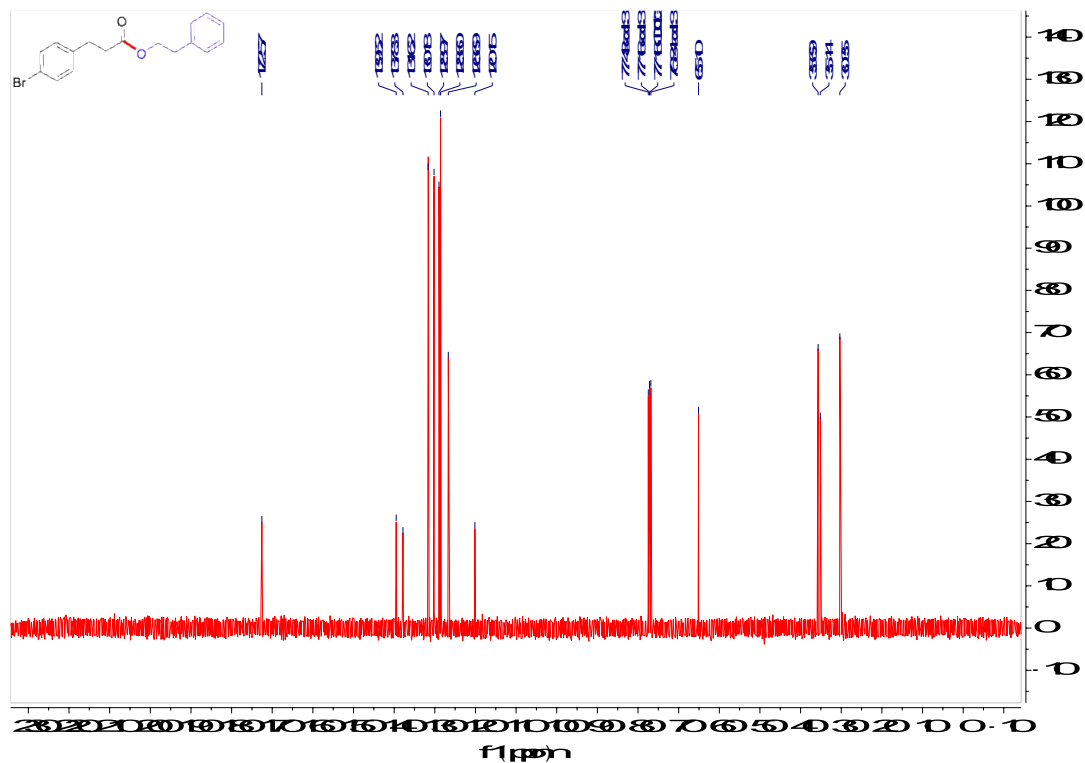
¹H NMR spectrum of Phenethyl 3-(4-cyanophenyl)propanoate (28)



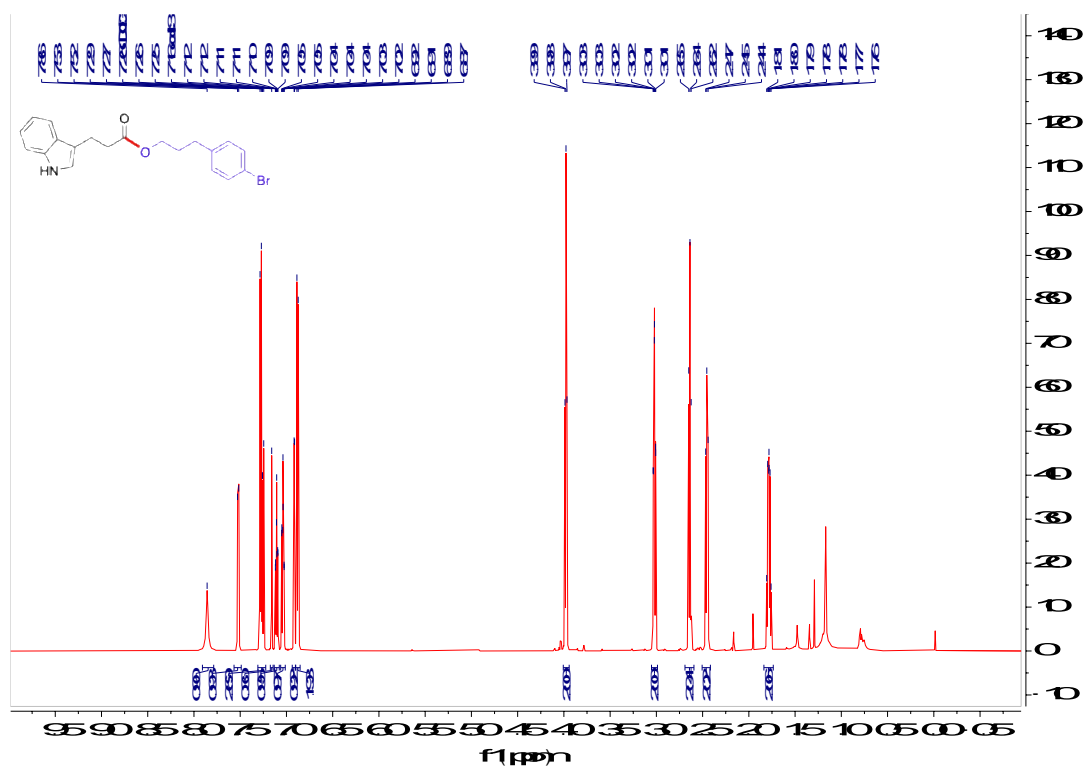
¹³C NMR spectrum of Phenethyl 3-(4-cyanophenyl)propanoate (28)



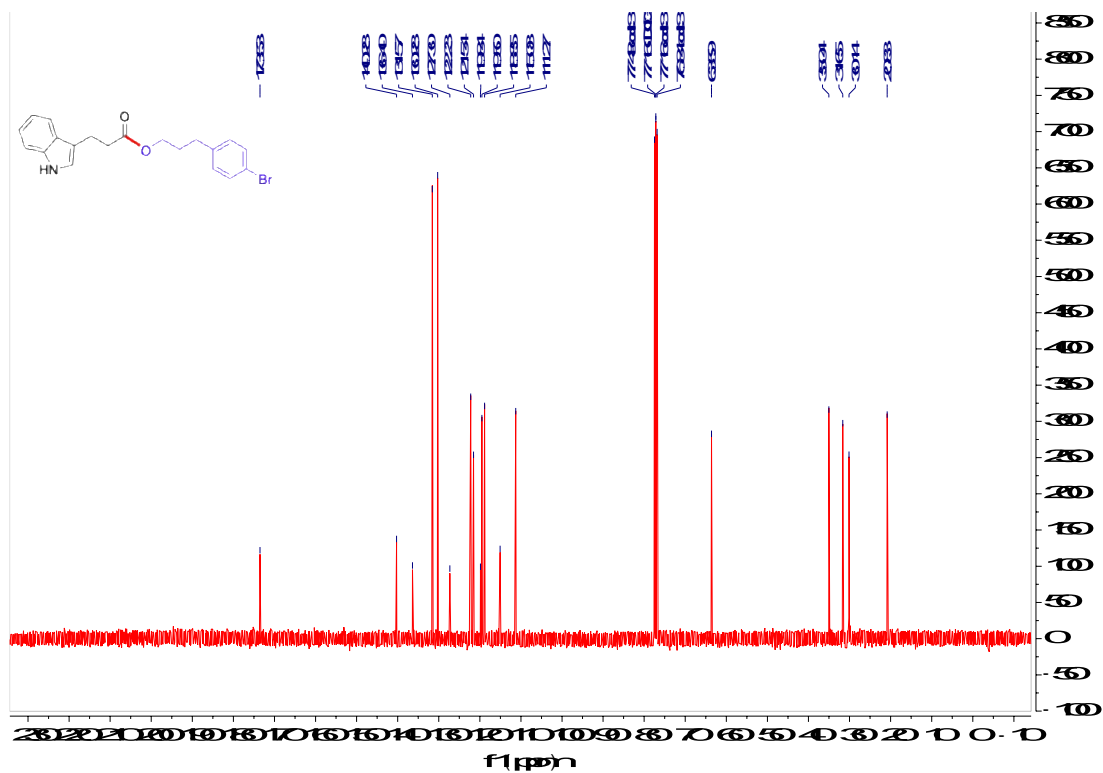
¹H NMR spectrum of Phenethyl 3-(4-bromophenyl)propanoate (29)



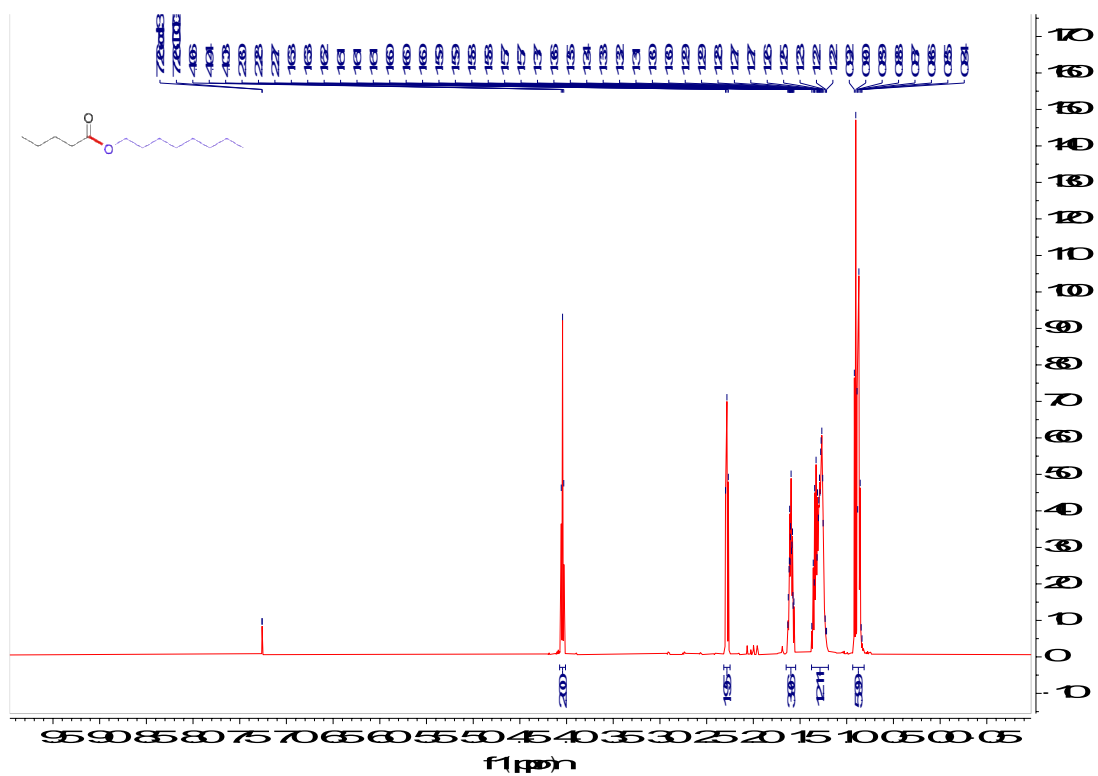
¹³C NMR spectrum of Phenethyl 3-(4-bromophenyl)propanoate (29)



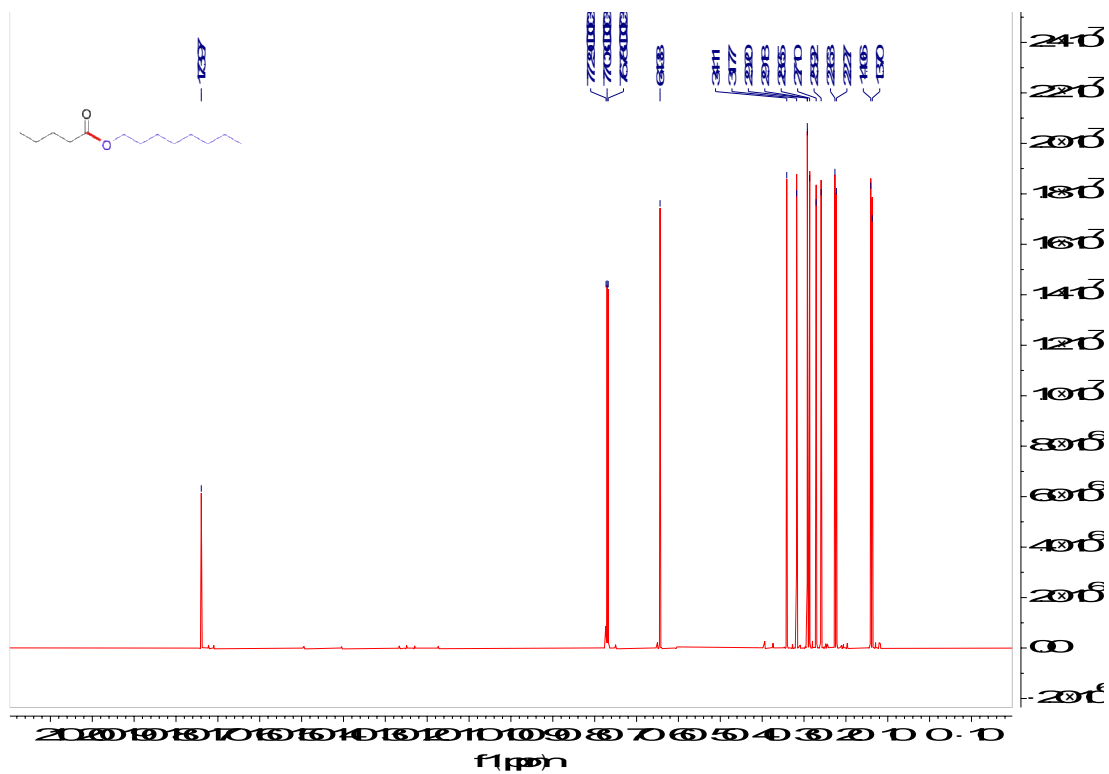
¹H NMR spectrum of 3-(4-Bromophenyl)propyl 3-(1H-indol-3-yl)propanoate (30)



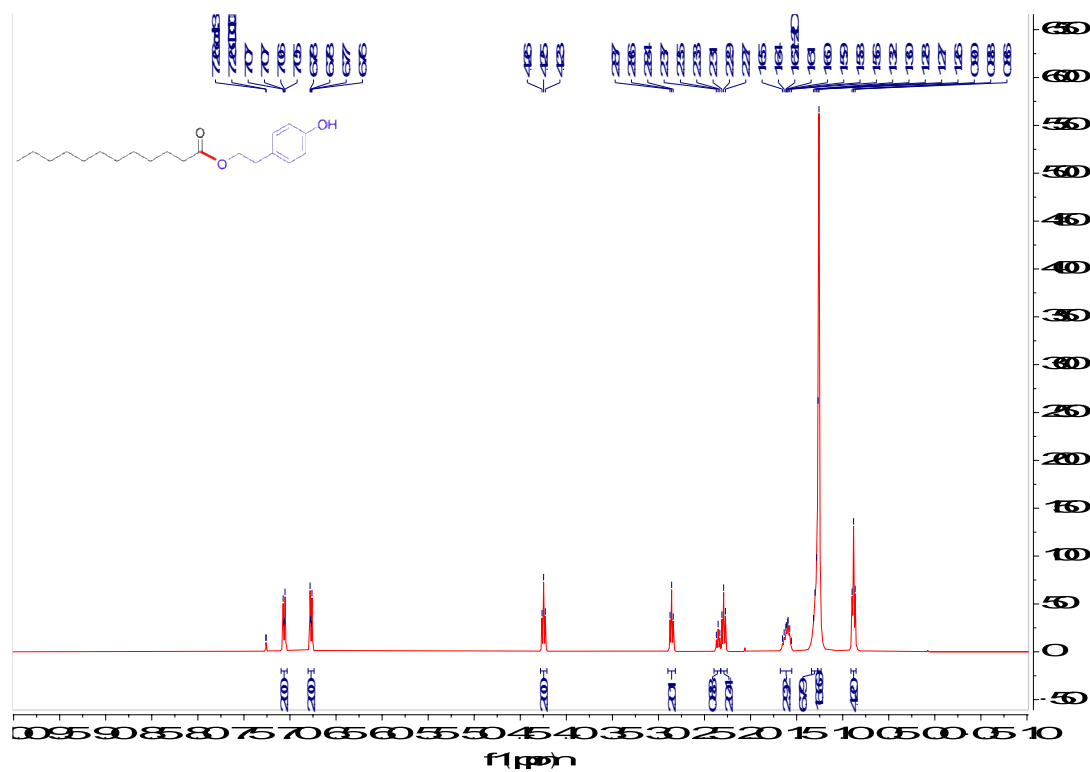
¹³C NMR spectrum of 3-(4-Bromophenyl)propyl 3-(1H-indol-3-yl)propanoate (30)



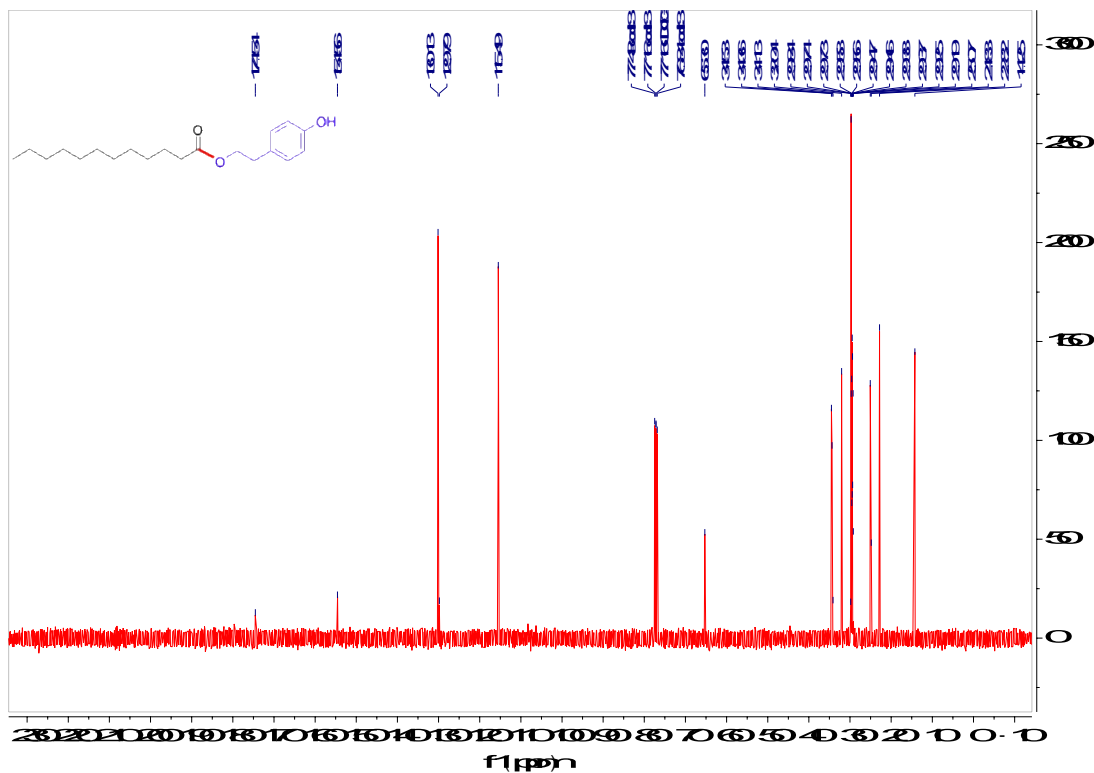
¹H NMR spectrum of *n*-Octyl pentanoate (35)



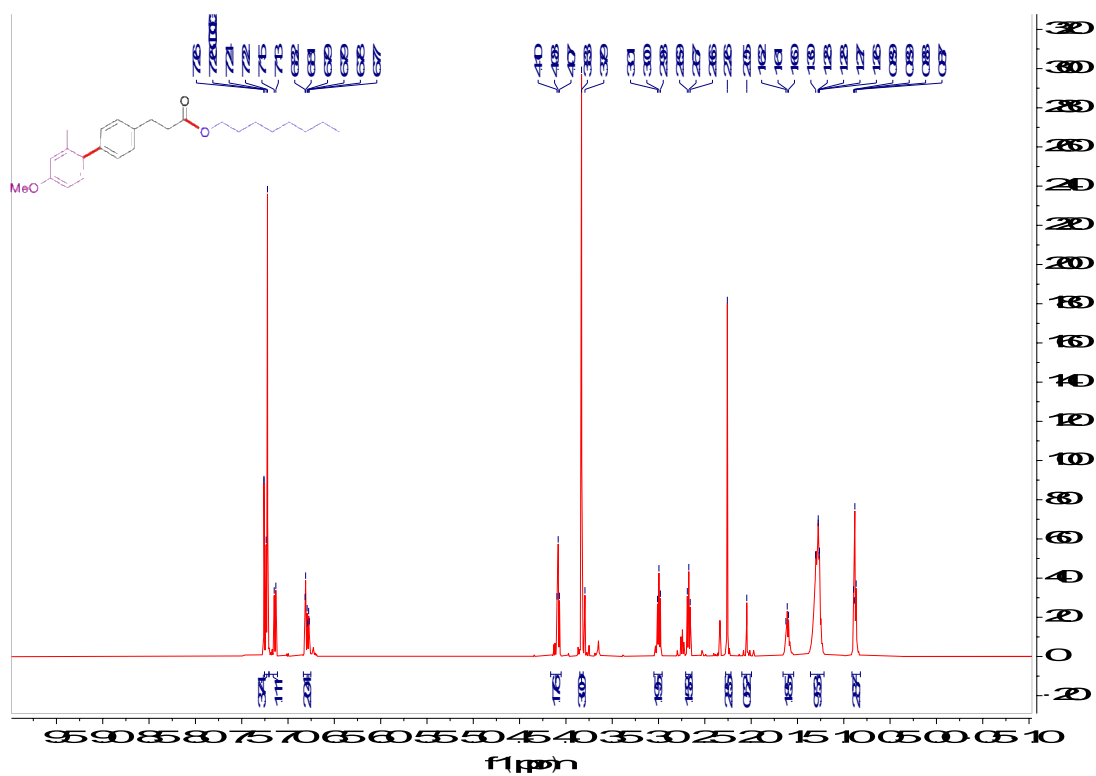
¹³C NMR spectrum of *n*-Octyl pentanoate (35)



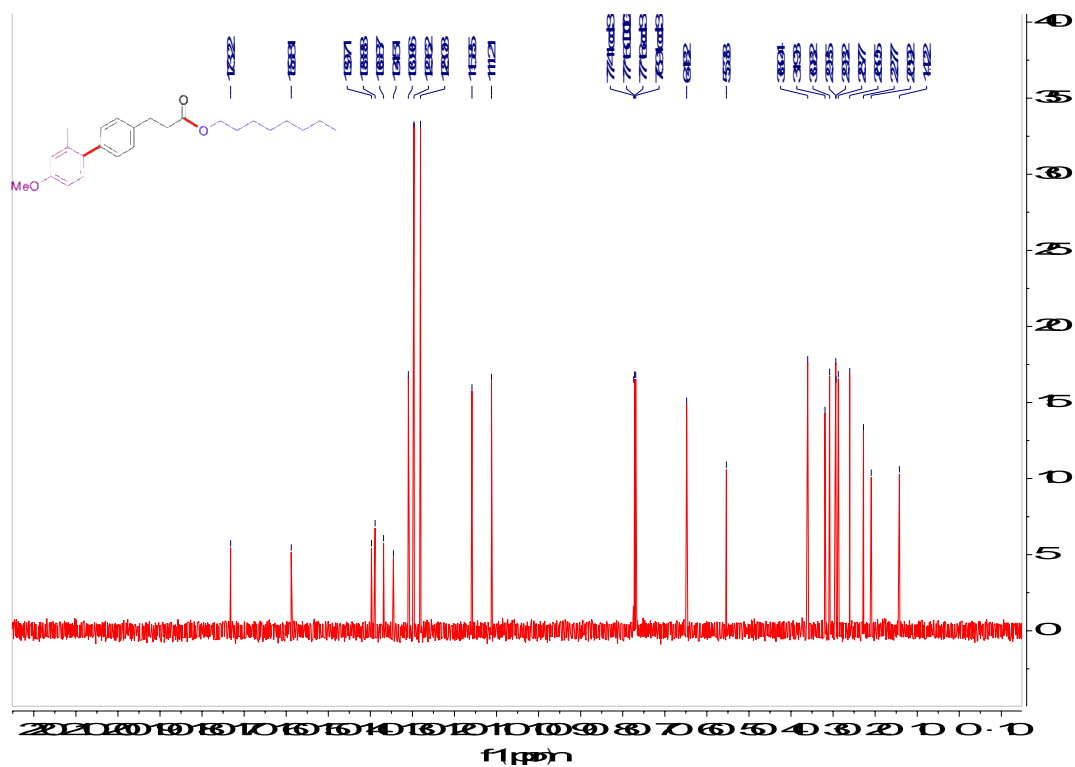
^1H NMR spectrum of 4-Hydroxyphenethyl dodecanoate (36)



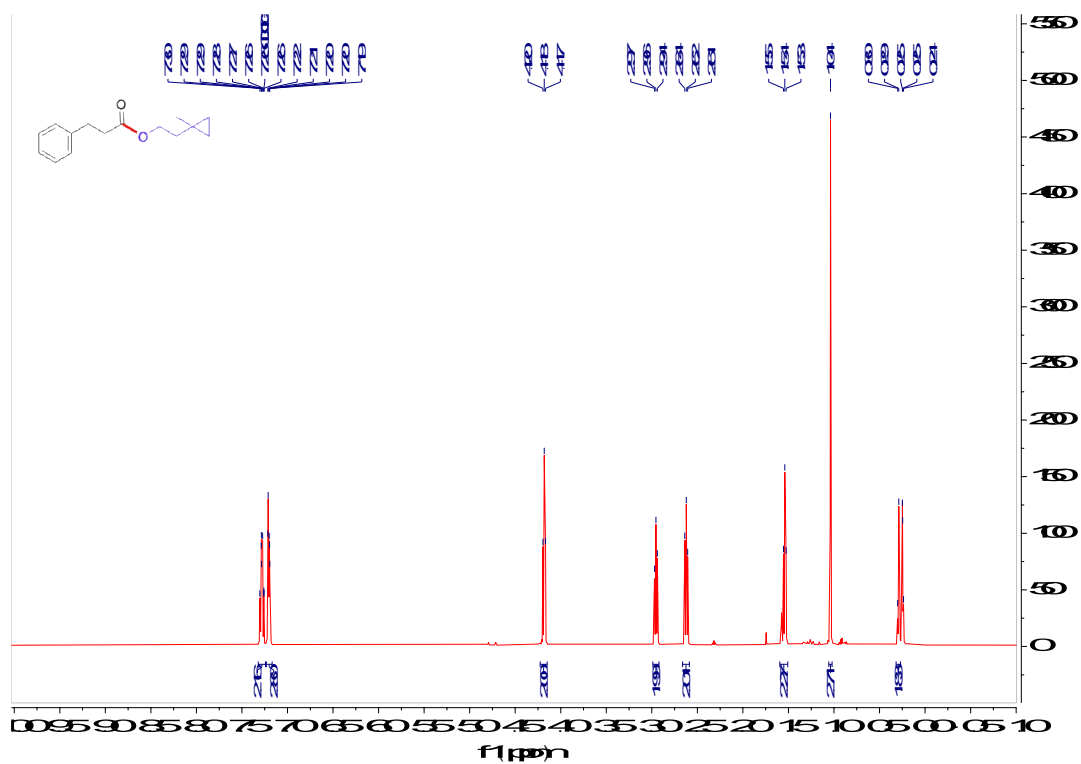
^{13}C NMR spectrum of 4-Hydroxyphenethyl dodecanoate (36)



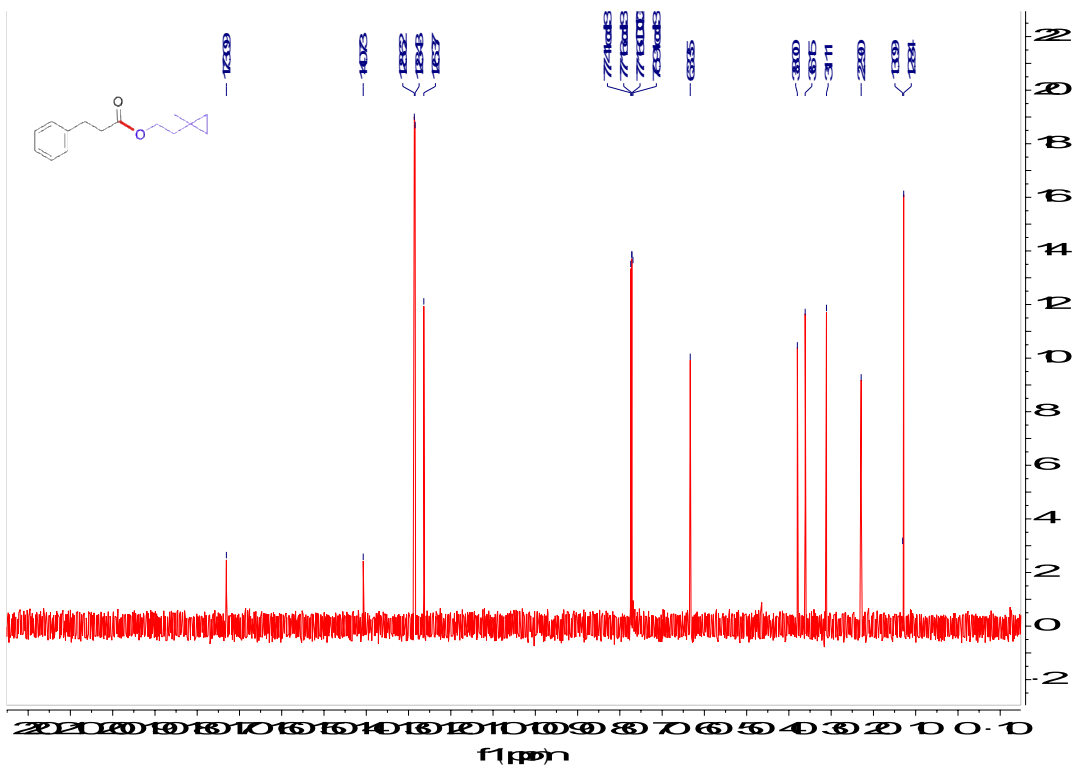
¹H NMR spectrum of Octyl 3-(4'-methoxy-2'-methyl-[1,1'-biphenyl]-4-yl)propanoate (44)



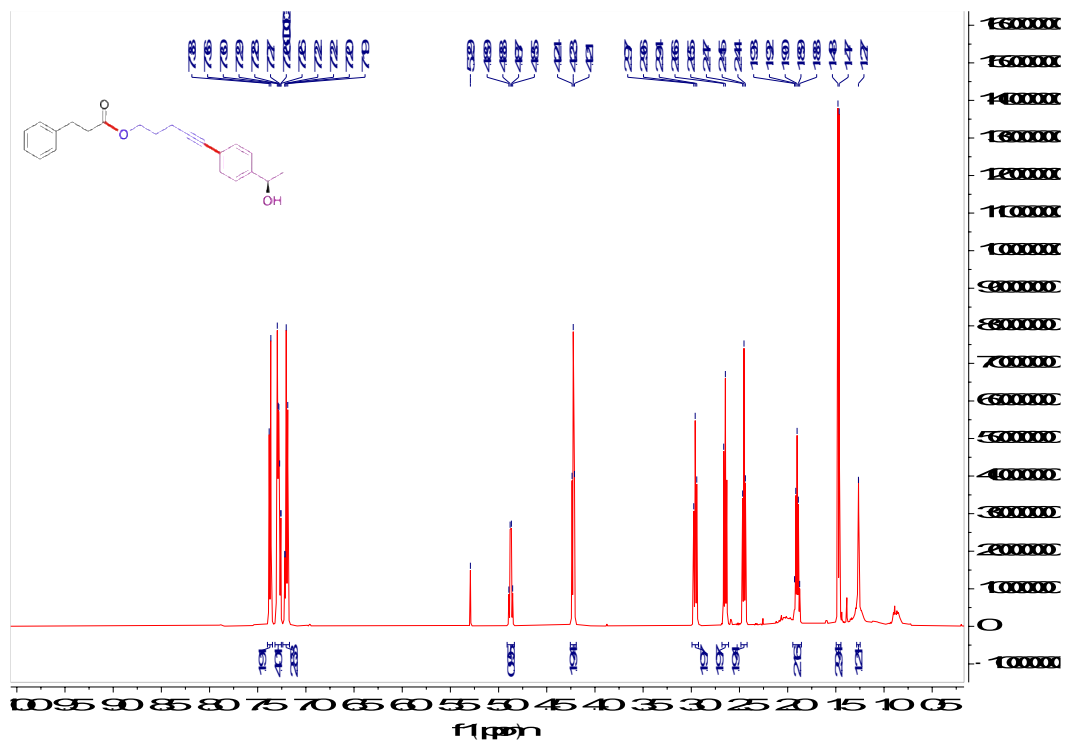
¹³C NMR spectrum of Octyl 3-(4'-methoxy-2'-methyl-[1,1'-biphenyl]-4-yl)propanoate (44)

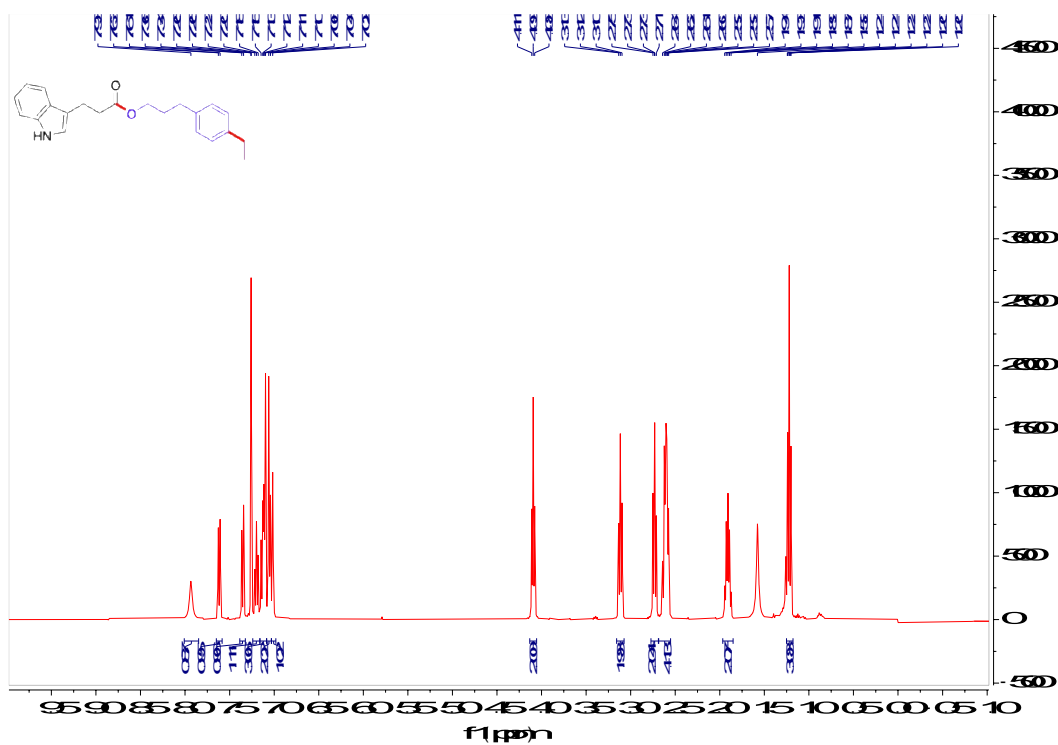


¹H NMR spectrum of 2-(1-Methylcyclopropyl)ethyl 3-phenylpropanoate (**48**)

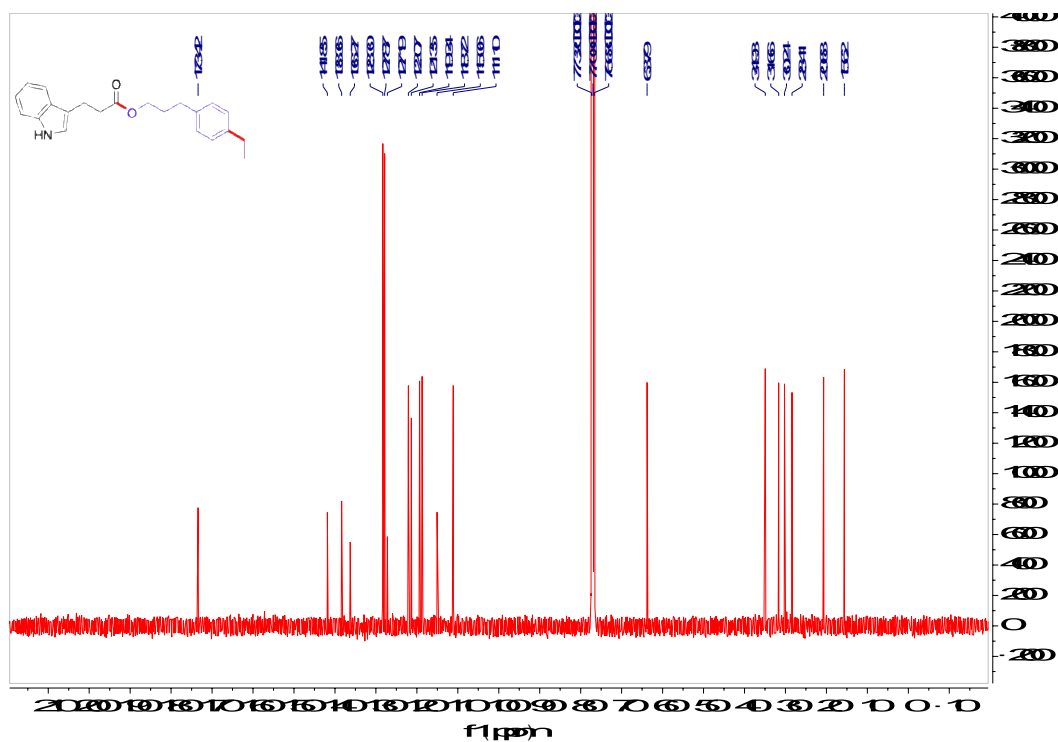


¹³C NMR spectrum of 2-(1-Methylcyclopropyl)ethyl 3-phenylpropanoate (**48**)





¹H NMR spectrum of 3-(4-Ethylphenyl)propyl 3-(1H-indol-3-yl)propanoate (57)



¹³C NMR spectrum of 3-(4-Ethylphenyl)propyl 3-(1H-indol-3-yl)propanoate (57)

2. A streamlined, sustainable synthesis of the anticancer drug erdafitinib

Singhania, V.; Nelson, C. B.; Reamey, M.; Morin, E.; Kavthe, R. D.; Lipshutz, B. H., A streamlined, green and sustainable synthesis of the anticancer agent erdafitinib *Org. Lett.* **2023**, Article ASAP.

DOI: [10.1021/acs.orglett.3c01380](https://doi.org/10.1021/acs.orglett.3c01380)

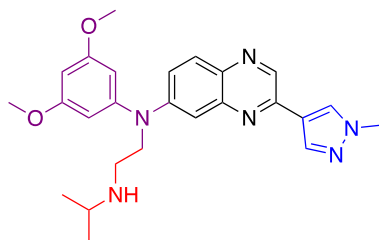
Copyright 2023 American Chemical Society.

Reproduced with permission.

2.1. Introduction and background

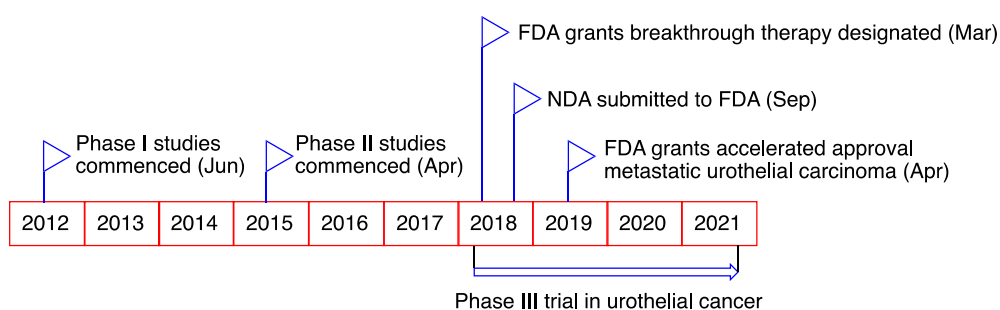
Erdafitinib, commercially sold under the brand name Balversa, is a potent anticancer drug that targets urothelial carcinoma, a very common type of bladder cancer, by acting as a selective small molecule tyrosine kinase inhibitor of pan-fibroblast growth factor receptor (FGFR).¹ It is one of the limited therapeutic options applicable to patients who have locally advanced or metastatic bladder cancer with tumors that have FGFR3 or FGFR2 mutation that has progressed during or after previously administered frontline platinum-containing chemotherapy.¹

Figure 1. Structure of the anticancer drug erdafitinib



It was first developed by Janssen in collaboration with Astex Pharmaceuticals and received accelerated approval from the US FDA in 2019 due to its established efficacy resulting from its oral administration in clinical trials (Figure 2).² Erdafitinib was dubbed a blockbuster that was in line for \$1 billion sales as the company was pricing it in the range of \$10,080 to \$22,680 for a month's supply depending on dosage (56 oral tablets of 3 mg each).³

Figure 2. Milestones in the development of erdafitinib



Currently, erdafitinib is also being investigated for its potential as a therapeutic agent for bile duct, liver, prostate, lymphoma, esophageal, and non-small cell lung cancers.⁴ An ongoing clinical trial, RAGNAR investigates evidence of efficacy or maximum response for erdafitinib in heavily pretreated patients with various hard to treat advanced malignances (Table 1). A total of 178 patients of median age 56.5 (range 12-79) were treated and responses in 14 distinct tumor types were observed.⁵

Table 1. Results from phase II clinical trial for erdafitinib

<u>entry</u>	<u>tumor type</u>	<u>number of patients treated</u>	<u>IA ORR* number (%)</u>
1	total	178	47 (26.4)
2	bile duct cancer	31	13 (41.9)
3	breast	14	6 (20.7)
4	pancreatic	13	4 (30.8)
5	lung cancer	11	3 (27.3)
6	endometrial	6	2 (33.3)
7	esophageal	6	1 (16.7)

8	ovarian	4	1 (25)
9	salivary gland	5	5 (100)
10	thyroid	1	1 (100)

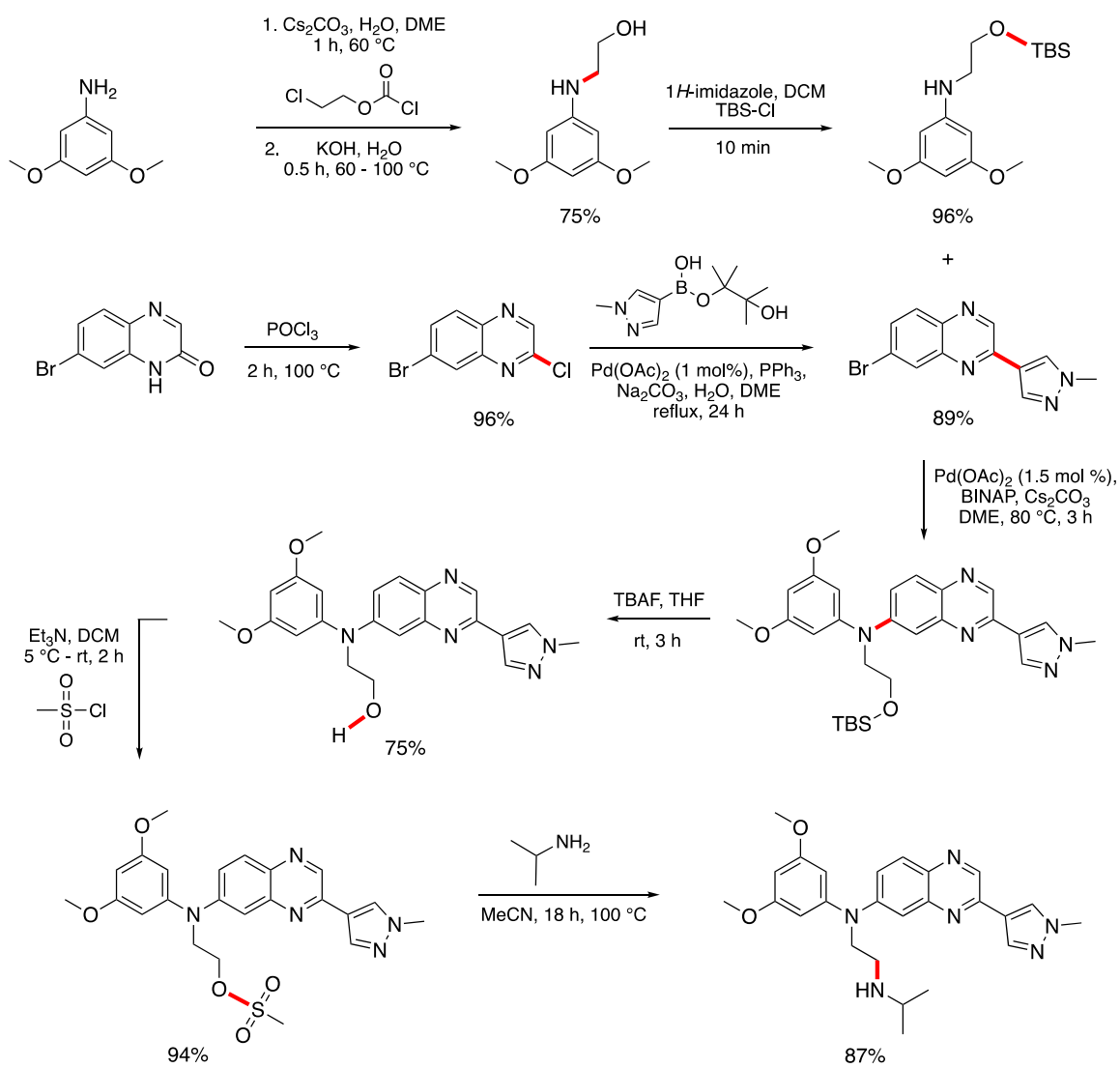
*Investigator assessed objective response rate

Unfortunately, while erdafitinib has shown considerable promise in these clinical applications, its current method of synthesis relies on several unattractive parameters, including (a) required elevated reaction temperatures, (b) unsustainable and costly loadings of precious metal (palladium)-based catalysts, and (c) reliance on toxic, flammable, and environmentally egregious organic solvents.⁶⁻¹⁰

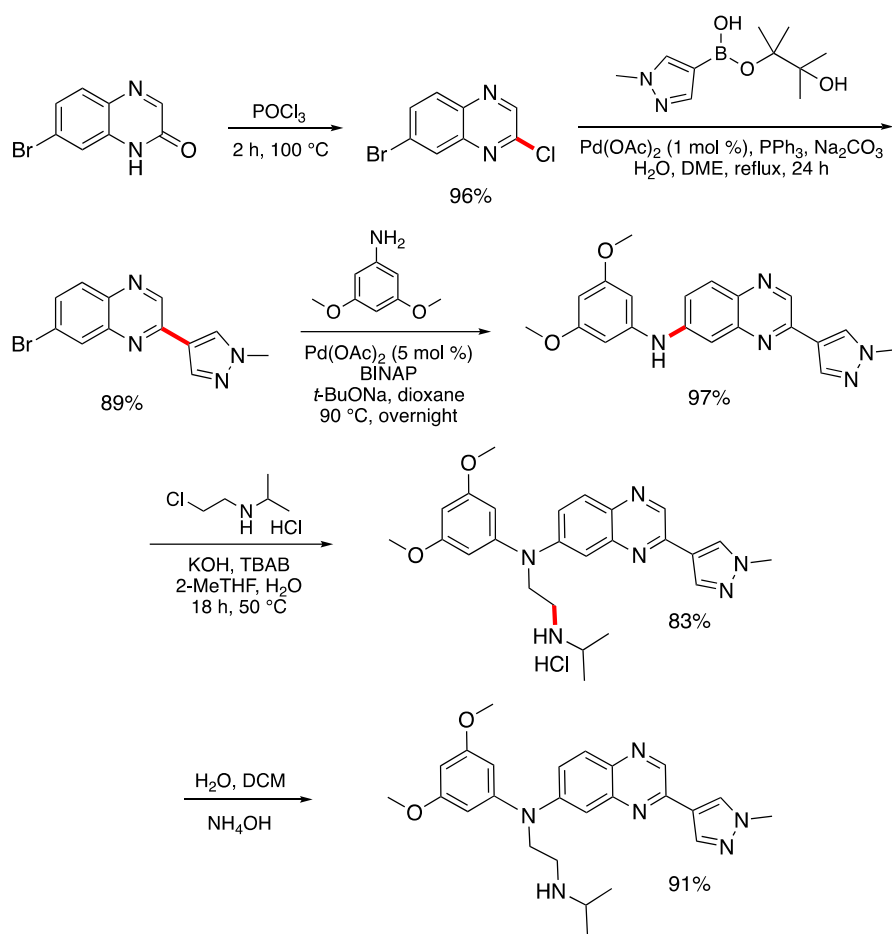
Amongst many, the reported 6-step convergent route and 4-step linear route described in the original patent is shown in Schemes 1 and 2, respectively.¹¹ Saxty from Astex Pharmaceuticals and co-workers describe the synthesis of erdafitinib and its analogs in the initial patent published in 2011.

The route to this pharmaceutical via a Suzuki-Miyaura cross-coupling and amination reaction has not been improved since. These processes require unsustainable and costly catalyst loadings and are oftentimes conducted in various waste-generating organic solvents. Hence, there is ample room for improvement in the category of ‘greenness’ of the methodology. Herein, we report a 3-step, 2-pot synthesis of erdafitinib enabled by aqueous micellar media using a biodegradable surfactant and a green solvent, 2-MeTHF.

Scheme 1. A 6-step, convergent route to erdafitinib (Astex Pharmaceuticals)



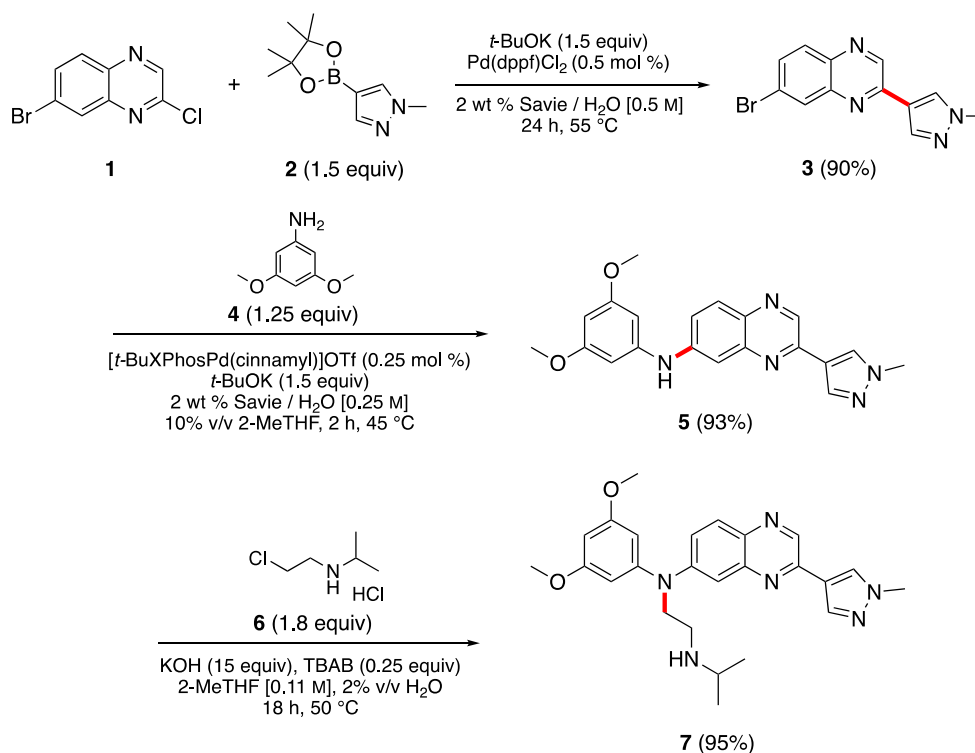
Scheme 2. A 4-step, linear route to erdafitinib (Astex Pharmaceuticals)



2.2. Results and Discussion

A new, improved and greener synthetic route to erdafitinib is outlined in Scheme 3. The synthesis was accomplished by performing two sequential, Pd-catalyzed cross-couplings; that is, an initial Suzuki-Miyaura reaction followed by an amination. These catalytic processes can be performed in a 1-pot fashion as well. The final step involved a nucleophilic substitution reaction that afforded the final drug in 80% overall yield.

Scheme 3. Greener and potentially economically attractive synthetic route to erdafitinib

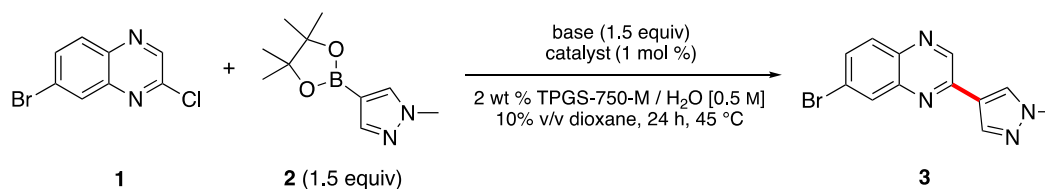


2.2.1. Optimization of Step 1: Suzuki-Miyaura reaction

For optimization of this first, C-C bond forming step, the heteroaryl chloride, 7-bromo-2-chloroquinoxaline (**1**) was treated with 1-methylpyrazole-4-boronic acid pinacol ester (**2**) to afford intermediate **3**, 7-bromo-2-(1-methyl-1*H*-pyrazol-4-yl)quinoxaline (Table 2). The reaction was initially performed at 45 °C with only 1 mol % of a Pd catalyst under aqueous micellar conditions.¹²⁻¹³ For optimization of the reaction conditions, base, surfactant, temperature, catalyst, along with catalyst loading were tested (Table 2, a-d). This screening led to commercially available Pd(dppf)Cl₂ as catalyst, accompanied by 1.5 equivalents of *t*-BuOK as the base as the most effective combination.

Table 2. Optimization of Suzuki-Miyaura reaction

a. Screening of catalyst and base

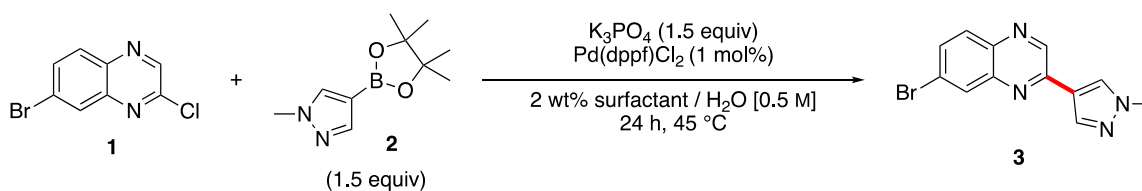


entry	catalyst (ligand)*	base	NMR yield (%)
1	Pd(PPh ₃) ₄	K ₃ PO ₄	35
2	Pd(OAc ₂) (SPhos)	K ₃ PO ₄	9
3	Pd(OAc ₂) (EvanPhos)	K ₃ PO ₄	19
4	[<i>t</i> -BuXPhosPd(allyl)]OTf	K ₃ PO ₄	2
5	Pd ₂ (dba) ₃	K ₃ PO ₄	2

6	Pd(dba) ₂	K ₃ PO ₄	2
7	XPhos-Pd-G3	K ₃ PO ₄	29
8	Pd-PEPPSI-IPent	K ₃ PO ₄	2
9	Pd(dppf)Cl ₂	K ₃ PO ₄	80
10	Pd(dppf)Cl ₂	NEt ₃	86
11	Pd(dppf)Cl ₂	K ₂ CO ₃	79
12	Pd(dppf)Cl ₂	<i>t</i> -BuONa	74
13	Pd(dppf)Cl ₂	<i>t</i> -BuOK	87
14	Pd(dppf)Cl ₂	<i>t</i> -BuOK (1.0 equiv)	67
15	Pd(dppf)Cl ₂	<i>t</i> -BuOK (2.0 equiv)	72

*catalyst : ligand (1 : 1.8)

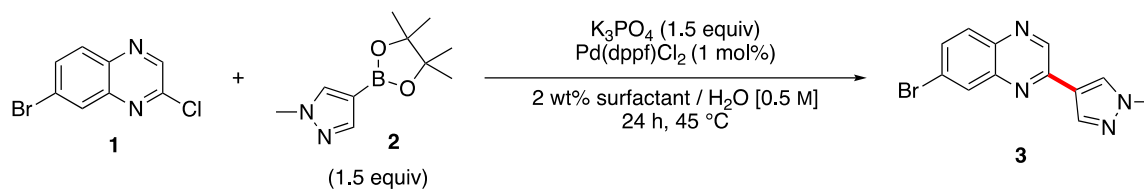
b. Screening of surfactant solution



entry	surfactant	NMR yield (%)
1	none	65
2	TPGS-750-M	80
3	Brij-30	52
4	PTS-600	77
5	MC1	54

6	DMF	62
7	Savie	80

c. Screening of base and temperature

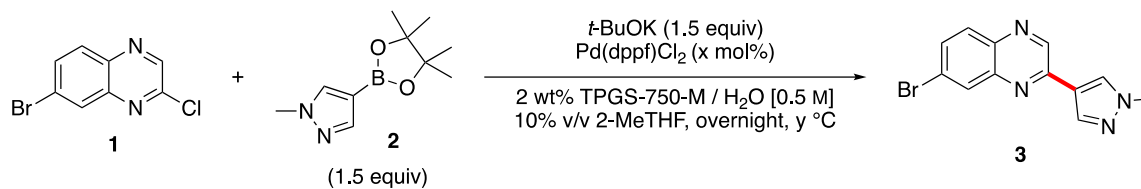


entry	base	temp. (°C)	NMR yield (%)
1	K_3PO_4	45	80
2	NEt_3	45	86
3	K_2CO_3	45	79
4	<i>t</i> -BuOK	25	73
5	<i>t</i> -BuOK	45	87
6	<i>t</i> -BuOK	60	60
7	<i>t</i> -BuONa	25	34
8	<i>t</i> -BuONa	45	74
9	<i>t</i> -BuONa	60	67
10	<i>t</i> -BuOK (1.0 equiv)	45	67
11	<i>t</i> -BuOK (2.0 equiv)	45	72
12	<i>t</i> -BuOK*	45	92
13	<i>t</i> -BuOK*	60	44

14	Cs ₂ CO ₃ *	45	76
15	Cs ₂ CO ₃ *	60	80

*no co-solvent

d. Screening of catalyst loading and temperature



entry	cat loading (mol%)	temp (°C)	NMR yield (%)
1	2.0	45	82
2	1.0	45	87
3	0.5	45	74
4	0.25	45	73
5	0.1	45	50
6	2.0	60	79
7	1.0	60	77
8	0.5	60	79
9	0.25	60	66
10	0.1	60	44

Note: Pd(dppf)Cl₂ (<2 mol %) was added by preparing a stock solution of Pd(dppf)Cl₂ in 2-MeTHF.

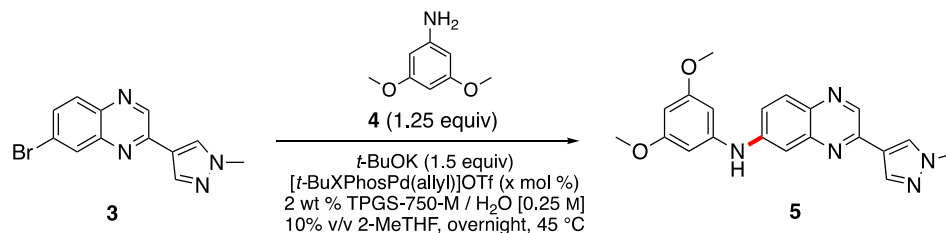
5	surfactant: Savie, no co-solvent, 0.5 mol % Pd, 55 °C	90*
---	---	-----

*Isolated yield using column chromatography

2.2.2. Optimization of Step 2: amination reaction

For optimization of the amination cross-coupling, aryl bromide (**3**) formed from step 1 was employed to perform amination using coupling partner, 3, 5-dimethoxyaniline (**4**) to afford the diarylamine **5**. To increase solubility of the reagents and starting materials in this aqueous reaction mixture, a small volume (10% v/v) of 2-MeTHF, a green co-solvent,¹⁵ was added and the reaction mixture was diluted to a 0.25 M global concentration (Table 4). As observed in the amination work done by Yitao and co-workers, out of the *t*-BuXPhos-based Pd complexes screened, the more lipophilic pre-catalyst, [*t*-BuXPhosPd(cinnamyl)]OTf demonstrated highest product conversions under micellar catalysis conditions,¹⁶ leading to complete consumption of starting material in less than two hours (entries 14-16). The biodegradable surfactant, Savie yet again, demonstrated greatest enabling properties, further strengthening the original claims associated with its potential use in sustainable drug syntheses.

Table 4. Optimization of the amination of bromide **3**



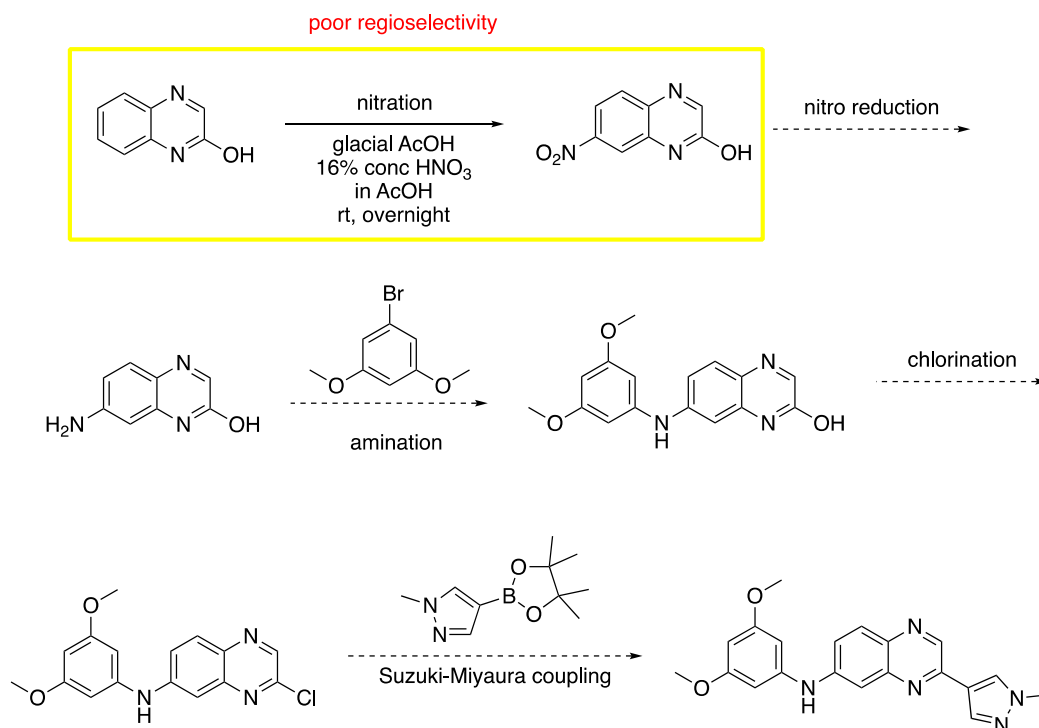
entry	catalyst loading (mol %)	deviation from standard conditions	NMR yield (%)
1	1	-	99
2	1	co-solvent: dioxane	83
3	1	0.5 M conc, co-solvent: dioxane	42
4	1	no co-solvent	72
5	-	no catalyst	trace
6	-	no catalyst, no co-solvent	trace
7	1	temperature: 60 °C	75
8	2	-	96
9	0.5	-	98
10	0.25	-	99
11	0.1	-	62
12	0.05	-	36
13	1	[<i>t</i> -BuXPhosPd(cinnamyl)]OTF	99
14	1	[<i>t</i> -BuXPhosPd(cinnamyl)]OTF, 4 h	99
15	1	[<i>t</i> -BuXPhosPd(cinnamyl)]OTF, 4 h, surfactant: Savie	99
16	0.25	[<i>t</i> -BuXPhosPd(cinnamyl)]OTF, 2 h, surfactant: Savie	93*

*Isolated yield by filtration

In this work, standalone amination employing water as reaction medium was very successful, affording diarylamine product **5** in two hours with a low Pd catalyst loading of only 0.25 mol % (i.e., 2500 ppm). This is in marked contrast to the far higher loadings of precious metal, Pd, typically required for such C-N bond formations in organic solvents.¹⁷ In addition, and also unlike the corresponding aminations in traditional Pd-catalyzed couplings, this far more sustainable method does not require column chromatography; the product can be easily isolated by filtration. Step 2 individually yielded 93% of pure product **5**.

Alternatively, compound **5** can be synthesized using a cheaper starting material, 2-quinoxalinol, however, it is a longer route involving a five step synthetic process (Scheme 4).

Scheme 4. Alternative route to amine **5**

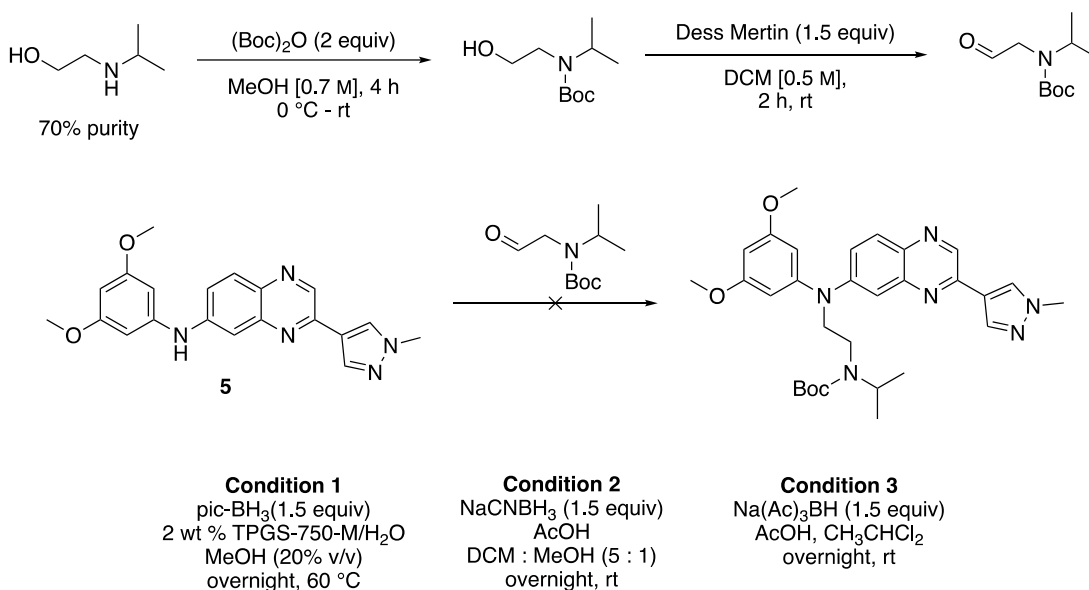


The first step of the method entails nitration of 2-quinoxalinol. Attempts to synthesize 7-nitro-2-quinoxalinol using the procedure outlined in the literature was successful in consuming the starting material but failed to result in high regioselectivity.¹⁸ Due to difficulty in isolation of the required nitro product, this route was not pursued further.

2.2.3. Optimization of the final step to erdafitinib

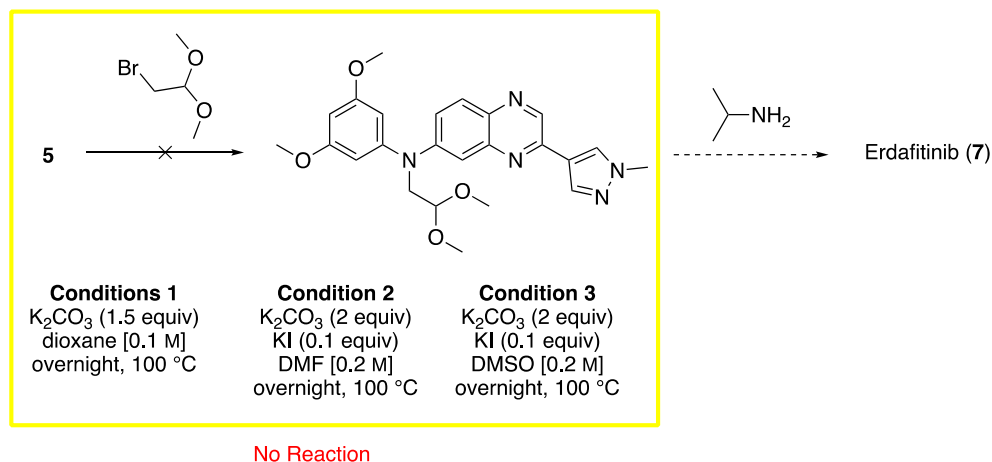
The third and final step of this short route to anticancer drug erdafitinib was the most challenging. Attempts to perform reductive amination utilizing diaryl amine **5** were in vain. Thus, the *N*-Boc-protected 2-(isopropylamino)acetaldehyde was synthesized using literature methodology (Scheme 5).¹⁹ Use of the acetaldehyde along with α -picolineborane, sodium cyanoborohydride or sodium triacetoxyborohydride failed to provide the targeted amine (Scheme 5).²⁰

Scheme 5. Attempts at reductive amination using amine **5**



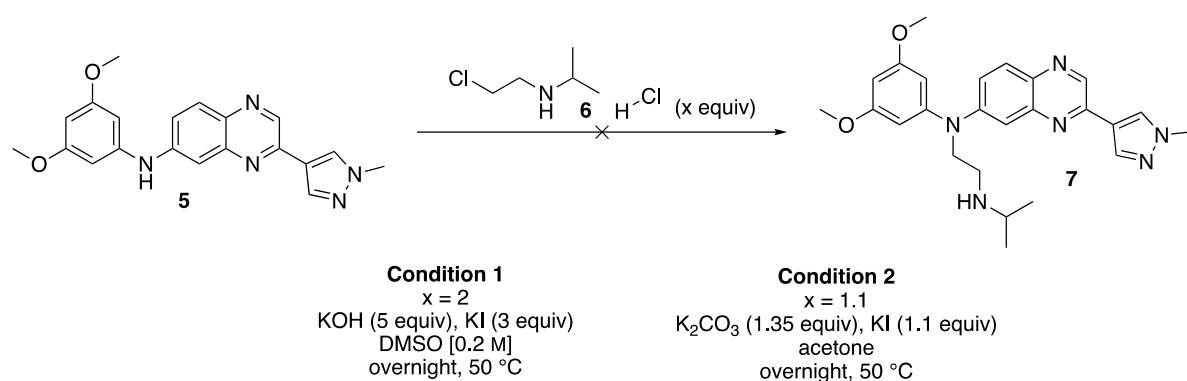
In attempts to attach the last piece of the molecule to erdafitinib, nucleophilic substitution reaction using **5** was attempted (Scheme 6). The economically attractive and commercially available halide, 2-bromo-1,1-dimethoxyethane was initially used to react with **5** which could ultimately undergo reductive amination with isopropyl amine to provide our final product drug, **7**. However, nucleophilic attack on alkyl bromide in various organic solvents was fruitless.

Scheme 6. Potential alternative route to erdafitinib



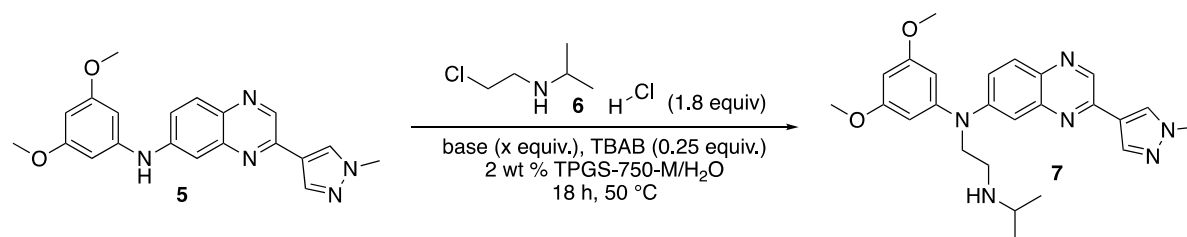
Due to poor reactivity using reductive amination, compound **6** was eventually used to perform nucleophilic substitution with amine **5**. Efforts to use DMSO or acetone as solvents with potassium iodide for in situ Finkelstein reaction were not successful (Scheme 7).

Scheme 7. Attempts at nucleophilic substitution reaction to synthesize erdafitinib



Next, efforts were made to use an S_N2 reaction mentioned in the initially patent¹¹ after modifications (Table 5). The reaction conditions and reagents were maintained while only changing the reaction medium from 2-MeTHF to aqueous micellar medium (2 wt % TPGS-750-M/ H_2O). Attempts to run the reaction using potassium hydroxide and potassium tert-butoxide were also not successful. We can potentially conclude from these experiments that high quantities of base are required for the process potentially due to the alkyl chloride being in a HCl salt form.

Table 5. Modification of literature route to erdafitinib under aqueous micellar conditions



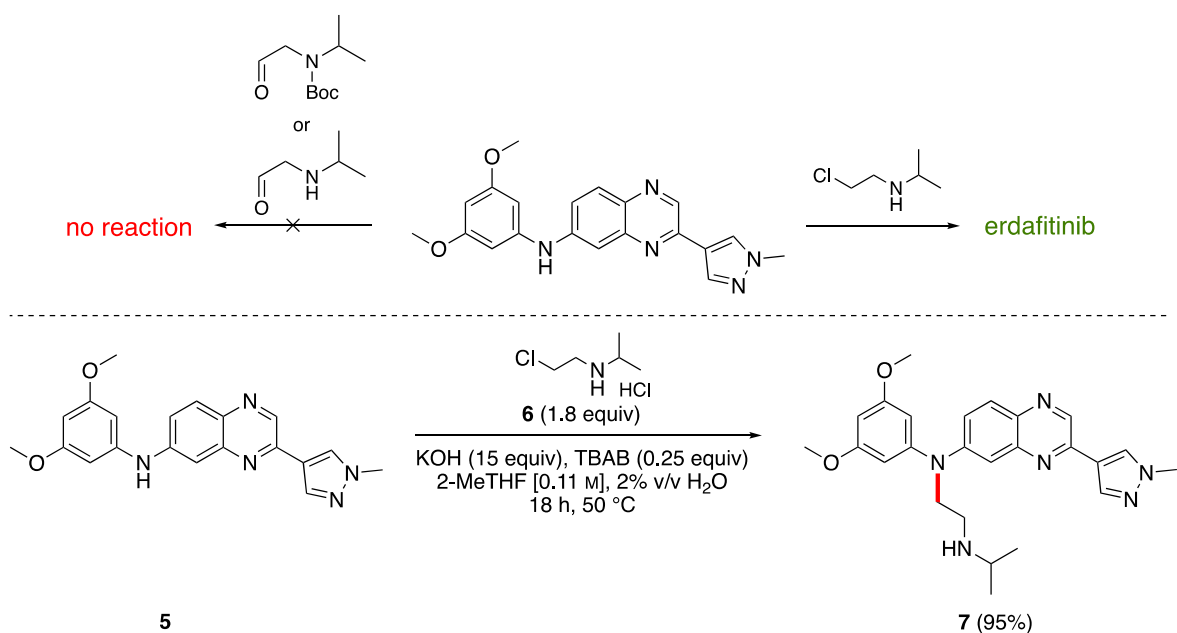
entry	base (x equiv)	observation
1	KOH (15)	trace

2	KO- <i>t</i> -Bu (15)	trace
3	KOH (1.5)	no reaction
4	KO- <i>t</i> -Bu (1.5)	no reaction

Eventually, nucleophilic substitution reported by Saxty and co-workers was employed with diarylamine **5** and HCl salt of *N*-(2-chloroethyl)propan-2-amine.¹¹ With KOH as base and tetrabutylammonium bromide (TBAB) as a phase transfer catalyst, an S_N2 reaction in 2-MeTHF gave **7** in 95% isolated yield after column chromatography (Scheme 8).

Scheme 8. Attempts at reductive amination and nucleophilic substitution reaction (top).

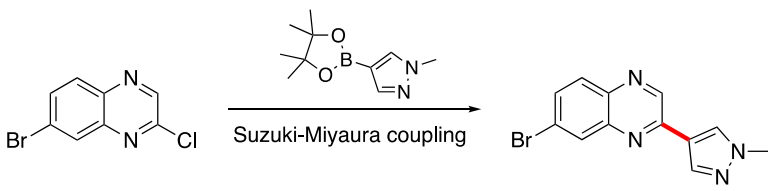
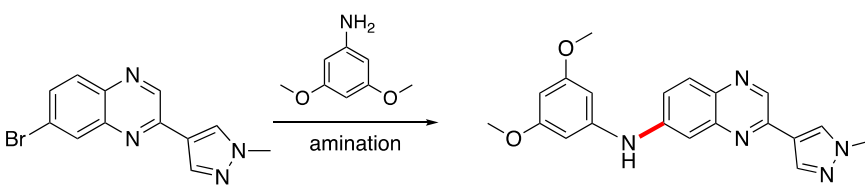
Third and final step for the synthesis (bottom)



2.2.4. Greener route to erdafitinib

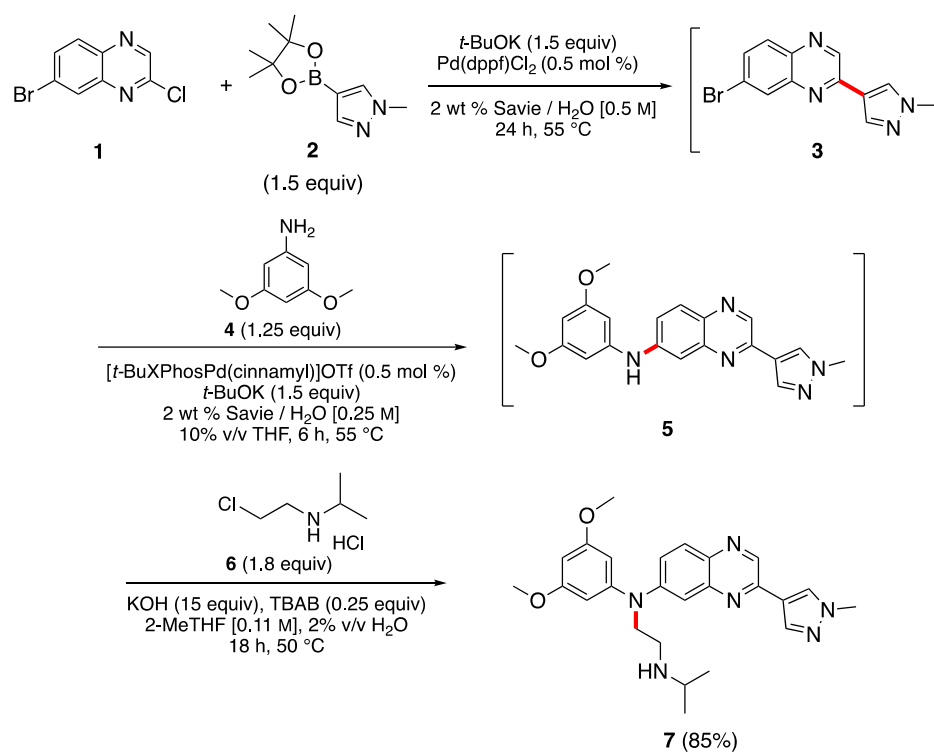
Overall, Table 6 shows comparisons between this work and the syntheses presented in the Astex patent, clearly showcasing the enhanced greenness and efficiency. The newly developed methodology, outlined in Scheme 9, leads to a significantly shortened 3-step process requiring only 2-pots, highlighting “time”²¹ and “pot”²² economies.

Table 6. Comparison between this work and literature conditions

reaction parameters	this work	literature conditions
		
Pd loading	0.50 mol % (5000 ppm)	1 mol%
reaction temperature	55 °C	85 °C
solvent/medium	in water (with biodegradable surfactant, Savie)	DME
E factor ²³	8.8	11.6
		
Pd loading	0.25 mol % (2500 ppm)	5 mol%

reaction temperature	45 °C	90 °C
reaction time	2 h	overnight
solvent/medium	in water (with biodegradable surfactant, Savie)	dioxane
E factor	12.3	128.5

Scheme 9. 3-Step, 2-pot sequence to erdafitinib (**7**)



The most attractive feature, however, is the complete elimination of any work-up. Intermediate **3** can be used directly without isolation to form product **5** after amination via this 2-step, 1-pot tandem sequence. However, when the amination reaction is run in a 1-pot fashion, an increased Pd catalyst loading of 0.5 mol % (5000 ppm) and increased reaction temperature (55 °C) are required to ensure complete consumption of coupling partner **3**. Even

though there is an increase in catalyst loading, it is still an order of magnitude lower than the existing literature process. Product **5** can then be employed without purification for subsequent conversion to **7**, obtained in 85% overall isolated yield.

2.3. Conclusion

To conclude, a sustainable and short synthetic route to the anticancer drug erdafitinib, a very useful treatment for urothelial carcinoma, has been described. The two main Pd-catalyzed reactions, Suzuki-Miyaura and amination reaction, only require a total investment of 0.75 mol % of a commercially available monomeric catalyst, and can be executed in a 1-pot fashion, thus, eliminating the need for work up. Both the steps are performed under aqueous micellar conditions using the biodegradable surfactant Savie making the downstream waste water process more straightforward. Overall, this sequence provides yet another example of designer surfactant-enabled chemistry in water that effectively replaces use of traditional, and unsustainable, synthetic chemistry in organic solvents.

2.4. References

- 1) Lorient, Y.; Necchi, A.; Park, S. H.; Garcia-Donas, J.; Huddart, R.; Burgess, E.; Fleming, M.; Rezazadeh, A.; Mellado, B.; Varlamov, S.; Joshi, M.; Duran, I.; Tagawa, S. T.; Zakharia, Y.; Zhong, B.; Stuyckens, K.; Santiago-Walker, A.; De Porre, P.; O'Hagan, A.; Avadhani, A.; Siefker-Radtke, A. O. Erdafitinib in Locally Advanced or Metastatic Urothelial Carcinoma. *N. Engl. J. Med.* **2019**, *381*, 338–348.
- 2) Markham, A. Erdafitinib: First Global Approval. *Drugs* **2019**, *79*, 1017–1021.
- 3) Fierce Pharma. <https://www.fiercepharma.com/pharma/j-j-s-balversa-wins-quick-blockbuster-nod-as-first-targeted-therapy-for-bladder-cancer> (2019)
- 4) Perera, T. P. S.; Jovcheva, E.; Mevellec, L.; Vialard, J.; De Lange, D.; Verhulst, T.; Paulussen, C.; Van De Ven, K.; King, P.; Freyne, E.; Rees, D. C.; Squires, M.; Saxty, G.; Page, M.; Murray, C. W.; Gilissen, R.; Ward, G.; Thompson, N. T.; Newell, D. R.; Cheng, N.; Xie, L.; Yang, J.; Platero, S. J.; Karkera, J. D.; Moy, C.; Angibaud, P.; Laquerre, S.; Lorenzi, M. V. Discovery and Pharmacological Characterization of JNJ-42756493 (Erdafitinib), a Functionally Selective Small-Molecule FGFR Family Inhibitor. *Mol. Cancer Ther.* **2017**, *16*, 1010–1020.
- 5) Lorient, Y.; Schuler, M. H.; Iyer, G.; Witt, O.; Doi, T.; Qin, S.; Tabernero, J.; Reardon, D. A.; Massard, C.; Palmer, D.; Lugowska, I.; Coward, J.; Corassa, M.; Stuyckens, K.; Liao, H.; Najmi, S.; Hammond, C.; Santiago-Walker, A. E.; Sweiti, H.; Pant, S. Tumor Agnostic Efficacy and Safety of Erdafitinib in Patients (Pts) with Advanced Solid Tumors with Prespecified Fibroblast Growth Factor Receptor Alterations (*FGFRalt*) in RAGNAR: Interim Analysis (IA) Results. *J. Clin. Oncol.* **2022**, *40*, 3007–3007.
- 6) Xu, Z.; Wang, H.; Jiang, S.; Lu, S.; Mao, Y. New and Convergent Synthesis of Erdafitinib. *J. Heterocycl. Chem.* **2022**, *59*, 2093–2097.
- 7) Rayadurgam, J.; Sana, S.; Sasikumar, M.; Gu, Q. Palladium Catalyzed C–C and C–N Bond Forming Reactions: An Update on the Synthesis of Pharmaceuticals from 2015–2020. *Org. Chem. Front.* **2021**, *8*, 384–414.
- 8) Semeniuchenko, V.; Braje, W. M.; Organ, M. G. Sodium Butylated Hydroxytoluene: A Functional Group Tolerant, Eco-Friendly Base for Solvent-Free, Pd-Catalysed Amination. *Chem. Eur. J.* **2021**, *27*, 12535–12539.
- 9) Liang, X.; Yang, Q.; Wu, P.; He, C.; Yin, L.; Xu, F.; Yin, Z.; Yue, G.; Zou, Y.; Li, L.; Song, X.; Lv, C.; Zhang, W.; Jing, B. The Synthesis Review of the Approved Tyrosine Kinase Inhibitors for Anticancer Therapy in 2015–2020. *Bioorg. Chem.* **2021**, *113*, 105011.
- 10) Yuan, S.; Yu, B.; Liu, H.-M. New Drug Approvals for 2019: Synthesis and Clinical Applications. *Eur. J. Med. Chem.* **2020**, *205*, 112667.
- 11) Saxty, G.; Murray, C. W.; Berdini, V.; Besong, G. E.; Hamlett, C. C. F.; Johnson, C. N.; Woodhead, S. J.; Reader, M.; Rees, D. C.; Mevellec, L. A.; Angibaud, P. R.; Freyne, E. J. E.; Govaerts, T. C. H.; Weerts, J. E. E.; Perera, T. P. S.; Gilissen, R. A. H. J.; Wroblowski, B.; Lacrampe, J. F. A.;

- Papanikos, A.; Querolle, O. A. G.; Pasquier, E. T. J.; Pilatte, I. N. C.; Bonnet, P. G. A.; Embrechts, W. C. J.; Akkari, R.; Meerpoel, L. Pyrazolyl quinazoline kinase inhibitors. *WO Pat.* WO2011135376A1, 2011.
- 12) Lipshutz, B. H.; Ghorai, S.; Abela, A. R.; Moser, R.; Nishikata, T.; Duplais, C.; Krasovskiy, A.; Gaston, R. D.; Gadwood, R. C. TPGS-750-M: A Second-Generation Amphiphile for Metal-Catalyzed Cross-Couplings in Water at Room Temperature. *J. Org. Chem.* **2011**, *76*, 4379–4391.
- 13) Landstrom, E. B.; Handa, S.; Aue, D. H.; Gallou, F.; Lipshutz, B. H. EvanPhos: A Ligand for ppm Level Pd-Catalyzed Suzuki–Miyaura Couplings in Either Organic Solvent or Water. *Green Chem.* **2018**, *20*, 3436–3443.
- 14) Kincaid, J. R. A.; Wong, M. J.; Akporji, N.; Gallou, F.; Fialho, D. M.; Lipshutz, B. H. Introducing Savie: A Biodegradable Surfactant Enabling Chemo- and Biocatalysis and Related Reactions in Recyclable Water. *J. Am. Chem. Soc.* **2023**, *145*, 4266–4278.
- 15) Pace, V.; Hoyos, P.; Castoldi, L.; Domínguez de María, P.; Alcántara, A. R. 2-Methyltetrahydrofuran (2-MeTHF): A Biomass-Derived Solvent with Broad Application in Organic Chemistry. *ChemSusChem* **2012**, *5*, 1369–1379.
- 16) Zhang, Y.; Takale, B. S.; Gallou, F.; Reilly, J.; Lipshutz, B. H. Sustainable Ppm Level Palladium-Catalyzed Aminations in Nanoreactors under Mild, Aqueous Conditions. *Chem. Sci.* **2019**, *10*, 10556–10561.
- 17) (a) Schlummer, B.; Scholz, U. Palladium-Catalyzed C–N and C–O Coupling—A Practical Guide from an Industrial Vantage Point †. *Adv. Synth. Catal.* **2004**, *346*, 1599–1626; (b) Corbet, J.-P.; Mignani, G. Selected Patented Cross-Coupling Reaction Technologies. *Chem. Rev.* **2006**, *106*, 2651–2710; (c) Torborg, C.; Beller, M. Recent Applications of Palladium-Catalyzed Coupling Reactions in the Pharmaceutical, Agrochemical, and Fine Chemical Industries. *Adv. Synth. Catal.* **2009**, *351*, 3027–3043; (d) Heravi, M. M.; Kheilkordi, Z.; Zadsirjan, V.; Heydari, M.; Malmir, M. Buchwald–Hartwig Reaction: An Overview. *J. Organomet. Chem.* **2018**, *861*, 17–104; (e) Ruiz-Castillo, P.; Buchwald, S. L. Applications of Palladium-Catalyzed C–N Cross-Coupling Reactions. *Chem. Rev.* **2016**, *116*, 12564–12649.
- 18) Zhu, H.; Mishra, R.; Yuan, L.; Abdul Salam, S. F.; Liu, J.; Gray, G.; Sterling, A. D.; Wunderlich, M.; Landero-Figueroa, J.; Garrett, J. T.; Merino, E. J. Oxidative Cyclization-Induced Activation of a Phosphoinositide 3-Kinase Inhibitor for Enhanced Selectivity of Cancer Chemotherapeutics. *ChemMedChem* **2019**, *14*, 1933–1939.
- 19) (a) Van Craen, D.; Begall, J.; Großkurth, J.; Himmel, L.; Linnenberg, O.; Isaak, E.; Albrecht, M. Hierarchically Assembled Helicates as Reaction Platform – from Stoichiometric Diels–Alder Reactions to Enamine Catalysis. *Beilstein J. Org. Chem.* **2020**, *16*, 2338–2345. (b) Ding, C. Z.; Chen, S.; Zhao, B.; Liu, X.; Xiao, L.; Ding, C.; Wang, F.; Li, J. Fused-ring or tricyclic aryl pyrimidine compound used as kinase inhibitor. *EP Pat.* EP3290419A1, 2016.
- 20) Li, X.; Iyer, K. S.; Thakore, R. R.; Leahy, D. K.; Bailey, J. D.; Lipshutz, B. H. Bisulfite Addition Compounds as Substrates for Reductive Aminations in Water. *Org. Lett.* **2021**, *23*, 7205–7208.
- 21) Hayashi, Y. Time Economy in Total Synthesis. *J. Org. Chem.* **2021**, *86*, 1–23.

22) Hayashi, Y. Pot Economy and One-Pot Synthesis. *Chem. Sci.* **2016**, *7*, 866–880.

23) Sheldon, R. A. The E Factor: Fifteen Years On. *Green Chem.* **2007**, *9*, 1273-1283.

2.5. General information

Reagents and chemicals were purchased from Sigma-Aldrich, Combi-Blocks, Alfa Aeser, or Acros Organics and used without further purification. Palladium catalyst Pd(dppf)Cl₂ was purchased from SigmaAldrich. Palladium complex [*t*-BuXPhosPd(cinnamyl)]OTf was synthesized using the reported procedure.¹¹ TPGS-750-M is available from Sigma-Aldrich (catalog #733857; solution, or #763896; wax) or can be prepared following the reported procedure.¹² Savie can be prepared following the reported procedure.¹³ The desired 2 wt % of surfactant solution in HPLC water (which was degassed with argon prior to use) was prepared by dissolving 2 g of surfactant together with 98 g of HPLC water and stored under argon.

¹H and ¹³C NMR spectra were recorded on a Bruker 400 MHz (400 MHz for ¹H, 101 MHz for ¹³C); DMSO-d₆ and CDCl₃ were used as NMR solvents. Residual peaks for CHCl₃ in CDCl₃ (¹H = 7.26 ppm, ¹³C = 77.20 ppm) and (CH₃)₂S=O in (CD₃)₂S=O (¹H = 2.50 ppm, ¹³C = 39.52 ppm) were used for assignments. Chemical shifts are reported in parts per million (ppm), the coupling constant J values are given in Hertz (Hz). Peak patterns are indicated as follows: s, singlet; d, doublet; t, triplet; q, quartet; p, pentet; m, multiplet. Thin layer

¹¹ DeAngelis, A. J.; Gildner, P. G.; Chow, R.; Colacot, T. J. Generating Active “L-Pd(0)” via Neutral or Cationic π -Allylpalladium Complexes Featuring Biaryl/Bipyrazolylphosphines: Synthetic, Mechanistic, and Structure–Activity Studies in Challenging Cross-Coupling Reactions. *J. Org. Chem.* **2015**, *80*, 6794–6813.

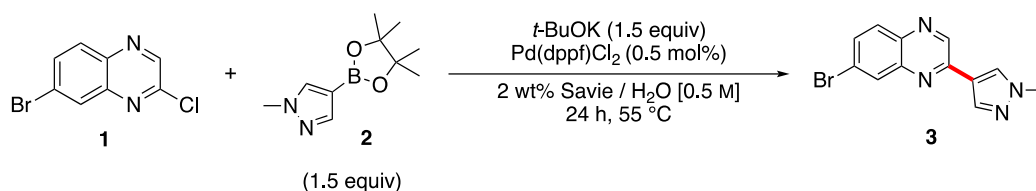
¹² Lipshutz, B. H.; Ghorai, S.; Abela, A. R.; Moser, R.; Nishikata, T.; Duplais, C.; Krasovskiy, A.; Gaston, R. D.; Gadwood, R. C. TPGS-750-M: A Second-Generation Amphiphile for Metal-Catalyzed Cross-Couplings in Water at Room Temperature. *J. Org. Chem.* **2011**, *76*, 4379–4391.

¹³ Kincaid, J. R. A.; Wong, M. J.; Akporji, N.; Gallou, F.; Fialho, D. M.; Lipshutz, B. H. Introducing Savie: A Biodegradable Surfactant Enabling Chemo- and Biocatalysis and Related Reactions in Recyclable Water. *J. Am. Chem. Soc.* **2023**, *145*, 4266–4278.

chromatography (TLC) was done using Silica Gel 60 F254 plates (Merck, 0.25 mm thick). Flash chromatography was done in glass columns using Silica Gel 60 (EMD, 40-63 μm). Chiral HPLC data was collected using an Agilent 1220 HPLC. HRMS data were recorded on a Waters Micromass LCT TOF ES+ Premier mass spectrometer using ESI ionization.

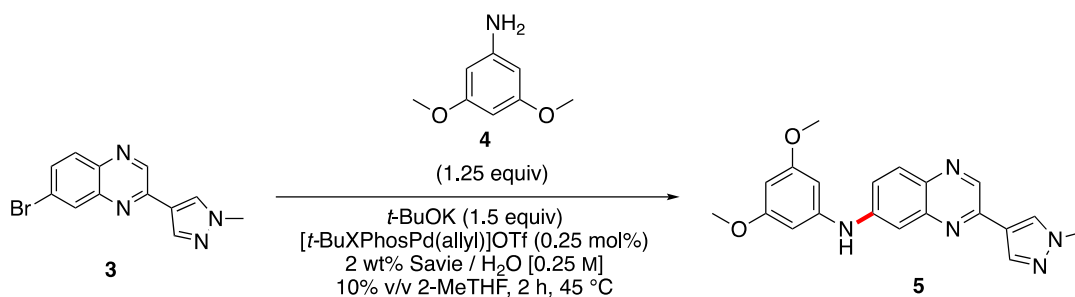
2.6. Experimental procedures

2.6.1. Suzuki-Miyaura cross coupling reaction



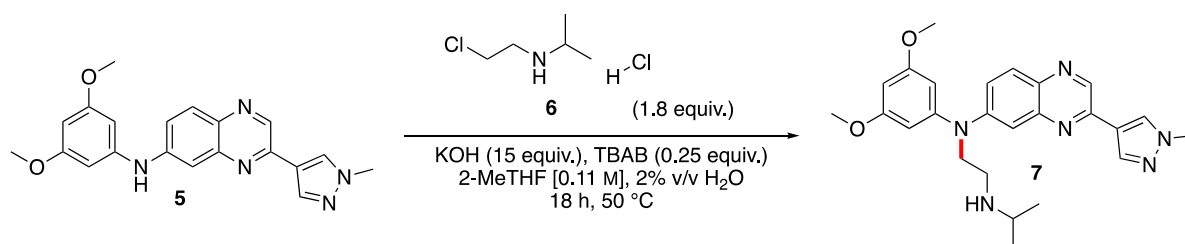
In a 1-dram vial equipped with a magnetic stir bar, 7-bromo-2-chloroquinoxaline (0.25 mmol) and 1-methylpyrazole-4-boronic acid pinacol ester (1.5 equiv., 0.375 mmol) were added. To the vial, Pd catalyst (0.5 - 1.0 mol %) and base (1.0-2.0 equiv) were added under argon. Aqueous 2 wt % surfactant solution (0.5 mL) (and co-solvent if applicable) was subsequently added and the reaction was allowed to stir on an isotherm aluminum reaction block on an IKA plate, at 45°C until completion (as monitored by TLC). The reaction mixture was then extracted with EtOAc (5 x 0.5 mL). The organic solvents were removed under vacuum to give crude product. The desired product was isolated by flash chromatography over silica gel and dried *in vacuo*.

2.6.2. Amination reaction



In a 1-dram vial equipped with a magnetic stir bar, 7-bromo-2-(1-methyl-1H-pyrazol-4-yl)quinoxaline (0.25 mmol) and 3,5-dimethoxyaniline (1.25 equiv, 0.313 mmol) were added. To the vial, Pd catalyst (0.05 - 2.0 mol %) and t -BuOK (1.5 mmol, 0.375 mmol) were added under argon. Aqueous 2 wt % surfactant solution (0.9 mL) and co-solvent (0.1 mL) were subsequently added and the reaction was allowed to stir on an isotherm aluminum reaction block on an IKA plate, at 45 °C until completion (as monitored by TLC). The reaction was allowed to cool to rt. Subsequently, saturated NaHCO₃ (2 mL) was added and the reaction mixture was cooled in the freezer. The precipitate was isolated via filtration and then dried *in vacuo*.

2.6.3. S_N2 reaction



In a 2-dram vial equipped with a magnetic stir bar, KOH was dissolved in a solution of 2% v/v H₂O (0.05 mL) and 2-MeTHF (2.25 mL). To the vial, N-(3,5-dimethoxyphenyl)-3-(1-

methyl-1*H*-pyrazol-4-yl)quinoxalin-6-amine (**5**) (0.25 mmol) and tetrabutylammonium bromide (0.25 equiv, 0.0625 mmol) were added. The reaction was allowed to stir on an isotherm aluminum reaction block on an IKA plate, at 50 °C for 1 h. *N*-(2-chloroethyl)-2-propanamine HCl (1.8 equiv, 0.45 mmol) was subsequently added and stirring was continued at 50 °C overnight. The reaction mixture was then allowed to cool to rt. The crude reaction mixture was loaded directly onto silica gel and the desired product was isolated by flash chromatography over silica gel and then dried *in vacuo*.

2.6.4. Procedure for synthesis of step 1 and step 2 in 1-pot

Step 1: Suzuki-Miyaura cross coupling reaction

In a 1-dram vial equipped with a magnetic stir bar, 7-bromo-2-chloroquinoxaline (0.25 mmol) and 1-methylpyrazole-4-boronic acid pinacol ester (1.5 equiv, 0.375 mmol) were added. To the vial, Pd(dppf)Cl₂ (0.5 mol %) and *t*-BuOK (1.5 equiv, 0.375 mmol) were added under argon. Aqueous 2 wt % TPGS-750-M solution (0.5 mL) was subsequently added and the reaction was allowed to stir on an isotherm aluminum reaction block on an IKA plate at 45 °C until completion (as monitored by TLC).

Step 2: Amination reaction

Once step 1 was completed, the vial was allowed to cool to rt. In a separate 1-dram vial, 3,5-dimethoxyaniline (1.25 equiv, 0.313 mmol) and *t*-BuOK (1.5 mmol, 0.375 mmol) were dissolved in 2 wt % TPGS-750-M solution (0.4 mL) under argon. The prepared solution was then added to the reaction mixture via syringe. In another 1-dram vial under argon, [*t*-BuXPhosPd(cinnamyl)]OTf (1 mol %) was dissolved in dry THF (0.1 mL). The prepared

solution was then added to the reaction mixture via syringe. The reaction mixture was then allowed to stir on an isotherm aluminum reaction block on an IKA plate at 55 °C until completion (as monitored by TLC). The reaction was allowed to cool to rt. Subsequently, saturated NaHCO₃ (2 mL) was added and the reaction mixture was cooled in the freezer. The precipitate was isolated via filtration and then dried *in vacuo*. The crude reaction mixture was used for step 3 without purification.

2.7. *E Factor calculation for erdafitinib*

$$E \text{ Factor} = \frac{\text{grams of wastes}}{\text{grams of product}}^{14}$$

Step 1:

This work:

Scale = 0.25 mmol

Product = 64.8 mg

Waste:

Excess boronic acid = 26 mg

t-BuOK = 42.1 mg

Surfactant (Savie) = 10 mg

H₂O = 490 mg

Pd complex = 0.9 mg

¹⁴ Sheldon, R. A. The E Factor: Fifteen Years On. *Green Chem.* **2007**, *9*, 1273-1283.

$$E \text{ Factor} = \frac{569 \text{ mg of wastes}}{64.8 \text{ mg of product}} = \mathbf{8.8}$$

Literature:

Scale = 2 mol

Product = 532.2 g

Waste:

Excess boronic acid = 63.7 g

Ligand = 10.82 g

Pd catalyst = 4.5 g

Na₂CO₃ = 240.37 g

DME = 5.48 L or 4751.2 g

H₂O = 1.13 L or 1130 g

$$E \text{ Factor} = \frac{6200.6 \text{ g of wastes}}{532.2 \text{ g of product}} = \mathbf{11.6}$$

Step 2:

This work:

Scale = 0.25 mmol

Product = 84.1 mg

Waste:

Excess amine = 9.7 mg

t-BuOK = 42.1 mg

Surfactant (Savie) = 18 mg

H₂O = 882 mg

2-MeTHF = 0.1 mL or 86 mg

Pd complex = 0.5 mg

$$E \text{ Factor} = \frac{1038 \text{ mg of wastes}}{84.1 \text{ mg of product}} = \mathbf{12.3}$$

Literature:

Scale = 69.2 mmol

Product = 4.2 g

Waste:

Ligand = 2.2 g

Pd catalyst = 0.78 g

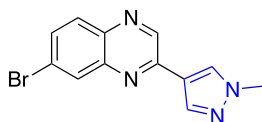
t-BuONa = 20 g

dioxane = 500 mL or 516.5 g

$$E \text{ Factor} = \frac{539.5 \text{ g of wastes}}{4.2 \text{ g of product}} = \mathbf{128.5}$$

2.8. Product characterization (NMR and HRMS)

7-Bromo-2-(1-methyl-1*H*-pyrazol-4-yl)quinoxaline (**3**)



¹H NMR (400 MHz, DMSO-*d*₆) δ 9.32 (s, 1H), 8.63 (s, 1H), 8.28 (d, *J* = 0.7 Hz, 1H), 8.18 (d, *J* = 2.2 Hz, 1H), 7.97 (d, *J* = 8.8 Hz, 1H), 7.86 (dd, *J* = 8.8, 2.2 Hz, 1H), 3.95 (s, 3H).

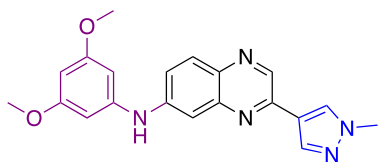
¹³C NMR (101 MHz, DMSO-*d*₆) δ 147.99, 144.47, 142.44, 139.19, 138.27, 131.73, 131.41, 130.78, 130.29, 123.34, 119.71, 38.96.

Yield: 90%; 64.8 mg; grey solid.

R_f = 0.22 (1 : 98.9 : 0.1, MeOH/DCM/NH₄OH).

Spectral data matched those previously reported.¹⁵

N-(3,5-Dimethoxyphenyl)-3-(1-methyl-1*H*-pyrazol-4-yl)quinoxalin-6-amine (**5**)



¹H NMR (400 MHz, DMSO-*d*₆) δ 8.97 (s, 1H), 8.84 (s, 1H), 8.57 (s, 1H), 8.23 (s, 1H), 7.84 (d, *J* = 9.7 Hz, 1H), 7.44 (dq, *J* = 4.7, 2.6 Hz, 2H), 6.43 (d, *J* = 2.2 Hz, 2H), 6.20 (t, *J* = 2.2 Hz, 1H), 3.93 (s, 3H), 3.75 (s, 6H).

¹⁵ Xu, Z.; Wang, H.; Jiang, S.; Lu, S.; Mao, Y. New and Convergent Synthesis of Erdafitinib. *J. Heterocycl. Chem.* **2022**, *59*, 2093–2097.

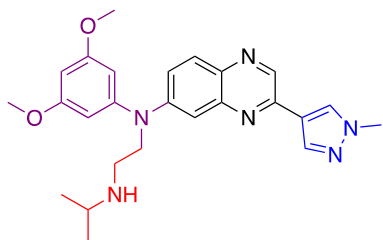
¹³C NMR (101 MHz, DMSO-d₆) δ 161.19, 147.11, 145.31, 143.63, 143.46, 139.66, 137.55, 135.96, 130.81, 129.67, 121.98, 120.33, 107.47, 97.27, 93.60, 55.13, 38.83.

Yield: 93%; 84.1 mg; yellow solid.

R_f = 0.25 (2 : 98, MeOH/DCM).

Spectral data matched those previously reported.¹⁶

*N*¹-(3,5-Dimethoxyphenyl)-*N*²-isopropyl-*N*¹-(3-(1-methyl-1*H*-pyrazol-4-yl)quinoxalin-6-yl)ethane-1,2-diamine (erdafitinib) (**7**)



¹H NMR (400 MHz, DMSO-d₆) δ 8.95 (s, 1H), 8.54 (s, 1H), 8.20 (d, *J* = 0.7 Hz, 1H), 7.76 (d, *J* = 9.2 Hz, 1H), 7.27 (dd, *J* = 9.2, 2.7 Hz, 1H), 7.14 (d, *J* = 2.7 Hz, 1H), 6.46 (d, *J* = 2.2 Hz, 2H), 6.41 (t, *J* = 2.2 Hz, 1H), 3.93 (s, 3H), 3.88 (t, *J* = 7.1 Hz, 2H), 3.74 (s, 6H), 2.80 (t, *J* = 7.0 Hz, 2H), 2.71 (p, *J* = 6.2 Hz, 1H), 0.95 (d, *J* = 6.2 Hz, 6H).

¹³C NMR (101 MHz, DMSO-d₆) δ 161.42, 149.08, 147.97, 147.06, 143.50, 139.63, 137.80, 135.46, 130.73, 129.03, 121.30, 120.38, 109.01, 103.89, 97.07, 55.31, 52.32, 48.08, 43.81, 38.86, 25.48, 22.86.

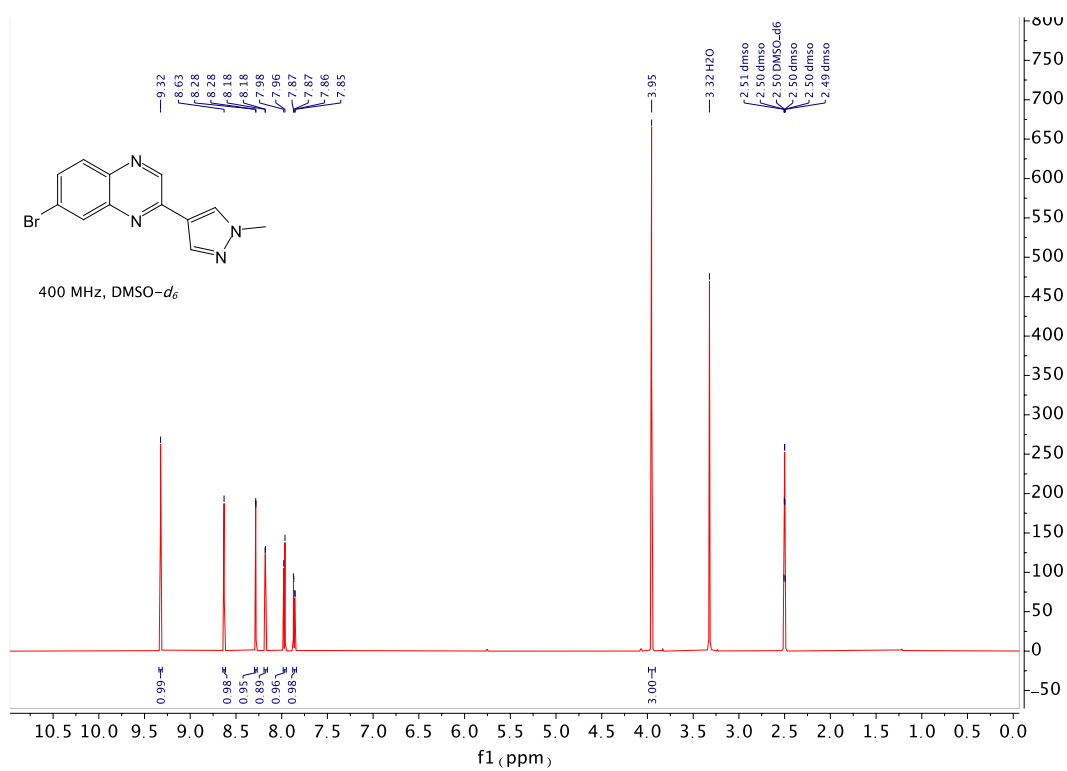
Yield: 95%; 105.9 mg; yellow powder.

¹⁶ Semeniuchenko, V.; Braje, W. M.; Organ, M. G. Sodium Butylated Hydroxytoluene: A Functional Group Tolerant, Eco-Friendly Base for Solvent-Free, Pd-Catalysed Amination. *Chem. Eur. J.* **2021**, *27*, 12535–12539.

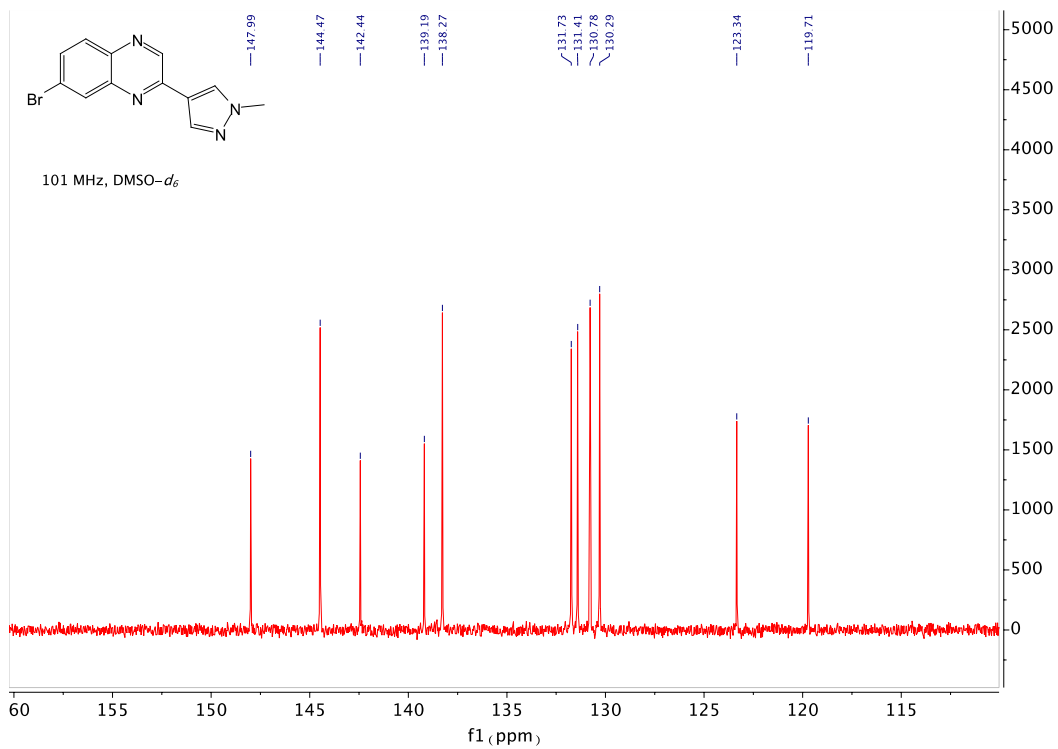
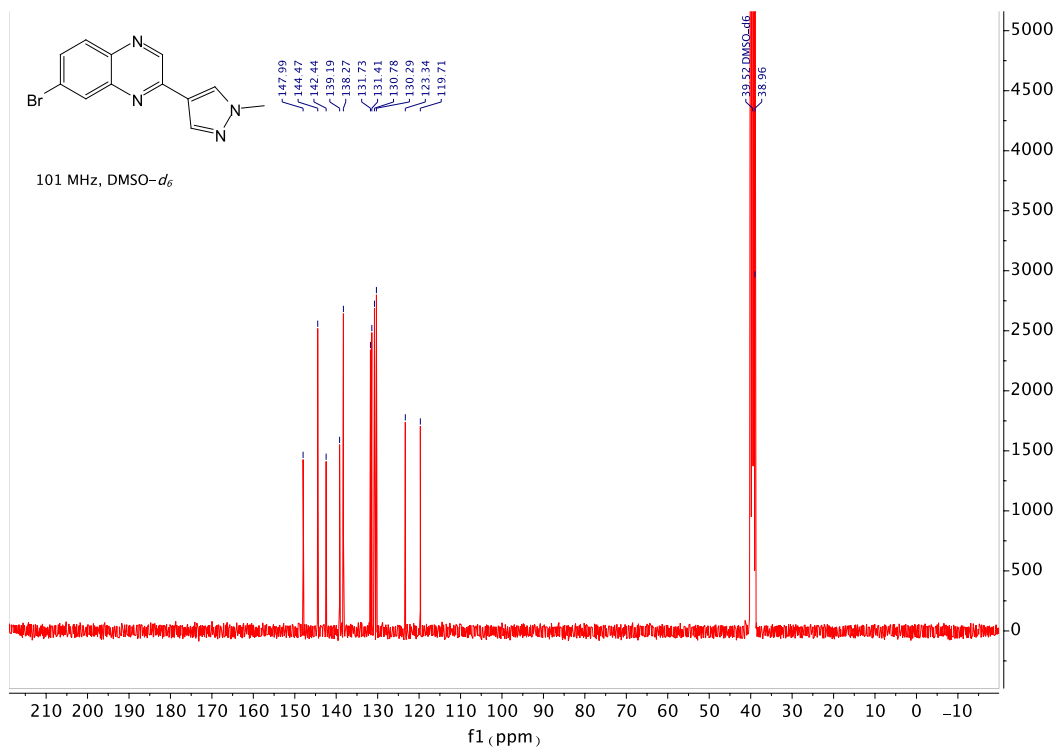
$R_f = 0.18$ (8 : 92, MeOH/DCM).

HRMS (ESI), m/z : $[M+1]^+$ calcd. for $C_{25}H_{31}N_6O_2$ 447.2508; found 447.2512.

2.9. NMR spectra

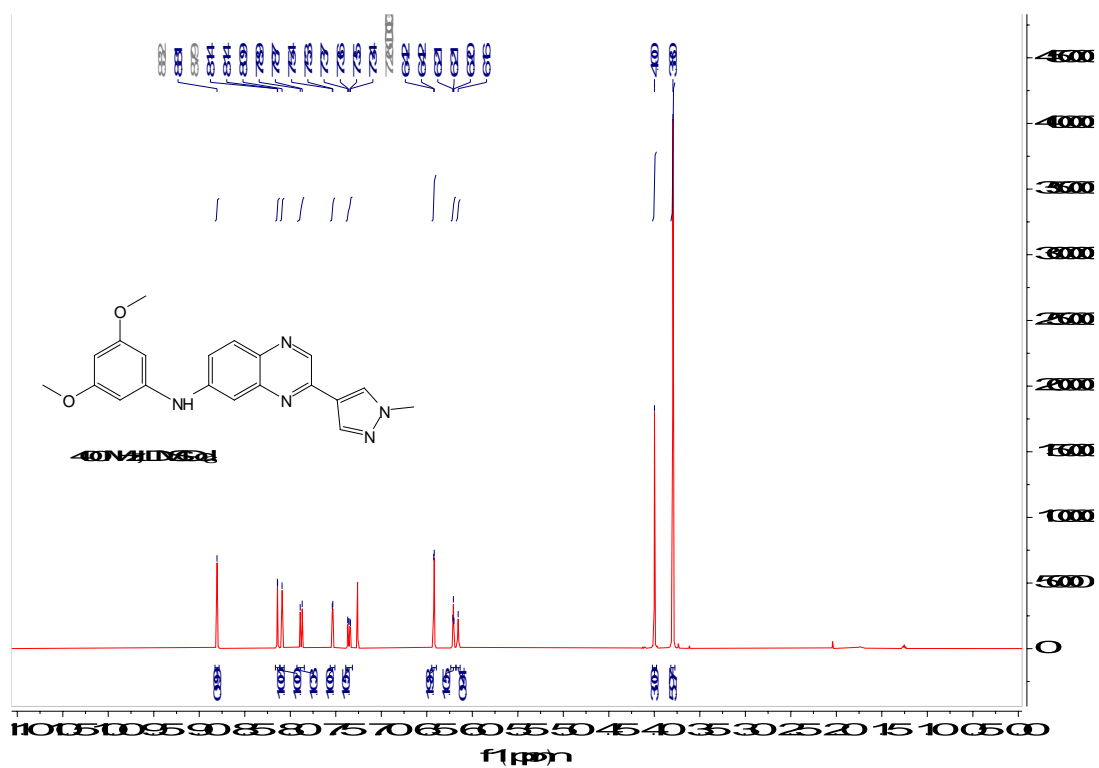


1H NMR spectrum of 7-bromo-2-(1-methyl-1H-pyrazol-4-yl)quinoxaline (**3**)

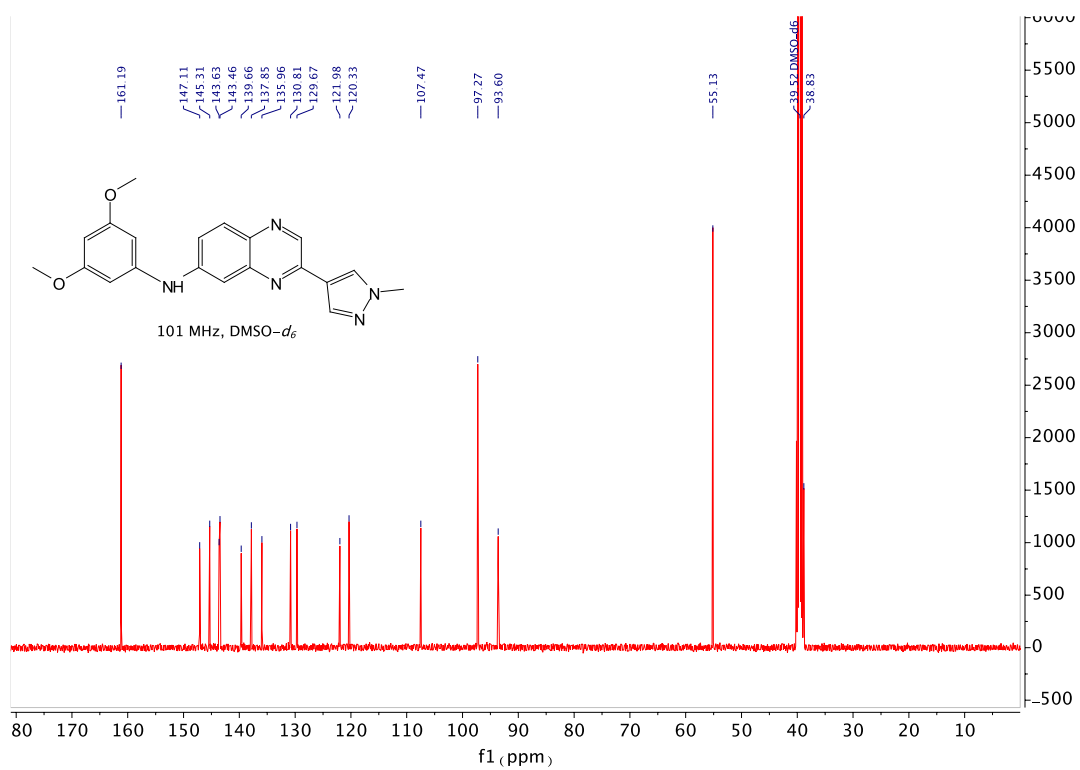


^{13}C NMR spectrum of 7-bromo-2-(1-methyl-1H-pyrazol-4-yl)quinoxaline (**3**)

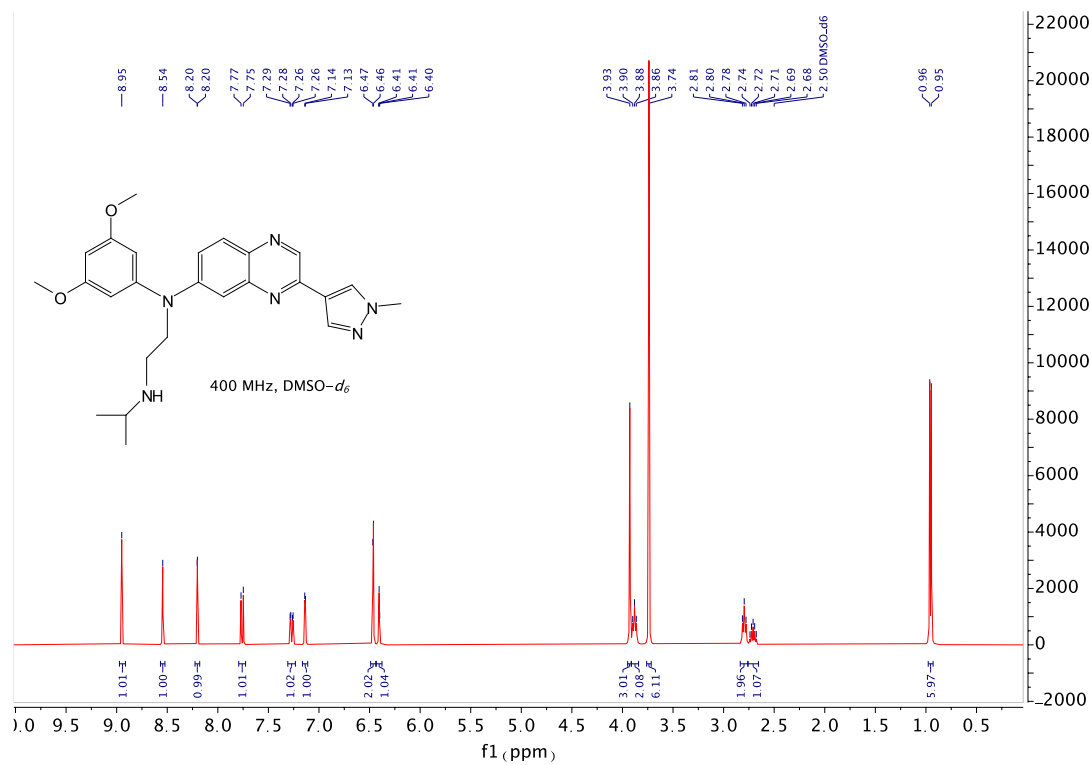
zoomed out (top); zoomed in (bottom)



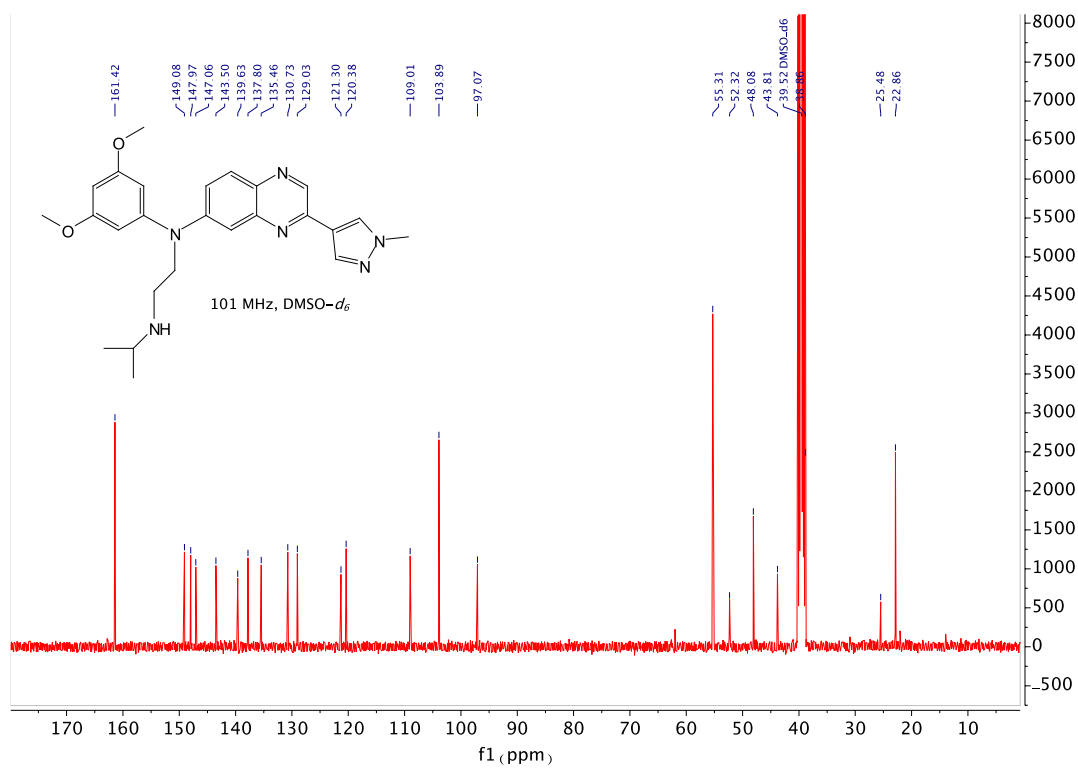
¹H NMR spectrum of *N*-(3,5-dimethoxyphenyl)-3-(1-methyl-1*H*-pyrazol-4-yl)quinoxalin-6-amine (**5**)



¹³C NMR spectrum of *N*-(3,5-dimethoxyphenyl)-3-(1-methyl-1*H*-pyrazol-4-yl)quinoxalin-6-amine (**5**)



¹H NMR spectrum of Erdafitinib (7)



¹³C NMR spectrum of Erdafitinib (7)

3. Nickel nanoparticle catalyzed mono- and di-reductions of *gem*-dibromocyclopropanes under mild, aqueous micellar conditions

Wood, A. B.; Cortes-Clerget, M.; Kincaid, J. R. A.; Akkachairin, B.; Singhanian, V.; Gallou, F.; Lipshutz, B. H. Nickel Nanoparticle-Catalyzed Mono- and Di-Reductions of *gem*-Dibromocyclopropanes Under Mild, Aqueous Micellar Conditions *Angew. Chem., Int. Ed.* **2020**, *59*, 17587–17593.

Copyright Wiley-VCH GmbH.

Reproduced with permission.

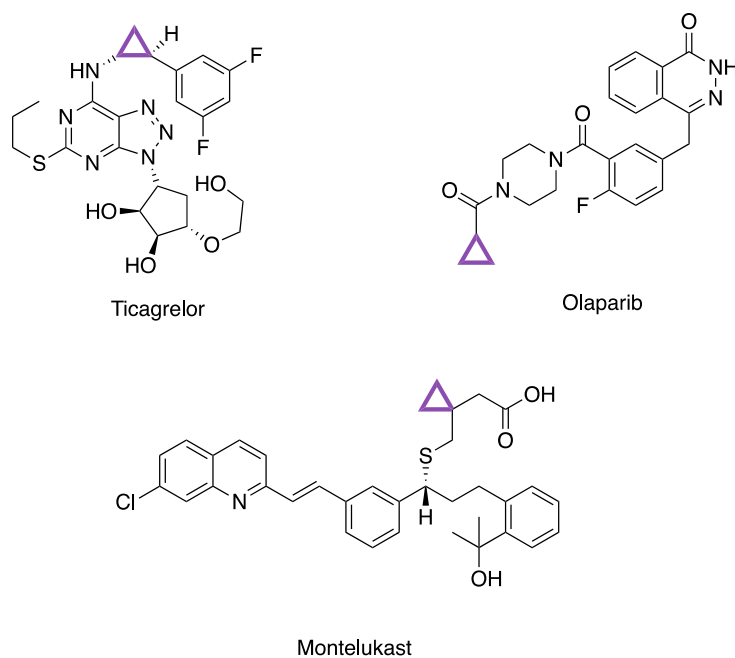
3.1. *Introduction and background*

Cyclopropyl rings are unique moieties found in several organic frameworks. They are coplanar three membered strained rings with shorter and more enhanced π -character of each C-C bond due to angle strain (60° vs. 109.5°). The C-H bonds are also shorter and stronger compared to those in alkanes. Due to these idiosyncratic properties, cyclopropyl rings have various biological advantages which explains their increased presence in many pharmaceuticals. They also have reduced off-target effects that, in turn, reduces side effects in drugs. They also have increased metabolic stability, as it is difficult to abstract a proton.¹

Cyclopropyl rings are bioisosteres that can replace labile moieties. For example, the coplanar structure of the cyclopropyl ring allows it to function as a more lipophilic phenyl ring, yet retaining a drug's properties which leads to enhanced potency of the drug. Cyclopropanes can also "lock" in stereochemistry when replacing an olefin, which can otherwise undergo isomerization *in vivo*. As a consequence of these desired effects on the drugs' biological and pharmacological profile, cyclopropyl rings are now found in hundreds of Active Pharmaceutical Ingredients including eleven of the top two hundred pharmaceuticals (Figure 1).²

There are multiple ways to introduce a cyclopropyl ring into a molecule. The current state-of-the-art method which is used both in academic and industrial labs is the initial preparation of *gem*-dihalocyclopropanes, by adding dihalocarbene to an olefin followed by reduction of the resulting halogens on the ring to yield the targeted cyclopropane.³

Figure 1. Cyclopropyl ring-containing APIs



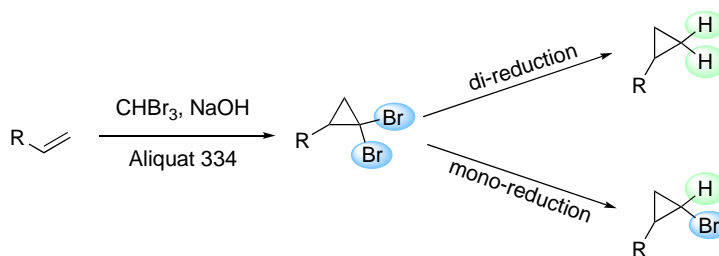
Existing reduction processes face serious limitations. They use stoichiometric amounts of toxic and dangerous hydride reagents, along with precious metals. These methodologies also use elevated temperatures or pressures while taking place in waste-generating organic solvents.⁴ These drawbacks include:

- Reduction using dangerous and toxic hydride reagents, such as tributyltin hydride and lithium aluminum hydride in refluxing THF or benzene.⁵
- Birch-type reduction conditions that are not chemoselective and require dangerous metals.⁶
- Reduction over large amounts of palladium on carbon or Raney nickel using hydrogen gas pressure at elevated temperatures.⁷

- Electrochemical reduction in toxic organic solvents using a leaded bronze cathode developed specifically for the process. This method requires high electron stoichiometry (9 F) and substantial amounts of supporting electrolyte MTES (*N*-methyl-*N,N,N*-triethylammonium methylsulfate).⁸

For this project a new nickel nanoparticle-catalyzed reduction of *gem*-dibromocyclopropanes in aqueous micellar solution was developed, consisting of the surfactant, TPGS-750-M, in the presence of sodium borohydride as hydride source (Figure 2). Small changes in reaction conditions allow access to mono-brominated cyclopropanes exclusively. These building blocks can be further derivatized and functionalized. We also dive into the mechanistic studies of the reduction process using deuterium incorporation while describing the synthesis of various isotopic analogs of cyclopropyl rings.

Figure 2. Synthesis of *gem*-dibromocyclopropane followed by mono- or di-reduction



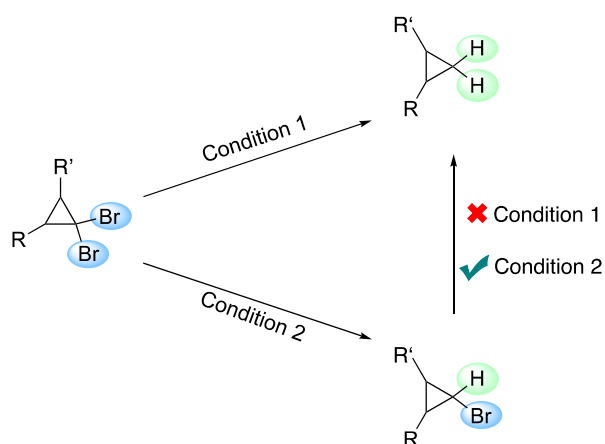
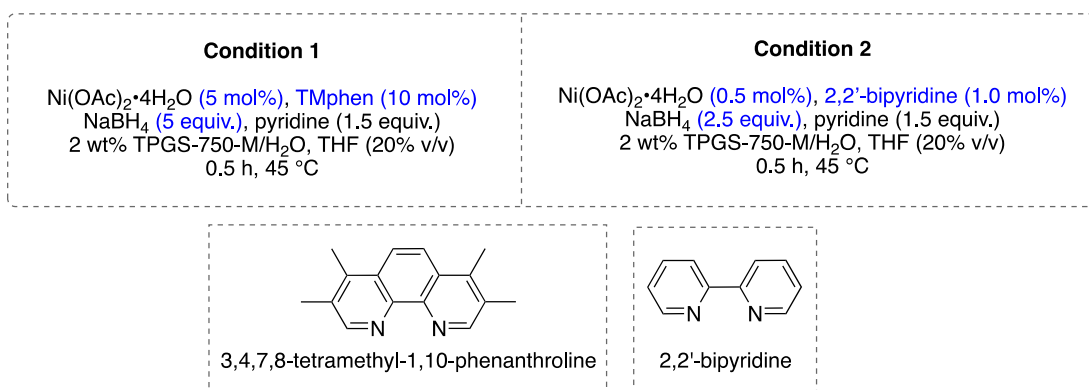
Deuterated cyclopropanes have been deemed beneficial and have recently gained attraction in the pharmaceutical industry. It has been found that substituting hydrogen with deuterium in a drug brings about no change in its biological properties. Owing to the size of the deuterium atom, the C-D bond is stronger than the C-H bond, making it harder to

metabolically breakdown the bond, in turn increasing the stability of the drug. The increased stability leads to increased half-life which helps reduce the dosage needed. Switching from hydrogen to deuterium also reduces toxicity by directing it to a more positive metabolic pathway.⁹

3.2. Results and Discussion

Conditions for di-reduction of *gem*-dibromocyclopropanes were optimized under aqueous micellar conditions (Figure 3). To completely reduce the starting material, 5 mol% of nickel chelated by the 3,4,7,8-tetramethyl-1, 10-phenanthroline (TMPhen) ligand was required along with sodium borohydride as reductant. A small volume of co-solvent (20% v/v) THF was necessary for generality to better solubilize and reduce more lipophilic substrates. Monobromocyclopropane could be accessed by simply reducing the catalyst loading by 10-fold, from 5 to 0.5 mol% and changing the ligand to the more flexible 2, 2'-bipyridine while reducing the amount of hydride source by half. Interestingly, for the reduction of monobromocyclopropane to the completely reduced cyclopropane, di-reduction conditions had to be employed with TMPhen. This potentially suggests different mechanisms for the two reduction steps.

Figure 3. Access to mono- and di-reduced cyclopropane



3.2.1. Mechanistic studies of mono-reduction of gem-dibromocyclopropane

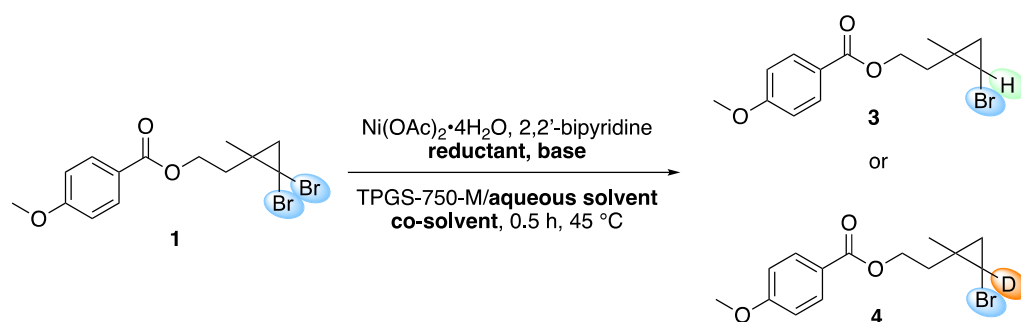
To acquire a mechanistic understanding of these reductions, various experiments were performed to synthesize deuterated analogs of both mono- and di-reduced products. Mono-reduction of the starting material **1** employing 2,2'-bipyridine was performed by both protonated and deuterated reagents and then compared. These reagents included reductants

(NaBH₄ vs. NaBD₄), co-solvents (THF vs. THF-*d*₈), base (pyridine vs. pyridine-*d*₅), as well as the bulk aqueous medium (H₂O vs. D₂O; Table 1).

Interestingly, using sodium borodeuteride as the only deuterated reagent was not very successful in incorporating deuterium into the product (entry 1). Only 18% of the mono-deuterated bromocyclopropane **4** was observed by NMR analysis of the crude reaction mixture.

To assess other possible hydride sources for the reduction, other deuterated reagents were tested. Using D₂O instead of H₂O as the bulk aqueous solvent was not beneficial either since no deuterium incorporation was observed (entry 2). As expected, due to the limited reagent quantities in the reaction mixture, reduction in the presence of THF-*d*₈ as co-solvent or pyridine-*d*₅ as base with NaBH₄ as hydride source led to only trace amounts of the mono-deuterated product (entries 3, 4).

Reduction reactions using other permutations of deuterated reagents under micellar catalysis conditions resulted in improved yields of the mono-deuterated product (30 - 84%; entries 5-7). The highest percentage of deuterium incorporation was observed when all four reagents (reductant, base, aqueous solvent and co-solvent) were in deuterated form in the presence of surfactant, TPGS-750-M. Intriguing results were observed when TPGS-750-M was entirely absent from the reaction medium and all other reagents were deuterated. Using NMR analysis of crude reaction mixture, 93% deuterium incorporation was detected under these conditions (entry 8).

Table 1. Optimization of reduction of **1** to mono-deuterated product **4**

entry	reductant	base	aqueous solvent	co-solvent	D incorporation
1	NaBD ₄	pyridine	H ₂ O	THF	18%
2	NaBH ₄	pyridine	D ₂ O	THF	0%
3	NaBH ₄	pyridine	H ₂ O	THF- <i>d</i> ₈	6%
4	NaBH ₄	pyridine- <i>d</i> ₅	H ₂ O	THF	3%
5	NaBD ₄	pyridine	D ₂ O	THF	30%
6	NaBD ₄	pyridine	D ₂ O	THF- <i>d</i> ₈	68%
7	NaBD ₄	pyridine- <i>d</i> ₅	D ₂ O	THF- <i>d</i> ₈	84%
8	NaBD ₄	pyridine- <i>d</i> ₅	D ₂ O (no surfactant)	THF- <i>d</i> ₈	93%

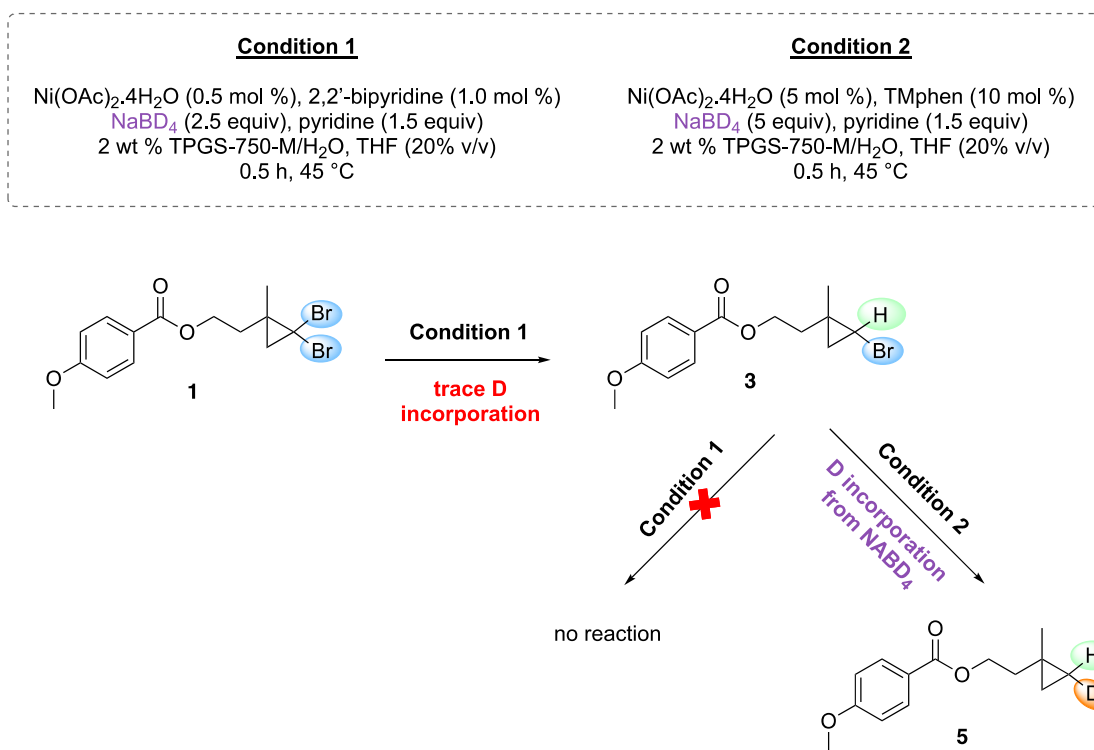
This interesting result provides some insight into the mechanism of the first debromination reaction. The surfactant, TPGS-750-M seems to unexpectedly be posing as a hydrogen sources. It is likely that a radical chain mechanism is in effect that competes with all other sources of deuterium. Holah, *et al.* observed that Ni(II) complex ligated by either 2,2'-bipyridine or phenanthroline and activated by sodium borohydride produces a Ni(I) species,

Ni(ligand)₂BH₄•2H₂O. This Ni(I) species may then be responsible for formation of the active borane radical anion that leads to the rapid proton/deuterium exchange reaction.¹⁰

3.2.2. Reduction of mono-bromocyclopropane

Attempts to reduce the mono-bromocyclopropane **3** under mono-reduction conditions were observed to be extremely slow, producing no product. On the other hand, subjecting **3** to di-reduction conditions using TMPhen as ligand and sodium borodeuteride as reductant resulted in complete formation of the di-reduced cyclopropane **5** and quantitative deuterium incorporation into the cyclopropane ring. These deuteration experiments also suggest the possibility that the two bromides are reduced stepwise via distinct mechanisms.

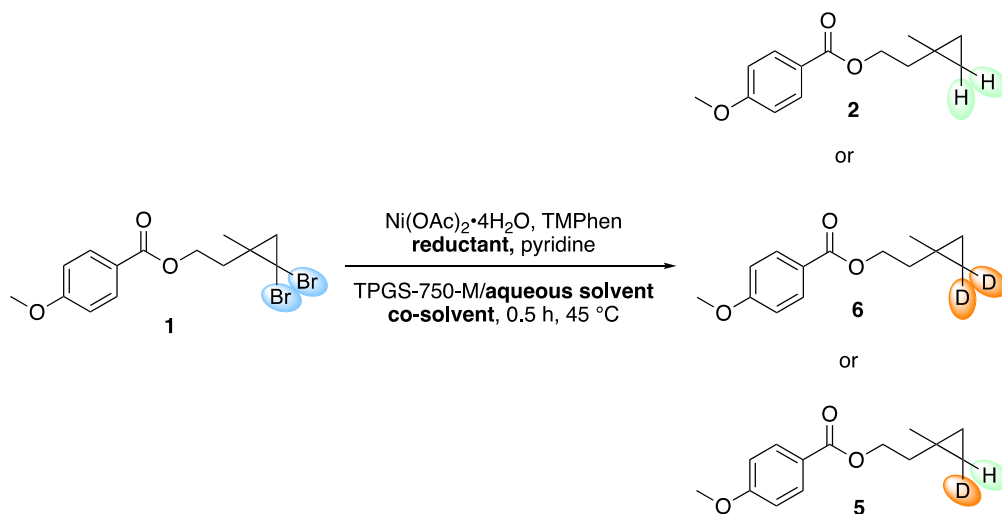
Figure 4. Two-step process towards the completely reduced, mono-deuterated product **5**



3.2.3. Mechanistic studies of di-reduction of *gem*-dibromocyclopropanes

To study deuteration of *gem*-dibromocyclopropane under di-reduction conditions, **1** was subjected to similar experiments with various permutations of deuterated reagents, as in the mono-reduction condition case (Table 2). Only mono-deuterated product **5** was detected by NMR analysis of crude reaction mixtures in the case where sodium borodeuteride was the only deuterated reagent used (entry 1). Use of THF-*d*₈ or D₂O did not lead to any deuterium incorporation and only product **2** was observed (entries 2-3). A combination of sodium borodeuteride with THF-*d*₈ or D₂O was not as selective and yielded a mixture of both mono- (**5**) and di-deuterated (**6**) products (entries 4-5). Finally, the combination of all three deuterated reagents resulted in complete deuterium incorporation and clean di-deuterated product **6**. The presence or absence of TPGS-750-M did not have any effect on deuterium incorporation in the direct di-deuteration case. The final di-deuterated product **6** could be separated via column chromatography to give 53% isolated yield (Figure 5).

Table 2. Optimization of reduction of **1** to di-deuterated product **6**



entry	reductant	aqueous solvent	co-solvent	deuterium incorporation
1	NaBD ₄	H ₂ O	THF	mono deuterated product
2	NaBH ₄	D ₂ O	THF	no deuterium incorporation
3	NaBH ₄	H ₂ O	THF- <i>d</i> ₈	no deuterium incorporation
4	NaBD ₄	D ₂ O	THF	mono- & di-deuterated product
5	NaBD ₄	H ₂ O	THF- <i>d</i> ₈	mono- & di-deuterated product
6	NaBD ₄	D ₂ O	THF- <i>d</i> ₈	di-deuterated product

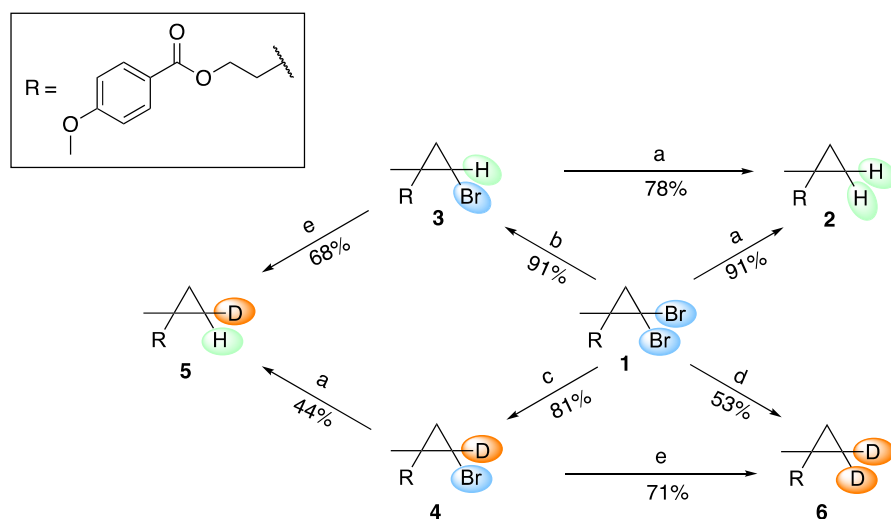
3.2.4. Access to a variety of isotopic analogs of reduced products of gem-dibromocyclopropanes

After optimization of conditions leading to both the mono- and di-deuteration products, it was possible to arrive at partially or fully debrominated cyclopropanes originating from the same *gem*-dibromocyclopropane. A variety of mono- and di-deuterated and proton containing cyclopropanes were synthesized in one or two steps from **1** (Figure 5). In all cases, separation of doubly reduced cyclopropane products from either the mono-reduced, or dibrominated starting material was quite straightforward.

Synthesis of deuterated products, either mono- or di-deuterated, are lower yielding reactions relative to those containing protonated species (i.e., see **4**, **5**, and **6** vs. **2** and **3**; Figure 5). This is expected due to kinetic isotope effects wherein sodium borohydride/borodeuteride resulted in a k_H/k_D of 4.4 for mono-reduction.¹¹ The large difference in reaction rates could potentially account for the considerable loss in yield, as well as unwanted protonated

cyclopropane side products that occur during this chemistry if the entire system is not completely deuterated. Interestingly, it was also observed that the yield associated with the overall 2-step process (77%) from **1** to **2** via **3** is lower compared to the 1-step direct double dehalogenation (91%).

Figure 5. Methodologies developed to access various isotopic analogs of reduced products from **1**



a) $\text{Ni}(\text{OAc})_2 \cdot 4\text{H}_2\text{O}$ (5 mol %), TMPhen (10 mol %), pyridine (1.5 equiv), and NaBH_4 (5 equiv) in 2 wt % TPGS-750-M/ H_2O (20% v/v THF). b) $\text{Ni}(\text{OAc})_2 \cdot 4\text{H}_2\text{O}$ (0.5 mol %), BiPy (1.0 mol %), pyridine (1.5 equiv), and NaBH_4 (2.5 equiv) in 2 wt % TPGS-750-M/ H_2O (20% v/v THF). c) $\text{Ni}(\text{OAc})_2 \cdot 4\text{H}_2\text{O}$ (0.5 mol %), BiPy (1.0 mol %), pyridine- d_5 (1.5 equiv), and NaBD_4 (2.5 equiv) in 2 wt % TPGS-750-M/ D_2O (20% v/v THF- d_8). d) $\text{Ni}(\text{OAc})_2 \cdot 4\text{H}_2\text{O}$ (5 mol %), TMPhen (10 mol %), pyridine (1.5 equiv), and NaBD_4 (5 equiv) in 2 wt % TPGS-750-M/ D_2O (20% v/v THF- d_8). e) $\text{Ni}(\text{OAc})_2 \cdot 4\text{H}_2\text{O}$ (5 mol %), TMPhen (10 mol %), pyridine (1.5 equiv), and NaBD_4 (5 equiv) in 2 wt % TPGS-750-M/ H_2O (20% v/v THF).

3.3. Conclusion

To conclude, an environmentally friendly methodology for the mono- and di-reduction of *gem*-dibromocyclopropanes in aqueous micellar media has been developed. This process uses an easily prepared nickel nanoparticle catalyst that requires an inexpensive and catalytic nickel(II) salt. TMPhen or 2,2'-bipyridine as ligands provide access to both mono- and di-reduced cyclopropane. Sodium borohydride as the reductant and pyridine as the base in 2 wt% TPGS-750-M/H₂O and small amount (20% v/v) of THF as organic co-solvent is all this 'green' methodology requires. The reactions are run at ambient temperatures and atmospheric pressure without the need for pressurized gases. This robust methodology can be utilized to incorporate deuterium onto the cyclopropyl rings. A variety of both mono- and di-deuterated and protonated cyclopropanes were synthesized. This provided interesting insight into the mechanism of the reduction reaction and suggested that the di-reduction undergoes a step-wise process with two separate reduction mechanisms. The studies also indicated that the mono-reduction of *gem*-dibromocyclopropane is potentially a radical-based process.

3.4. References

- 1) T. T. Talele, *J. Med. Chem.* **2016**, *59*, 8712-8756.
- 2) Njardarson Group, Top 200 Pharmaceutical Products by Retail Sales in 2018—https://Njardarson.Lab.Arizona.Edu/Sites/Njardarson.Lab.Arizona.Edu/Files/2018Top200PharmaceuticalRetailSalesPosterLowRes_0.Pdf, **2019**.
- 3) W. von E. Doering, A. K. Hoffmann, *J. Am. Chem. Soc.* **1954**, *76*, 6162–6165.
- 4) a) E. B. Averina, E. M. Budynina, Y. K. Grishin, A. N. Zefirov, T. S. Kuznetsova, N. S. Zefirov, *Russ. J. Org. Chem.* **2001**, *37*, 1409–1413; b) J. E. Baldwin, R. M. Adlington, D. G. Marquess, A. R. Pitt, M. J. Porter, A. T. Russell, *Tetrahedron* **1996**, *52*, 2515–2536; c) H. Tsue, H. Imahori, T. Kaneda, Y. Tanaka, T. Okada, K. Tamaki, Y. J. Sakata, *J. Am. Chem. Soc.* **2000**, *122*, 2279–2288; d) E. Fernandez-Megia, N. Gourlaouen, S. V. Ley, G. J. Rowlands, *Synlett* **1998**, 991–994; e) D. Seyferth, H. Yamazaki, D. L. Alleston, *J. Org. Chem.* **1963**, *28*, 703–706; f) S. Mataka, T. Sawada, M. Tashiro, M. Taniguchi, Y. Mitroma, *J. Chem. Res.* **1997**, 48–49; g) C. W. Jefford, D. Kirkpatrick, F. Delay, *J. Am. Chem. Soc.* **1972**, *94*, 8905–8907; h) C. V. Ramana, R. Murali, M. Nagarajan, *J. Org. Chem.* **1997**, *62*, 7694–7703.
- 5) M. Bänziger, C. Bucher, *Chim. Oggi.*, **2015**, *33*, 50-55.
- 6) a) M. von Seebach, S. I. Kozhushkov, R. Boese, J. Benet-Buchholz, D. S. Yufit, J. A. K. Howard, A. de Meijere, *Angew. Chem. Int. Ed.* **2000**, *39*, 2495–2498; *Angew. Chem.* **2000**, *112*, 2617–2620; b) A. Oku, H. Tsuji, M. Yoshida, N. Yoshiura, *J. Am. Chem. Soc.* **1981**, *103*, 1244–1246; c) J. A. Martínez-Perez, L. Sarandeses, J. Granja, J. Palenzuela, A. Mourino, *Tetrahedron Lett.* **1998**, *39*, 4725–4728; d) E. Vogel, W. Wiedemann, H. D. Roth, J. Eimer, H. Günther, *Justus Liebig's Ann. Chem.* **1972**, *759*, 1–36; e) T. Sugimura, T. Futagawa, T. Katagiri, N. Nishiyama, A. Tai, *Tetrahedron Lett.* **1996**, *37*, 7303–7306; f) L. A. Paquette, E. Chamot, A. R. Browne, *J. Am. Chem. Soc.* **1980**, *102*, 637–643; g) J. E. Baldwin, R. Shukla, *J. Phys. Chem. A* **1999**, *103*, 7821–7825; h) W. Kraus, G. Klein, H. Sadlo, W. Rothenwohrer, *Synthesis* **1972**, 485–487; i) Y. M. Sheikh, J. Leclercq, C. Djerassi, *J. Chem. Soc. Perkin Trans. 2* **1974**, 909–914.
- 7) T. S. Kuznetsova, O. V. Kokoreva, E. B. Averina, A. N. Zefirov, Y. K. Grishin, N. S. Zefirov, *Russ. Chem. Bull.* **1999**, *48*, 929–933; b) M. S. Baird, P. Licence, V. V. Tverezovsky, I. G. Bolesov, W. Clegg, *Tetrahedron* **1999**, *55*, 2773–2784; c) R. J. de Lang, L. Brandsma, *Synth. Commun.* **1998**, *28*, 225–232.
- 8) C. Gütz, M. Selt, M. Bänziger, C. Bucher, C. Romelt, N. Hecken, F. Gallou, T. R. Galvao, S. R. Waldvogel, *Chem. Eur. J.* **2015**, *21*, 13878–13882.
- 9) R. B. Raffa, R. Taylor, *J. Pharm. Pharmacol* **2018**, *9*, 440-446.
- 10) D. G. Holah, A. N. Hughes, B. C. Hui, *Can. J. Chem.* **1977**, *55*, 4048–4055.
- 11) J. T. Groves, K. W. Ma, *J. Am. Chem. Soc.* **1974**, *96*, 6527–6529.

3.5. *General experimental information*

A solution of 2 wt % surfactant/H₂O was prepared by dissolving the surfactant in degassed HPLC grade water and was stored under argon. TPGS-750-M is available from Sigma-Aldrich (catalog #733857 (solution) or #763896 (wax)) or can be prepared following the reported procedure.¹⁷ All commercially available reagents were used without further purification. Thin layer chromatography (TLC) was done using Silica Gel 60 F254 plates (Merck, 0.25 mm thick). Flash chromatography was done in glass columns using Silica Gel 60 (EMD, 40-63 μm). ¹H and ¹³C NMR were recorded at 25 °C either on a Varian Unity Inova 400 MHz, a Varian Unity Inova 500 MHz or on a Varian Unity Inova 600 MHz spectrometers in CDCl₃ with residual CHCl₃ (¹H = 7.27 ppm, ¹³C = 77.16 ppm) as internal standard. Chemical shifts are reported in parts per million (ppm). Data are reported as follows: chemical shift, multiplicity (s = singlet, d = doublet, t = triplet, q = quartet, quin = quintet, m = multiplet), coupling constant (if applicable) and integration. HRMS data were recorded on a Waters Micromass LCT TOF ES+ Premier mass spectrometer using ESI ionization.

¹⁷ Lipshutz, B. H.; Ghorai, S.; Abela, A. R.; Moser, R.; Nishikata, T.; Duplais, C.; Krasovskiy, A.; Gaston, R. D.; Gadwood, R. C. TPGS-750-M: A Second-Generation Amphiphile for Metal-Catalyzed Cross-Couplings in Water at Room Temperature. *J. Org. Chem.* **2011**, *76*, 4379–4391.

3.6. General procedure

3.6.1. General procedure for the di-reduction of *gem*- *dibromocyclopropanes*

In a 5 mL round-bottom flask, was added Ni(OAc)₂•4H₂O (2.5 mg, 5 mol %) and 3,4,7,8-tetramethyl-1,10-phenanthroline (TMPhen - 4.7 mg, 10 mol %). A septum was adapted and the flask was purged with argon. A 2 wt % solution of TPGS-750- M/H₂O (0.32 mL, 0.5 M total) was added. Formation of a purple complex was allowed by stirring the solution for 10 min. Pyridine (24 μL, 0.3 mmol, 1.5 equiv) was added. After 5 min, NaBH₄ (37.8 mg, 1 mmol, 5 equiv) was added in one portion and the vial was capped again and sealed to prevent any leak. The *gem*-dibromocyclopropane (0.2 mmol, 1 equiv) was dissolved in THF (80 μL, 20% v/v) and added as a solution to the flask through the septum. A 6 mL syringe (containing 0.1 mL THF) was added through the septum to accept evolving hydrogen gas. The reaction was stirred for 30 min at 45 °C (Note: in the cases of fused cycles 6 and 7, the reaction was performed at rt). If the volume of gas generated exceeds the volume of the syringe, the syringe must be emptied outside of the flask and the ballast adapted again. After completion, the reaction was dissolved in EtOAc (3 mL) and filtered through a pad of silica. The pad was rinsed with EtOAc (3 x 3 mL). The organic layer was dried over anhydrous MgSO₄, filtered, and concentrated under vacuum. Purification by flash chromatography was then performed.

3.6.2. General procedure for the mono-reduction of *gem*- *dibromocyclopropanes*

In a 5 mL round-bottom flask was added Ni(OAc)₂•4H₂O (1.2 mg, 0.5 mol %) and bipyridine (1.6 mg, 1 mol %). A septum was adapted and the flask was purged with argon. A 2 wt % solution of TPGS-750-M/H₂O (2.0 mL, 0.5 M) was added. Formation of a purple complex is allowed by stirring the solution for 10 min. Pyridine (121 μL, 1.5 mmol, 1.5 equiv) was added. After 5 min, NaBH₄ (94.6 mg, 5 mmol, 5 equiv) was added in one portion and the vial was capped again and sealed to prevent any leak. The *gem*-dibromocyclopropane (1.0 mmol, 1 equiv) was dissolved in THF (0.4 mL, 20% v/v) and added as a solution to the flask through the septum. A 6 mL syringe (containing 0.1 mL THF) was added as through the top of the septum to accept evolving hydrogen gas. The reaction was stirred for 30 min at 45 °C. If the volume of gas generated exceeds the volume of the syringe, the syringe must be emptied outside of the flask and adapted again. After completion, the reaction was dissolved in EtOAc (3 mL) and filtered through a pad of silica. The pad was rinsed with EtOAc (3 x 3 mL). The organic layer was dried over anhydrous MgSO₄, filtered, and concentrated under vacuum. Purification by flash chromatography was then performed.

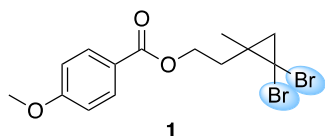
3.6.3. General procedure for deuteration studies

In a 5 mL round-bottom flask, was added the catalyst (5 mol %) and 3,4,7,8-tetramethyl-1,10-phenanthroline (TMPhen - 4.7 mg, 10 mol %). A septum was adapted and the flask was purged with argon. TPGS-750-M/2 wt % in H₂O or D₂O (0.32 mL, 0.5 M total) was added. The formation of a purple complex was observed upon stirring the solution for 10 min. Pyridine or pyridine-*d*₅ (24 μL, 0.3 mmol, 1.5 equiv) was added. After 5 min, the NaBH₄ or NaBD₄ (1 mmol, 5 equiv) was added in one portion and the vial was capped again and sealed to prevent any leak. The *gem*-dibromocyclopropane (0.2 mmol, 1 equiv) was dissolved in THF

or THF- d_8 (80 μ L, 20% v/v) and added as a solution to the flask through the septum. A 6 mL syringe (containing 0.1 mL THF) was added through the septum to accept evolving gas. The reaction was stirred for 30 min at 45 °C. If the volume of gas generated exceed the volume of the syringe, the syringe must be emptied outside of the flask and the syringe adapted again. After completion, the reaction was dissolved in EtOAc (3 mL), filtered through a pad of silica and the crude was analyzed by ^1H NMR to determine the percentage of deuterium incorporated.

3.7. Product characterization (NMR and HRMS)

2-(2,2-Dibromo-1-methylcyclopropyl)ethyl 4-methoxybenzoate (**1**)



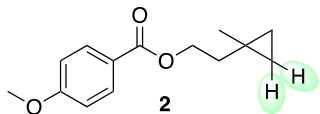
^1H NMR (400 MHz, CDCl_3) δ 8.16 – 7.88 (m, 2H, Ar-H), 7.04 – 6.84 (m, 2H, Ar-H), 4.51 (td, $J = 6.8, 2.2$, 2H, O- CH_2), 3.87 (s, 3H, O- CH_3), 2.16 (hept, $J = 7.6, 7.2$, 2H, CH_2), 1.57 (d, $J = 7.5$, 1H, CH_2), 1.49 (d, $J = 2.4$, 1H, CH_2), 1.48 (s, 3H, CH_3);

^{13}C NMR (101 MHz, CDCl_3) δ 166.4, 163.5, 131.8, 122.6, 113.8, 62.2, 55.6, 38.4, 37.1, 34.6, 27.8, 22.8. brown solid.

$R_f = 0.26$ (90:10 hexanes/EtOAc).

Chemical Formula: HRMS (ESI) m/z : $[\text{M}+\text{Na}]^+$ calcd. for $\text{C}_{14}\text{H}_{16}\text{Br}_2\text{O}_3\text{Na}$ 412.9364; found: 412.9367.

2-(1-Methylcyclopropyl)ethyl 4-methoxybenzoate (**2**)



¹H NMR (400 MHz, CDCl₃) δ 7.99 (d, 2H, Ar-H), 6.91 (d, 2H, Ar-H), 4.40 (t, $J = 6.9$, 2H, O-CH₂), 3.85 (s, 3H, O-CH₃), 1.69 (t, $J = 6.9$, 2H, CH₂), 1.11 (s, 3H, CH₃), 0.38 – 0.25 (m, 4H, 2 x CH₂);

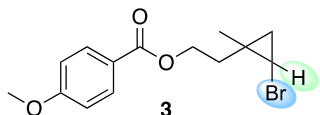
¹³C NMR (101 MHz, CDCl₃) δ 166.6, 163.3, 131.7, 123.1, 113.7, 63.5, 55.5, 38.2, 23.0, 13.2, 12.9.

Yield: 91%, 42.5 mg, colorless oil.

R_f = 0.40 (95:5 hexanes/EtOAc).

Chemical Formula: HRMS (ESI) m/z : [M+Na]⁺ calcd. for C₁₄H₁₈O₃Na 257.1154; found: 257.1148.

2-(2-Bromo-1-methylcyclopropyl)ethyl 4-methoxybenzoate (**3**)



¹H NMR (500 MHz, CDCl₃) major diastereoisomers δ 8.01 (tt, $J = 8.5, 1.6$, 2H, Ar-H), 6.99 – 6.87 (m, 2H, Ar-H), 4.45 – 4.34 (m, 2H, CH₂), 3.96 – 3.78 (s, 3H, CH₃), 2.95 (ddd, $J = 6.2, 4.5, 1.6$, 1H, CH-Br), 2.03 (td, $J = 7.0, 1.9$, 1H, CH₂), 1.76 – 1.66 (m, 1H, CH₂), 1.35 (s, 3H, CH₃), 1.14 – 1.07 (m, 1H, CH₂), 0.71 (ddd, $J = 6.4, 4.4, 1.8$, 1H, CH₂); minor diastereoisomers δ 8.01 (tt, $J = 8.5, 1.6$, 2H, Ar-H), 6.99 – 6.86 (m, 2H, Ar-H), 4.48 (tdd, $J = 7.3, 4.3, 2.9$, 2H,

CH₂), 3.96 – 3.78 (s, 3H, CH₃), 2.88 (ddd, *J* = 7.7, 4.4, 1.7, 1H, CH-Br), 2.03 (td, *J* = 7.0, 1.9, 1H, CH₂), 1.80 (dtd, *J* = 12.5, 6.2, 1.7, 1H, CH₂), 1.24 – 1.17 (s, 3H, CH₃), 1.05 (ddd, *J* = 8.1, 6.3, 1.8, 1H, CH₂), 0.80 (ddd, *J* = 6.5, 4.6, 1.9, 1H, CH₂);

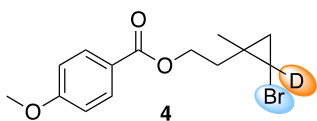
¹³C NMR (126 MHz, CDCl₃) major diastereoisomers δ 166.4, 163.5, 131.8, 122.8, 113.8, 62.4, 55.6, 37.7, 35.3, 29.4, 22.3, 20.3, 19.1; minor diastereoisomers δ 166.5, 163.5, 131.8, 122.9, 113.8, 62.8, 55.6, 37.7, 35.3, 29.5, 22.8, 22.6, 20.3, 19.2.

Yield: 91%, 285.7 mg, colorless oil.

R_f = 0.74 (80:20 hexanes/EtOAc).

Chemical Formula: HRMS (ESI) *m/z*: [M+Na]⁺ calcd. for C₁₄H₁₇BrO₃Na 335.0259; found: 335.0268.

2-(2-Bromo-1-methylcyclopropyl-2-*d*)ethyl 4-methoxybenzoate (**4**)



¹H NMR (400 MHz, CDCl₃) major diastereomers δ 8.05 – 7.96 (m, 2H), 6.96 – 6.90 (m, 2H, ArH), 4.52 – 4.33 (m, 2H), 3.86 (s, 3H), 2.02 (t, *J* = 6.9 Hz, 1H), 1.70 (dt, *J* = 14.2, 7.0 Hz, 1H), 1.34 (s, 3H), 1.09 (d, *J* = 6.3 Hz, 1H), 0.69 (d, *J* = 6.3 Hz, 1H); minor diastereomers δ 8.05 – 7.96 (m, 2H), 6.96 – 6.90 (m, 2H), 4.52 – 4.33 (m, 2H), 3.86 (s, 3H), 2.02 (t, *J* = 6.9 Hz, 1H), 1.79 (dt, *J* = 14.2, 6.2 Hz, 1H), 1.19 (s, 3H), 1.03 (d, *J* = 6.3 Hz, 1H), 0.78 (d, *J* = 6.3 Hz, 1H);

¹³C NMR (101 MHz, CDCl₃) major diastereomers δ 166.25 (s), 163.34 (s), 131.57 (s), 122.53 (s), 113.60 (s), 62.23 (s), 55.41 (s), 37.43 (s), 35.07 (s), 22.41 (s), 20.14 (s), 18.86 (s);

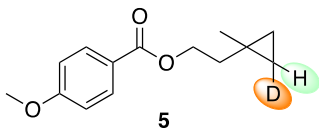
minor diastereomers δ 166.33 (s), 163.34 (s), 131.57 (s), 122.70 (s), 113.57 (s), 62.67 (s), 55.41 (s), 37.43 (s), 35.07 (s), 22.33 (s), 21.95 (s), 18.90 (s);

Yield: 81%, 127.2 mg, colorless oil.

R_f = 0.45 (90:10 hexane/EtOAc).

Chemical Formula: HRMS (ESI) m/z : $[M+Na]^+$ calcd. for C₁₄H₁₆Br DO₃Na 336.0322; found: 336.0325.

2-(1-Methylcyclopropyl-2-*d*)ethyl 4-methoxybenzoate (**5**)



¹H NMR (400 MHz, CDCl₃) mixture of diastereomers δ 7.99 (d, J = 8.9 Hz, 2H), 6.92 (d, J = 8.9 Hz, 2H), 4.40 (t, J = 6.9 Hz, 2H), 3.86 (s, 3H), 1.69 (t, J = 6.9 Hz, 2H), 1.11 (s, 3H), 0.37 – 0.25 (m, 3H);

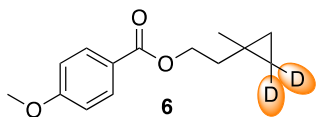
¹³C NMR (101 MHz, CDCl₃) δ 166.41 (s), 163.19 (s), 131.49 (s), 122.92 (s), 113.53 (s), 63.37 (s), 55.38 (s), 37.99 (s), 22.79 (s), 12.97 (s), 12.66 (s), 12.81 – 12.41 (m).

Yield: 44%, 20.6 mg, colorless oil.

R_f = 0.43 (90:10 hexane/EtOAc).

Chemical Formula: HRMS (ESI) m/z : $[M+Na+CH_3OH]^+$ calcd. for C₁₄H₁₇DO₃NaCH₃OH: 290.1479; found: 290.1471.

2-(1-Methylcyclopropyl-2,2-*d*₂)ethyl 4-methoxybenzoate (**6**)



^1H NMR (400 MHz, CDCl_3) δ 7.99 (d, 2H), 6.92 (d, 2H), 4.40 (t, $J = 6.9$ Hz, 2H), 3.86 (s, 3H), 1.69 (t, $J = 6.9$ Hz, 2H), 1.11 (s, 3H), 0.31 (dd, $J = 26.0, 4.6$ Hz, 2H);

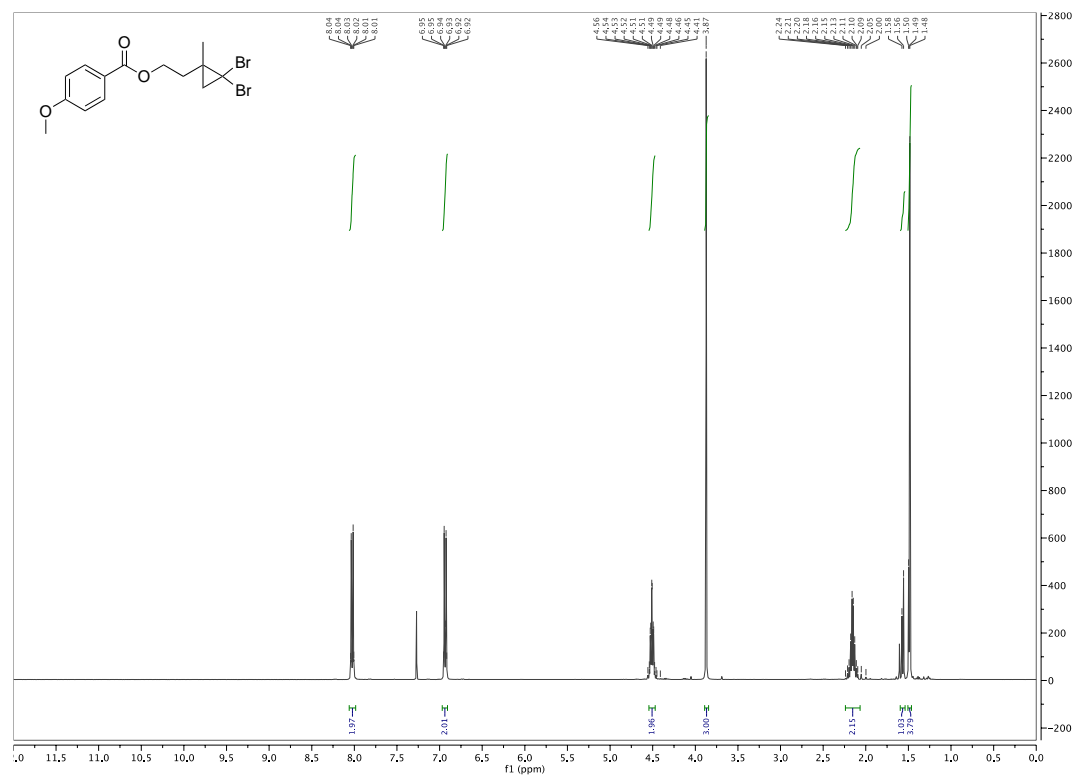
^{13}C NMR (101 MHz, CDCl_3) δ 166.40 (s), 163.19 (s), 131.49 (s), 122.92 (s), 113.53 (s), 63.37 (s), 55.38 (s), 37.95 (s), 22.75 (s), 12.87 (s), 12.66 (s), 12.54 (s).

Yield: 53%, 24.9 mg, colorless oil.

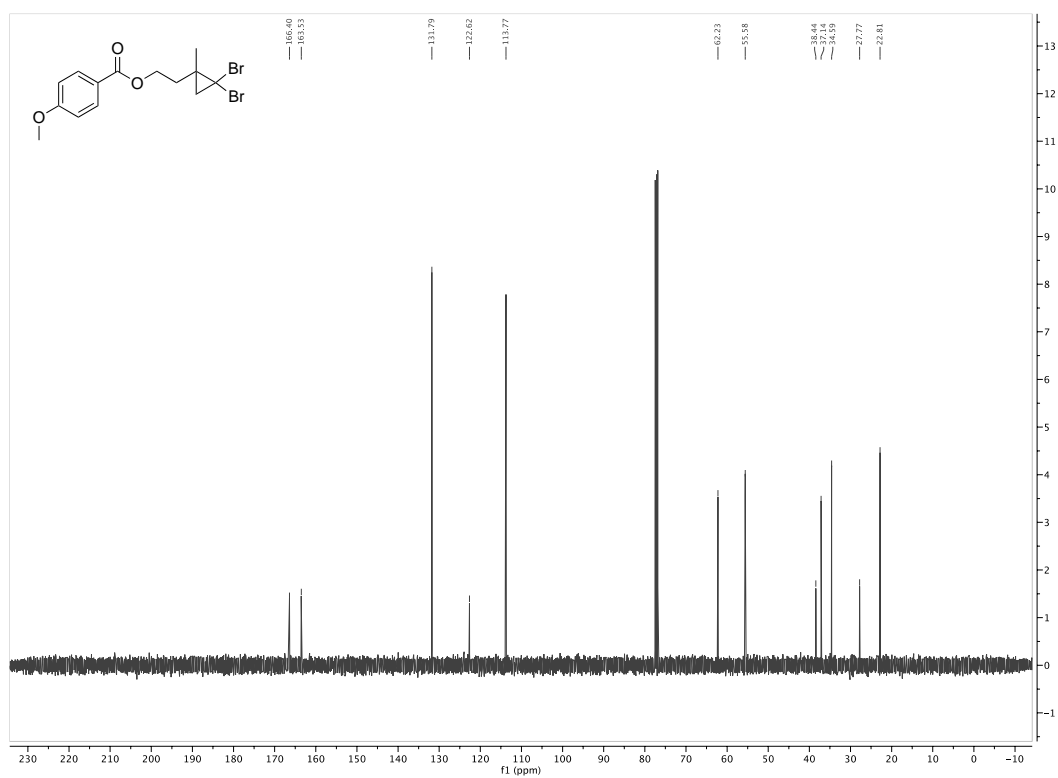
R_f = 0.53 (90:10 hexane/EtOAc).

Chemical Formula: HRMS (ESI) m/z : $[\text{M}+\text{Na}+\text{CH}_3\text{OH}]^+$ calcd. for $\text{C}_{14}\text{H}_{16}\text{D}_2\text{O}_3\text{NaCH}_3\text{OH}$: 291.1541; found: 291.1541.

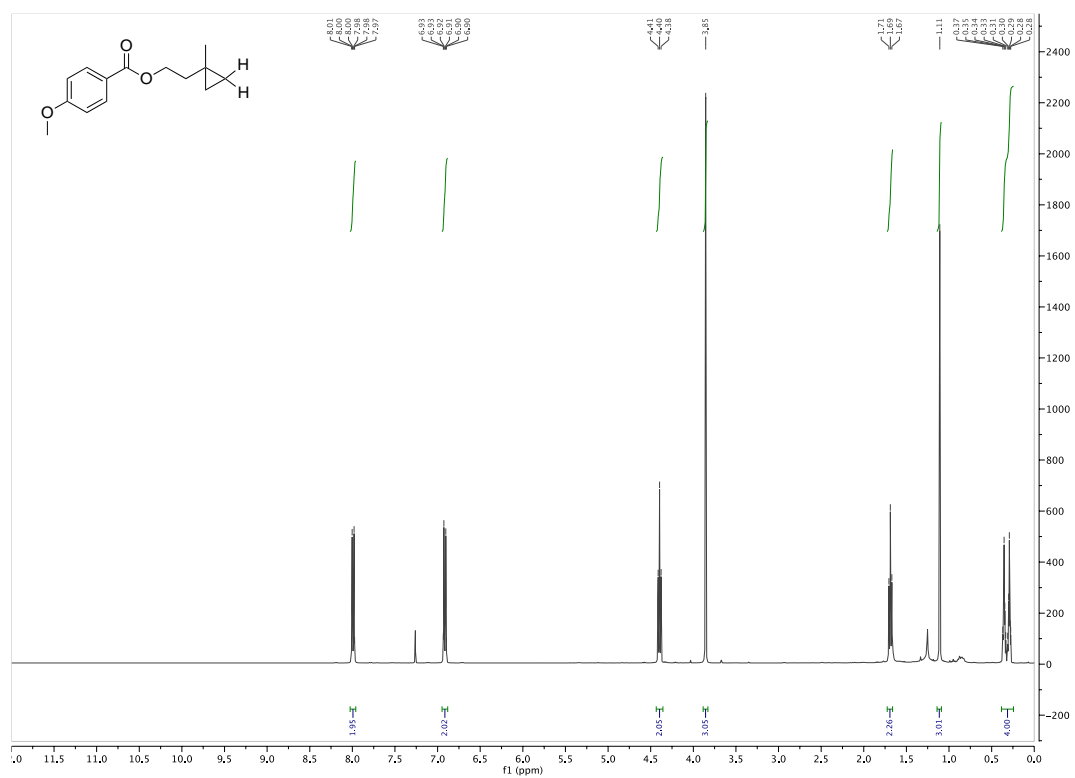
3.8. NMR spectra



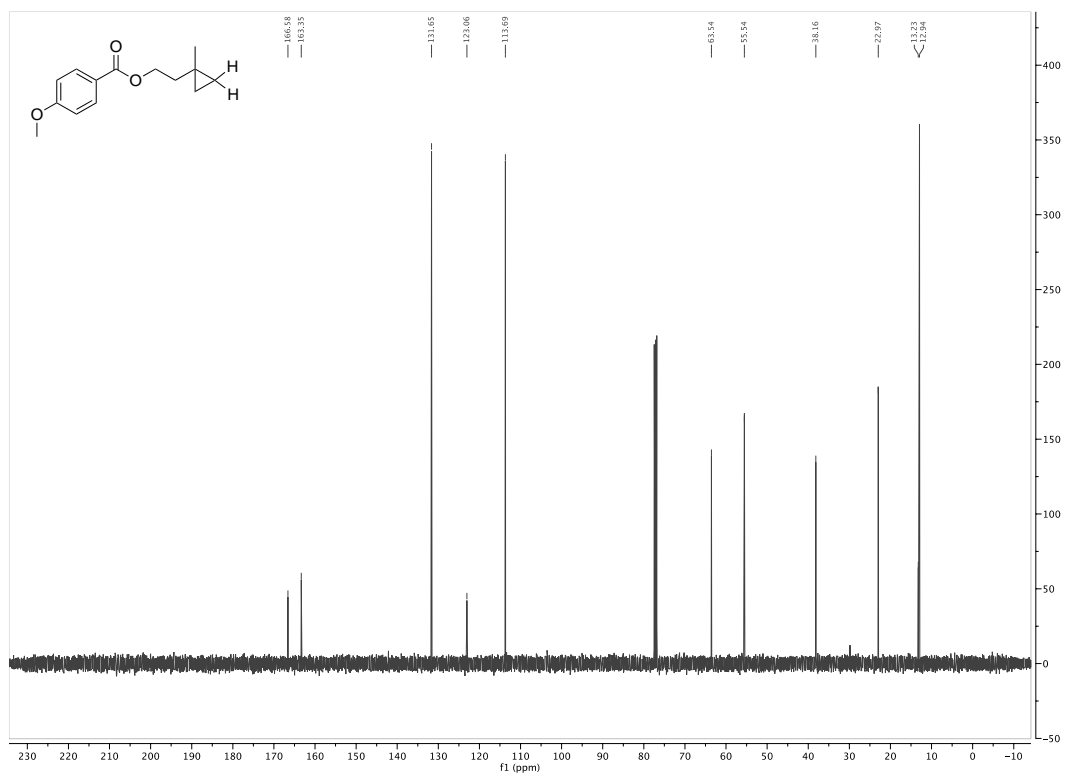
¹H NMR spectra of 2-(2,2-Dibromo-1-methylcyclopropyl)ethyl 4-methoxybenzoate (**1**)



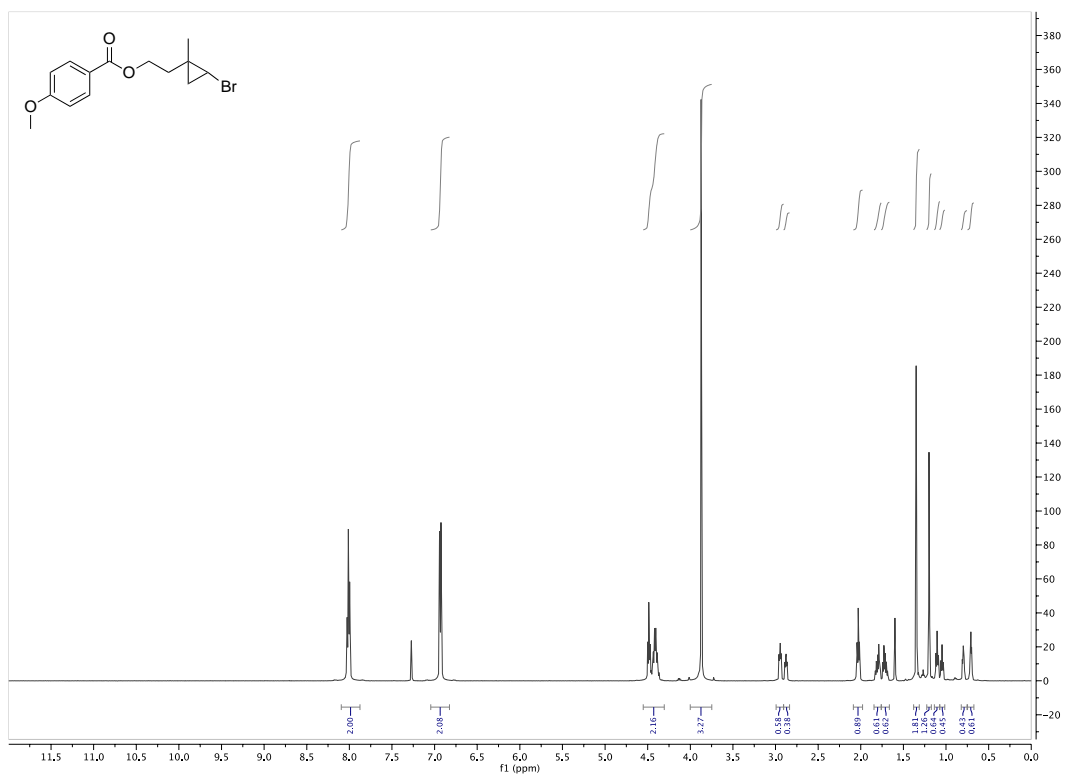
^{13}C NMR spectra of 2-(2,2-Dibromo-1-methylcyclopropyl)ethyl 4-methoxybenzoate (**1**)



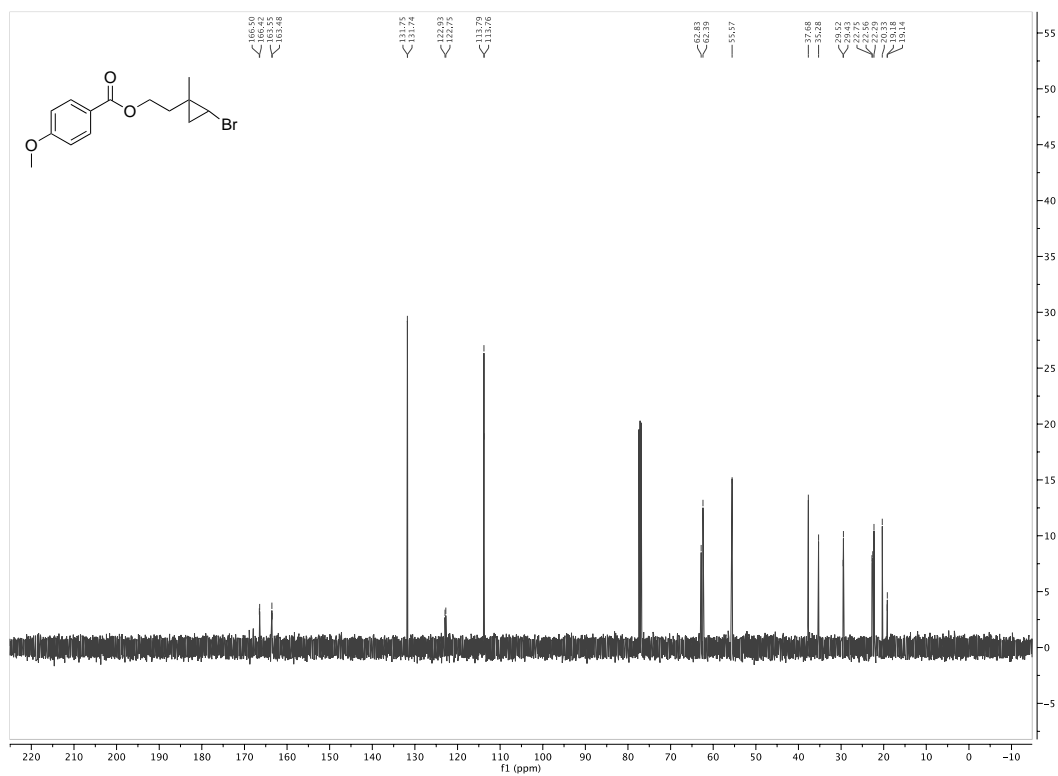
¹H NMR spectra of 2-(1-Methylcyclopropyl)ethyl 4-methoxybenzoate (**2**)



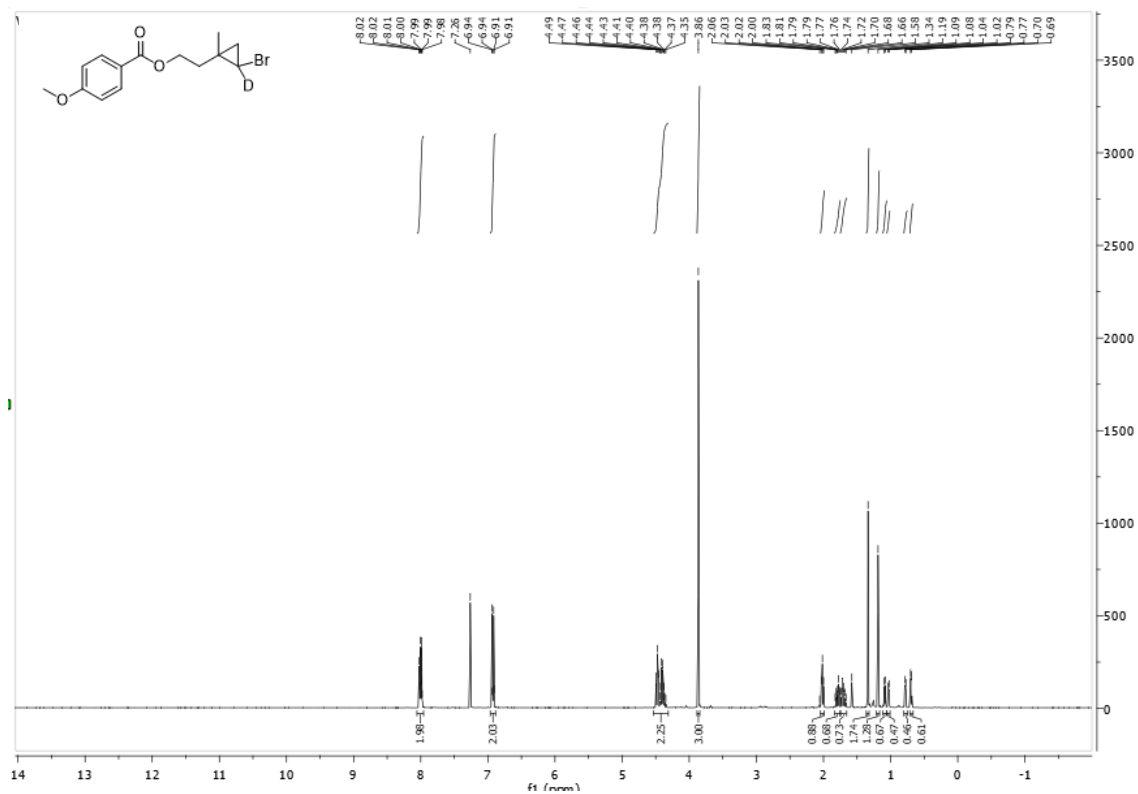
^{13}C NMR spectra of 2-(1-Methylcyclopropyl)ethyl 4-methoxybenzoate (2)



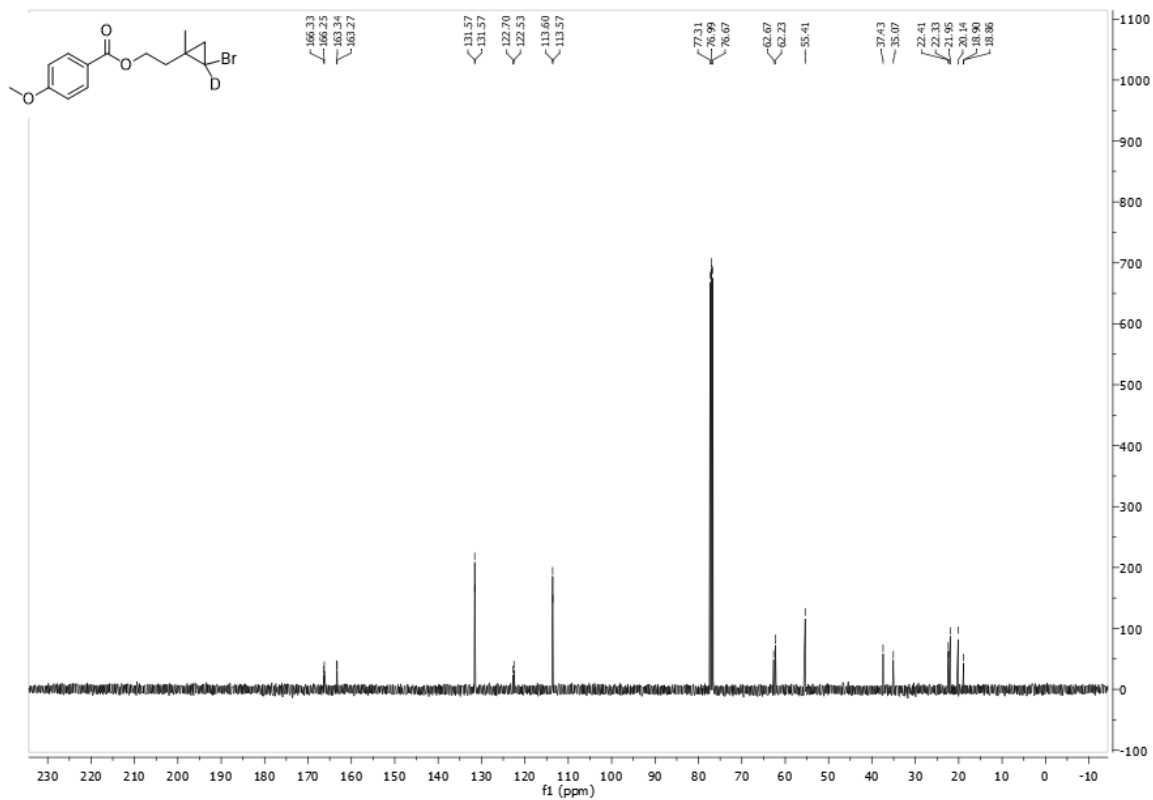
¹H NMR spectra of 2-(2-bromo-1-methylcyclopropyl)ethyl 4-methoxybenzoate (**3**)



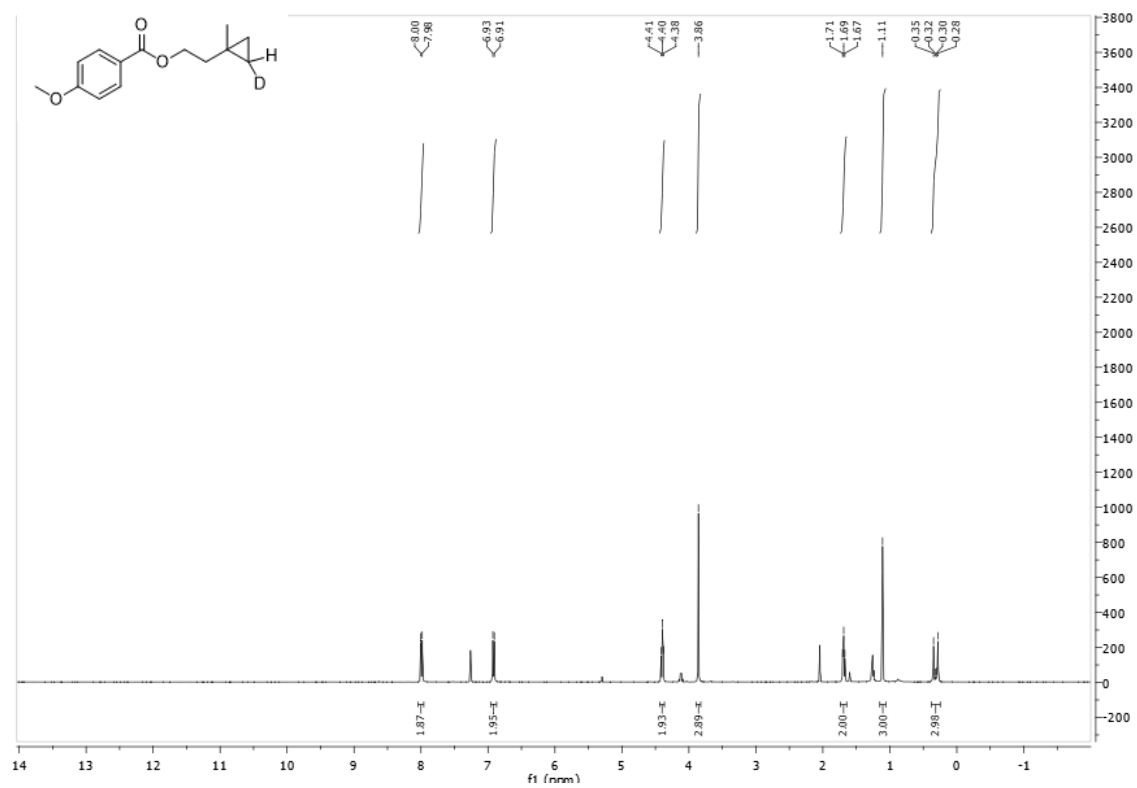
¹³C NMR spectra of 2-(2-Bromo-1-methylcyclopropyl)ethyl 4-methoxybenzoate (**3**)



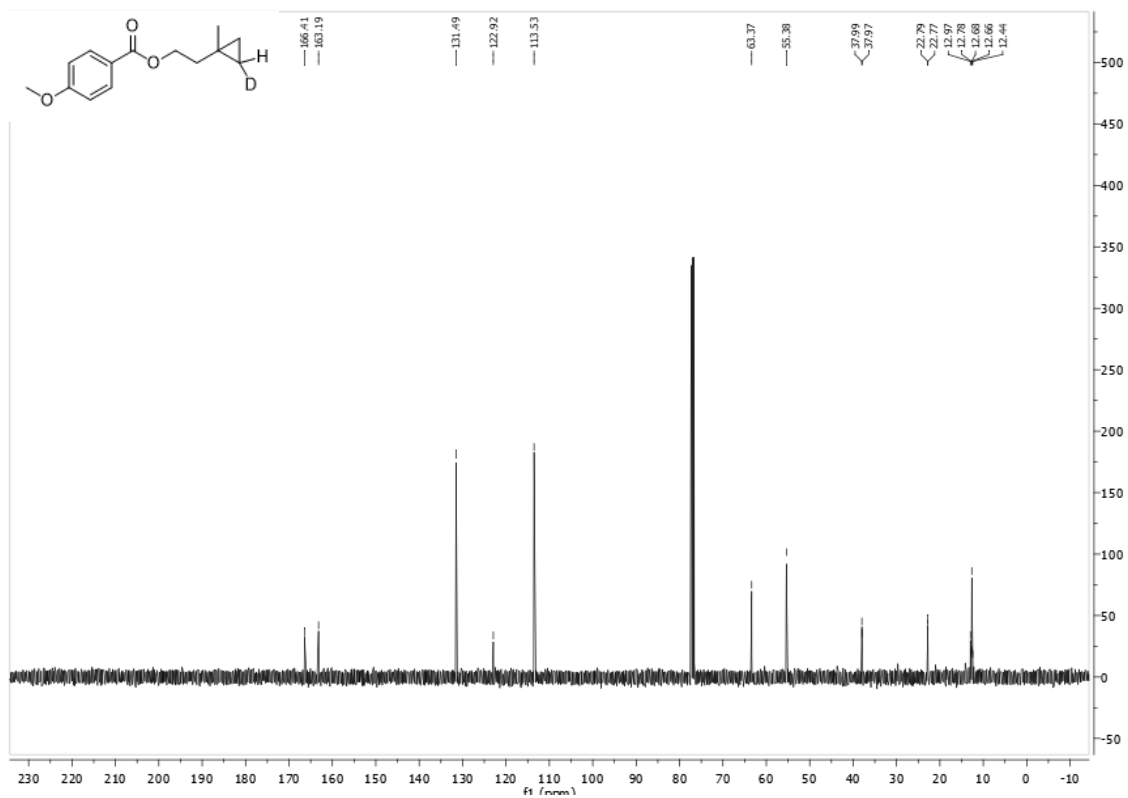
¹H NMR spectra of 2-(2-Bromo-1-methylcyclopropyl-2-d)ethyl 4-methoxybenzoate (**4**)



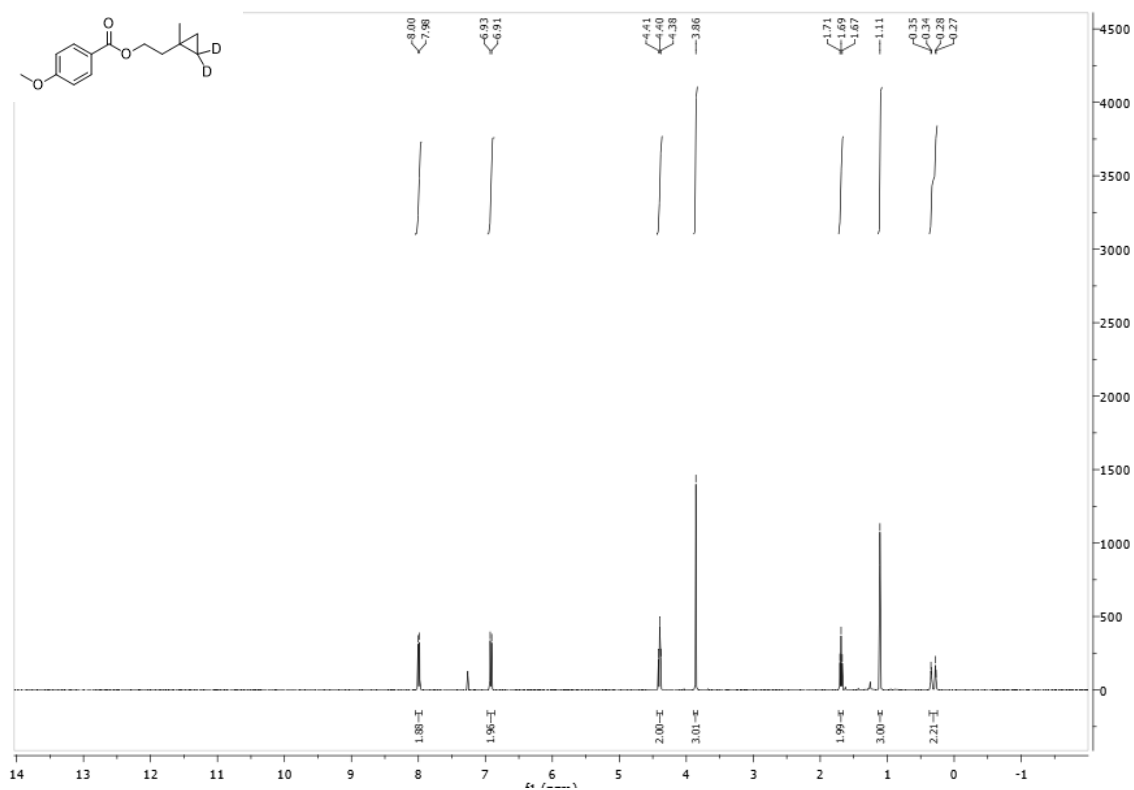
^{13}C NMR spectra of 2-(2-Bromo-1-methylcyclopropyl-2-*d*)ethyl 4-methoxybenzoate (**4**)



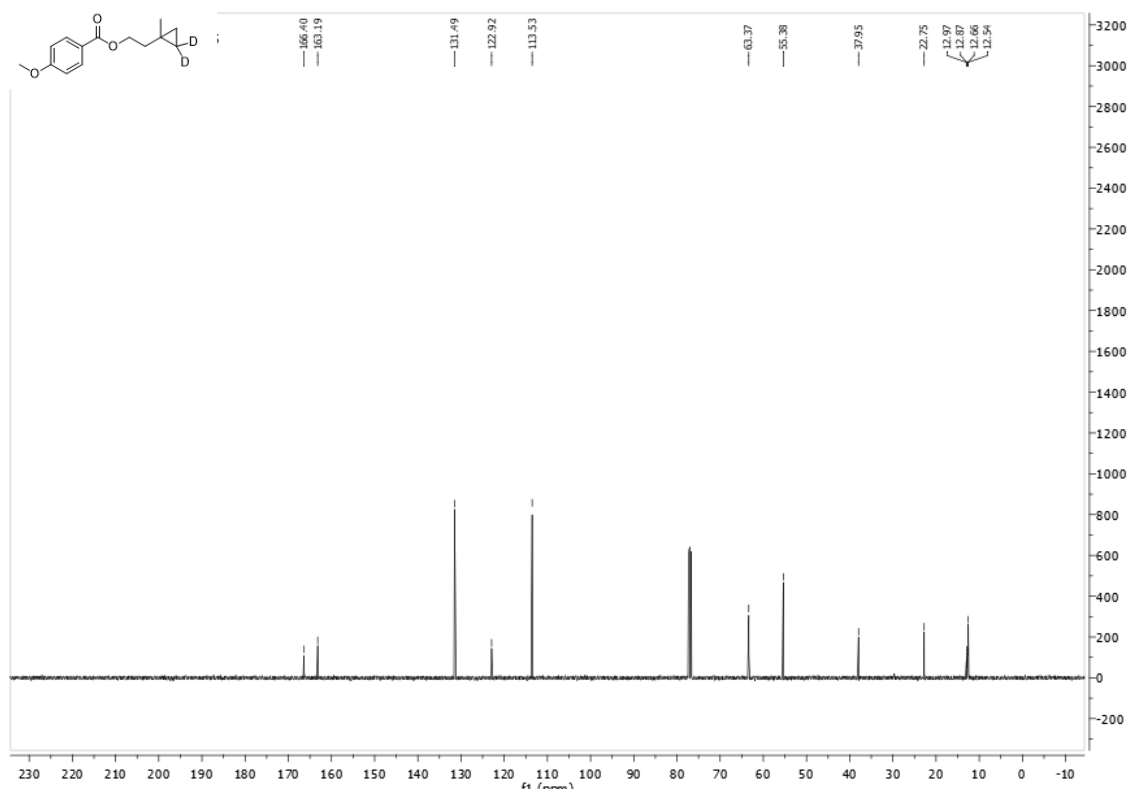
¹H NMR spectra of 2-(1-Methylcyclopropyl-2-d)ethyl 4-methoxybenzoate (**5**)



^{13}C NMR spectra of 2-(1-Methylcyclopropyl-2-*d*)ethyl 4-methoxybenzoate (**5**)



¹H NMR spectra of 2-(1-Methylcyclopropyl-2,2-d₂)ethyl 4-methoxybenzoate (**6**)



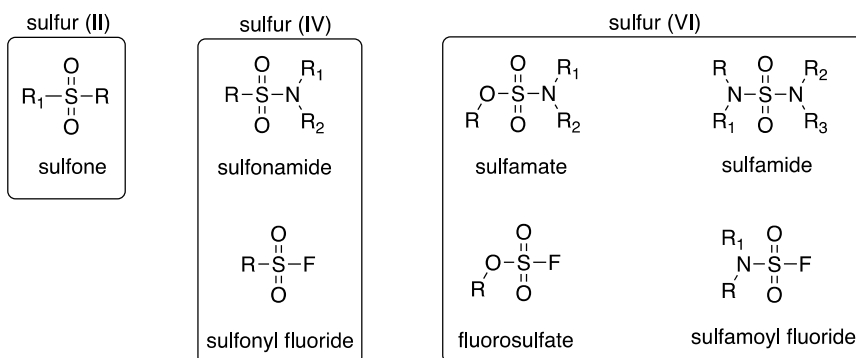
¹³C NMR spectra of 2-(1-Methylcyclopropyl-2,2-*d*₂)ethyl 4-methoxybenzoate (**6**)

4. Synthesis of sulfamate esters

4.1. Introduction and background

Sulfur containing functional groups often exist in pharmaceuticals and natural products.¹ The versatility in the functionalities arise from various oxidation states of sulfur that range from -2 to +6 (Figure 1). Sulfur (VI) containing motifs such as sulfamate, sulfamide, fluorosulfate and sulfamoyl fluoride are widely used by medicinal chemists. Sulfamate and sulfamide can pose as both hydrogen-bond donor and acceptor in a chemical structure and are often used as bioisosteres for amides, ureas, and carbamates.¹

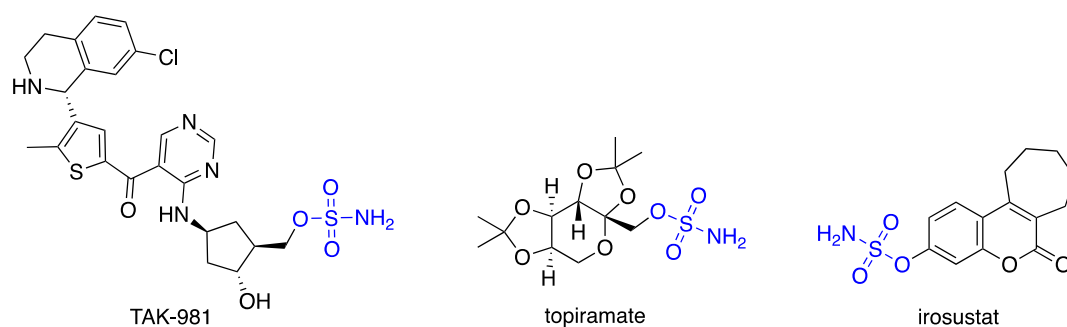
Figure 1. Sulfur-containing functional groups with various oxidation states



Steroid sulfatase (STS) is an enzyme responsible for formation of both active estrogens and androgens post-hydrolysis of steroid sulfates. These active species invigorate hormone-dependent cancer cell proliferation leading to breast cancer tumorigenesis.¹ Thus, a number of STS inhibitors have been reported in the past 20 years and many of them contain the sulfur (VI) motif, sulfamate.² The aryl *O*-sulfamate pharmacophore exists in many steroidal and non-

steroidal drugs that are in clinical and pre-clinical trials for oncology and women's health. For example, irosustat, is an irreversible and nonsteroidal STS inhibitor in clinical trials for treatment of hormone-sensitive tumors such as breast, prostate, and endometrial cancers (Figure 2). Topiramate is another sulfamate containing drug that is very commonly prescribed for the treatment of epilepsy and migraine. Currently, the drug is being evaluated for treatment of severe pediatric obesity and alcohol use disorder.² Recently, in 2021, Takeda identified another enzyme inhibitor, TAK-981 that is being evaluated in clinical trials for the treatment of metastatic solid tumor and lymphoma.³

Figure 2. Sulfamate-containing therapeutics



The sulfamate functional group can either be obtained from its sulfamoyl halide or halide sulfate counterpart. Chlorides and fluorides are more widely used than bromides or iodides since the latter is more prone to reduction and radical reaction than nucleophilic substitution.⁴ While comparing the bond strengths of S-F and S-Cl, the homolytic bond dissociation of S-F in SO₂F₂ is ~85 kcal mol⁻¹ whereas that of S-Cl in SO₂Cl₂ is ~46 kcal mol⁻¹ indicating that -SO₂F containing reagents are more likely to undergo nucleophilic substitution.⁴ Even though S-F bonds provide more stability, it has reduced reactivity which can be easily overcome by

polarizing the bond via hydrogen bonding or exposure to Lewis acids. Reactions involving the $-\text{SO}_2\text{F}$ group can also be accelerated by stabilizing the fluoride ion which makes it a better leaving group during elimination. These stabilized S(VI)-F bonds can also be activated by coupling agents such as DMAP and DBU. Thus, between chlorides and fluorides, S(VI)-F moieties provide more chemoselectivity, thermal stability, and hydrolytic stability giving rise to a new type of click chemistry known as sulfur (VI) fluoride exchange (SuFEx). (Table 1). Hence, it is clear that nucleophilic attack on S(VI) fluoride occurs exclusively at the sulfur atom using the SuFEx mechanism, making this a more favorable method to synthesize sulfamates.

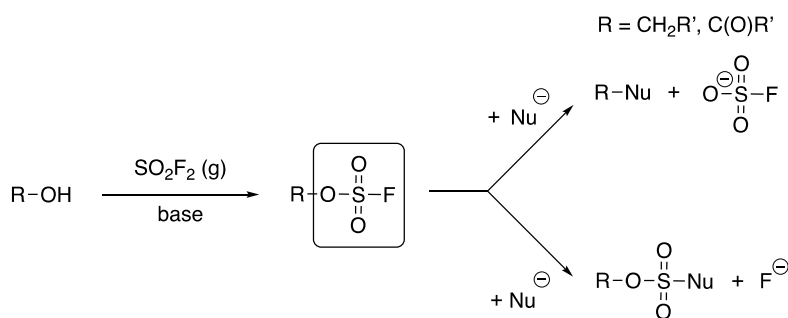
Table 1. Differences between sulfonyl fluoride and sulfonyl chloride

sulfonyl chloride	sulfonyl fluoroide
homolytic scission – easily irreversibly reduced	heterolytic cleavage – resistant to reduction
thermally and hydrolytically fragile	more stable towards thermolysis and hydrolysis
mixed products from nucleophilic attack - sulfonylation and chlorination	reaction with nucleophiles gives only sulfonylation product

Fluorosulfates have been taken advantage of to prepare sulfamates by simply relying on nucleophilic attack by an amine (Figure 3). Fluorosulfates can be synthesized from an alcohol using SO_2F_2 gas at high temperatures in the presence of a base. Depending on the substituent on the fluorosulfate, the $-\text{OSO}_2\text{F}$ can either be a good leaving group or a sturdy connector.⁴

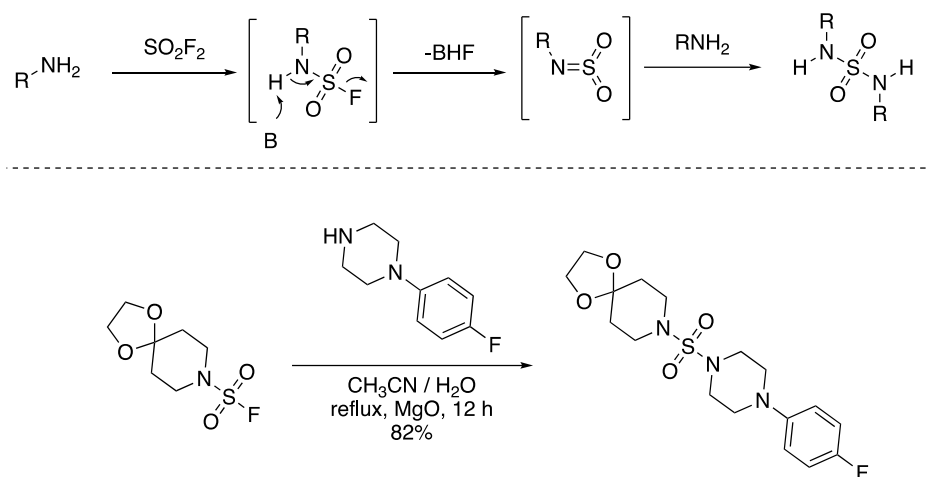
Mono-substituted sulfamoyl fluorides are difficult to synthesize using SO_2F_2 since they rapidly undergo elimination to form the azasulfene intermediate (Scheme 1, top). Owing to the acidic nature of the proton on the nitrogen of this sulfamoyl fluoride basic pH can immediately collapse the functional group to the facile intermediate which, however, can be captured by an amine to produce a sulfamide.⁴

Figure 3. Synthesis and reactivity of fluorosulfates



Di-*N*-substituted sulfamoyl fluoride, on the other hand, are very stable compounds that can be synthesized from SO_2F_2 . However, this requires forcing conditions for further reactivity.⁵ This functional group is surprisingly inert to various nucleophiles, such as amines, phosphines, thiols, organolithium, Grignard reagent, hydride, phenoxide and hydroxide, at room temperature in organic solvents.⁴ One of the very few examples of a SuFEx reaction with di-*N*-substituted sulfamoyl fluoride was described by Sharpless that used magnesium oxide to activate the S-F bond to form the sulfamide (Scheme 1, bottom).

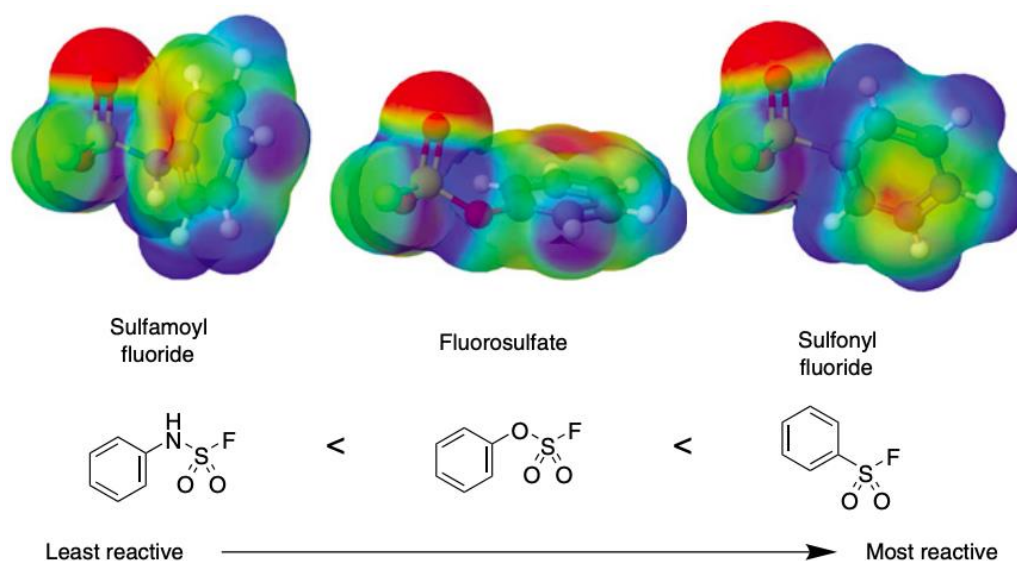
Scheme 1. Reactivity of primary (top) and secondary (bottom) sulfamoyl fluoride



In order to compare the relative reactivity of various S(VI)-F moieties such as sulfamoyl fluoride, fluorosulfate and sulfonyl fluoride, the resonance stabilization along the S-X (X = N, O, C) bond can be considered (Figure 4). As mentioned above, sulfamoyl fluorides are the most stable functional group in this category due to resonance stabilization from the electron donation from the nitrogen lone pairs.⁵ Even though there is resonance stabilization in the fluorosulfates along the S-O bond, the electronegative oxygen makes this moiety more reactive. Comparatively, sulfonyl fluorides are the most reactive due to the absence of lone pairs on the carbon connected to the sulfur.

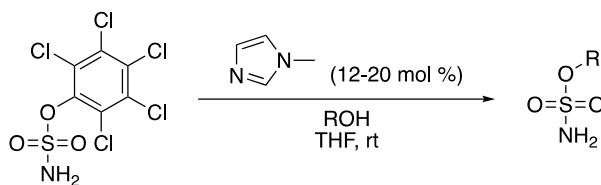
Thus, based on the resonance and electron density distribution, sulfonyl fluorides contain the most electrophilic sulfur atom.⁵ This also indicates that fluorosulfates have a more electrophilic sulfur atom than does a sulfamoyl fluoride, eluding to why the former has been explored more extensively for sulfamate synthesis.

Figure 4. Relative reactivity of sulfur atom in S(VI)-F bond containing moieties



So far, SuFEx type reactions via nucleophilic attack by an alcohol or alkoxide on a mono- or *N*-disubstituted sulfamoyl fluoride to form sulfamate has not been reported. However, other leaving groups instead of fluoride are being explored for sulfamate synthesis. For example, in 2020, Miller reported pentachlorophenyl sulfamate as a highly electron-deficient sulfamate donor for the synthesis of primary sulfamates (Scheme 2).⁶

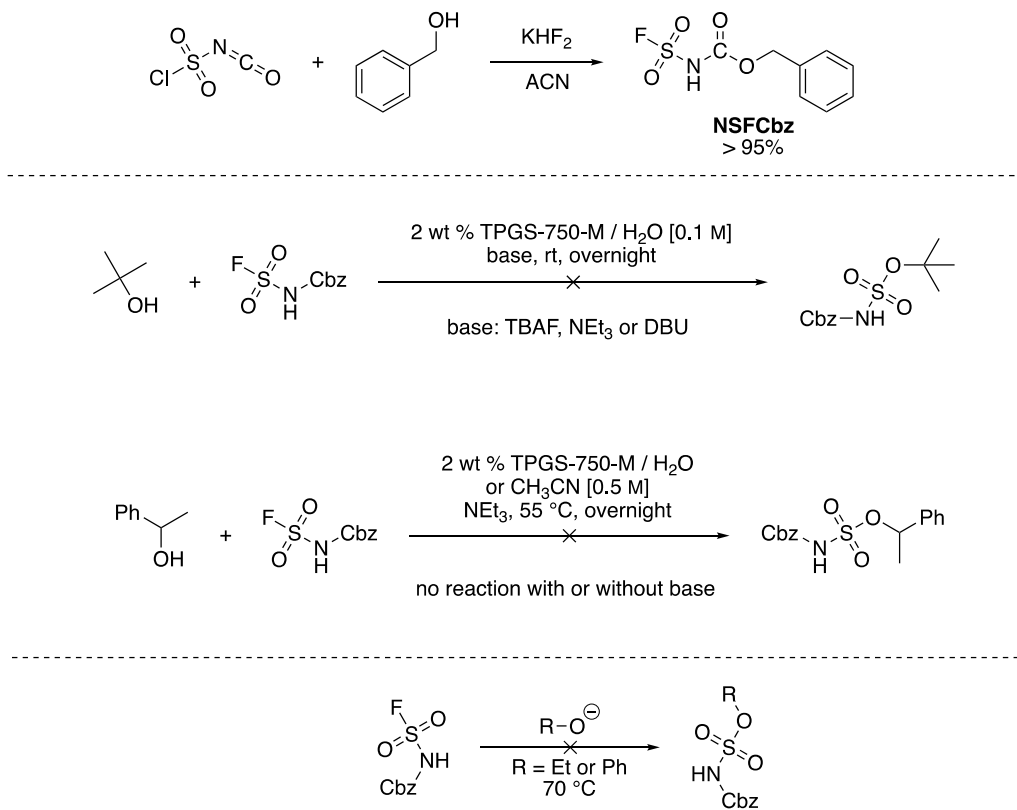
Scheme 2. Alcohol sulfamoylation using an electron deficient aryl sulfamate



4.2. Results and Discussion

Considering the limited amount of literature on sulfamate synthesis from sulfamoyl fluoride, attempts were made to subject sulfamoyl fluoride to alcohol under basic conditions. Benzyl(fluorosulfonyl)carbamate reagent (Cbz-NSF) was synthesized in good yields using chlorosulfonyl isocyanate and benzyl alcohol without the need for purification (Scheme 3).⁷ ¹⁹F NMR was used to confirm the reagent synthesis and absence of degradation via an azasulfene mechanism.

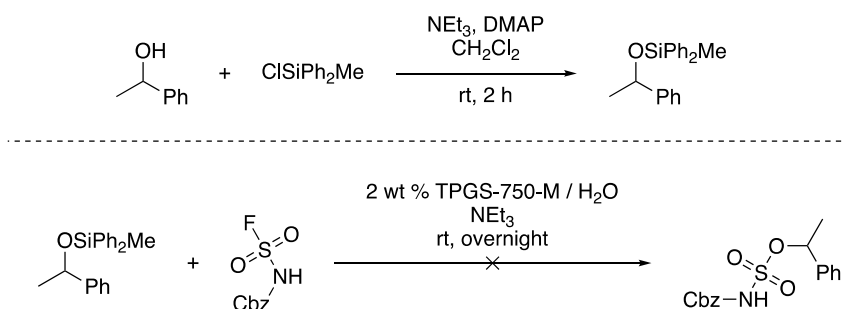
Scheme 3. Synthesis of Cbz-protected sulfamoyl fluoride reagent (top). Reaction of the reagent with alcohol (middle) and alkoxide (bottom)



The Cbz-NSF reagent was subjected to butanol at room temperature under aqueous micellar conditions (Scheme 3). Neither of the bases used yielded the desired product. The reagent was unreactive with 1-phenylethanol as well under both aqueous micellar conditions and in organic solvent. Surprisingly, reaction of the reagent with alkoxide at high temperature was also ineffective.

To facilitate fluorine elimination from the sulfamoyl fluoride, attempts were made to take advantage of fluorine's affinity for silicon. 1-Phenylethanol was protected using chloro-(methyl)diphenylsilane (Scheme 4).⁸ However, reaction of the protected alcohol with Cbz-NSF did not yield the desired product even in a protic solvent. A possible explanation could be that the azasulfene is formed under basic conditions even before there is an opportunity for Si-F bond formation and the silyl ether is a poor nucleophile that does not attack the azasulfene.

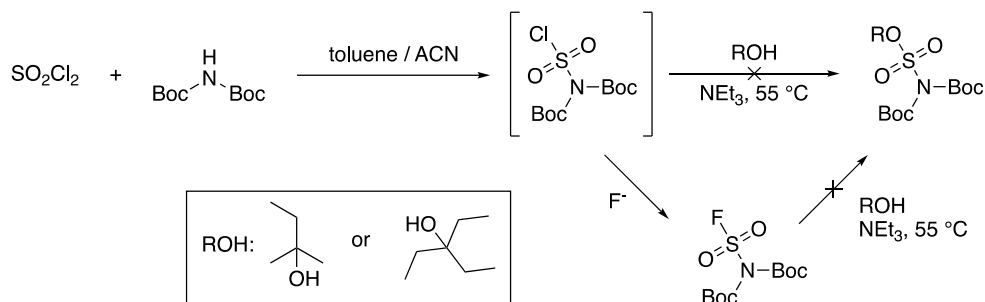
Scheme 4. Synthesis and use of a silyl ether as nucleophile



To avoid the possibility of reagent degradation of the mono-substituted sulfamoyl fluoride, attempted were made to synthesize both *N*-disubstituted sulfamoyl chloride and *N*-

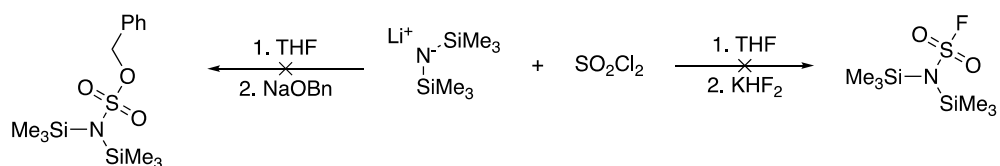
disubstituted sulfamoyl fluoride from sulfonyl chloride and *bis-N*-Boc amine (Scheme 5).⁷ Unfortunately, the reagents were unreactive with tertiary alcohols.

Scheme 5. Use of *N*-disubstituted sulfamoyl halide for sulfamate synthesis



Synthesis of *N*-disubstituted sulfamoyl fluoride using lithium *bis*(trimethylsilyl)amide (LiHMDS) was also unfruitful (Scheme 6). Attack of sodium benzoate on *in situ*-formed sulfamoyl chloride was also not successful. These experiments confirm that *N*-disubstituted sulfamoyl fluorides are difficult to synthesize and are fairly inert to alcohols and alkoxides.

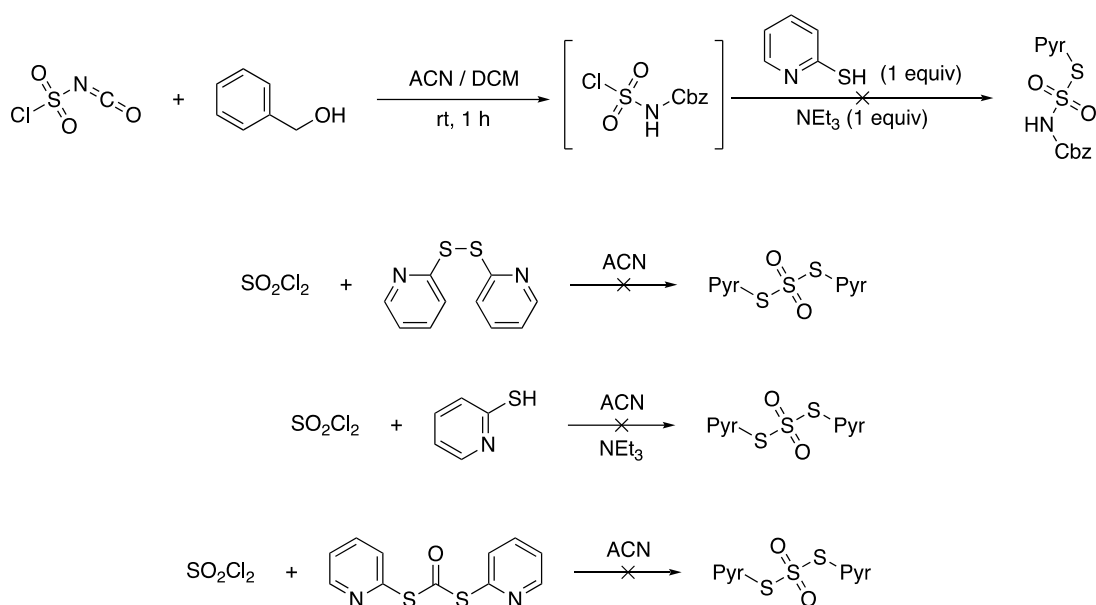
Scheme 6. Use of LiHMDS for sulfamate synthesis



With lack of success with SuFEx type reactions using sulfamoyl fluoride, efforts were made to use a different functional group to increase the electrophilicity of sulfur(VI). Recently, DiPyridylDiThioCarbonate (DPDTC) was used as a coupling reagent for amide

bond formation.⁹ The same concept was applied in an effort to synthesize an active reagent with thiopyridyl as leaving group (Scheme 7). Use of 2-mercaptopyridine to substitute chloride in the Cbz-protected sulfamoyl chloride was futile. Attempts to synthesize a DPDTC type reagent containing -SO₂ instead of -CO was unsuccessful with dipyridyl disulfide, 2-mercaptopyridine, and DPDTC itself.

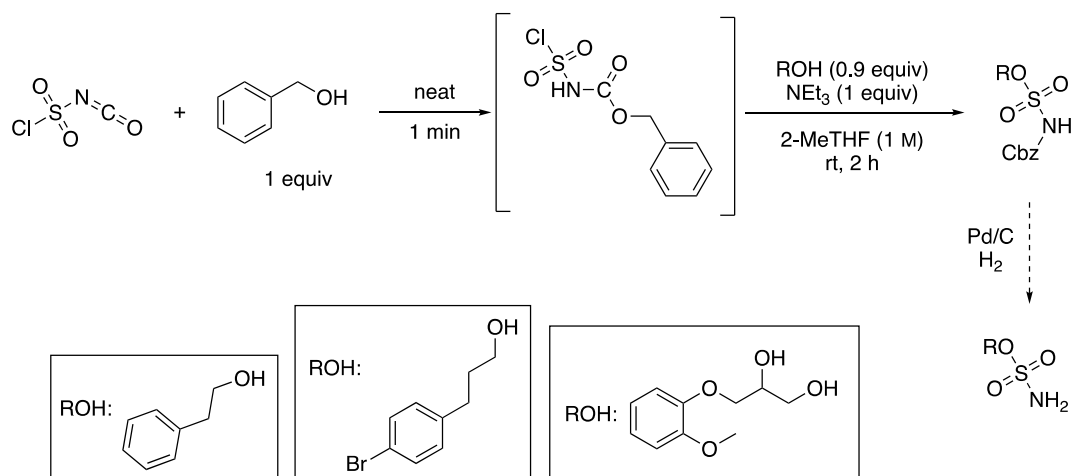
Scheme 7. Attempts to synthesize DPDTC type reagent



After dissatisfactory results in attempts to use other leaving groups, the next pursuit was to *in situ* generate sulfamoyl chloride from chlorosulfonyl isocyanate and benzyl alcohol and subject the reagent to alcohol under basic conditions (Scheme 8). To generate a better nucleophile, the alcohol was pre-mixed with triethylamine in a green solvent, 2-MeTHF and then added to the sulfamoyl chloride reaction vessel. Liquid alcohols were directly added to the reaction vessel prior to deprotonation. Cbz-protected sulfamates were successfully

synthesized and were confirmed by HRMS. Due to the polarity of sulfamate, the product was difficult to isolate and preparative TLC was used to obtain the material. Interestingly, HRMS results indicated that the diol experienced sulfamoylation on both the primary and secondary alcohols thus, indicating the lack of selectivity of the process.

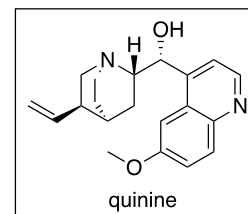
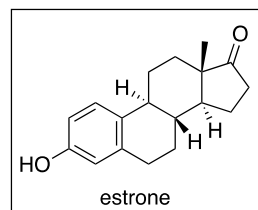
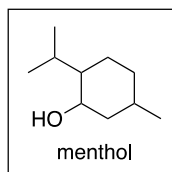
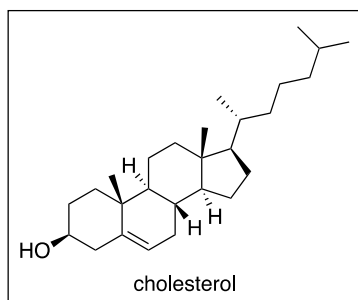
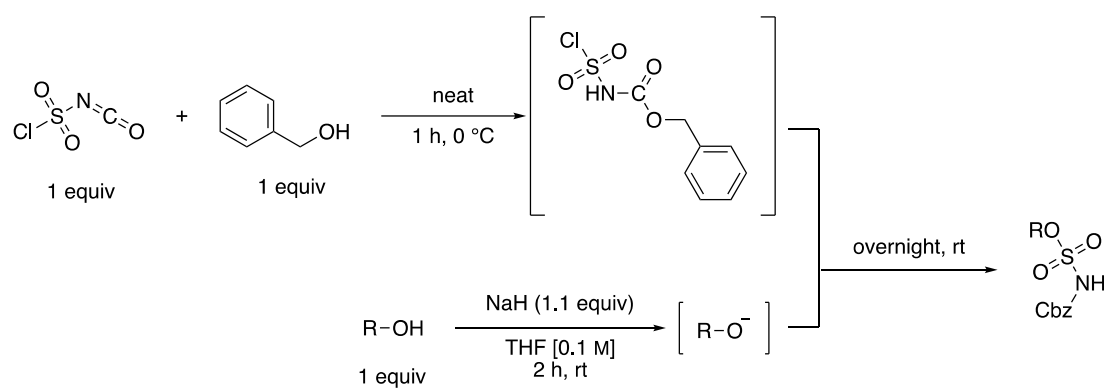
Scheme 8. Nucleophilic attack by alcohol on in-situ generated sulfamoyl chloride



For challenging substrates such as cholesterol, menthol, estrone, and quinine, the alkoxide was generated using sodium hydride prior to the sulfamoylation reaction (Scheme 9). Even though these substrates are more lipophilic, they were difficult to isolate and were low yielding. Overall, this method of sulfamate synthesis was not robust and was limited in substrate scope.

Thus, these results indicate that synthesis of sulfamate from sulfamoyl halide is challenging and hence not well known. The poor nucleophilicity of alcohol could play a part however, it is surprising that formation of alkoxide is not helpful either.

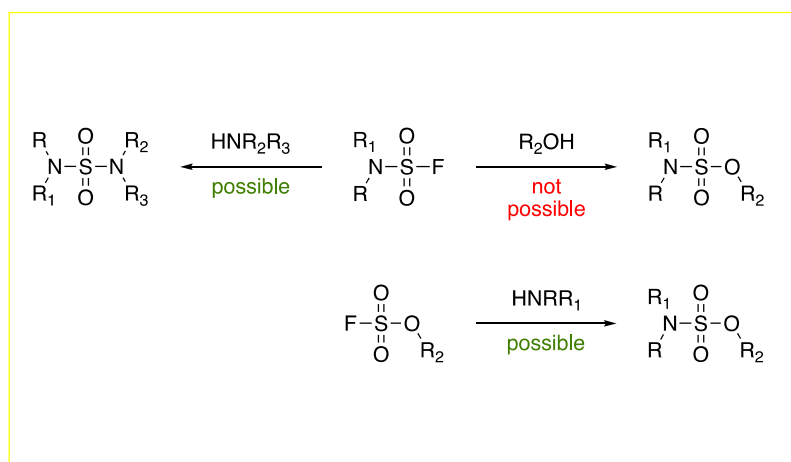
Scheme 9. Sulfamoylation of challenging alcohols



4.3. Conclusion

To conclude, this study indicates that synthesis of sulfamate from sulfamoyl fluoride via alcohol nucleophilic attack is not a favorable process (Figure 5). *N*-Disubstituted sulfamoyl fluorides are extremely stable species that do not undergo SuFEx type reactions to eliminate fluoride ion in the presence of a nucleophile, especially a weak nucleophile like alcohol.¹⁰ However, they are able to form sulfamide in the presence of group 2 metal complexes.¹¹ By contrast, mono-substituted sulfamoyl fluorides readily eliminate fluoride ion and collapse within minutes to form the azasulfene intermediate which in the presence of amine can form sulfamide as well.^{10, 12} Preliminary results did indicate that sulfamide synthesis from sulfamoyl fluoride is possible under aqueous micellar conditions using more environmentally friendly tools.

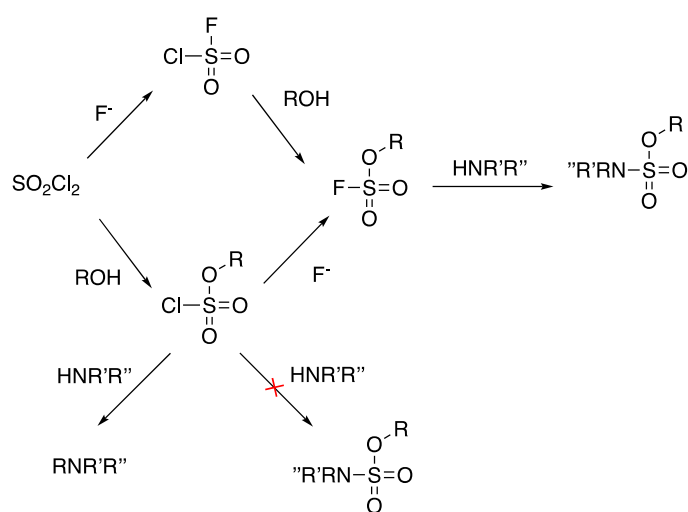
Figure 5. Potential reactivity of sulfamoyl fluoride and fluorosulfate



As for synthesis of sulfamates using SuFEx type reactions, it is more plausible to subject fluorosulfate to nucleophilic attack by an amine. Fluorosulfate can potentially be prepared via

sulfuryl chloride in two ways (Figure 6): (1) SO_2Cl_2 can be fluorinated and then treated with alcohol or, (2) SO_2Cl_2 can be exposed to alcohol to form chlorosulfate that can then be fluorinated to give the fluorosulfate product. Unfortunately, treatment of chlorosulfate with an amine does not undergo sulfonylation but instead forms the C-N bond at sulfur in the chlorosulfate.¹³

Figure 6. Potential ways to get to sulfamate from sulfuryl chloride



There are a number of ways to use Burgess reagent or Burgess-type reagent to synthesize sulfamate or use sulfamoyl chloride with alcohol to form sulfamate, but as of this date there is no evidence of SuFEx type reactions on sulfamoyl fluoride can serve to form sulfamates.¹⁴

4.4. References

- 1) Mustafa, M.; Winum, J.-Y. The Importance of Sulfur-Containing Motifs in Drug Design and Discovery. *Expert Opinion on Drug Discovery* **2022**, *17*, 501–512.
- 2) Thomas, M. P.; Potter, B. V. L. Discovery and Development of the Aryl *O* -Sulfamate Pharmacophore for Oncology and Women's Health. *J. Med. Chem.* **2015**, *58*, 7634–7658.
- 3) Langston, S. P.; Grossman, S.; England, D.; Afroze, R.; Bence, N.; Bowman, D.; Bump, N.; Chau, R.; Chuang, B.-C.; Claiborne, C.; Cohen, L.; Connolly, K.; Duffey, M.; Durvasula, N.; Freeze, S.; Gallery, M.; Galvin, K.; Gaulin, J.; Gershman, R.; Greenspan, P.; Grieves, J.; Guo, J.; Gulavita, N.; Hailu, S.; He, X.; Hoar, K.; Hu, Y.; Hu, Z.; Ito, M.; Kim, M.-S.; Lane, S. W.; Lok, D.; Lublinsky, A.; Mallender, W.; McIntyre, C.; Minissale, J.; Mizutani, H.; Mizutani, M.; Molchinova, N.; Ono, K.; Patil, A.; Qian, M.; Riceberg, J.; Shindi, V.; Sintchak, M. D.; Song, K.; Soucy, T.; Wang, Y.; Xu, H.; Yang, X.; Zawadzka, A.; Zhang, J.; Pulukuri, S. M. Discovery of TAK-981, a First-in-Class Inhibitor of SUMO-Activating Enzyme for the Treatment of Cancer. *J. Med. Chem.* **2021**, *64*, 2501–2520.
- 4) Dong, J.; Krasnova, L.; Finn, M. G.; Sharpless, K. B. Sulfur(VI) Fluoride Exchange (SuFEx): Another Good Reaction for Click Chemistry. *Angew. Chem., Int. Ed.* **2014**, *53*, 9430–9448.
- 5) *Emerging Fluorinated Motifs: Synthesis, Properties, and Applications*, 1st ed.; Ma, J., Cahard, D., Eds.; Wiley, 2020.
- 6) Rapp, P. B.; Murai, K.; Ichiishi, N.; Leahy, D. K.; Miller, S. J. Catalytic Sulfamoylation of Alcohols with Activated Aryl Sulfamates. *Org. Lett.* **2020**, *22*, 168–174.
- 7) Wata, C.; Hashimoto, T. Organoiodine-Catalyzed Enantioselective Intermolecular Oxyamination of Alkenes. *J. Am. Chem. Soc.* **2021**, *143*, 1745–1751.
- 8) Fujiki, K.; Tanaka, K. Exploration of the Fluoride Reactivity of Aryltrifluoroborate on Selective Cleavage of Diphenylmethylsilyl Groups: Exploration of the Fluoride Reactivity of Aryltrifluoroborate on Selective Cleavage of Diphenylmethylsilyl Groups. *Eur. J. Org. Chem.* **2020**, *2020*, 4616–4620.
- 9) Freiberg, K. M.; Kavthe, R. D.; Thomas, R. M.; Fialho, D. M.; Dee, P.; Scurria, M.; Lipshutz, B. H. Direct Formation of Amide/Peptide Bonds from Carboxylic Acids: No Traditional Coupling Reagents, 1-Pot, and Green. *Chem. Sci.* **2023**, *14*, 3462–3469.
- 10) Carneiro, S. N.; Khasnavis, S. R.; Lee, J.; Butler, T. W.; Majmudar, J. D.; am Ende, C. W.; Ball, N. D. Sulfur(VI) Fluorides as Tools in Biomolecular and Medicinal Chemistry. *Org. Biomol. Chem.* **2023**, *21*, 1356–1372.
- 11) Mahapatra, S.; Woroch, C. P.; Butler, T. W.; Carneiro, S. N.; Kwan, S. C.; Khasnavis, S. R.; Gu, J.; Dutra, J. K.; Vetelino, B. C.; Bellenger, J.; am Ende, C. W.; Ball, N. D. SuFEx Activation with Ca(NTf₂)₂: A Unified Strategy to Access Sulfamides, Sulfamates, and Sulfonamides from S(VI) Fluorides. *Org. Lett.* **2020**, *22*, 4389–4394.

- 12) Chrominski, M.; Ziemkiewicz, K.; Kowalska, J.; Jemielity, J. Introducing SuFNucs: Sulfamoyl-Fluoride-Functionalized Nucleosides That Undergo Sulfur Fluoride Exchange Reaction. *Org. Lett.* **2022**, *24*, 4977–4981.
- 13) Ko, E. C. F.; Robertson, R. E. The Mechanism for Hydrolysis of Primary Alkyl Chlorosulfates in Water. The Kinetic Solvent Isotope Effect and the Secondary Deuterium Isotope Effect. *Can. J. Chem.* **1972**, *50*, 434–437.
- 14) a) Blackburn, J. M.; Short, M. A.; Castanheiro, T.; Ayer, S. K.; Muellers, T. D.; Roizen, J. L. Synthesis of *N*-Substituted Sulfamate Esters from Sulfamic Acid Salts by Activation with Triphenylphosphine Ditriflate. *Org. Lett.* **2017**, *19*, 6012–6015. b) Binkley, W. W.; Degering, Ed. F. Organic Syntheses with Sulfuryl Chloride. *J. Am. Chem. Soc.* **1939**, *61*, 3250–3251. c) Spillane, W.; Malaubier, J.-B. Sulfamic Acid and Its *N*- and *O*-Substituted Derivatives. *Chem. Rev.* **2014**, *114*, 2507–2586.

5. Hydrosilylation of carboxylic acid to primary alcohol

5.1. Introduction and background

Alcohols are an important functional group as they serve as building blocks in various industries, including pharmaceuticals.¹ One of the most common ways to synthesize alcohols is reduction of commercially available and inexpensive carboxylic acids. Conventional reduction methods use hazardous chemicals such as lithium aluminum hydride (LAH) and diisobutylaluminum hydride (DIBAL-H) that are moisture sensitive and react violently in the presence of water (Table 1).²

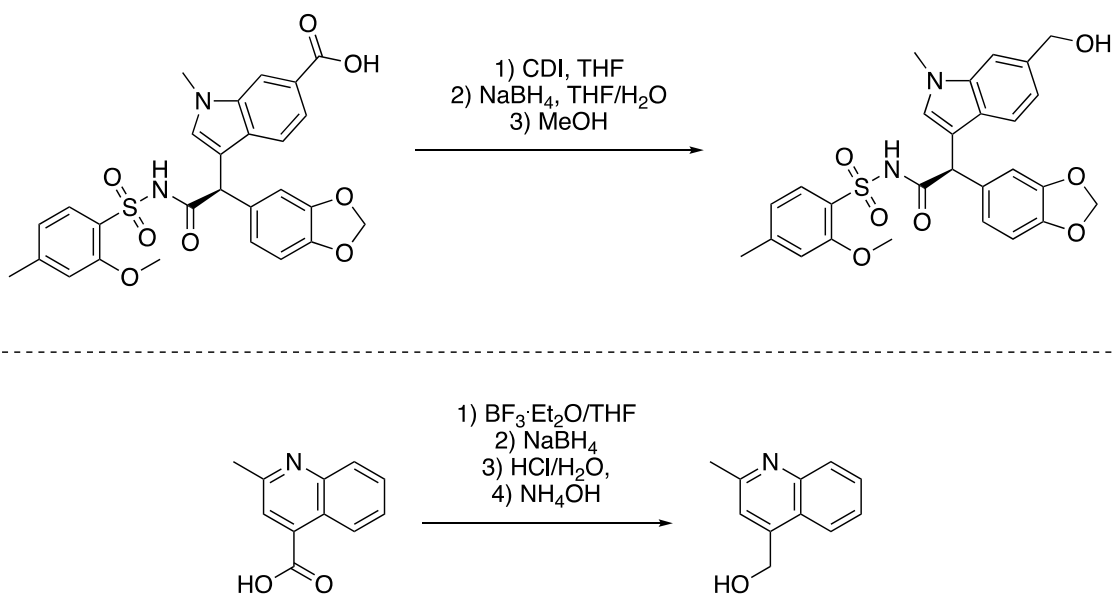
Table 1. Disadvantages of current carboxylic acid reduction methods

conventional methods	disadvantages
LAH and DIBAL-H	<ul style="list-style-type: none">• hazardous chemicals• violent reaction with water
NaBH ₄ and other borane derivatives	<ul style="list-style-type: none">• incompatible with other functional groups• exothermic reactions• spontaneously combustible
catalytic hydrogenation	<ul style="list-style-type: none">• use of harsh conditions: H₂ pressure• limited literature

Sodium borohydride and other borane derivatives as reducing agents are incompatible with various functional groups and require tedious extra handling since they are moisture-

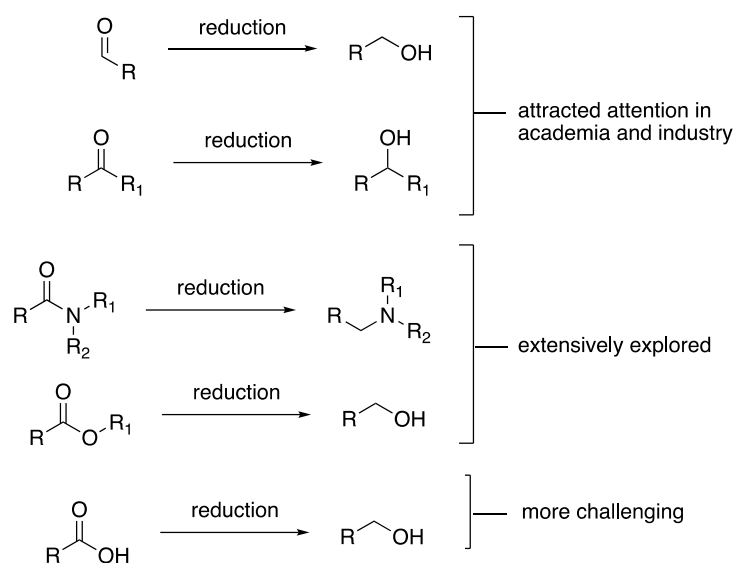
sensitive and waste generating.³ Scheme 1 showcases two industrial reduction processes using borane reagents that are low yielding due to required carbonyl activation and reduction of other functional groups in the molecule.⁴ Similarly, catalytic hydrogenations are not an ideal reduction method as they require harsh conditions and high pressurized systems.

Scheme 1. Unfavorable literature methods for reduction of carboxylic acid to alcohol



Thus, hydrosilylation is a safer alternative to other reduction processes since the reagents are easier to handle and the byproducts generated are easy to eliminate as they are either volatile or water soluble.² While hydrosilylation of amides and esters have been thoroughly studied, reduction of aldehydes and ketones have recently attracted attention in both academia and industry (Figure 1). However, hydrosilylation of carboxylic acids still remains challenging due to poor electrophilicity of the unactivated carbonyl in the molecule.

Figure 1. Hydrosilylation of various carbonyl containing functional groups



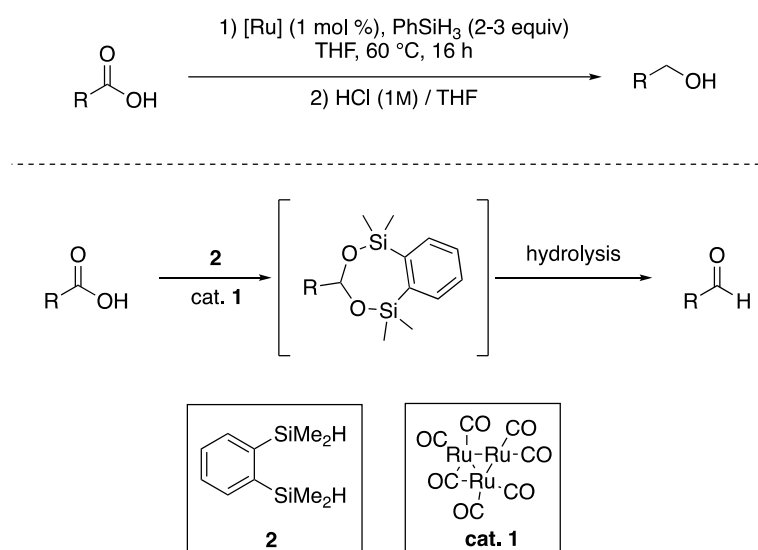
Some of the commonly used metals to catalyze hydrosilylation reactions are ruthenium and iron. In 2014, Jose and co-workers described a general method to selectively reduce carboxylic acids to primary alcohols under mild conditions (Scheme 2, top).⁵

The Ru complex used is commercially available and relatively easy to synthesize in a 2-step, 1-pot process. However, their reduction process has a limited substrate scope and requires waste-generating solvents, such as THF. Ruthenium can also be used to catalyze selective reduction of a carboxylic acid to aldehyde (Scheme 2, bottom).⁶ A restrictive, bifunctional organosilane, 1,2-*bis*(dimethylsilyl)benzene is used as the reductant along with a Ru complex to carry out the transformation.

Anthem Biosciences developed a phosphine ligand-free ruthenium complex to perform hydrosilylations on various functional groups.⁷ The purpose of developing the complex was to avoid phosphine-containing waste. Human exposure to phosphine gases can lead to severe convulsions, bronchitis, and pulmonary edema. Additionally, phosphine-based ligands often

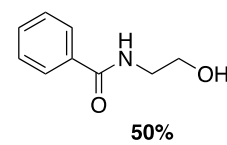
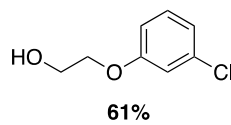
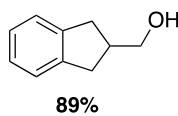
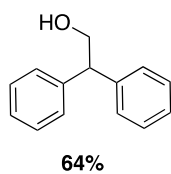
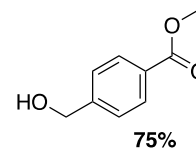
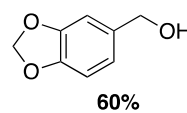
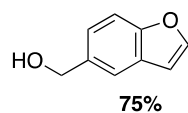
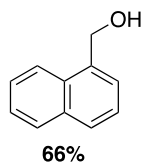
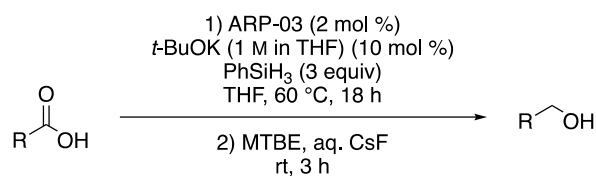
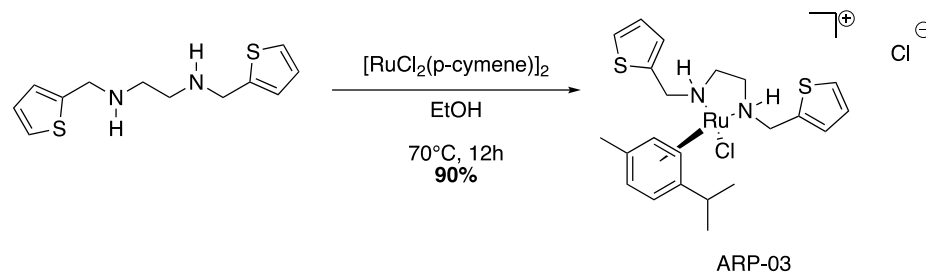
require inert conditions due to its proclivity towards air oxidation, making phosphines potentially difficult to use in large-scale applications. The Ru complex was synthesized using dichloro(*p*-cymene)ruthenium(II) dimer, a commonly used organometallic compound. Thiophenyl moieties on the ligand act as a hemilabile ligand that stabilizes reactive intermediates.

Scheme 2. Ruthenium catalyzed hydrosilylation of carboxylic acid



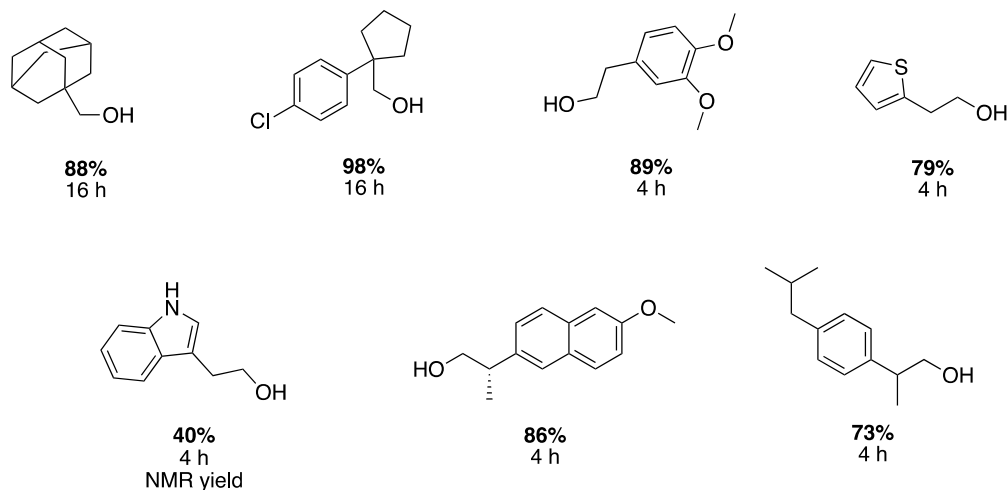
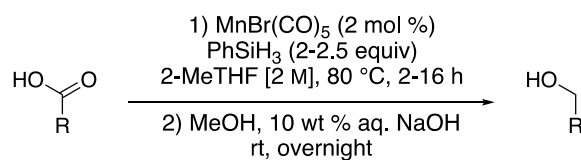
This phosphine-free ruthenium catalyst was used to perform hydrosilylation on carboxylic acids (Scheme 3).¹ Both aromatic and aliphatic carboxylic acids were reduced to their corresponding primary alcohols using phenylsilane as the hydride source. However, this transformation was yet again performed in the organic solvent, THF, affording relatively low yields of products. Moreover, a limited substrate scope was reported, with heteroatoms such as basic nitrogen and sulfur not present in the edicts.

Scheme 3. Phosphine free ruthenium catalyst (top). Use of this catalyst for hydrosilylation of carboxylic acids (bottom)



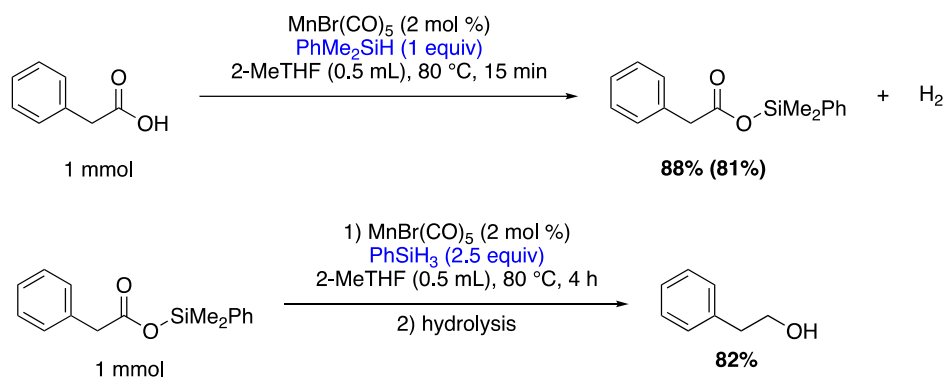
Recently, in 2021, Emanuele and co-workers used an economical and commercially available manganese catalyst, $Mn(CO)_5Br$ to reduce carboxylic acids to alcohols using phenylsilane (Scheme 4).⁸ This methodology involved an earth-abundant metal under milder conditions and in a greener solvent, 2-MeTHF. Even though they used a higher temperature (80 °C), their reduction process only required 2-16 hours for completion.

Scheme 4. Manganese-catalyzed hydrosilylation of carboxylic acids



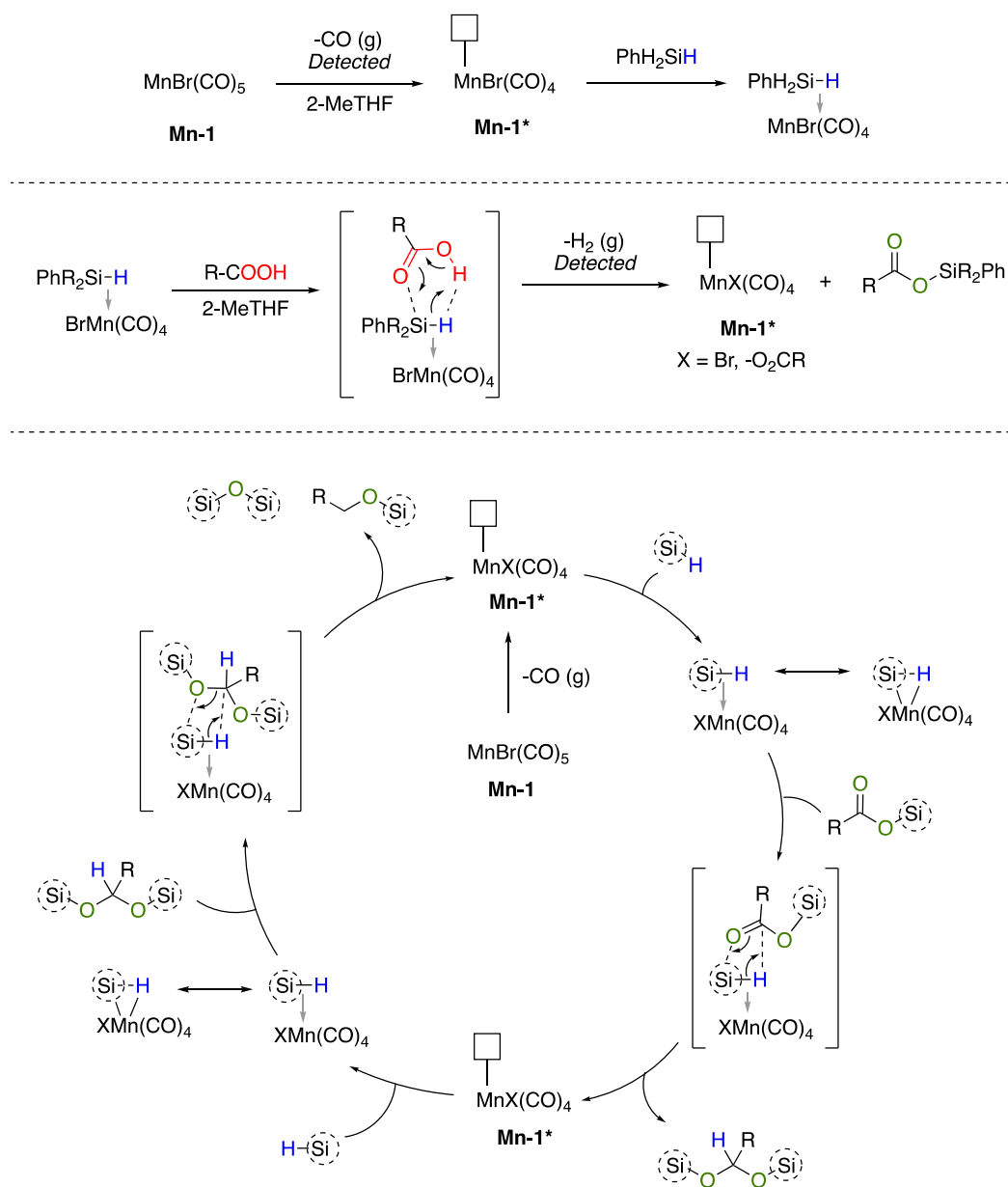
Mechanistic studies indicate that the first step of the process involves the immediate (15 minutes) formation of a silyl ester (Scheme 5). During the first step, evolution of hydrogen gas was detected. After the release of the detected gas, the resulting silyl ester is reduced to the alcohol in good yields, indicating that the hydrogen does not participate in the reduction process. The same reduction reaction in the absence of $\text{Mn}(\text{CO})_5\text{Br}$ yielded no product indicating that the complex is necessary for the hydrosilylation process.

Scheme 5. Silyl ester formation and H₂ gas release during the hydrosilylation process



Gas phase analysis also indicated that only one equivalent of CO is lost from the Mn complex, providing a coordination site during the dehydrogenative coupling of the carboxylic acid and the silane (Figure 2). The proposed mechanism hypothesizes that the second step of the process is the Si-H addition into the carbonyl to form the disilylacetal. This disilylacetal undergoes hydrolysis to form the aldehyde, as shown in Scheme 2 (bottom). Finally, reductive cleavage of the C-O bond in the disilylacetal gives the silyl ether that is then hydrolyzed to form the desired alcohol product.

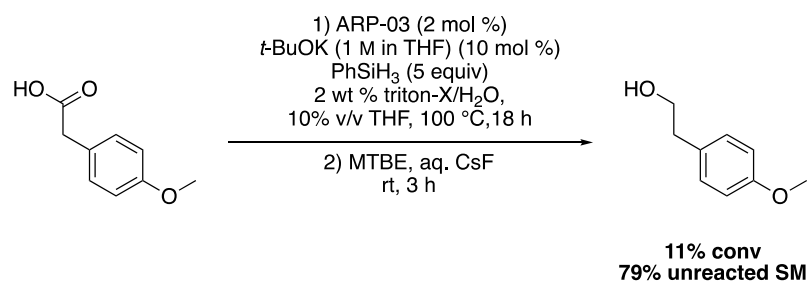
Figure 2. Proposed mechanism for the Mn catalyzed hydrosilylation of carboxylic acid



5.2. Results and Discussion

In order to make the Ru catalyzed hydrosilylation process more environmentally friendly, Anthem Biosciences attempted application of micellar technology (Scheme 6). They employed Triton X-100 as surfactant along with the same catalyst and reaction conditions. However, their reaction temperature was higher than the cloud point of the surfactant that most likely led to low conversion to the product.

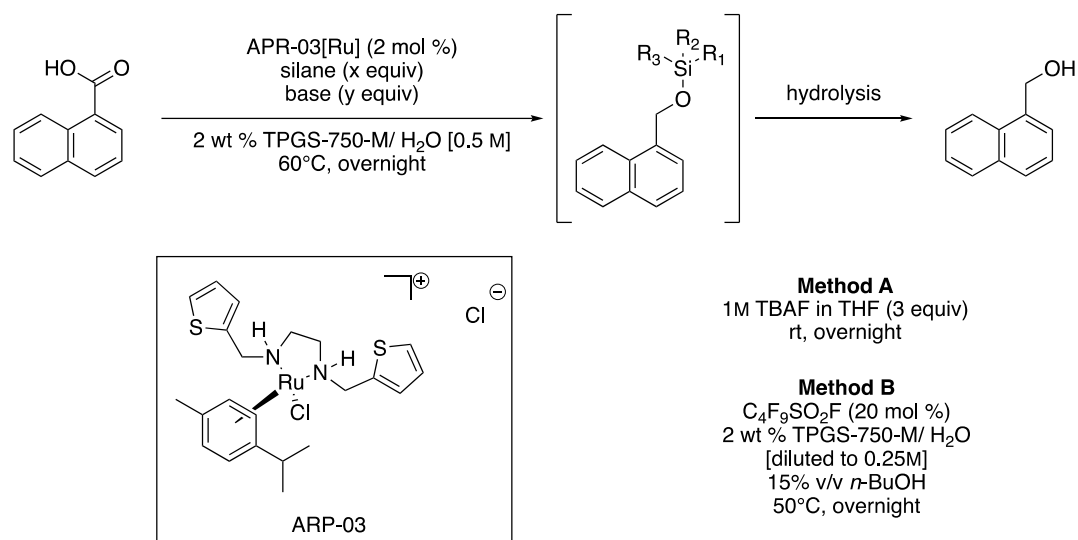
Scheme 6. Hydrosilylation in a micellar system attempted by Anthem Biosciences



The goal of this project was to develop an environmentally responsible method for hydrosilylation of carboxylic acids to alcohols. TPGS-750-M, the more commonly used surfactant for micellar catalysis in the Lipshutz group, was subjected to the Ru complex developed by Anthem Biosciences in the presence of a silane and a base (Table 2).⁷ Two different hydrolysis methods were examined to obtain the final alcohol product from the silyl ether.⁹ While optimizing reaction conditions for the reduction of 2-naphthoic acid, diphenyl silane as the hydride source, and potassium phosphate as the base were identified as the ideal combination of reagents (entry 4). The hydrolysis method using the surfactant system proved to be more beneficial (compare entries 1 and 2). Unfortunately, more economical silane

sources such as tetramethyldisiloxane (TMDS) and polymethylhydrosiloxane (PMHS) formed a difficult to handle gel like consistency which was most likely due to polymerization initiated by the reagents (entries 9 and 10).

Table 2. Optimization of Ru catalyzed hydrosilylation under micellar conditions



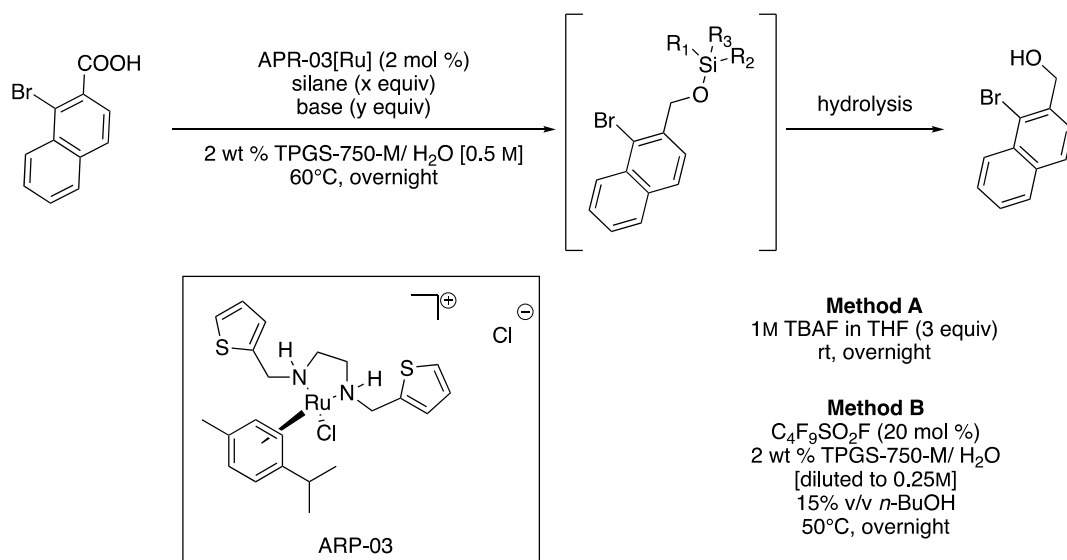
entry	silane (x equiv)	base (y equiv)	hydrolysis method	NMR yield (%)
1	Ph ₂ SiH ₂ (5)	-	A	12*
2	Ph ₂ SiH ₂ (5)	-	B	39
3	Ph ₂ SiH ₂ (5)	<i>t</i> -BuOK (0.1)	B	55
4	Ph ₂ SiH ₂ (5)	K ₃ PO ₄ (0.1)	B	76*
5	Ph ₂ SiH ₂ (5)	NEt ₃ (0.1)	B	55
6	Ph ₂ SiH ₂ (2)	K ₃ PO ₄ (0.1)	B	23
7	Ph ₂ SiH ₂ (3)	K ₃ PO ₄ (0.1)	B	38

8	Ph ₂ SiH ₂ (4)	K ₃ PO ₄ (0.1)	B	50
9	TMDS (5)	K ₃ PO ₄ (0.1)	B	34
10	PMHS (5)	K ₃ PO ₄ (0.1)	B	41

*Isolated yield.

Further silane screening indicated that the more lipophilic silane, diphenylmethylsilane, resulted in higher product conversion (Table 3). However, this result was not consistent with results using other carboxylic acids.

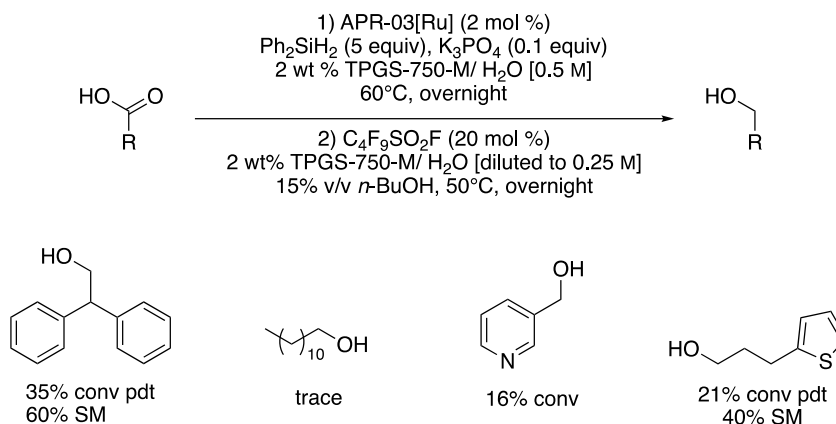
Table 3. Silane screening for carboxylic acid reduction process



entry	silane (x equiv)	base (y equiv)	hydrolysis	NMR yield
			method	(%)
1	PhSiH ₃ (5)	K ₃ PO ₄ (0.2)	A	messy
2	Ph ₂ SiH ₂ (5)	K ₃ PO ₄ (0.2)	A	47
3	Ph ₂ MeSiH (5)	K ₃ PO ₄ (0.2)	A	54

When the optimized conditions were applied to various carboxylic acids, the results were not encouraging (Scheme 7). The reduction products were very low yielding and the results were not consistent. Upon further examination it was discovered that the Ru complex that was claimed to be bench stable was degrading over time and thus losing activity. Even after synthesis of fresh catalyst the hydrosilylation process in water remained challenging with the given system.

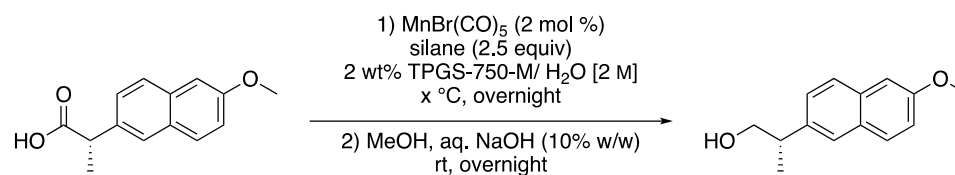
Scheme 7. Final results obtained from hydrosilylation performed by the Ru complex



After obtaining unsatisfactory results from use of this ruthenium catalyst, attention was diverted to the commercially available catalyst, $\text{Mn}(\text{CO})_5\text{Br}$. This manganese catalyst was used in water in the presence of a small amount of the surfactant, TPGS-750-M to reduce naproxen (Table 4). Silane sources such as diphenylsilane (Ph_2SiH_2), phenylsilane (PhSiH_3), TMDS, diphenylmethylsilane (Ph_2MeSiH), triethylsilane (Et_3SiH), and triethoxysilane ($(\text{EtO})_3\text{SiH}$) were tested. Surprisingly, none of the silanes worked well in water even at a high

temperature (80 °C). However, an undesired side product was observed. The best result was observed with (EtO)₃SiH at 65 °C (entry 11).

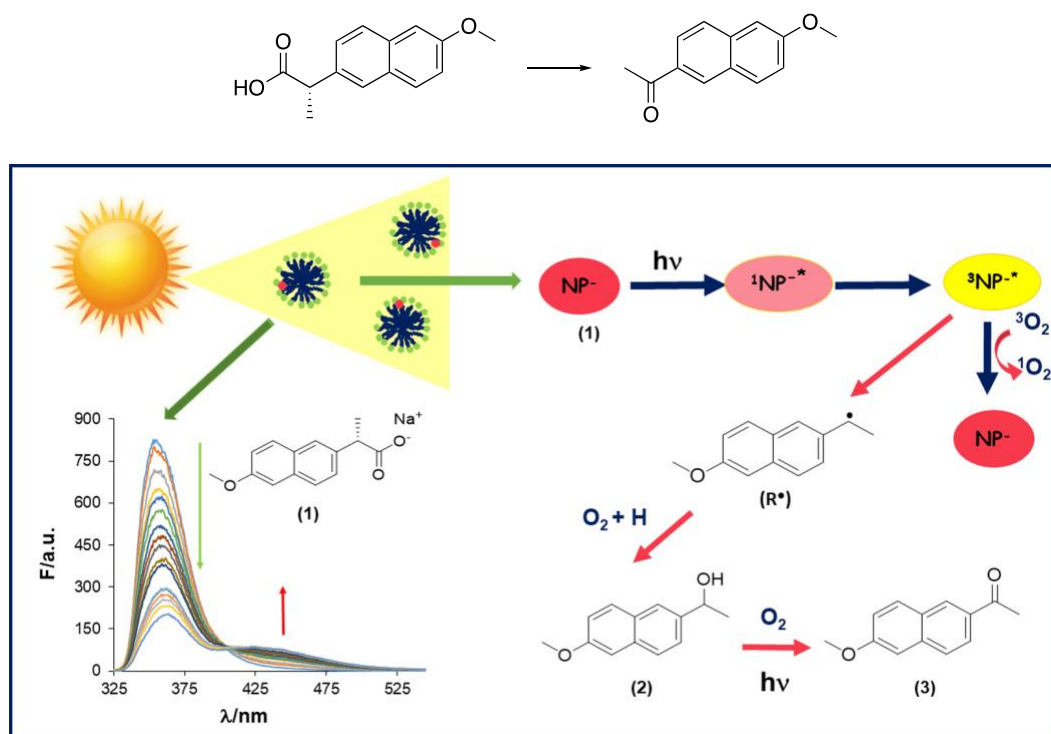
Table 4. Optimization of silane source and temperature for the Mn catalyzed hydrosilylation of carboxylic acid



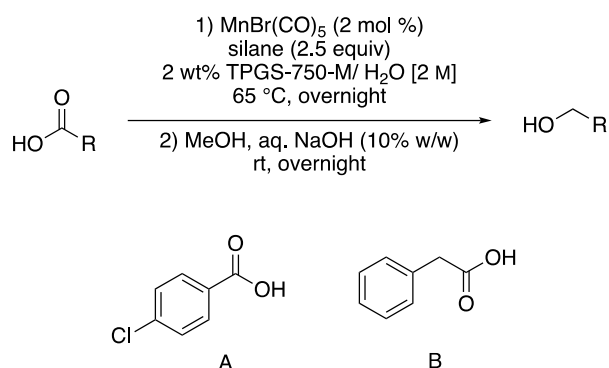
entry	silane	temp (°C)	NMR yield (%)
1	Ph ₂ SiH ₂	80	trace
2	PhSiH ₃	80	14
3	PhSiH ₃	75	11
4	PhSiH ₃	65	12
5	PhSiH ₃	55	trace
6	PhSiH ₃	45	trace
7	PhSiH ₃	65	12
8	TMDS	65	trace
9	MePh ₂ SiH	65	trace
10	Et ₃ SiH	65	trace
11	(EtO) ₃ SiH	65	25

An extensive literature search revealed that naproxen undergoes a unique radical process in the presence of micelles or manganese (Figure 3).¹⁰ It follows a radical pathway to perform decarboxylative oxygenation of the carboxylic acid to form the methyl ketone.¹¹

Figure 3. Decarboxylative oxygenation of naproxen using a radical pathway



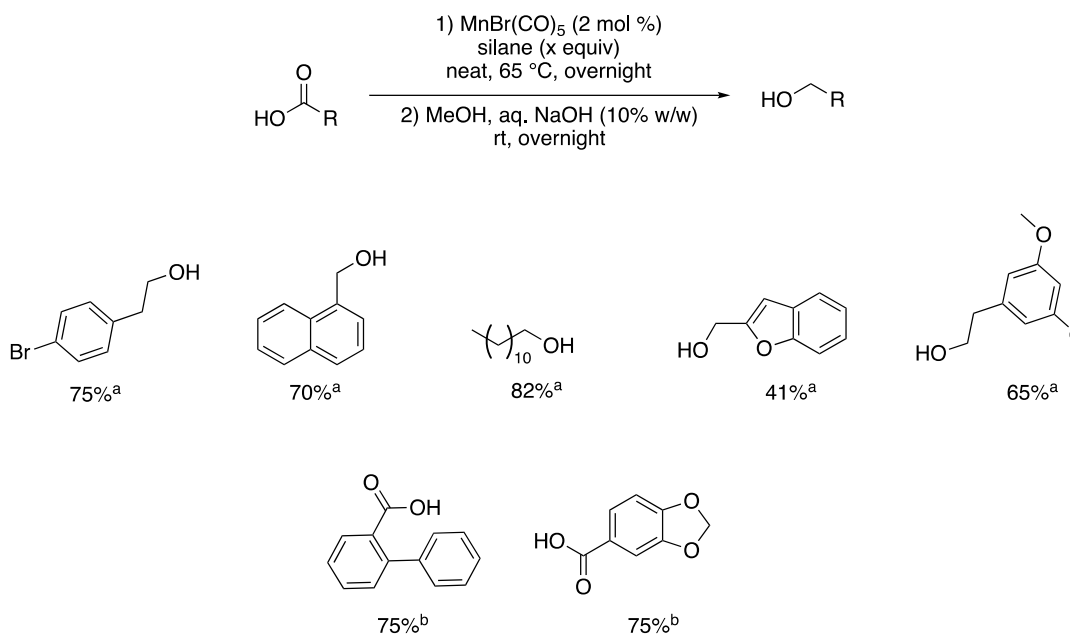
Other substrates such as 4-chlorobenzoic acid and phenylacetic acid were reduced to their alcohol derivatives in decent yields with $(\text{EtO})_3\text{SiH}$ using only 2 mol % of $\text{Mn}(\text{CO})_5\text{Br}$ under aqueous micellar conditions (Table 5, entries 2 and 4). Interestingly, no solvent was required for the transformation and thus, the hydrosilylation could be carried out under neat conditions providing the product in full conversion (entry 5).

Table 5. Silane and reaction medium optimization for the reduction process

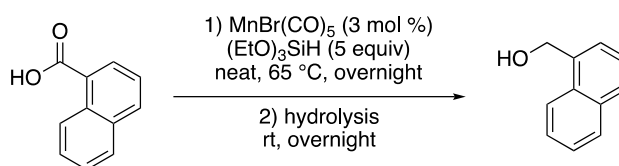
entry	silane	substrate	NMR yield (%)
1	PhSiH_3	A	only SM
2	$(\text{EtO})_3\text{SiH}$	A	full conv
3	PhSiH_3	B	25
4	$(\text{EtO})_3\text{SiH}$	B	70
5	$(\text{EtO})_3\text{SiH}$ (neat)	B	full conv

From the obtained results a generic hydrosilylation method was developed to reduce carboxylic acids to alcohols in the absence of any solvent using only 2 mol % of $\text{Mn}(\text{CO})_5\text{Br}$ at 65 °C (Scheme 8). Both PhSiH_3 and the relatively cheaper $(\text{EtO})_3\text{SiH}$ can be used as the hydride source. However, PhSiH_3 only requires 2.5 equivalents whereas the quantity of silane is doubled to five equivalents for $(\text{EtO})_3\text{SiH}$ to ensure ample availability of hydride ions since the tertiary silane only contains one hydride compared to three hydrides in the primary silane. Even with the increase in quantity this process is cheaper using $(\text{EtO})_3\text{SiH}$. It is important to note that this methodology is performed under neat conditions and at a lower temperature compared to the known literature.⁸

Scheme 8. General reaction parameters for hydrosilylation under neat conditions



The hydrolysis process reported in the literature requires large amounts of MeOH and aq. NaOH (total volume: 10 mL for 1 mmol scale). Many functional groups are sensitive to basic conditions (NaOH) thus making this hydrolysis process not selective for complex molecules. An improved hydrolysis method was required that was less waste generating and more functional group compatible. Hydrolysis performed in 2 wt % TPGS-750-M is not only higher in substrate concentration but also improves the product yield (Table 6). A readily available, easy to use, and functional group compatible fluoride source, potassium fluoride can be utilized to break the Si-O bond in the silyl ether to give the alcohol product (entry 6).

Table 6. Optimization of hydrolysis conditions

entry	condition	NMR yield (%)
1	MeOH + 10 wt % aq. NaOH	70*
2	THF + HCl (1 M)	14*
3	95% EtOH + 2.5 M NaOH	83
4	2 wt % TPGS-750-M/ H ₂ O + 5 M NaOH	77
5	2 wt % TPGS-750-M/ H ₂ O + TBAF (2.5 equiv)	77
6	2 wt % TPGS-750-M/ H ₂ O + KF (5 equiv)	86
7	2 wt % TPGS-750-M/ H ₂ O + CsF (5 equiv)	42

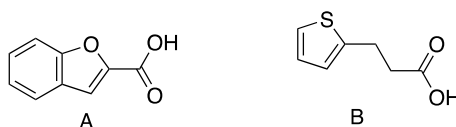
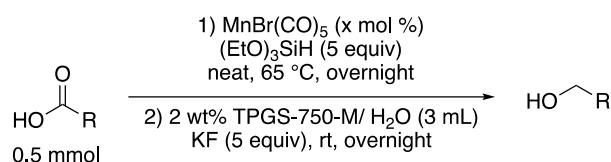
*Isolated yields.

It is important to note that higher amounts of Mn catalyst were used for the hydrolysis study due to the instability of the complex. Even though the catalyst is claimed to be air-stable, it loses its activity over time.^{8,12,13} The inconsistencies in the catalyst loading trends (Table 7) clearly indicate that $\text{Mn}(\text{CO})_5\text{Br}$ is not air and moisture stable over a long period of time and the methodology begins to show reproducibility issues.

With the new hydrolysis conditions, carboxylic acid reductions were almost 20% higher in product conversion (Scheme 9 compared to Scheme 8). However, yet again these experiments were run using 3 mol % of Mn catalyst making it difficult to conclude if the

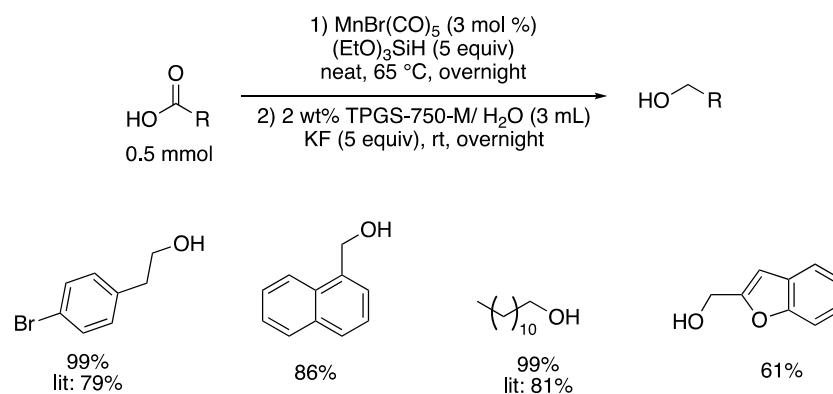
increase in yield is due to the improved hydrolysis conditions or the higher loading of compromised catalyst.

Table 7. Impact of catalyst loading on the product conversion



entry	catalyst loading	substrate	NMR yield (%)
1	2	A	61
2	3	A	45
3	2	B	18
4	3	B	30

Scheme 9.



5.3. *Conclusion*

Hydrosilylation of carboxylic acid to primary alcohol is an important transformation that has not been studied extensively. The methodologies that exist use waste-generating organic solvents and are performed at high temperatures.

A phosphine-free ruthenium complex developed by Anthem Biosciences is claimed to be bench stable. However, experiments indicated otherwise since activity of the catalyst deteriorated over time. The methodology developed in aqueous micellar conditions was not robust and was not generally applicable to various carboxylic acids with additional functional groups.

Commercially available $\text{Mn}(\text{CO})_5\text{Br}$ is also claimed to be bench stable, however, it is seen to degrade over time. This catalyst is also on indefinite back order that makes it not easily attainable. Unsatisfactory quality of reagents leads to reproducibility issues that indicates that the method developed is not reliable and requires further experimentation.

5.4. References

- 1) Abhilash, V.; Hegde, S. N.; Jacob, A.; Mathivanan, N.; Lamees, T.; Gadakh, A. V.; Sathiyarayanan, A. M.; Karthik, C. S.; Ganesh, S. Chemoselective Hydrosilylation of Carboxylic Acids Using a Phosphine-Free Ruthenium Complex and Phenylsilane. *J. Organomet. Chem.* **2022**, *963*, 122288.
- 2) Fan, S.; Li, H. Metal Catalyzed Hydrosilylation Reaction for Biomass Upgrading. *Fuel* **2022**, *312*, 122836.
- 3) Ashcroft, C. P.; Challenger, S.; Clifford, D.; Derrick, A. M.; Hajikarimian, Y.; Slucock, K.; Silk, T. V.; Thomson, N. M.; Williams, J. R. An Efficient and Scalable Synthesis of the Endothelin Antagonists UK-350,926 and UK-349,862 Using a Dynamic Resolution Process. *Org. Process Res. Dev.* **2005**, *9*, 663–669.
- 4) Wang, Y.; Papamichelakis, M.; Chew, W.; Sellstedt, J.; Noureldin, R.; Tadayon, S.; Daigneault, S.; Galante, R. J.; Sun, J. Development of a Suitable Process for the Preparation of a TNF- α Converting Enzyme Inhibitor, WAY-281418. *Org. Process Res. Dev.* **2008**, *12*, 1253–1260.
- 5) Fernández-Salas, J. A.; Manzini, S.; Nolan, S. P. Chemoselective Ruthenium-Catalysed Reduction of Carboxylic Acids. *Adv. Synth. Catal.* **2014**, *356*, 308–312.
- 6) Miyamoto, K.; Motoyama, Y.; Nagashima, H. Selective Reduction of Carboxylic Acids to Aldehydes by a Ruthenium-Catalyzed Reaction with 1,2-Bis(Dimethylsilyl)Benzene. *Chem. Lett.* **2012**, *41*, 229–231.
- 7) Shashikumar, K.; Maldode, S. B.; Sajjanar, S.; Hegde, S. N.; Sattineni, S.; Avasare, V. D.; Gadakh, A. V.; Ganesh, S.; Sathiyarayanan, A. M. Phosphine-Free Ruthenium Complex for Hydrogenation of Carbonyl Compounds: Synthesis and Applications. *ChemistrySelect* **2021**, *6*, 8411–8415.
- 8) Antico, E.; Schlichter, P.; Werlé, C.; Leitner, W. Reduction of Carboxylic Acids to Alcohols via Manganese(I) Catalyzed Hydrosilylation. *JACS Au* **2021**, *1*, 742–749.
- 9) Akporji, N.; Lieberman, J.; Maser, M.; Yoshimura, M.; Boskovic, Z.; Lipshutz, B. H. Selective Deprotection of the Diphenylmethylsilyl (DPMS) Hydroxyl Protecting Group under Environmentally Responsible, Aqueous Conditions. *ChemCatChem* **2019**, *11*, 5743–5747.
- 10) Valero, M.; Sultimova, N. B.; Houston, J. E.; Levin, P. P. Naproxen Sodium Salt Photochemistry in Aqueous Sodium Dodecyl Sulfate (SDS) Ellipsoidal Micelles. *J. Mol. Liq.* **2021**, *324*, 114724.
- 11) Guan, R.; Bennett, E. L.; Huang, Z.; Xiao, J. Decarboxylative Oxygenation of Carboxylic Acids with O₂ via a Non-Heme Manganese Catalyst. *Green Chem.* **2022**, *24*, 2946–2952.
- 12) Li, J.; Kerr, A.; Song, Q.; Yang, J.; Häkkinen, S.; Pan, X.; Zhang, Z.; Zhu, J.; Perrier, S. Manganese-Catalyzed Batch and Continuous Flow Cationic RAFT Polymerization Induced by Visible Light. *ACS Macro Lett.* **2021**, *10*, 570–575.

- 13) Hu, Y.; Wang, C. Bromopentacarbonylmanganese(I). In *Encyclopedia of Reagents for Organic Synthesis*; John Wiley & Sons, Ltd: Chichester, UK, 2016; pp 1–3.